NASA Contractor Report 189079

NASA-CR-189079
19920011436

Advanced Development of the Boundary Element Method for Elastic and Inelastic Thermal Stress Analysis

Donald P. Henry, Jr.
State University of New York at Buffalo
Buffalo, New York

December 1991

Prepared for
Lewis Research Center
Under Grant NAG3–712

National Aeronautics and
Space Administration

ABSTRACT

The focus of this dissertation is on advanced development of the boundary element method for elastic and inelastic thermal stress analysis. New formulations for the treatment of body forces and nonlinear effects are derived. These formulations, which are based on particular integral theory, eliminate the need for volume integrals or extra surface integrals to account for these effects. The formulations are presented for axisymmetric, two- and three-dimensional analysis. Also in this dissertation, two-dimensional and axisymmetric formulations for elastic and inelastic, inhomogeneous stress analysis are introduced. The derivations account for inhomogeneities due to spatially dependent material parameters, and thermally induced inhomogeneities.

The nonlinear formulations of the present work are based on a incremental initial stress approach. Two inelastic solutions algorithms are implemented: an iterative; and a variable stiffness type approach. The Von Mises yield criterion with variable hardening and the associated flow rule are adopted in these algorithms.

All formulations are implemented in a general purpose, multi-region computer code with the capability of local definition of boundary conditions. Quadratic, isoparametric shape functions are used to model the geometry and field variables of the boundary (and domain) of the problem. The multi-region implementation permits a body to be modeled in substructured parts; thus dramatically reducing

the cost of the analysis. Furthermore, it allows a body consisting of regions of different (homogeneous) material to be studied.

To test the program, results obtained for simple test cases are checked against their analytical solutions. Thereafter, a range of problems of practical interest are analyzed. In addition to displacement and traction loads, problems with body forces due to self-weight, centrifugal, and thermal loads are considered.

ACKNOWLEDGEMENT

I wish to express my sincere gratitude to my advisor, Professor P.K. Banerjee for his guidance, support, and encouragement during the course of this research.

I would also like to thank Dr. S. Ahmad and Dr. S.T. Raveendra for their assistance and Dr. R.B. Wilson of Pratt and Whitney (United Technologies) for his influential suggestions.

The author is indebted to Dr. C.C. Chamis, Project Manager at NASA Lewis-Research Center (Cleveland, Ohio) and Dr. E.S. Todd, Program Manager at Pratt and Whitney (Hartford, Connecticut) for their financial support which made this research possible.

Finally, I wish to thank Carm Gosden for her exceptional typing of this dissertation.

CONTENTS

LIST OF TABLES

LIST OF FIGURES

NOTATION

A short list of notation is given below. All other symbols are defined when first introduced. A few symbols have different meaning in different context, but no confusion should arise. Matrices are indicated by bold print throughout this dissertation.

$\mathbf{A}^b, \mathbf{B}^b, \mathbf{C}^b$	Boundary system matrices in assembled form
$\mathbf{A}^\sigma, \mathbf{B}^\sigma, \mathbf{C}^\sigma$	Coefficient matrices of the stress equations in assembled form
$C_{ij}(\xi)$	A tensor dependent on location of the field point ξ
$C^e_{ijkl}, C^{ep}_{ijkl}$	Elastic and elastoplastic constitutive tensors
$D^e_{ijkl}, D^{ep}_{ijkl}$	Elastic and elastoplastic constitutive tensors
E	Young's modulus (in the Appendix, E represents the complete elliptic integral of the second kind)
f_i	Body force
$F(\sigma_{ij,h})$	Yield function
g	Gravitational acceleration
G_{ij}, F_{ij}, B_{ijk}	Kernels of the displacement equation
$B^\varepsilon_{ijk}, F^\varepsilon_{ijk}, B^\varepsilon_{ijkl}$	Kernels of the strain equation
$G^\sigma_{ijk}, F^\sigma_{ijk}, B^\sigma_{ijkl}$	Kernels of the stress equation
h	The slope of the uniaxial equivalent stress, equivalent plastic strain curve

J^{σ}_{ijkl}	Jump term (free term) tensor
K	Complete elliptic integral of the first kind
K_{ij}, L_{ij}	Functions depended on the current state of stress
L( )	Linear differential operator
n_i	Unit direction normals
$N^{\gamma}(\eta)$	Shape function
r,z	Cylindrical coordinates of field point
R,Z	Cylindrical coordinates of integration (Gauss) point
S_{ij}	Deviatoric stress
t_i	Traction
T	Temperature change
$T_i(x)$	Imposed boundary traction
u_i	Displacement
$U_i(x)$	Imposed boundary displacement
x	Refers to global coordinates of an integration point
$\mathbf{x}$	System vector of unknown boundary quantities
$\mathbf{y}$	System vector of known boundary quantities
α	Coefficient of thermal expansion

β	$= \alpha(3\lambda+2\mu)$
δ_{ij}	Kronecker delta
ε_{ij}	Total strain
ε^{e}_{ij}	Elastic strain
ε^{h}_{ij}	Homogeneous part of elastic strain
ε^{i}_{ij}	Inhomogeneous part of elastic strain
ε^{m}_{ij}	Mechanical strain
ε^{p}_{ij}	Plastic strain
ε^{t}_{ij}	Thermal strain
η	Refers to local coordinate of an integration point
λ	Lamé constant
$\dot{\lambda}$	Incremental plastic flow factor
μ	Shear modulus
ν	Poisson's ratio
ξ	Refers to coordinates of a field point
π	Archimedes number
ρ	Mass density
σ_{ij}	(Real) stress

σ^p_{ij}	(Corrective) plastic part of initial stress
σ^e_{ij}	Elastic stress
σ^i_{ij}	Inhomogeneous part of initial stress
σ^o_{ij}	Initial stress
σ^t_{ij}	Thermal part of initial stress
σ_o	Yield stress
$\boldsymbol{\sigma}^o$	System vector of initial stress
$\emptyset(\xi)$	Fictitious particular integral density
ω	Angular velocity

Superscript

c	Components related to complementary function
p	Components related to particular integral (not to be confused with plastic component)
.	(Incremental) time rate of change

Subscript

,	Spatial derivative
i,j,k	Indicial notation i,j,k = 1,2 in two-dimensions i,j,k = 1,2,3 in three-dimensions i,j,k = r,z in axisymmetry
r,θ,z	Directions of cylindrical components

CHAPTER 1

INTRODUCTION

1.1 GENERAL REMARKS

1.2 THE HISTORICAL DEVELOPMENT OF BEM IN STRESS ANALYSIS

1.3 SCOPE OF THE PRESENT WORK

CHAPTER ONE

INTRODUCTION

1.1 GENERAL REMARKS

Through the years, scientists have formulated mathematical equations to describe the behavior of many physical phenomena in the field of continuum mechanics. However, due to the complexity of these equations, closed-form solutions are unobtainable for all but the simplest problems. In developing applications, engineers must therefore resort to approximate techniques for the solutions to physical problems.

In the 1950s, the advent of the digital computer spurred the development of new approximate techniques or 'numerical methods'. Essentially, three numerical techniques evolved: the finite difference method; the finite element method (FEM); and the boundary element method (BEM).

The finite difference method, which employed 'difference equations' for the generation of equation system, was the forerunner of these methods. However, the large size of the resulting equation system and its inability to readily deal with irregular boundaries limited its success.

A more powerful and popular approach known as the finite element method (FEM) emerged. In this procedure the domain is divided into discrete elements, and trial functions are used to approximate the

functional variables across each element. Variational principles are applied to obtain a best fit solution for an appropriate set of boundary conditions. This method is very proficient in elastic and inelastic stress analyses and reasonable success has been achieved in dynamics.

Owing to their mathematical and numerical simplicity, the development of these two methods was rapid. In contrast, the development was slower for a more complex technique known as the boundary element method (BEM). In recent years, however, researchers have focused considerable attention on this method mainly due to its advantages over the former methods. These advantages include: the ability to solve three-dimensional problems with greater efficiency, higher resolution results for stress concentration problems, increased accuracy, and greater ease in application for problems of infinite or semi-infinite regions. Moreover, the system equations are written only at nodal points on the surface of the body of interest, rather than throughout the entire domain. This leads to a set of equations that is smaller than that of competing methods.

Two distinct, yet equivalent (Lamb, 1932) boundary element formulations exist. An indirect method, which introduces a ficticious set of functions as an intermediate step in the solution process, and a more popular direct formulation, which utilizes all real, physical variables. Essentially, both methods consist of transforming the governing differential equation into a boundary integral equation. The surface of a body is divided into boundary elements, and shape functions are used to represent variation of quantities across the elements in terms of their nodal values. These integral equations are

integrated numerically, generating a system of equations at boundary nodes. Standard solution procedures are employed to obtain results for a prescribed set of boundary conditions.

1.2 THE HISTORICAL DEVELOPMENT OF BEM IN STRESS ANALYSIS

The first rigorous work on integral equations was published by Fredholm in 1903. Since that time, extensive research has been carried out by a number of researchers such as Kellog (1929), Muskhelishvili (1953), Kupradze (1964) and Smirhovi (1964). The most notable work related to elastostatics was conducted by Mikhlin (1957, 1964,1965). However, due to the complexity of finding analytical solutions, most of these early works were of mathematical nature dealing in topics of existence and uniqueness.

The advent of the digital computer brought about a change in the usefulness of these mathematical formulations. The first application in elastostatics by Jaswon and Ponter (1963) dealt with torsion in elastic bars. A general elastostatic (direct BEM) approach based on the displacement formulation derived from the Somigliana's identity (1885) was established by Rizzo (1967). Further contributions were made by Cruse (1969, 1973), and Lachat and Watson (1976). An alternative, indirect, elastostatic formulation was developed by Banerjee (1969), Butterfield and Banerjee (1971), Watson (1973), Tomlin (1973), and others.

As the method developed, the analysis was extended to other areas. Cruse (1967) pioneered the study on transient elastodynamics, and Rizzo and Shippy (1977) laid forth an efficient procedure to account for steady-state body forces such as centrifugal and thermal

loadings. Kermanidis (1975) produced the first elastic, axisymmetric formulation, followed by Cruse, Snow and Wilson (1977) who extended the axisymmetric analysis to include thermal and centrifugal body force effects. And in 1979, Nigam (1979) introduced an axisymmetric formulation capable of handling non-axisymmetric boundary conditions.

It soon became apparent that material nonlinearities, in the form of initial stress (or initial strain), could be incorporated into the elastic analysis through a volume integral in a manner analogous to body force, and therefore, quasi-static algorithms for plasticity and creep analysis were developed. Swedlow and Cruse (1971) presented the first elastoplastic BEM formulation, followed by Riccardella (1973) who is credited with the first two-dimensional formulation. Further development by other workers followed: Rzasnik and Mendelson (1975), Mendelson and Albers (1975), and Chaudonneret (1977). These authors, however, overlooked the strong singularity present in the domain integral of the interior stress rate equation. In 1978, Bui (1978) presented a correct treatment of this integral and indicated the existence of the free term. Nevertheless, this integral was strongly singular and the numerical integration was still difficult.

Banerjee and co-workers developed a two-dimensional (Banerjee and Mustoe, 1978), elastoplastic BEM formulation and were the first to extend the analysis to three-dimensional (Banerjee, Cathie, and Davies, 1979) and axisymmetric (Cathie and Banerjee, 1980) media. And in 1982, Cathie and Banerjee (1982) presented a time independent inelastic analysis. Their work is unique in the sense that the stress rates are calculated via numerical differentiated displacement rates, and therefore, the strongly singular domain integral is avoided. The

method is computationally efficient, however, some accuracy is lost in the numerical differentiation.

Mukherjee and co-workers also have concentrated considerable effort in this area. Their contributions included: a time-dependent inelastic analysis using power creep; and the constitutive relations due to Hart (Mukherjee and Kunar, 1978); and the implementation of an axisymmetric visco-plastic analysis (Sarihan and Mukherjee, 1982). In addition, they have presented an integral equation for stress rates written as a function of a gradient of initial strain rates which eliminates the appearance of the strongly singular Lebesque integral over the domain in favor of a weaker volume integral.

Other researchers, such as Telles and Brebbia (1981), Kobayashi and Nishimura (1980), and Telles (1983), have presented formulations and have solved a variety of plasticity problems.

The most notable advancement in stress analysis via the boundary element method is the development of the general purpose, three-dimensional, dynamic and inelastic, stress analysis program - BEST3D - developed for the National Aeronautics and Space Administration (NASA) by Banerjee, Wilson and Miller (1985), Banerjee and Ahmad (1985) and Banerjee and Raveendra (1986). Highlighted in this work is the use of isoparametric quadratic shape functions for modeling the variation of functions over the boundary elements and volume cells. In addition, the system includes a sophisticated numerical integration scheme (Banerjee, Wilson, Miller, 1985) and a multi-region facility.

The BEST3D system contains the most advanced plasticity analysis to date. A Von Mises model, a two-surface model and a thermally sensitive anisotropic plasticity model, are all contained in the

system. Furthermore, an iteration acceleration scheme is used to reduce the number of iterations needed for convergence.

All the aforementioned plasticity formulations are based on iterative procedures that work successfully, but often takes unduly large number of iterations to converge to the correct solution, particularly in problems involving a high degree of nonlinearity such as the loading close to the collapse state of stress when significant amount of plastic zones develop. It was to this end that Banerjee and Raveendra (1987) presented the first direct or 'non-iterative' two-dimensional elastoplastic analysis which is comparable to the variable stiffness method in the finite element analysis.

In any thermal stress analysis, it is important to account for the variations in elastic modulus. In 1968, Rizzo and Shippy (1968) presented a BEM formulation for inhomogeneous elastic inclusions. More recently Tanaka and Tanaka (1980) introduced a thermoelastic formulation for inhomogeneous material. In this analysis the material parameters are independent of temperature, and vary only as a function of position. Finally, Ghosh and Mukherjee (1984) presented a two-dimensional iterative formulation for thermoelastic deformation of inhomogeneous media. In their work, they assumed the shear modulus varied linearly with temperature. In spite of these efforts the problem of elastic inhomogeneity remains essentially unresolved.

1.3 SCOPE OF THE PRESENT WORK

Once considered an analysis for mathematicians, the boundary element method is now accepted in the engineering community as a powerful and versatile tool for solving practical problems. In many applications, the boundary element method has proven itself superior

to other numerical methods, particularly in three-dimensional linear analysis. However, further refinement is necessary if inelastic boundary element analysis is to assert a similar claim. The primary objective of the present work is to rectify some of the deficiencies in this area. Furthermore, in this dissertation, considerable effort is put forth in extending all formulations to their axisymmetric form. The realization that many stress analysis problems of industrial interest are axisymmetric in nature, and the fact that the axisymmetric analysis costs a fraction of the three-dimensional counterpart, makes the axisymmetric analysis an invaluable tool.

To better appreciate the new boundary element formulations presented in this dissertation, the conventional BEM formulations for elastic and inelastic thermal analyses are first presented in Chapter 2. Included is a comprehensive look at the details of axisymmetric inelastic stress analysis.

The need for only surface discretization is a significant advantage BEM has over other methods requiring full domain discretization. However, this advantage is partially diminished in thermal and inelastic analysis where volume integration is required. To rectify the matter, a new formulation, based on particular integral theory is developed. This new procedure, incorporates the body force effect into the boundary element system without additional surface or volume integration. Application of the method for gravitational, centrifugal and thermal body forces is presented in Chapter 3 and in Chapter 4, the formulation is also extended to the inelastic analysis.

In Chapter 5 one of BEM's greatest deficiencies is addressed; that being its inability to deal with material inhomogeneities. Both

natural material inhomogeneities as well as thermally induced inhomogeneities are considered for both linear and non-linear thermal analysis.

All formulations of the present work are implemented into a general purpose, multi-region system capable of local definition of boundary conditions. Quadratic isoparametric shape functions are used to model the geometry and the field variables of both the boundary element and volume cells. In Chapter 6, a variety of linear and nonlinear problems are presented. In addition to displacement and traction boundary loads, body forces due to self-weight, centrifugal, and thermal loads are considered. In most problems, the body of interest is sub-structured for a multi-region analysis. This dramatically reduces the time and cost of the analysis as will be discussed.

CHAPTER 2

CONVENTIONAL BOUNDARY ELEMENT FORMULATION FOR ELASTIC AND INELASTIC STRESS ANALYSIS

CHAPTER TWO

CONVENTIONAL BOUNDARY ELEMENT FORMULATION FOR ELASTIC AND INELASTIC STRESS ANALYSIS

2.1 INTRODUCTION

In this chapter, the conventional formulation of the boundary integral equations for elastic and inelastic thermal stress analysis is presented. In addition to the two- and three-dimensional formulations, the axisymmetric case is also developed. The body forces and nonlinear effects are incorporated in these formulations in the conventional manner through volume integrals or addition surface integrals.

After a brief discussion on the elastoplastic constitutive relations, two BEM algorithms for the solution of inelastic problems are described. The first algorithm is an iterative procedure which includes a time saving feature which reduces the number of iterations needed for convergence by utilizing the past history of initial stress rates to estimate the values of the initial stress rates of the next load increment. The second algorithm is a direct procedure similar to the variable stiffness approach in the finite element method. This procedure exploits certain features of the constitutive relationship to express the unknown nonlinear initial stress rate tensor as a scalar quantity which then can be eliminated from the boundary equation system through a back substitution of the (modified) stress rate equations.

The axisymmetric, two- and three-dimensional formulations are implemented in a multi-region code which utilizes quadratic isoparametric shape functions to model the geometry and field variables of the boundary and domain of the body. Numerical implementation procedures are briefly discussed, including techniques that are used to calculate coefficients of the integrals over strong singularity points on the boundary and domain of the body. Finally, a number of examples are included to demonstrate the accuracy and convergence of the plasticity algorithms.

2.2 BOUNDARY INTEGRAL FORMULATION

2.2.1 Governing Equations

The governing equation of stress for a body in equilibrium with domain V and surface S can be expressed in a cartesian system x_i as

$$\sigma_{ij,j} + f_i = 0 \qquad (2.1)$$

$i,j = 1,2$ for two-dimensional

$i,j = 1,2,3$ for three-dimensional

where $\sigma_{ij} = \sigma_{ij}(x)$ is the stress tensor,

$f_i = f_i(x)$ represents the total contribution of all body forces present, and

the comma indicates spatial derivatives.

Throughout this dissertation, when the dimension of the problem is irrelevant to the point of the discussion, three-dimension will be assumed. Solutions of equations (2.1) are subject to boundary conditions:

$$u_i = U_i(x) \quad \text{on } S_1 \tag{2.2a}$$

or

$$t_i = \sigma_{ij}\, n_j = T_i(x) \quad \text{on } S_2 \tag{2.2b}$$

or

a compatible combination of the two on S_3 (2.2c)

where $S = S_1 + S_2 + S_3$,

u_i is the displacement vector,

t_i is the traction vector,

n_j is the boundary normal vector,

$U_i(x)$ are the imposed displacements, and

$T_i(x)$ are the imposed tractions.

In equation (2.2b) we have used the Cauchy traction relation

$$t_i = \sigma_{ij}\, n_j \tag{2.3}$$

and displacements are related to strain via

$$\varepsilon_{ij} = 1/2\ (u_{i,j}+u_{j,i}) \tag{2.4}$$

The (total) strain tensor ε_{ij} can be decomposed into an elastic strain ε^e_{ij} and an initial strain ε^o_{ij}

$$\varepsilon_{ij} = \varepsilon^e_{ij} + \varepsilon^o_{ij} \tag{2.5}$$

The elastic strain is directly related to stress through the elastic constitutive relations

$$\sigma_{ij} = D^e_{ijkl}\, \varepsilon^e_{kl} \tag{2.6a}$$

$$\varepsilon^e_{ij} = C^e_{ijkl}\, \sigma_{kl} \tag{2.6b}$$

where

$$D^e_{ijkl} = 2\mu\, \delta_{ik}\, \delta_{jl} + \lambda\, \delta_{ij}\, \delta_{kl} \tag{2.7a}$$

$$C^e_{ijkl} = \frac{1+\nu}{E}\,\delta_{ik}\,\delta_{jl} - \frac{\nu}{E}\,\delta_{ij}\,\delta_{kl} \qquad (2.7b)$$

δ_{ij} is the Kronecker delta

λ and μ are Lamé constants

E is the modulus of elasticity, and

ν is Poisson's ratio

Note: $$D^e_{ijkl}\,C^e_{klpq} = \delta_{ip}\,\delta_{jq} \qquad (2.8)$$

D^e_{ijkl} and C^e_{ijkl} are symmetric with respect to (ij) and (kl)

The initial strain, by definition, is the difference between the total strain and the elastic strain. The initial strain occurs from various effects, such as plastic deformation, thermal loading, or strain present in a body before loading occurs. In a thermoplastic analysis, initial strain will be defined as the summation of plastic strain ε^p_{ij} and thermal strain ε^t_{ij}

$$\varepsilon^o_{ij} = \varepsilon^p_{ij} + \varepsilon^t_{ij} \qquad (2.9)$$

Substituting equation (2.5) into equation (2.6) yields a relation between total strain and stress

$$\sigma_{ij} = D^e_{ijkl}\,\varepsilon_{kl} - \sigma^o_{ij} \qquad (2.10a)$$

$$\varepsilon_{ij} = C^e_{ijkl}\,\sigma_{kl} + \varepsilon^o_{ij} \qquad (2.10b)$$

where

$$\sigma^o_{ij} = D^e_{ijkl}\,\varepsilon^o_{kl} \qquad (2.10c)$$

Substituting equation (2.4) and (2.10a) into equation (2.1) produces the governing differential equation of equilibrium in terms

of displacement, body force, and initial stress:

$$(\lambda+\mu)\, u_{j,ij} + \mu\, u_{i,jj} + f_i = \sigma^{o}_{ij,j} \tag{2.11}$$

This is the Navier equation with an initial stress term present.

2.2.2 Two- and Three-Dimensional Integral Formulation

In deriving the boundary integral equations for general elastic and inelastic analysis, we consider an elastic body under two distinct equilibrium states. The first state (u_i, t_i, f_i, ε^{e}_{ij}, σ_{ij}) will be considered the real state, and the second state ($\bar{u}_i$, $\bar{t}_i$, $\bar{f}_i$, $\bar{\varepsilon}^{e}_{ij}$, $\bar{\sigma}_{ij}$) will be considered an arbitrary state.

The following integral statement can be inferred from equations (2.6) and symmetry property of D^{e}_{ijkl}

$$\int_V \bar{\sigma}_{ij}\, \varepsilon^{e}_{ij}\, dV = \int_V \bar{\varepsilon}^{e}_{ij}\, \sigma_{ij}\, dV \tag{2.12}$$

Using equation (2.5) this equation can be rewritten in terms of total strain as

$$\int_V \bar{\sigma}_{ij}\, \varepsilon_{ij}\, dV = \int_V \bar{\varepsilon}^{e}_{ij}\, \sigma_{ij}\, dV + \int_V \bar{\sigma}_{ij}\, \varepsilon^{o}_{ij}\, dV \tag{2.13}$$

Using equations (2.6b), (2.10c), and the symmetry property of D^{e}_{ijkl} we can show

$$\int_V \bar{\sigma}_{ij}\, \varepsilon^{o}_{ij}\, dV = \int_V \bar{\varepsilon}^{e}_{ij}\, \sigma^{o}_{ij}\, dV \tag{2.14}$$

Substituting this result in equation (2.13) gives

$$\int_V \bar{\sigma}_{ij}\, \varepsilon_{ij}\, dV = \int_V \bar{\varepsilon}^e_{ij}\, \sigma_{ij}\, dV + \int_V \bar{\varepsilon}^e_{ij}\, \sigma^o_{ij}\, dV \qquad (2.15)$$

Employing equation (2.4) and utilizing the symmetry property of the stress tensor, equation (2.15) is transformed into

$$\int_V \bar{\sigma}_{ij}\, u_{i,j}\, dV = \int_V \bar{u}^e_{i,j}\, \sigma_{ij}\, dV + \int_V \bar{\varepsilon}^e_{ij}\, \sigma^o_{ij}\, dV \qquad (2.16)$$

Applying the divergence theorem to the first two terms of the above equation and substituting equations (2.1) and (2.3) into this result we arrive at

$$\int_S \bar{t}_i(x)\, u_i(x)\, dS + \int_V \bar{f}_i(x)\, u_i(x)\, dV = \int_S \bar{u}^e_i(x)\, t_i(x)\, dS + \int_V \bar{u}^e_i(x)\, f_i(x)\, dV + \int_V \bar{\varepsilon}^e_{ij}\, \sigma^o_{ij}\, dV \qquad (2.17)$$

In the absence of initial stress, this equation reduces to the celebrated Betti's reciprocal work theorem.

We now define the arbitrary, elastic stress state to be equivalent to the state of stress given by the Kelvin point force solution for point force $e_k(\xi)$ acting at ξ_i.

$$\begin{aligned} \bar{f}_i(x) &= \delta(x,\xi)\, \delta_{ik}\, e_k(\xi) \\ \bar{u}^e_i(x) &= G_{ik}(x,\xi)\, e_k(\xi) \\ \bar{\varepsilon}^e_{ij}(x) &= B_{ijk}(x,\xi)\, e_k(\xi) \\ \bar{t}_i(x) &= F_{ik}(x\xi)\, e_k(\xi) \end{aligned} \qquad (2.18)$$

where

$\delta(x,\xi)$ is the Dirac delta function, and

G_{ik}, B_{ijk}, and F_{ik} represent the displacement, strain and stress at point x_i in an infinite space due to a unit point force at ξ_i (both the two- and three-dimensional functions are defined in the appendix). Noting the properties of the Dirac delta function, we can show that

$$\int \bar{f}_i(x)\, u_i(x)\, dV = \int \delta(x,\xi)\, \delta_{ik}\, e_k(\xi)\, u_i(x)\, dV = u_k(\xi)\, e_k(\xi) \tag{2.19}$$

Substituting equations (2.18) and (2.19) into equation (2.17) and using the orthogonality property to separate the three independent components (and cancelling the $e_k(\xi)$), the displacement at point ξ_i can be expressed as

$$C_{ij}(\xi)\, u_i(\xi) = \int_S [G_{ij}(x,\xi)\, t_i(x) - F_{ij}(x,\xi)\, u_i(x)]\, dS(x) + \int_V G_{ij}(x,\xi)\, f_i(x)\, dV(x) + \int_V B_{ikj}(x,\xi)\, \sigma^o_{ik}(x)\, dV(x) \tag{2.20}$$

where $C_{ij}(\xi) = \delta_{ij}$ for a point in the interior of the domain. When point ξ_i is brought to the boundary x_o, $C_{ij}(x_o)$ must be derived from the singular treatment of surface integral involving the F_{ij} kernel. The resulting tensor function C_{ij} is depended on the subtended angle of the tangent plane at x_o. For a point on the smooth surface $C_{ij} = 1/2\ \delta_{ij}$. The surface integral involving kernel F_{ij} in equation (2.20) must be treated as a Lebesgue integral.

The integral equation for the strain at an interior point is found analytically by substituting equation (2.20) (with $C_{ij} = \delta_{ij}$) into the strain-displacement relations, where differentiation is with respect to the field point ξ :

$$\varepsilon_{ij}(\xi) = \int_S [G^{\varepsilon}_{kij}(x,\xi)t_k(x) - F^{\varepsilon}_{kij}(x,\xi)u_k(x)]dS(x)$$

$$+ \int_V G^{\varepsilon}_{kij}(x,\xi)f_k(x)dV(x) + \int_V B^{\varepsilon}_{klij}(x,\xi)\sigma^{o}_{kl}(x)dV(x) \qquad (2.21)$$

By introducing this result into the stress-strain equation (2.10a) the stress integral equation is derived:

$$\sigma_{ij}(\xi) = \int_S [G^{\sigma}_{kij}(x,\xi)t_k(x) - F^{\sigma}_{kij}(x,\xi)u_k(x)]dS(x)$$

$$+ \int_V G^{\sigma}_{kij}(x,\xi)f_k(x)dA(x) + \int_V B^{\sigma}_{klij}(x,\xi)\sigma^{o}_{kl}(x)dV(x) \qquad (2.22)$$

The kernels G^{σ}_{kij}, F^{σ}_{kij} and B^{σ}_{klij} are defined in the Appendix.

The last integral in equations (2.21) and (2.22) is strongly singular and must be treated as Lebesgue integral. Treatment of these integrals is discussed in subsequent sections.

Due to strong singularities in the kernel functions, equations (2.21) and (2.22) are not used for calculations of stresses and strains on the boundary. Instead, an alternate procedure will be presented in later sections.

2.2.3 Axisymmetric Integral Formulation

The axisymmetric boundary integral equations can be derived from the three-dimensional BEM equation (2.20) which satisfies the governing differential equation (2.11). In principle this is accomplished by: recasting the three-dimensional BEM equation in cylindrical coordinates; applying appropriate tensor transformations; and integrating analytically to remove the angular (θ) dependency. However, once the axisymmetric displacement kernel G_{ij} is known, the

F_{ij} and B_{ijk} kernels can be derived an alternate way starting with the solution (the G_{ij} kernel) for the displacements due to a ring load intensity (Cathie and Banerjee, 1980). The strain due a ring load (the B_{ijk} kernel) is obtained by substitution of the G_{ij} kernel into the axisymmetric strain-displacement equations, where differentiation is with respect to x. The surface traction due to a ring load (the F_{ij} kernel) is found by introducing the B_{ijk} kernel into Hooke's law and multiplying by appropriate normals.

The axisymmetric form of the displacement integral equation can then be expressed as:

$$C_{ij}(\xi)u_i(\xi) = \int_C [G_{ij}(x,\xi)t_i(x) - F_{ij}(x,\xi)u_i(x)]dC(x)$$

$$+ \int_A G_{ij}(x,\xi)f_i(x)dA(x) + \int_A B_{ikj}(x,\xi)\sigma^o_{ik}(x)dA(x) \qquad (2.23)$$

$$i,j,k = r,z \quad ,$$

where

u_i, t_i, f_i, and σ^o_{ik} are expressed in radial and axial components,

$C_{ij} = \delta_{ij}$ for interior points and is dependent on the surface geometry at ξ for boundary points, and

G_{ij} , F_{ij} and B_{ijk} are defined in the Appendix.

Note that the surface integration is over a curve dC and the volume integration is over an area dA. Furthermore, the $2\pi R$ term which appears after integration in the θ direction has been absorbed in the kernels. The domain integral need only be evaluated where the initial stresses are non-zero.

Axisymmetric integral equations for stress and strain at interior points are derived in a manner analogous to the two- and three-dimensional case.

2.3 NUMERICAL IMPLEMENTATION

The integral equations discussed in the preceding sections become of practical interest only when numerical techniques are employed for their solution. It should be noted that these integral equations are exact statements, and any error in the final BEM solution is caused by approximations in the numerical implementation.

The numerical implementations of the integral equations consist of: discretization of the surface of the body (and domain when necessary) and discretization of the integral equations; numerical integration; assembly, and solution of these equations.

2.3.1 Discretization and Numerical Integration

Discretization - The body under consideration is divided into discrete boundary elements and, when applicable, volume cells. Quadratic isoparametric curvilinear shape functions, presented in Appendix I, are used to approximate the geometry and the field variables over the boundary elements and volume cells in terms of their nodal values. After discretization, the boundary displacement equation can be expressed in the following manner.

$$C_{ij}u_i(\xi) = \sum_{m=1}^{M}\left[\int_{S^m} G_{ij}(x,\xi)N^{\gamma}(\eta)dS^m\right]\bar{t}_i^{\gamma m} - \sum_{m-1}^{M}\left[\int_{S^m} F_{ij}(x,\xi)N^{\gamma}(\eta)dS^m\right]\bar{u}_i^{\gamma m}$$

$$+\sum_{P=1}^{P}\left[\int_{V^p} G_{ij}(x,\xi)N^{\beta}(\eta)\ dV^p\right]\bar{f}_i{}^{\beta p}$$

$$+\sum_{p=1}^{P}\left[\int_{V^p} B_{ikj}(x,\xi)N^{\beta}(\eta)dV^p\right](\bar{\sigma}^o_{ik})^{\beta p} \qquad (2.24)$$

where i,j,k = r,z

M = number of boundary elements,

P = number of volume cells,

$N^{\gamma}(\eta)$ represents shape function of boundary elements, and

$N^{\beta}(\eta)$ represents shape function of volume cells.

Summation over γ and β is implied.

The bars indicate nodal values and the integration coordinate x has been expressed in local coordinates η via the above shape functions.

The stress equation can be discretized in a similar fashion:

$$\sigma_{ij}(\xi) = \sum_{m=1}^{M}\left[\int_{S^m} G^{\sigma}_{kij}(x,\xi)N^{\gamma}(\eta)\ dS^m\right]\bar{t}^{\gamma m}_k$$

$$-\sum_{m=1}^{M}\left[\int_{S^m} F^{\sigma}_{kij}(x,\xi)N^{\gamma}(\eta)\ dS^m\right]\bar{u}^{\gamma m}_k$$

$$+\sum_{p=1}^{P}\left[\int_{V^p} G^{\sigma}_{kij}(x,\xi)N^{\beta}(\eta)\ dV^p\right]\bar{f}^{\beta p}_k$$

$$+\sum_{P=1}^{P}\left[\int_{V^p} B^{\sigma}_{klij}(x,\xi)N^{\beta}(\eta)\ dV^p\right](\bar{\sigma}^o_{kl})^{\beta p} \qquad (2.25)$$

A similar discretization of the strain equation is possible, however, the implementation is unnecessary. Once the stress state at

a point is known, the strains can be calculated by a direct application of the constitutive relation.

Numerical Integration - The complexity of the integral in the discretize equation necessitates the use of numerical integration for their evaluation. The steps in the integration process for a given element is outlined below:

1. Using appropriate Jacobian transformations (given in Appendix I), the curvilinear line element, surface element or volume element is mapped on to a unit line, a plane unit cell or a three-dimensional unit cell, respectively.

2. Depending on the proximity between the field point (ξ_i) and the element under consideration, there may be element sub-division and additional mapping for improved accuracy (Banerjee and Raveendra, 1986).

3. Gaussian quadrature (Appendix I) formulas are employed for the evaluation of the discretized integral over each element (or sub-element). These formulas approximate the integral as a sum of weighted function values at designated points. The error in the approximation is dependent on the order of the (Gauss) points employed in the formula. To minimize error while at the same time maintaining computational efficiency, optimization schemes are used to choose the best number of points for a particular field point and element (Watson, 1979).

2.3.2 Treatment of the Singular Integrals

The integration of the kernel functions are singular and require special attention when an integration point (x) coincides with the field point (ξ).

The Displacement Equation - The integrations of the G_{ij} and B_{ijk} kernels of the displacement equation are weakly singular under this circumstance and can be integrated numerically using element subdivisions near the singular point (Banerjee and Raveendra, 1986). On the other hand, the integration of the F_{ij} kernel of the displacement equation is strongly singular and must be integrated as a Lebesgue integral over the singular element. This integral can be decomposed into a free term and a Cauchy principal-value integral, but accurate numerical integration is still difficult (Banerjee and Raveendra, 1986). When constructing the equations for the boundary system, the singular integration involving the F_{ij} kernel can be circumvented by using the 'rigid body' displacement technique (Swedlow and Cruse, 1971) or the analogous 'inflation mode,' for axisymmetry (Nigam, 1979). A brief description of these procedures is given below.

Rigid Body: For every boundary node of the system there is a 2 by 2 (or 3 by 3 for three-dimension) block of coefficients on the diagonal of the **F** matrix, corresponding to the singular node, which is difficult to determine by numerical integration. Each of these terms, however, can be determined independently by assuming two (or three) different admissible displacement fields corresponding to a rigid body displacement in each of the two (or three) directions. All tractions (and body forces) are zero for this calculation.

Inflation Mode: Since a rigid body displacement is not admissible for the radial direction in axisymmetry, the two unknown coefficients (corresponding to the radial displacement) are determined by an inflation mode (i.e. a linear displacement in the radial direction), $u_r = r$ and $u_z = 0$. With body forces set to zero, the tractions related to this displacement are $t_r = 2(\lambda + \mu)\, n_r$ and $t_z = 2\lambda n_z$, in which n_r and n_z are normals on the boundary and λ and μ are Lamé constants. The remaining two unknown coefficients in the displacement equation for the z-direction are determined by using a rigid body displacement in this direction.

It should be noted that when displacements are required on the boundary between nodal points, the values should be calculated via the shape function of the boundary element.

The Stress Equation - The stress (or strain) calculation is handled in two ways depending on whether the field point falls on the boundary or in the interior of the domain.

Stress on the Boundary: For a point on the boundary, all kernel functions of the stress equation are all strongly singular and difficult to integrate numerically. However, the stress on the boundary can be obtained from the boundary tractions and discplacements without any integration as originally proposed by Cruse (1974). A slight modification must be made to incorporate the initial stress. In this procedure the stress-strain relations, the Cauchy traction equation and the equations relating local and global gradients of displacements are utilized in writing an expression for the boundary stress. Demonstrated for the axisymmetric case, these equations can be written in matrix form as follows

$$\begin{bmatrix} 0 & 0 & 0 & 0 & n_r & 0 & n_z & 0 \\ 0 & 0 & 0 & 0 & 0 & n_z & n_r & 0 \\ -n_z & 0 & n_r & 0 & 0 & 0 & 0 & 0 \\ 0 & -n_z & 0 & n_r & 0 & 0 & 0 & 0 \\ -c_1 & 0 & 0 & -c_2 & 1 & 0 & 0 & 0 \\ -c_2 & 0 & 0 & -c_1 & 0 & 1 & 0 & 0 \\ 0 & -\mu & -\mu & 0 & 0 & 0 & 1 & 0 \\ -c_2 & 0 & 0 & -c_2 & 0 & 0 & 0 & 1 \end{bmatrix} \begin{Bmatrix} u_{r,r} \\ u_{z,r} \\ u_{r,z} \\ u_{z,z} \\ \sigma_{rr} \\ \sigma_{zz} \\ \sigma_{rz} \\ \sigma_{\theta\theta} \end{Bmatrix} = \begin{Bmatrix} t_r \\ t_z \\ u_{r,s} \\ u_{z,s} \\ c_2\varepsilon_\theta \\ c_2\varepsilon_\theta \\ 0 \\ c_1\varepsilon_\theta \end{Bmatrix} - \begin{Bmatrix} 0 \\ 0 \\ 0 \\ 0 \\ \sigma^o_{rr} \\ \sigma^o_{zz} \\ \sigma^o_{rz} \\ \sigma^o_{\theta\theta} \end{Bmatrix} \tag{2.26}$$

where $c_1 = \lambda + 2\mu$ $\qquad$ $c_2 = \lambda$

n_r and n_z are normals on the boundary, and

$u_{r,s}$ and $u_{z,s}$ are the local displacement gradients on the boundary.

Using shape functions and their first derivatives the vectors on the right hand side of equations (2.26) can be expanded as a matrix multiplied by a vector consisting of nodal values of displacement, traction and initial stress. Equation (2.26)is then pre-multiplied by the inverse of the matrix on the left hand side.

Stress in the Interior: When the field point lies in the interior of the body, the G^{σ}_{ijk} and F^{σ}_{ijk} kernels of the stress equations are well behaved and require no special attention. However, the B^{σ}_{ijkl} kernel is strongly singular and must be integrated as a Lebesgue integral over the singular point. Once again, this type of integral can be decomposed into a free term (given in the Appendix) and a Cauchy principal-value integral. Although difficult and expensive, reasonable accuracy can be obtained when this integral is

numerically integrated using techniques described by Banerjee and Raveendra (1986). However, for high accuracy, the coefficients of the B^{σ}_{ijkl} kernel corresponding to a singular nodal point should be evaluated using a procedure known as the 'Initial Stress Expansion Technique,' described below.

2.3.3 Initial Stress Expansion Technique

In this procedure, the coefficients of the stress equations related to the non-singular nodes are integrated in the usual manner. In each stress equation there remains three undetermined coefficients in 2-D (six in 3-D, or four in a axisymmetry) corresponding to the initial stress at the singular node. In a manner analogous to the 'rigid body' technique, each of these coefficients are calculated by assuming one of the three (six or four) admissible stress states and compatible displacement fields given in Table 2.1 (2.2 or 2.3). For each stress state, one unknown coefficient in each stress equation can be determined. It should be noted that in order to apply this method the entire region must be covered with cells. In an iso-thermal analysis in which the plastic yield zone is small, this technique appears inefficient since it requires the presence of volume cells throughout the elastic region which otherwise would be unnecessary. Although this is true in a single region program, such is not the case in multi-region code since the technique is applied to each region independently and only used in regions where volume cells exist. Therefore, the zones in which plastic yielding is expected to occur are isolated in separate regions fully populated with cells, and the elastic regions remain free of any volume cells.

2.3.4 Singularities at the Origin in Axisymmetry

Additional singularities exist in the axisymmetric kernel when the field point falls on the origin ($\xi_r = 0$). This problem is resolved by moving the field point a small radial distance from the origin. This is a common practice also employed in the finite element analysis of axisymmetric problems. In the equations for stress and strain, the minimum distance should be 0.5% of the difference between the maximum and minimum z coordinates at the origin. For the displacement equation this distance can be considerably less. Alternatively, a separate limiting form of the displacement kernels for a field point on the origin can be derived (Bakr and Fenner, 1983).

Finally, for circumferential strain on the boundary at the origin, the relation $\varepsilon_\theta = \varepsilon_r = \partial u_r/\partial r$ proves useful instead of the usual $\varepsilon_\theta = u_r/r$.

2.3.5 Assembly and Solution of Equations

A displacement equation is written for each boundary node and a stress equation is written at points of interest. The resulting coefficients are modified appropriately for cases where the functions (boundary conditions) are referred to local boundaries. The displacement and stress equations are assembled by collecting the known and unknown values of tractions and displacements and their coefficients together. At the common interface of substructured regions, the equilibrium and compatibility conditions are invoked in a manner described by Banerjee and Butterfield (1981). The final system equations can be cast as:

$$A^b x = B^b y + C^b \sigma^o \tag{2.27a}$$

$$\sigma = A^\sigma x + B^\sigma y + C^\sigma \sigma^o \tag{2.27b}$$

where

x is the vector of unknown variables at boundary and interface nodes.

y is the vector of known variables,

σ^o is the vector of initial stress (includes thermal load contribution)

A^b, B^b, C^b are the coefficient matrices of the boundary (displacement) system, and

$A^\sigma, B^\sigma, C^\sigma$ are the coefficient matrices of the stress equations.

It should be noted that A^b is a square matrix. Furthermore, in a substructured system the matrices A^b and B^b are block banded whereas matrices C^b, A^σ, B^σ and C^σ are block diagonal.

Solution: Standard numerical procedures are used to solve for the knowns in equations (2.27a), after which the stresses in equation (2.27b) can be determined.

The solver, employed in this work, is part of a software package from LINPACK (Dongarra, et al, 1979), which decomposes the A^b matrix into an upper triangular submatrix by the Gaussian reduction process. This procedure allows for an efficient resolution for vectors of different values on the right hand side of the same equation. This is essential for an efficient plasticity algorithm.

2.4 CONVENTIONAL BEM FORMULATION WITH BODY FORCES

The general form of the governing differential equation for the deformation of a homogeneous isotropic body subjected to gravitational, centrifugal and thermal loading is given in equation (2.11) and is repeated here.

$$(\lambda+\mu)\, u_{j,ji} + \mu\, u_{i,jj} + f_i = \sigma^{o}_{ij,j} \tag{2.28}$$

in which

$f_i = f_i^g + f_i^c$

$f_i^g = \rho\, g\, e_3$ for gravity loading in z direction

$f_i^c = \rho\omega^2(x_1 e_1 + x_2 e_2)$ for centrifugal loading about z axis

$\sigma^{o}_{ij} = \beta T\, \delta_{ij}$ for thermal loading

ρ is the material density, g is the gravitational acceleration, e_i is a unit vector in the i direction, ω is the angular velocity, and x_i is the spatial coordinate from the center of rotation, $\beta = \alpha\,(3\lambda+2\mu)$, α is thermal coefficient of expansion, and T is the change in temperature.

For simplicity, rotation is assumed to be centered at the origin about the z axis. The above equation is subject to boundary conditions given in equation (2.2).

The three-dimensional boundary integral equation for displacement satisfying equation (2.28) is given in equation (2.20) and is repeated here.

$$C_{ij}(\xi)u_i(\xi) = \int_S [G_{ij}(x,\xi)t_i(x) - F_{ij}(x,\xi)u_i(x)]\, dS(x)$$

$$+ \int_V G_{ij}(x,\xi)f_i(x)\, dV(x) + \int_V B_{ikj}(x,\xi)\sigma^{o}_{ik}(x)\, dV(x) \tag{2.29}$$

and the corresponding equation for stress is given in equation (2.22).

Two drawbacks exist in the formulation. First, numerical volume integration is time consuming and expensive, and second, the volume integrals of the stress equation are strongly singular leading to difficulties in the numerical integration.

For these reasons, Rizzo and Shippy (1977) (and Cruse, Snow and Wilson, 1977 in axisymmetry) transformed the volume integrals of equation (2.29) into a surface integral, through an application of the divergence theorem (assuming a steady-state temperature distribution). The three-dimensional version is expressed as

$$C_{ij}(\xi)u_i(\xi) = \int_S [G_{ij}(x,\xi)\ \{t_i(x) - h(x)\ n_i(x)\} - F_{ij}(x,\xi)u_i(x)]\ dS$$

$$+ \mu_o \int_S \{h(x)+\beta T(x)\} \frac{\partial r_{,j}}{\partial n} - \frac{\partial}{\partial n}\{h(x)+\beta T(x)\}\ r_{,j} + 3\rho\omega^2 n_j(x) r]\ dS \qquad (2.30)$$

where

r is the eucidean distance between x and ξ,

$T(x)$ is the temperature change at x,

$n_i(x)$ is the boundary normals at x,

$\mu_o = (1-2\mu)/16\pi\mu(1-\nu)$; ν is Poisson's ratio, and

$f_i = h_{,i}(x)$.

The method is effective in many applications, particularly for gravitational and centrifugal analysis, but is restricted to steady-state temperature distribution and still requires additional surface integration. However, Rizzo (1977) and Shippy stated that the concept is applicable to diffusive systems and Masinda (1984) has, without evidence of implementations, produced formulations. Nevertheless, the

formulation is restricted to problems in which no heat sources are present and is only valid for uniform initial temperature distribution. For a general transient thermoelastic analysis, one still requires the use of volume internals.

2.5 INELASTIC BEM FORMULATION BASED ON VOLUME INTEGRALS

2.5.1 Incremental Theory of Plasticity

Before proceeding with the inelastic BEM formulation, it is necessary to explore the constitutive relations that govern the material nonlinearities. The stress-strain relationships based on the 'path independence in the small' theory of plasticity essentially have three components.

1. A yield criterion - defines the limit of elastic behavior.
2. A plastic flow rule - relates the irrecoverable plastic strain increment to the state of stress in a material.
3. A hardening rule - defines the expansion or contraction of the subsequent yield surfaces resulting from continuous plastic flow.

The nature of the yield surface and hardening parameters are material dependent. In this dissertation the Von Mises yield criterion with strain hardening, Drucker's postulate for associated plastic flow, and isotropic hardening is assumed. These assumptions provide a good model for ductile material, such as metal, under monotonic loading.

The Von Mises Yield Criterion - The Von Mises Yield Criterion with strain hardening is assumed in the present work. This can be expressed in terms of the deviatoric stress tensor S_{ij} and plastic

strain ε_{ij}^{p} as

$$F = \left(\frac{3}{2} S_{ij} S_{ij}\right)^{1/2} - h \left(\frac{2}{3} \varepsilon_{ij}^{p} \varepsilon_{ij}^{p}\right)^{1/2} \qquad (2.31)$$

where

$S_{ij} = \sigma_{ij} - \frac{1}{3} \delta_{ij} \sigma_{kk}$

$\sigma_o = \sigma_o(\varepsilon_{ij}^{p})$ is the uniaxial yield stress, and

h = the slope of the uniaxial equivalent stress plastic strain curve.

Plastic Flow Rule - The plastic flow rule (Drucker, 1952) states that the plastic strain rate tensor is linearly related to the gradient of the plastic potential Q through the stress point. This implies that the plastic strain rate tensor is normal to the surface of the plastic potential. This condition known as normality principle is generally expressed as

$$\dot{\varepsilon}_{ij}^{p} = K_{ij}\dot{\lambda} \qquad (2.32)$$

$$K_{ij} = \frac{\partial Q}{\partial \sigma_{ij}}$$

where

$\dot{\lambda}$ is non-negative scalar variable which depends on the current stress rates and the past history of loading.

For metals, 'associated flow' (i.e., $Q = F$) is usually assumed and will be adopted in this work. Other materials, such as soil, require more complicated functions, and therefore 'non-associated

flow' ($Q \neq F$) is often assumed.

Isotropic Hardening - A hardening rule defines the subsequent yield surfaces resulting from continuous plastic deformation. Different hardening rules have been proposed to model the behavior of various materials and loadings.

The isotropic hardening rule which is employed in the present work, assumes the yield surface uniformly expands about the origin in the stress space while maintaining its shape, center and orientation during plastic flow. Figure 2.1 illustrates this behavior. During loading along path OA, the stress state is elastic. At point A, the elastic limit is reached and additional loading along path AB expands the yield surface to point B. Upon unloading, the behavior is elastic along path BC until point C is reached, beyond which yielding occurs only once.

Let us assume a yield function for isotropic hardening material can be expressed as

$$F(\sigma_{ij}, \varepsilon^p_{ij}, h) = 0 \tag{2.33}$$

where σ_{ij} is the current state of stress, ε^p_{ij} is the total plastic strain and h is the hardening that may vary with plastic strain.

Since consistency relation requires the stress point must remain on newly developed surface during isotropic hardening, we have

$$dF = \frac{\partial F}{\partial \sigma_{ij}} \dot{\sigma}_{ij} + \frac{\partial F}{\partial \varepsilon^p_{ij}} \dot{\varepsilon}^p_{ij} + \frac{\partial F}{\partial h} \dot{h} = 0 \tag{2.34}$$

$\dot{h}$ can generally be expressed as a function of irrecoverable strain rates.

$$\dot{h} = \frac{\partial h}{\partial \varepsilon^p_{ij}} \dot{\varepsilon}^p_{ij}$$

and substituting this in equation (2.34) yields

$$dF = \frac{\partial F}{\partial \sigma_{ij}} \dot{\sigma}_{ij} + \frac{\partial F}{\partial \varepsilon^p_{ij}} \dot{\varepsilon}^p_{ij} + \frac{\partial F}{\partial h} \frac{\partial h}{\partial \varepsilon^p_{ij}} \dot{\varepsilon}^p_{ij} = 0 \qquad (2.35)$$

Equation (2.35) together with the normality condition (2.32) yields an expression for $\dot{\lambda}$

$$\dot{\lambda} = L^{\sigma}_{ij} \dot{\sigma}_{ij} \qquad (2.36)$$

where

$$L^{\sigma}_{ij} = \frac{1}{H} \frac{\partial F}{\partial \sigma_{ij}} \qquad (2.37)$$

$$H = - \left[\frac{\partial F}{\partial \varepsilon^p_{mn}} + \frac{\partial F}{\partial h} \frac{\partial h}{\partial \varepsilon^p_{mn}} \right] \frac{\partial F}{\partial \sigma_{mn}} \qquad (2.38)$$

Note the relationship given by equation (2.36) does not exist for ideal plasticity since H vanishes for zero hardening. This can be avoided by reformulating the above expression in terms of strain increments. In the absence of thermal strains we have

$$\dot{\lambda} = L^{\varepsilon}_{ij} \dot{\varepsilon}_{ij} \qquad (2.39)$$

where

$$L^{\varepsilon}_{ij} = \frac{1}{H^1} \frac{\partial F}{\partial \sigma_{kl}} D^e_{klij} \qquad (2.40)$$

$$H^1 = \frac{\partial F}{\partial \sigma_{ki}} D^e_{klmn} \frac{\partial F}{\partial \sigma_{mn}} - \left(\frac{\partial F}{\partial \varepsilon^p_{kl}} + \frac{\partial F}{\partial h} \frac{\partial h}{\partial \sigma^p_{kl}} \right) \frac{\partial F}{\partial \sigma_{kl}} \qquad (2.41)$$

and it is obvious that for ideal plasticity H^1 does not vanish. In the above equations, L^{σ}_{ij} and L^{ε}_{ij} are functions of the current state of stress.

Having found a relation for $\dot{\lambda}$, the plastic strain rate can now be found utilizing the normality condition (2.32), and the elastic strain increment is determined using Hooke's law.

$$\dot{\varepsilon}^{p}_{ij} = C^{p}_{ijkl}\,\dot{\sigma}_{kl} \tag{2.42a}$$

$$\dot{\varepsilon}^{e}_{ij} = C^{e}_{ijkl}\,\dot{\sigma}_{kl} \tag{2.42b}$$

where

$$C^{p}_{ijkl} = L_{ij}\,\frac{\partial F}{\partial \sigma_{kl}} \tag{2.43}$$

The total strain increment is a summation of the plastic, elastic and thermal strain:

$$\varepsilon_{ij} = \varepsilon^{p}_{ij} + \varepsilon^{e}_{ij} + \varepsilon^{t}_{ij} \tag{2.44}$$

where

$$\varepsilon^{t}_{ij} = \delta_{ij}\,\alpha\,T \tag{2.45}$$

and therefore the mechanical strain can be defined as

$$\varepsilon^{m}_{ij} = (\varepsilon_{ij} - \alpha\,\delta_{ij}\,\dot{T}) = \varepsilon^{e}_{ij} + \varepsilon^{p}_{ij} \tag{2.46}$$

or using equation (2.42)

$$\varepsilon^{m}_{ij} = C^{ep}_{ijkl}\,\sigma_{kl} \tag{2.47}$$

where

$$C^{ep}_{ijkl} = C^{e}_{ijkl} + C^{p}_{ijkl} \tag{2.48}$$

Upon inversion of the above equation, a relation for the stress increment can be found in terms of the mechanical strain increment

$$\dot{\sigma}_{ij} = D^{ep}_{ijkl} \dot{\varepsilon}^{m}_{kl} \tag{2.49}$$

Where D^{ep}_{ijkl} is the elastoplastic constitutive tensor. More specifically for the isotropic, strain-hardening Von Mises material

$$D^{ep}_{ijkl} = 2\mu \, \delta_{ik} \, \delta_{jl} + \lambda \, \delta_{ij} \, \delta_{kl} - \frac{3\mu \, S_{ij} \, S_{kl}}{\sigma_o^2 \, (1+h/3\mu)} \tag{2.50}$$

2.5.2 Incremental Inelastic BEM Formulation

The governing differential equation of equilibrium is given in equation (2.11). Expressing it in incremental form:

$$(\lambda+\mu) \, \dot{u}_{j,ji} + \mu \, \dot{u}_{i,jj} + \dot{f}_i = \dot{\sigma}^{o}_{ij,j} \tag{2.51}$$

Boundary conditions, similar in form to equation (2.2), are imposed on an incremental scale and incremental body forces are applied in a manner analogous to section 2.4.

The initial stress rate $\dot{\sigma}^{o}_{ij}$ is defined for the general case of thermoplasticity as a summation of the thermal stress rate $\dot{\sigma}^{t}_{ij}$ and a plastic stress rate $\dot{\sigma}^{p}_{ij}$ resulting from the nonlinearities present in the plastic domain. For the purpose of the thermoplastic BEM algorithm these can be defined as:

$$\dot{\sigma}^{o}_{ij} = \dot{\sigma}^{t}_{ij} + \dot{\sigma}^{p}_{ij} \tag{2.52a}$$

$$\dot{\sigma}^{t}_{ij} = \delta_{ij} \, (3\lambda+2\mu) \, \alpha \dot{T} \tag{2.52b}$$

$$\dot{\sigma}^{p}_{ij} = D^{e}_{ijkl} \, \dot{\varepsilon}^{m}_{kl} - D^{ep}_{ijkl} \, \dot{\varepsilon}^{m}_{kl} \tag{2.52c}$$

$$\dot{\varepsilon}^{m}_{kl} = \dot{\varepsilon}_{kl} - \delta_{kl}\,\alpha\,\dot{T} \qquad (2.52d)$$

where D^{e}_{ijkl}, D^{ep}_{ijkl} are the elastic and elastoplastic constitutive tensors respectively, E is the modulus of elasticity, α is the coefficient of thermal expansion, $\dot{T}$ is the incremental temperature change, and $\dot{\varepsilon}^{m}_{kl}$ is the mechanical strain.

The axisymmetric, two-, and three-dimensional boundary integral formulation derived in section 2.2 and rewritten in incremental form are all applicable to inelastic BEM analysis. It is understood that the field variables are incremental quantities, and the nonlinearities are incorporated into the analysis through the initial stress rate $\dot{\sigma}^{o}_{ij}$ as defined in equation (2.52).

2.5.3 Iterative Solution Algorithm for Thermoplasticity

The algorithm described here provides the solution for an incremental, assembled system, analogous to the system defined by equation (2.27). The solution requires complete knowledge of the initial stress distribution $\dot{\sigma}^{o}$ within the yielded region that is induced by the imposition of the boundary loading, body forces, and thermal loads. Unfortunately the nonlinear part $\dot{\sigma}^{p}$ of the initial stress is not known a priori for a particular load increment and therefore an iterative process must be employed within each loading stage.

An important feature incorporated in the iterative algorithm of the present work is an iteration acceleration scheme (Raveendra, 1984) which utilizes plastic stresses generated by the past history. In this procedure, the path followed by the previous load increment is used to extrapolate the plastic stresses at the beginning of the

current increment before the iterative operations. This results in substantial reduction in computer time. This procedure is graphically illustrated in Figure 2.2 for a simple tension problem with a variable hardening parameter. The initial loading from point A generates plastic stresses which are distributed during the iterations to arrive at the solution at B . Upon loading from state B the extrapolated path BC is followed. At C the resulting corrective stresses are distributed to reach state D .

The incremental algorithm is described below. Note, this algorithm requires that a stress equation be written at each cell node.

(a) Obtain the elastic solution for an arbitrary increment of boundary loading $\dot{\mathbf{y}}$ (and thermal loading $\dot{\mathbf{T}}$) from

$$\dot{\mathbf{x}} = [\mathbf{A}^b]^{-1}[\mathbf{B}^b\dot{\mathbf{y}} + \mathbf{C}^b\dot{\sigma}^t]$$

and (2.53)

$$\dot{\sigma} = \mathbf{A}^\sigma\dot{\mathbf{x}} + \mathbf{B}^\sigma\dot{\mathbf{y}} + \mathbf{C}^\sigma\dot{\sigma}^t$$

(b) Scale the elastic solution such that the highly stressed node is at yield. In the case of nonproportional loading this onset of yielding cannot be reached by scaling. Instead, incremental loads must be applied until yielding is reached.

(c) Impose a small load increment $\dot{\mathbf{y}}$ (and $\dot{\mathbf{T}}$), (usually less than five percent of the yield load) plus the estimated value of the plastic stress rates accumulated from the previous load step and evaluate

$$\dot{x} = [A^b]^{-1}[B^b\dot{y} + C^b\dot{\sigma}^o]$$

and (2.54)

$$\dot{\sigma} = A^\sigma\dot{x} + B^\sigma\dot{y} + C^\sigma\dot{\sigma}^o$$

where $\dot{\sigma}^o$ is a combination of the estimated plastic stress rates and the incremental thermal stress rates. If no prior plastic history exists, the value of the estimated plastic stress rates are zero.

(d) Accumulate all incremental quantities of stress, traction and displacement rates and use equation (2.52d) to calculate the mechanical strain of this increment.

(e) Evaluate the current constitutive matrix using the new stress history and calculate the current plastic stress rates via

$$\dot{\sigma}^p_{ij} = (D^e_{ijkl} - D^{ep}_{ijkl})\ \dot{\varepsilon}^m_{kl} \qquad (2.55)$$

Accumulate the plastic stress history of this load increment to be used as the estimated rate for the next load increment in step (c).

(f) If the current increment of plastic stress rates, computed in equation (2.55), is greater than a prescribed tolerance (normally 0.005 times the yield stress) at any node, then calculate the incremental quantities due to these rates using

$$\dot{x} = [A^b]^{-1}[C^b\dot{\sigma}^p] \quad \text{and} \quad \dot{\sigma} = A^\sigma\dot{x} + C^\sigma\dot{\sigma}^p \qquad (2.56)$$

and return to step (d) for the next iteration. If the value is less than the prescribed tolerance go to step (g). Note the boundary and thermal loading is zero for this calculation and the mechanical strain rate will therefore be equal to the total strain rate. If the number of iterations is greater than a specified limit (usually 50) the system is assumed to have reached the state of failure.

(g) Return to step (c) and apply the next load increment and the accumulated plastic stress rates from this load step. (If the size of the load increment changes the estimated plastic stress rates should be scaled proportionally.)

Any residual plastic stress at the end of the iteration is carried forward and applied to the system with the next load increment.

2.5.4 Variable Stiffness Plasticity Approach

The above nonlinear formulations include initial stress rates in the governing equations which are not known a priori and therefore are solved by using iterative procedures. A non-iterative, direct solution procedure is made feasible by reducing the number of unknowns in the governing equations by utilizing certain features of the incremental theory of plasticity expressed by equations (2.32), (2.36) and (2.39). This non-iterative or variable stiffness approach was introduced by Raveendra (1984) in a single-region, two-dimensional context. For the first time, this method is implemented in an axisymmetric, two- and three-dimensional, multiregion computer program.

The initial stress rates $\overset{o}{\sigma}_{ij}$ appearing in the incremental form of integral equations (2.20) to (2.22) can be expressed in the context of an elastoplastic deformation as:

$$\dot{\overset{o}{\sigma}}_{ij} = K_{ij}\dot{\lambda} \tag{2.57}$$

where $K_{ij} = D^{e}_{ijkl}\dfrac{\partial F}{\partial \sigma_{kl}}$

Substituting equations (2.36) and (2.57) in equation (2.20) and (2.22) we obtain (in the absence of body forces):

$$c_{ij}\dot{u}_i(\xi) = \int_S [G_{ij}(x,\xi)\dot{t}_i(x) - F_{ij}(x,\xi)\dot{u}_i(x)]dS(x)$$

$$+ \int_V B_{ipj}(x,\xi)K_{ip}(x)\dot{\lambda}(x)dV(x) \tag{2.58}$$

and

$$\dot{\lambda}(\xi) = L^{\sigma}_{jk}(\xi)\int_S [G^{\sigma}_{ijk}(x,\xi)\dot{t}_i(x) - F^{\sigma}_{ijk}(x,\xi)\dot{u}_i(x)]dS(x)$$

$$+ L^{\sigma}_{jk}(\xi)\int_V B^{\sigma}_{ipjk}(x,\xi)K_{ip}(x)\dot{\lambda}(x)dV(x) \tag{2.59}$$

Equations (2.58) and (2.59) can be solved simultaneously to evaluate the unknown values of displacements, traction rates and the scalar variable $\dot{\lambda}$.

Although equation (2.59) can be applied to any elastoplastic strain hardening problem, L^{σ}_{ij} becomes indeterminate for the case of ideal plasticity (zero strain hardening), therefore, it cannot be used for ideal plasticity. However, this minor problem can be circumvented either by specifying a small amount of strain hardening or more

appropriately replacing equation (2.59) by the strain rate equations (2.39) and (2.21). Thus using equations (2.39) and (2.57) in (2.21) we obtain

$$\dot{\lambda}(\xi) = L^{\varepsilon}_{jk}(\xi) \int_S [G^{\varepsilon}_{ijk}(x,\xi)\dot{t}_i(x) - F^{\varepsilon}_{ijk}(x,d)\dot{u}_i(x)]dS(x)$$

$$+ L^{\varepsilon}_{jk}(\xi) \int_V B^{\varepsilon}_{ipjk}(x,\xi)K_{ip}(x)\dot{\lambda}(x)dV(x) \qquad (2.60)$$

Equation (2.60) can now be applied to any problems of elastoplasticity (both strain hardening and ideal plasticity).

Assembly of System Equations for the Variable Stiffness Method - Although equations (2.36), (2.39) and (2.57) were substituted into the analytic form of the integral equations for the presentation, during actual implementation, these equations are substituted, on a nodal basis, into the incremental form of the assembled equation system (2.27). Therefore, using the incremental form of equation (2.27) as a starting point, equations (2.36) and (2.57) are employed to arrive at the following system:

$$\mathbf{A}^{b}\dot{\mathbf{x}} = \mathbf{B}^{b}\dot{\mathbf{y}} + \mathbf{C}^{b}\mathbf{K}\dot{\boldsymbol{\lambda}}$$

and (2.61)

$$\dot{\boldsymbol{\lambda}} = \mathbf{L}\mathbf{A}^{\sigma}\dot{\mathbf{x}} + \mathbf{L}\mathbf{B}^{\sigma}\dot{\mathbf{y}} + \mathbf{L}\mathbf{C}^{\sigma}\mathbf{K}\dot{\boldsymbol{\lambda}}$$

where $\dot{\mathbf{y}}$ are the known incremental boundary conditions and $\dot{\mathbf{x}}$ are the unknown. Matrices $\mathbf{A}, \mathbf{B}, \mathbf{C}$ and $\mathbf{A}^{\sigma}, \mathbf{B}^{\sigma}, \mathbf{C}^{\sigma}$ are constant for a given problem and matrices $\mathbf{K}, \mathbf{L}$ are dependent upon state variables, and are assumed to be constant during each small load step.

It should be noted that the second equation is written only for the cell nodes that are expected to yield during the current load step.

The above equations can be rewritten as:

$$A^{b}\dot{x} = \dot{b}^{b} + C^{\lambda b}\dot{\lambda} \tag{2.62a}$$

and

$$\dot{\lambda} = A^{\lambda}\dot{x} + \dot{b}^{\lambda} + C^{\lambda}\dot{\lambda} \tag{2.62b}$$

or upon rearranging the equation (2.62b) we have

$$H\dot{\lambda} = A^{\lambda}\dot{x} + \dot{b}^{\lambda} \tag{2.63}$$

where $\dot{b}^{b} = B^{b}\dot{y}$, $C^{\lambda b} = C^{b}K$, $A^{\lambda} = LA^{\sigma}$,

$\dot{b}^{\lambda} = LB^{\sigma}\dot{y}$, $C^{\lambda} = LC^{\sigma}K$, $H = I - C^{\lambda}$, and

I is the identity matrix.

Equation (2.63) can then be recast as

$$\dot{\lambda} = A^{o}\dot{x} + \dot{b}^{o} \tag{2.64}$$

where

$$A^{o} = H^{-1}A^{\lambda}$$

$$\dot{b}^{o} = H^{-1}\dot{b}^{\lambda}$$

Substituting the above equation into equation (2.62a) results in the final system equations:

$$A^{r}\dot{x} = \dot{b}^{r} \tag{2.65}$$

where

$$A^r = A^b - C^{\lambda b} A^o$$

$$\dot{b}^r = \dot{b}^b + C^{\lambda b} \dot{b}^o$$

The above equation can be solved to evaluate the unknown vector $\dot{x}$ at boundary nodes for every increment of loading. The present formulation is similar to the variable stiffness approach used in the finite element method since the system matrix on the boundary as well as the right hand side vector are modified for each increment of loading. For a multi-region system the inversion of H can be carried out for each region separately.

Solution Process for Variable Stiffness Approach - As previously mentioned, the solution process does not involve any iterative procedure, instead the substantial part of the solution effort is spent on assembly of the system equations for each load step. These operations can be described as follows:

(a) Impose an arbitrary boundary loading and solve the elastic problem in the usual manner.

(b) Scale the elastic solution such that the highest stressed node is at yield.

(c) Apply a small load increment (usually < five percent of the yield load) and compute K and L matrices using the past stress history.

(d) Form the system equation (2.65) and solve for $\dot{x}$.

(e) Evaluate the initial stress rates $\dot{\sigma}^o$ using equations (2.57) and

(2.64):

$$\dot{\sigma}^{o} = K\,\dot{\lambda} = K[A^{o}\dot{x} + \dot{b}^{o}]$$

(f) Evaluate interior quantities displacement and stress rates using the incremental form of equations (2.24) and (2.25).

(g) Return to step (c) if the strains are less than a specified norm. Otherwise, failure is assumed to have occurred.

It is of importance to note that the matrices **K, L** do not exist in the elastic region, therefore, the corresponding equations involving these matrices are formed and $\dot{\sigma}^{o}$ is determined, only for the nodes that are at yield. Any small deviation from the yield surface can be corrected by applying the stress rate difference (i.e. the initial stress rate) during the next load step.

2.6 ACCURACY AND CONVERGENCE

In order to test the accuracy and convergence of the elastoplastic formulations, simple problems with known solutions, such as cubes, spheres, and cylinders, were analyzed. Axisymmetric, two- and three-dimensional inelastic formulations were coupled with both the iterative and variable stiffness solution algorithms. All possible combinations were tested and in all cases excellent agreement with the analytical solutions was obtained. A few of these examples are presented here.

2.6.1 Two-dimensional Analysis of a Thick Cylinder

In order to verify convergence and accuracy of the two-dimensional, iterative plasticity algorithm, an analysis of a thick

cylinder subjected to increasing internal pressure is carried out under the plane stress condition. The discretization of the cylinder (1:2 ratio), shown in figure 2.3, has ten elements and four volume cells. In figure 2.4, the hoop strain vs. pressure for the inner and outer surfaces are compared to the analytic solution (Hill, 1950). Excellent agreement is obtained. Other numerical results, to within 1% error of the analytical solutions were obtained for the radial and hoop stress through the cylinder at different load pressures, and the displacement versus internal pressure response. In figure 2.5, the axial strain vs. pressure is compared with the theoretical solution, and slight deviation is observed. A possible explanation for this error is that the theoretical solution assumes the Tresca yield criterion, where the present analysis is based on the Von Mises criterion. The computational time using the two-dimensional analysis was found to be approximately 5% of the time required for the three-dimensional BEM analysis.

2.6.2 Three-dimensional Analysis of a Thick Cylinder

A three-dimensional elastoplastic analysis of a thick cylinder (in plane strain) is carried out using the variable stiffness algorithm. The discretization of the cylinder (1:2 ratio), shown in figure 2.6, has eighteen boundary elements and four (twenty-noded) isoparametric cells. The material properties are (given in consistent units):

$E = 2600$

$\nu = 0.3$

$\sigma_o = 600$ (Von Mises yield criterion assumed)

In figure 2.7, the load-displacement response (assuming ideal plasticity) is compared to the theoretical result (Hill, 1950). In figure 2.8, the circumferential stress distribution through the thick cylinder is presented for two different load levels. Good agreement with the analytical solution is observed in both figures.

In a second analysis, the material is assumed to exhibit variable plastic strain hardening according to:

Stress	vs.	Plastic Strain
600		0.0
640		0.1
660		0.2
660		10.0

In figure 2.9, the load-displacement response at the inner and outer surface is presented. Results obtained from the iterative procedure (with 5% load increments) are compared with two sets of results from the variable stiffness method. One set is obtained using 2% load increments, and the other 5% increments. Results are generally within 1% of one another.

2.6.3 Axisymmetric Analysis of a Hollow Sphere

A hollow sphere (1:2 ratio) subjected to internal pressure is used to demonstrate the axisymmetric elastoplastic formulation. Nine boundary elements and ten (eight noded) cells are used in the discretization of the sphere as shown in figure 2.10. The mesh utilizes spherical symmetry and contains points on the origin. The incline face is subjected to a roller boundary condition. The load-displacement response is shown in figure 2.11 and the hoop stress through the sphere at different load levels is given in figure 2.12.

The BEM solution obtained using the iterative method is in good agreement with the analytical result (Hill, 1950).

2.7 CONCLUDING REMARKS

The conventional boundary element formulations for elastic and inelastic thermal stress analysis were presented. The inelastic axisymmetric implementation presented in this chapter, with its use of quadratic elements and multi-region facility, is the most advanced implementation of its kind. Two inelastic algorithms, an iterative and a variable stiffness type approach were employed, the latter for the first time in axisymmetric and three-dimensional analysis. By comparing results of test problems to their analytical solutions, the accuracy of both methods was demonstrated. In Chapter 6, the methods will be used to analyze larger problems of practical interest.

The body force and nonlinear effects in the present formulation were incorporated in the system through volume integrals or extra surface integrals. In the next two chapters, new approaches for the treatment of these effects will be presented.

TABLE 1

STRESS STATES FOR INITIAL STRESS EXPANSION TECHNQIUE
IN TWO-DIMENSIONAL PLANE STRAIN
(PLAIN STRESS) ANALYSIS

Stress State	Coefficient to be determined corresponds to	Nodal Values of Assumed Stress State				
		σ^o_{xx}	σ^o_{yy}	σ^o_{xy}	u_x	u_y
1	σ^o_{xx}	E	0	0	$(1-\nu^2)x$	$-\nu(1+\nu)y$
2	σ^o_{yy}	0	E	0	$-\nu(1+\nu)x$	$(1-\nu^2)y$
3	σ^o_{xy}	0	0	E	$(1+\nu)y$	$(1+\nu)x$

where

E is the modulus of elasticity,

ν is the Poisson's ratio, and

x and y are the nodal coordinates.

All stresses and tractions are zero for all stress states.

The stress states for two-dimensional plane strain analysis, given in the table above, can be applied to the plane stress case, if the modified material parameters, defined below, are used.

$$\bar{E} = \frac{E(1+2\nu)}{(1+\nu)^2} \qquad \bar{\nu} = \frac{\nu}{1+\nu}$$

TABLE 2

STRESS STATES FOR INITIAL STRESS EXPANSION TECHNIQUE
IN THREE-DIMENSIONAL ANALYSIS

Stress State	Coefficient to be determined corresponds to	Nodal Values of Assumed Stress State								
		σ^o_{xx}	σ^o_{yy}	σ^o_{zz}	σ^o_{xy}	σ^o_{xz}	σ^o_{yz}	u_x	u_y	u_z
1	σ^o_{xx}	E	0	0	0	0	0	x	$-\nu y$	$-\nu z$
2	σ^o_{yy}	0	E	0	0	0	0	$-\nu x$	y	$-\nu z$
3	σ^o_{zz}	0	0	E	0	0	0	$-\nu x$	$-\nu y$	z
4	σ^o_{xy}	0	0	0	E	0	0	$(1+\nu)y$	$(1+\nu)x$	0
5	σ^o_{xz}	0	0	0	0	E	0	$(1+\nu)z$	0	$(1+\nu)x$
6	σ^o_{yz}	0	0	0	0	0	E	0	$(1+\nu)z$	$(1+\nu)y$

where

E is the modulus of elasticity,

ν is the Poisson's ratio, and

x,y, and z are nodal coordinates.

All stresses and tractions are zero for all stress states.

TABLE 3

STRESS STATES FOR INITIAL STRESS EXPANSION TECHNIQUE IN AXISYMMETRIC ANALYSIS

Stress State number	Coefficient to be determined corresponds to	Nodal values of assumed stress states											
		σ_{rr}	σ_{zz}	$\sigma_{\theta\theta}$	σ_{rz}	σ^o_{rr}	σ^o_{zz}	$\sigma^o_{\theta\theta}$	σ^o_{rz}	u_r	u_z	t_r	t_z
1	$\sigma^o_{\theta\theta}$	$\frac{(2-\nu)E}{3(1-\nu)C}r$	$\frac{\nu E}{(1-\nu)C}r$	$2\sigma_{rr}$	0	0	0	$\frac{-E}{C}r$	0	$\frac{(1+\nu)(1-2\nu)}{3(1-\nu)C}r^2$	0	$\sigma_{rr}n_r$	$\sigma_{zz}n_z$
2	σ^o_{rr}	0	0	0	0	E	0	E	0	$(1-\nu)r$	$-2\nu z$	0	0
3	σ^o_{zz}	0	0	0	0	0	E	0	0	$-\nu r$	z	0	0
4	σ^o_{rz}	0	0	0	0	0	0	0	μ	0	r	0	0

where E modulus of elasticity

μ shear modulus

ν Poisson's ratio

r and z are nodal coordinates

n_r and n_z are normals of the boundary

C arbitrary parameter with dimensions of length, added to insure dimensional homogeneity. The value can be equated to one for simplicity.

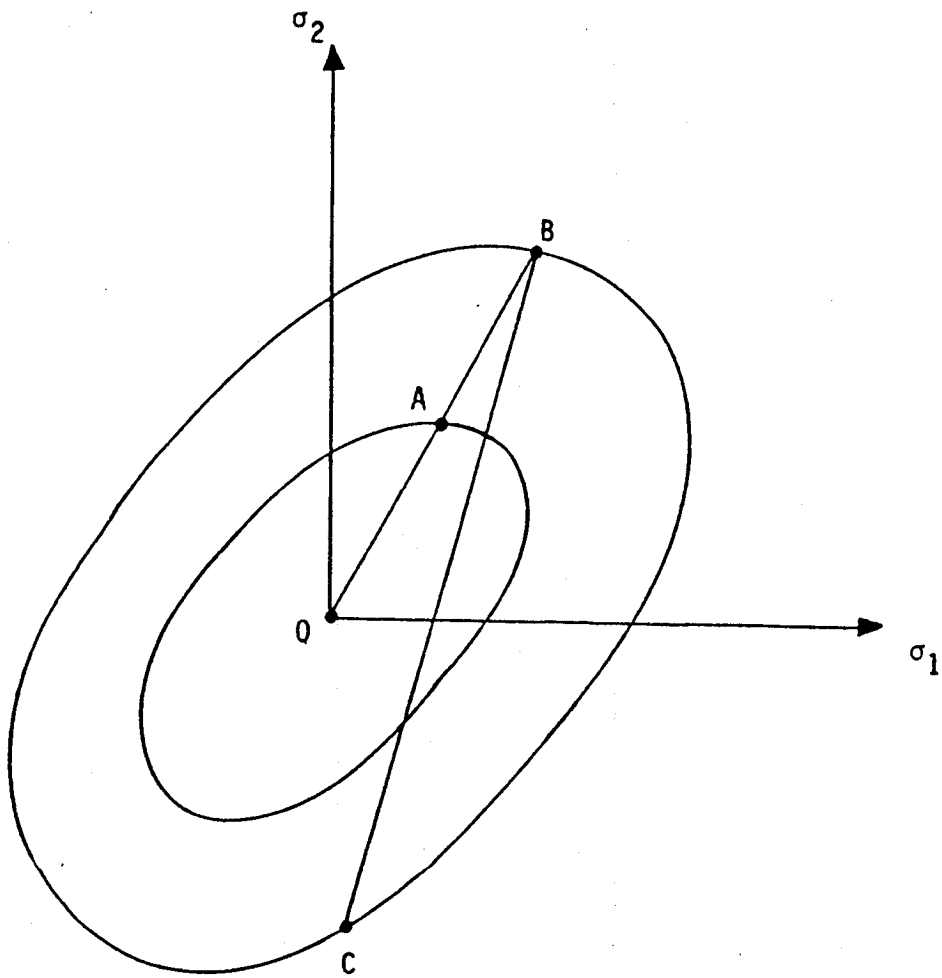

Figure 2.1
Isotropic Hardening Behavior

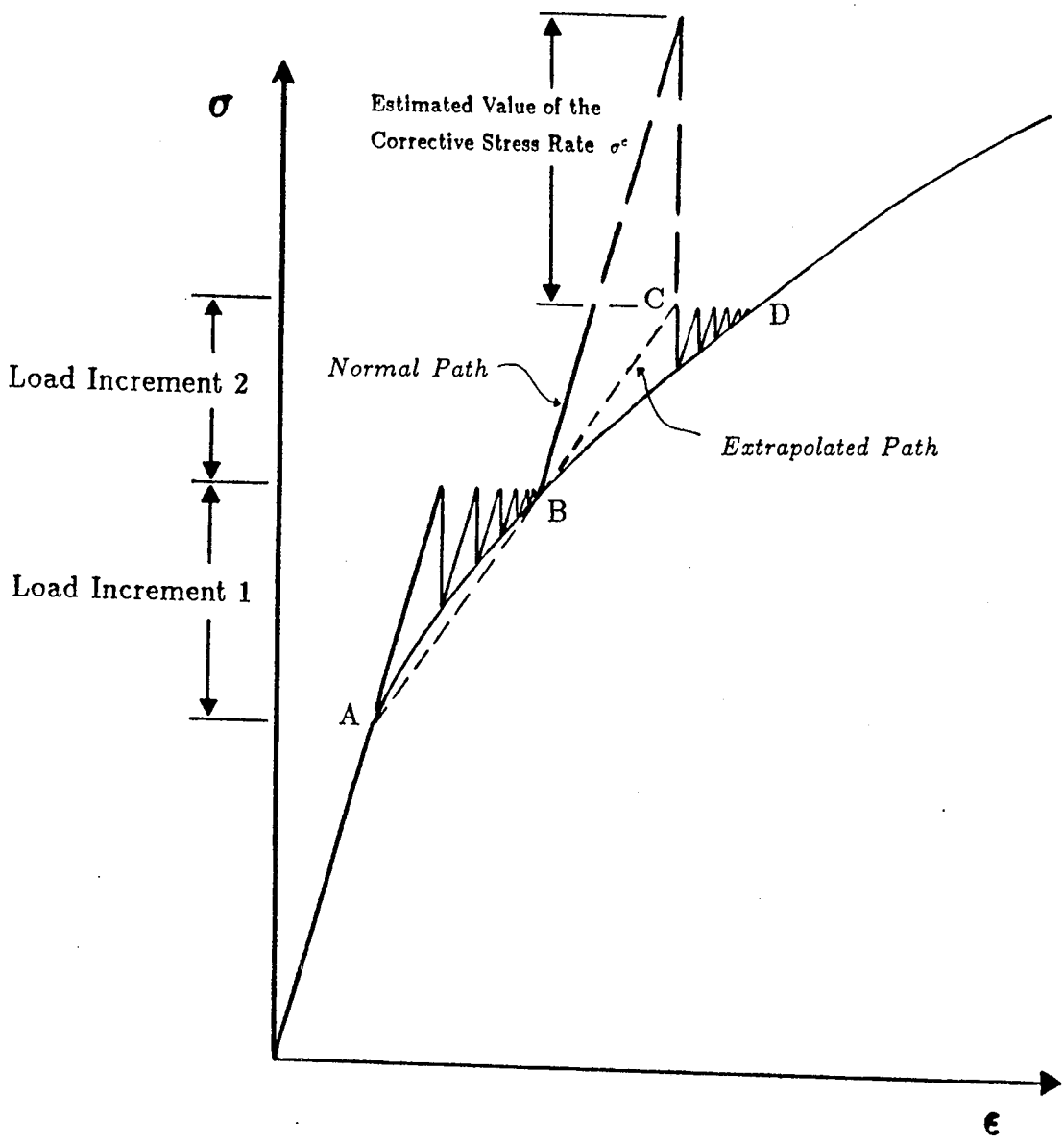

Figure 2.2
Accelerated Iterative Scheme

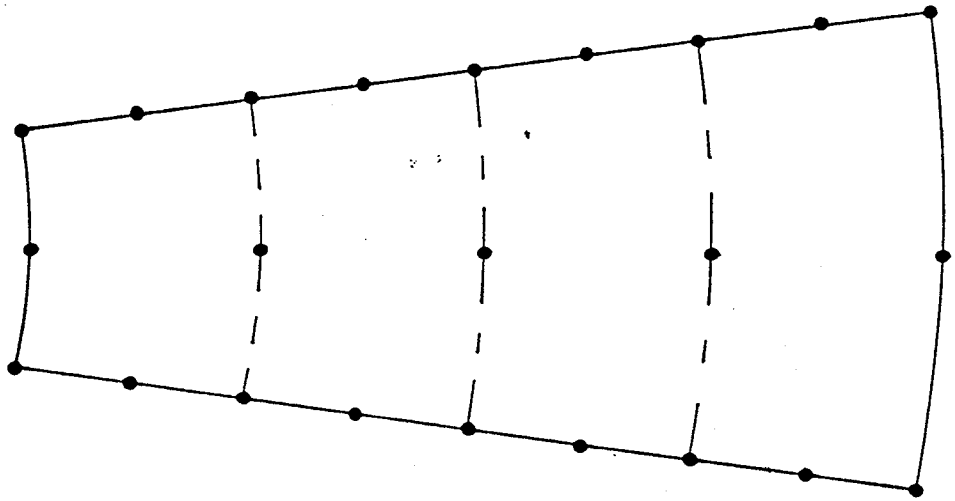

Figure 2.3
Two-dimensional Discretization of a Thick Cylinder (Diameter Ratio 1:2)

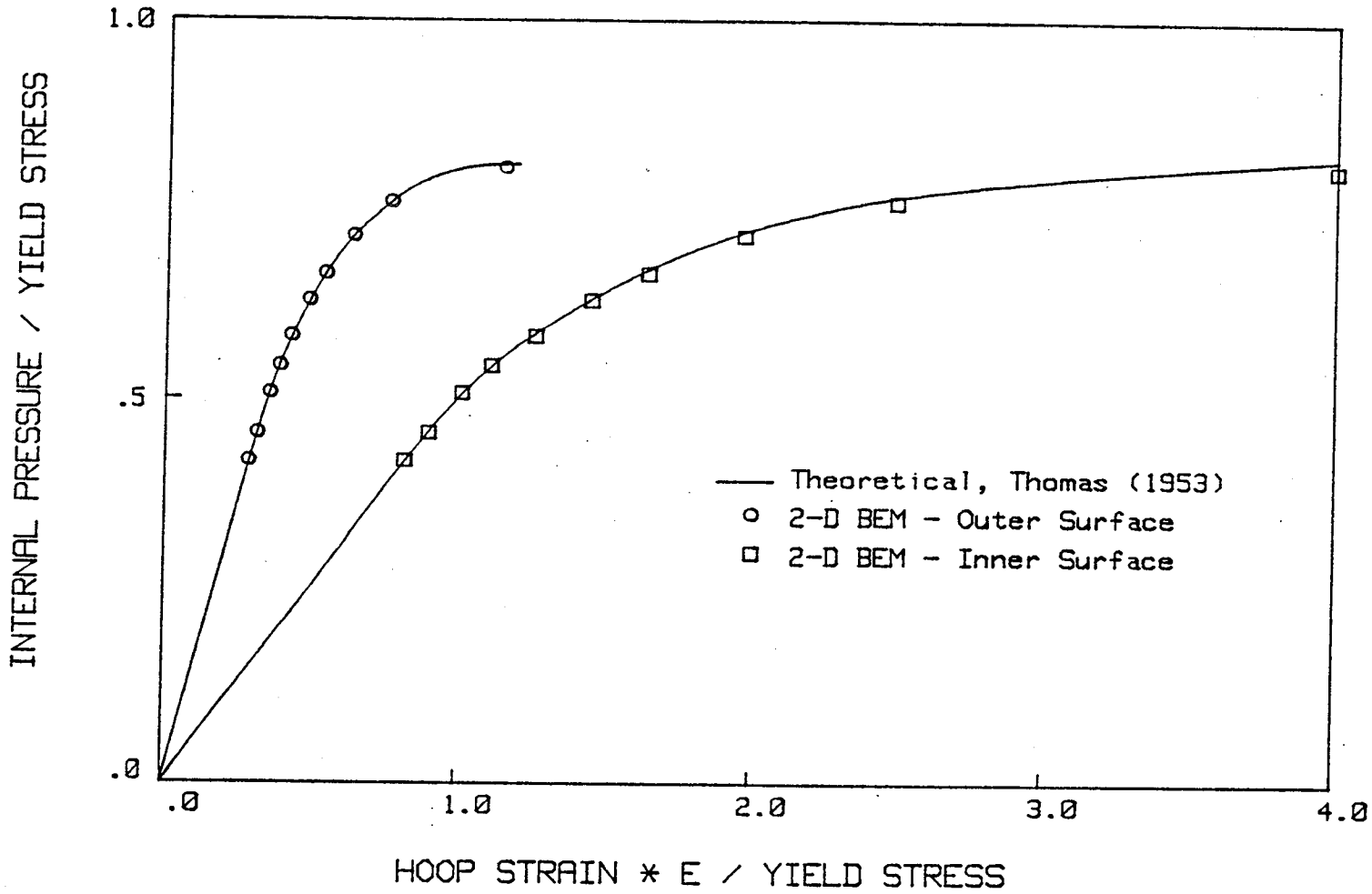

Figure 2.4
Hoop Strain in a Thick Cylinder under Internal Pressure (Plane Stress)

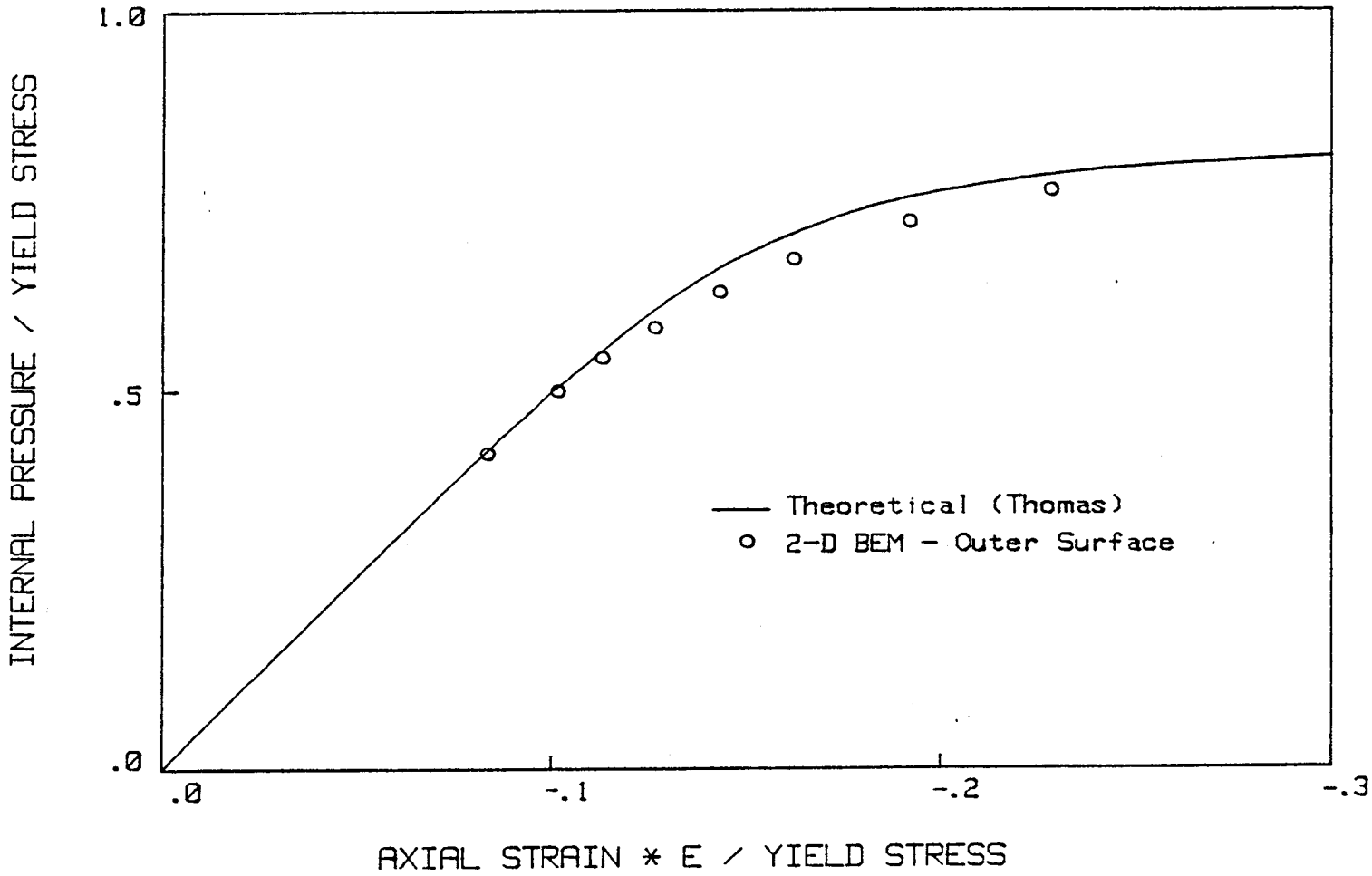

Figure 2.5
Axial Strain at the Outer Surface of Thick Cylinder under Internal Pressure (Plane Stress)

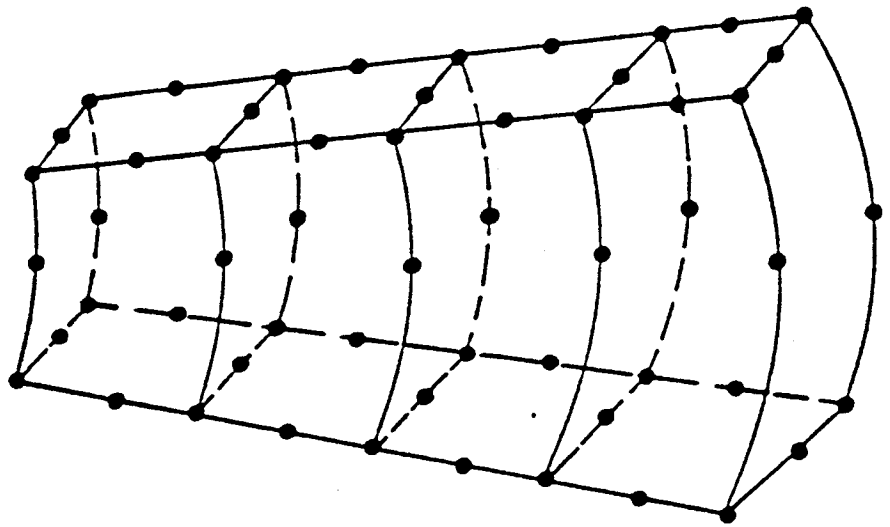

Figure 2.6
Three-dimensional Discretization of a Thick Cylinder (Diameter Ratio 1:2)

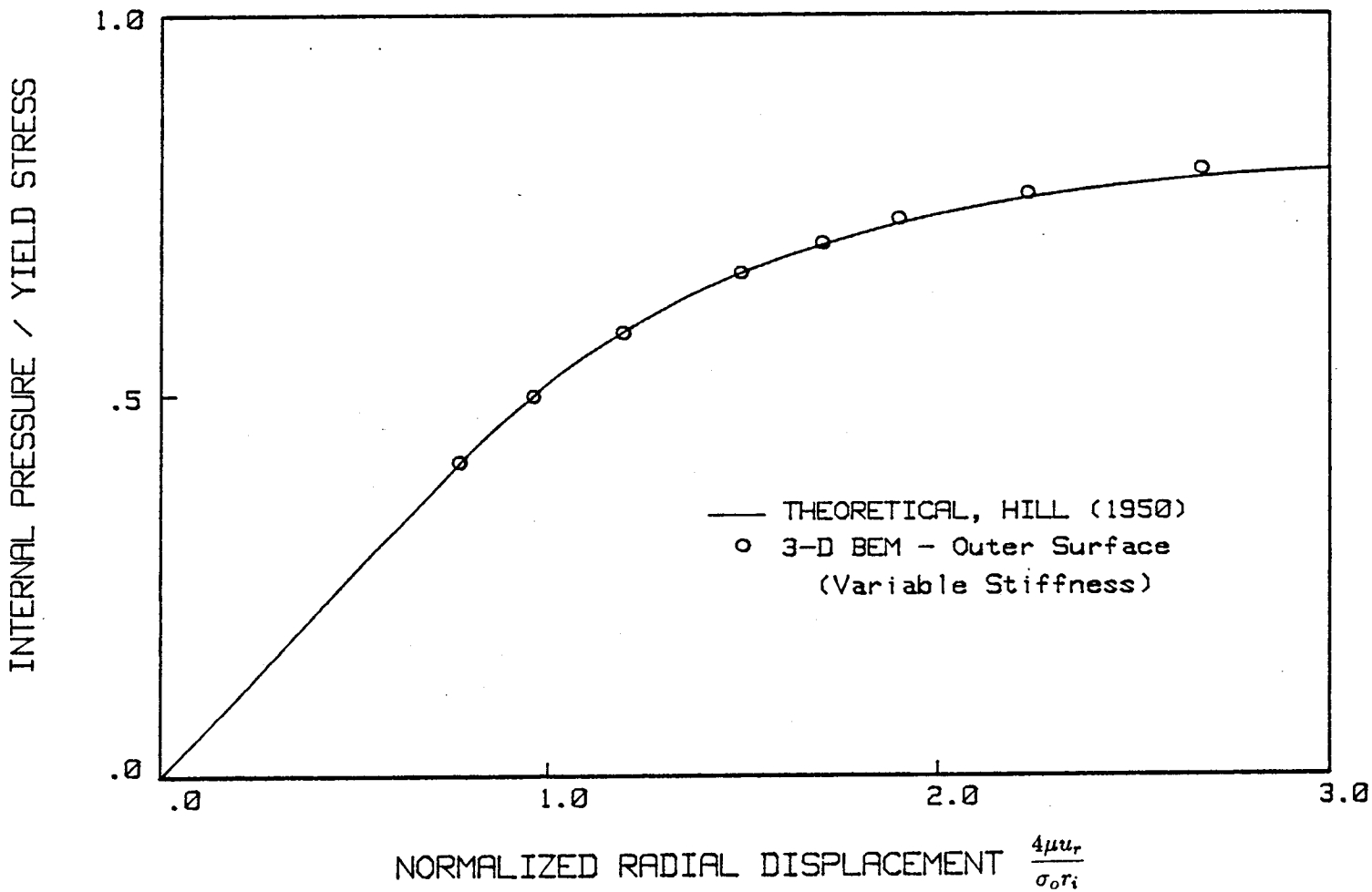

Figure 2.7
Radial Displacement of the Outer Surface of a Thick Cylinder under Internal Pressure (Plane Strain)

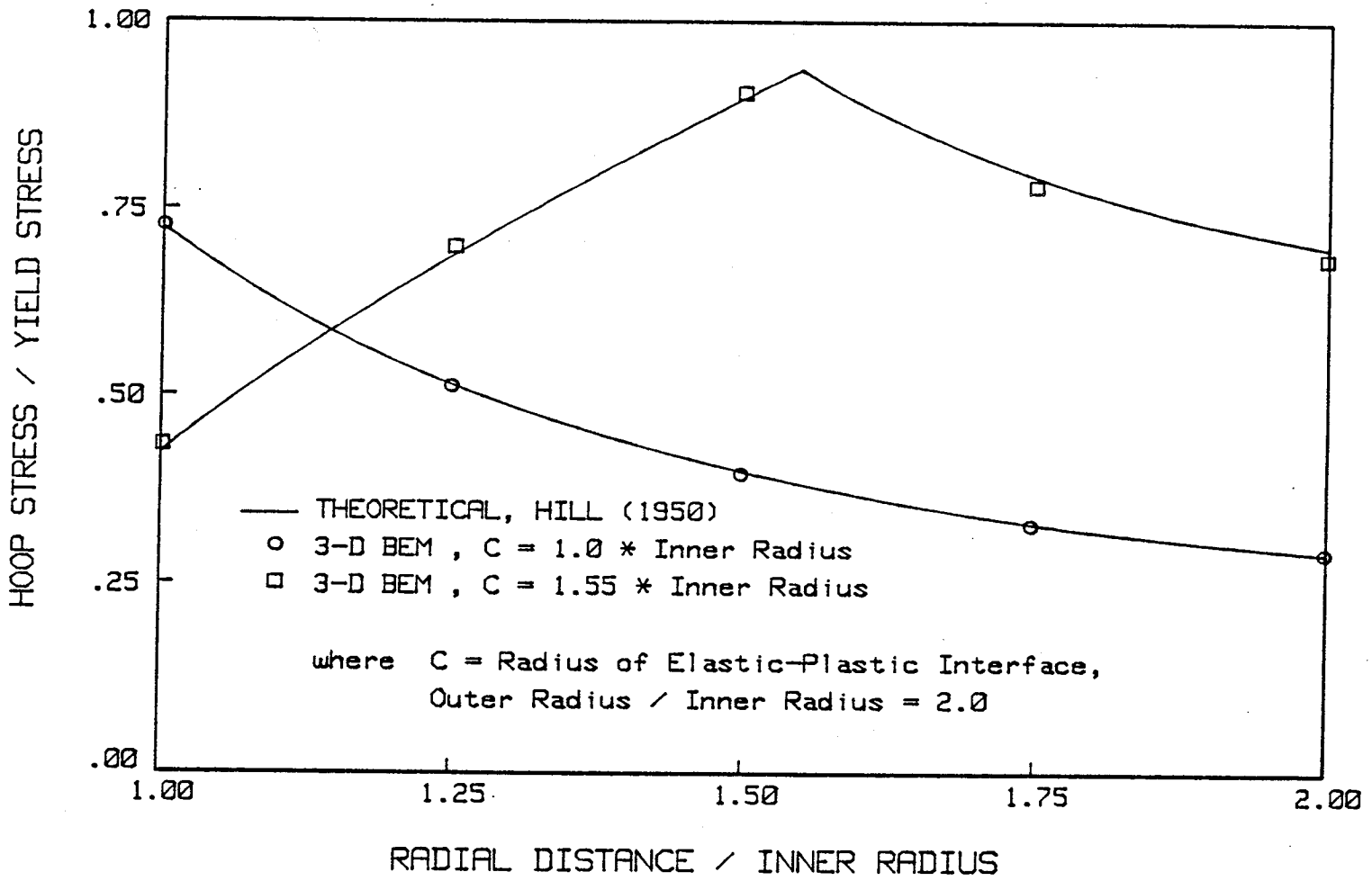

Figure 2.8
Circumferential Stress Distribution through a Thick Cylinder under Internal Pressure (Plane Strain)

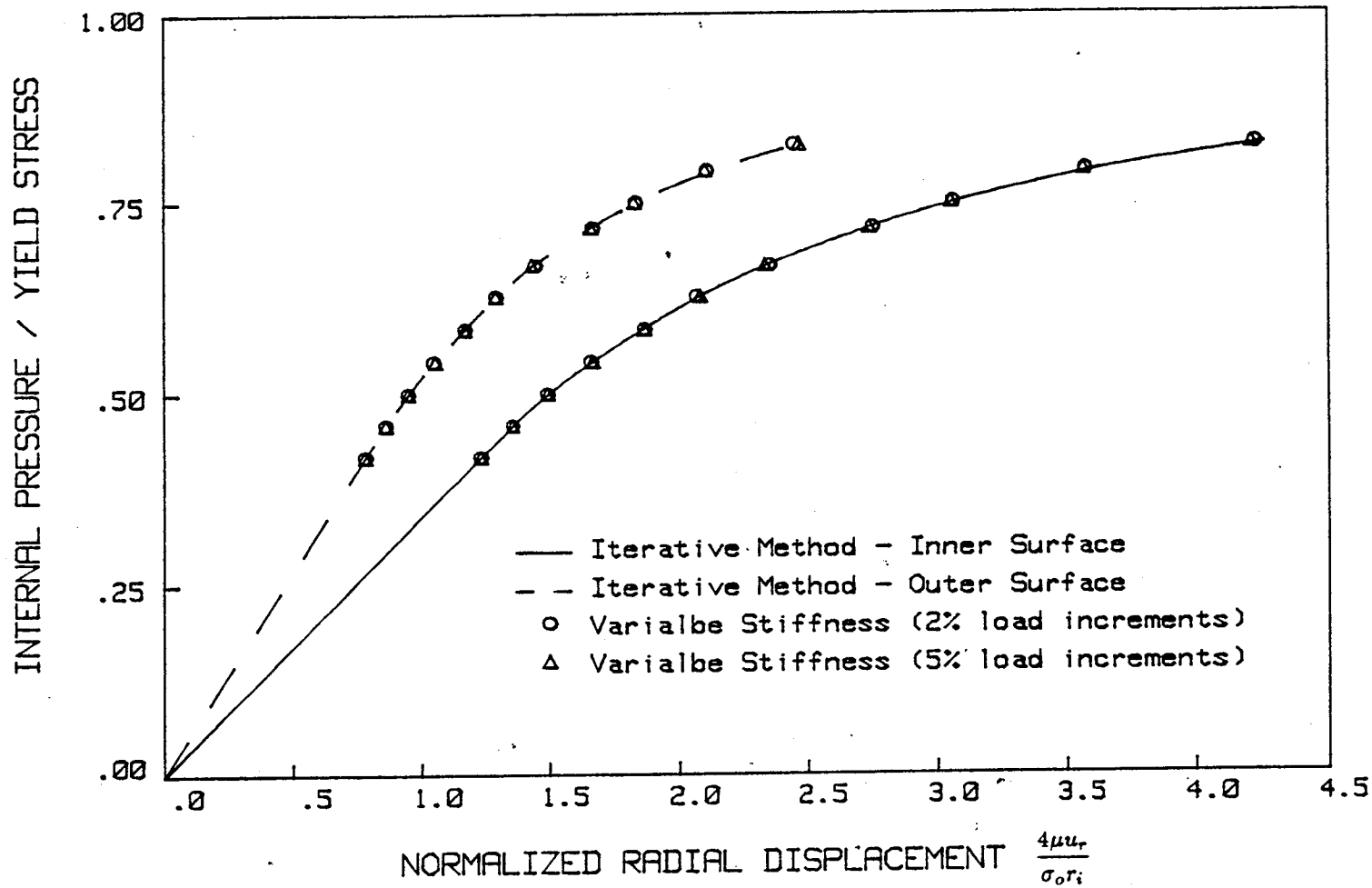

Figure 2.9

Load versus Radial Displacement of the Inner and Outer Surfaces of a 3-D Thick Cylinder with Hardening (Plane Strain)

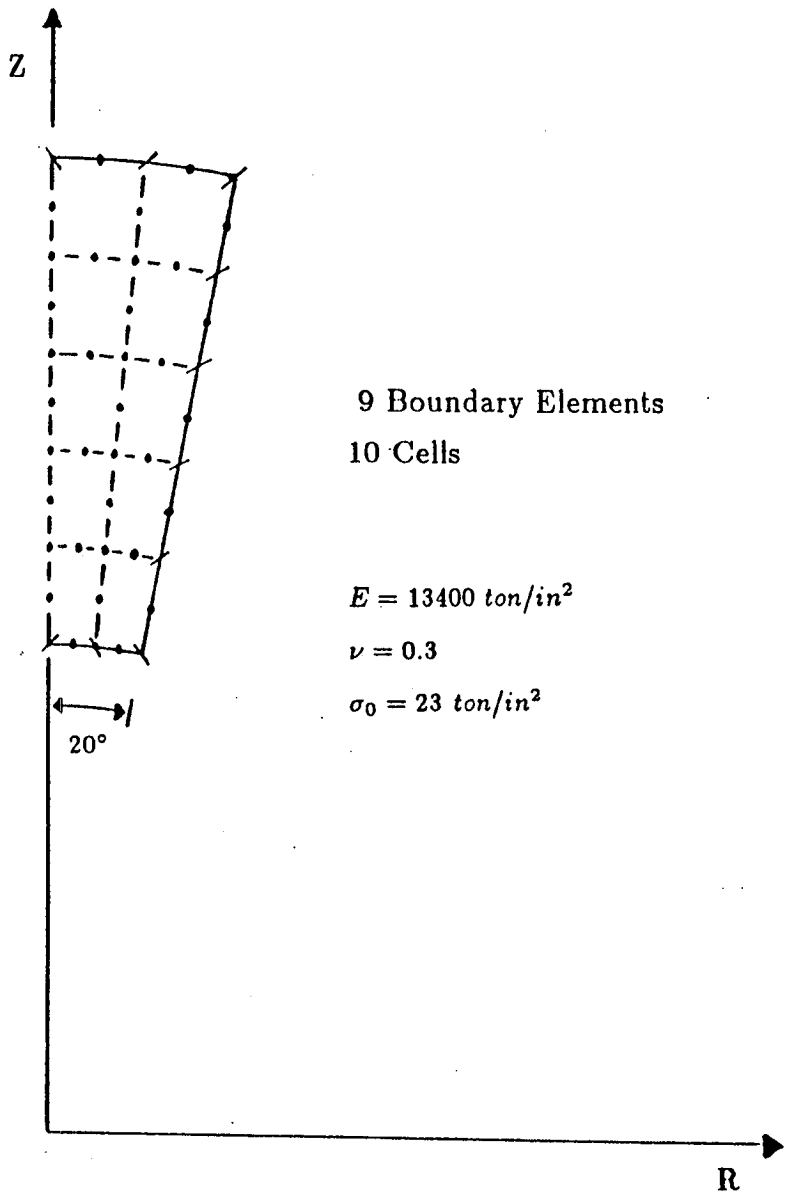

Figure 2.10
Hollow Sphere (1:2 Ratio)

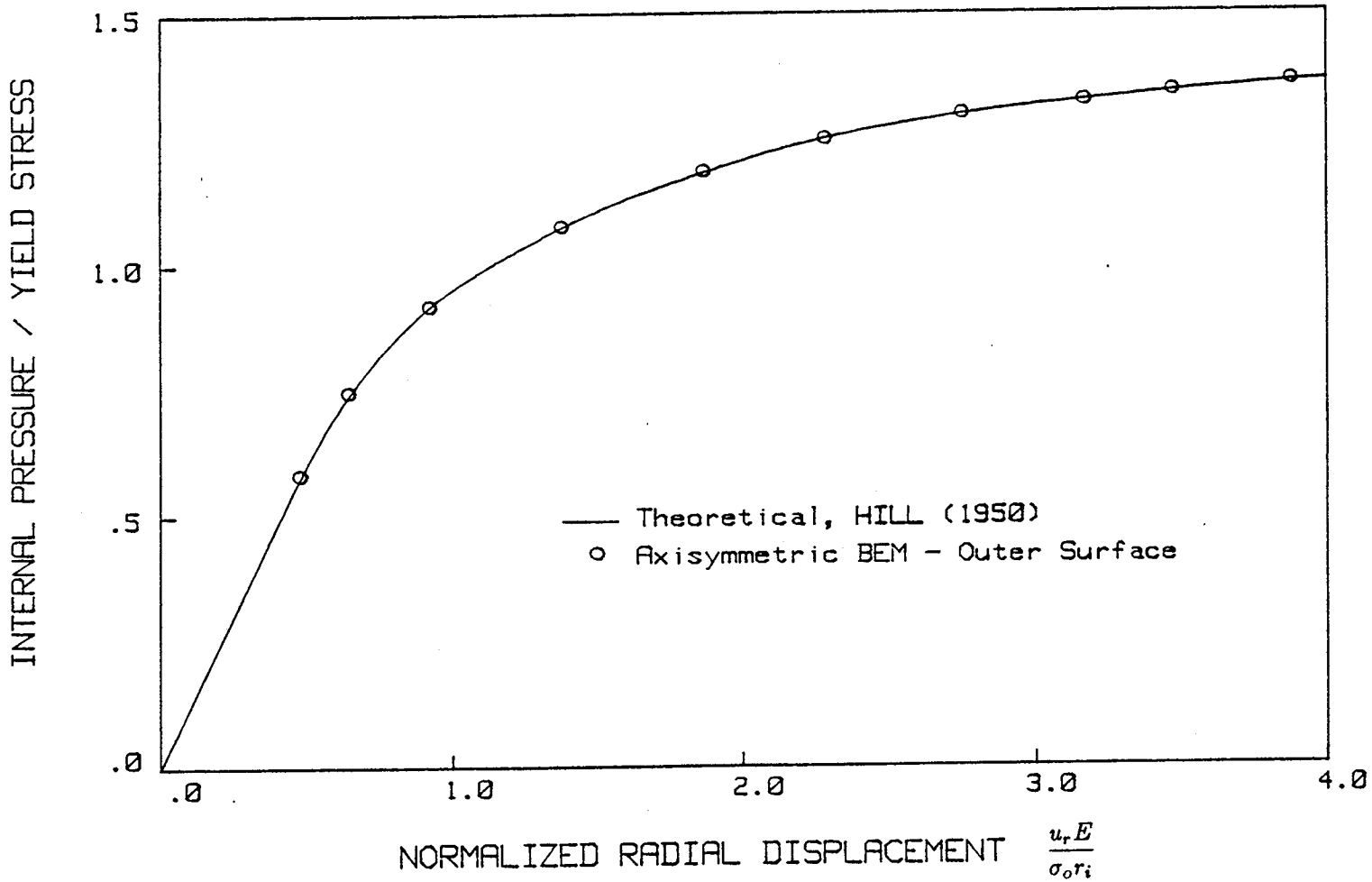

Figure 2.11
Radial Displacement in a Hollow Sphere subjected to Internal Pressure

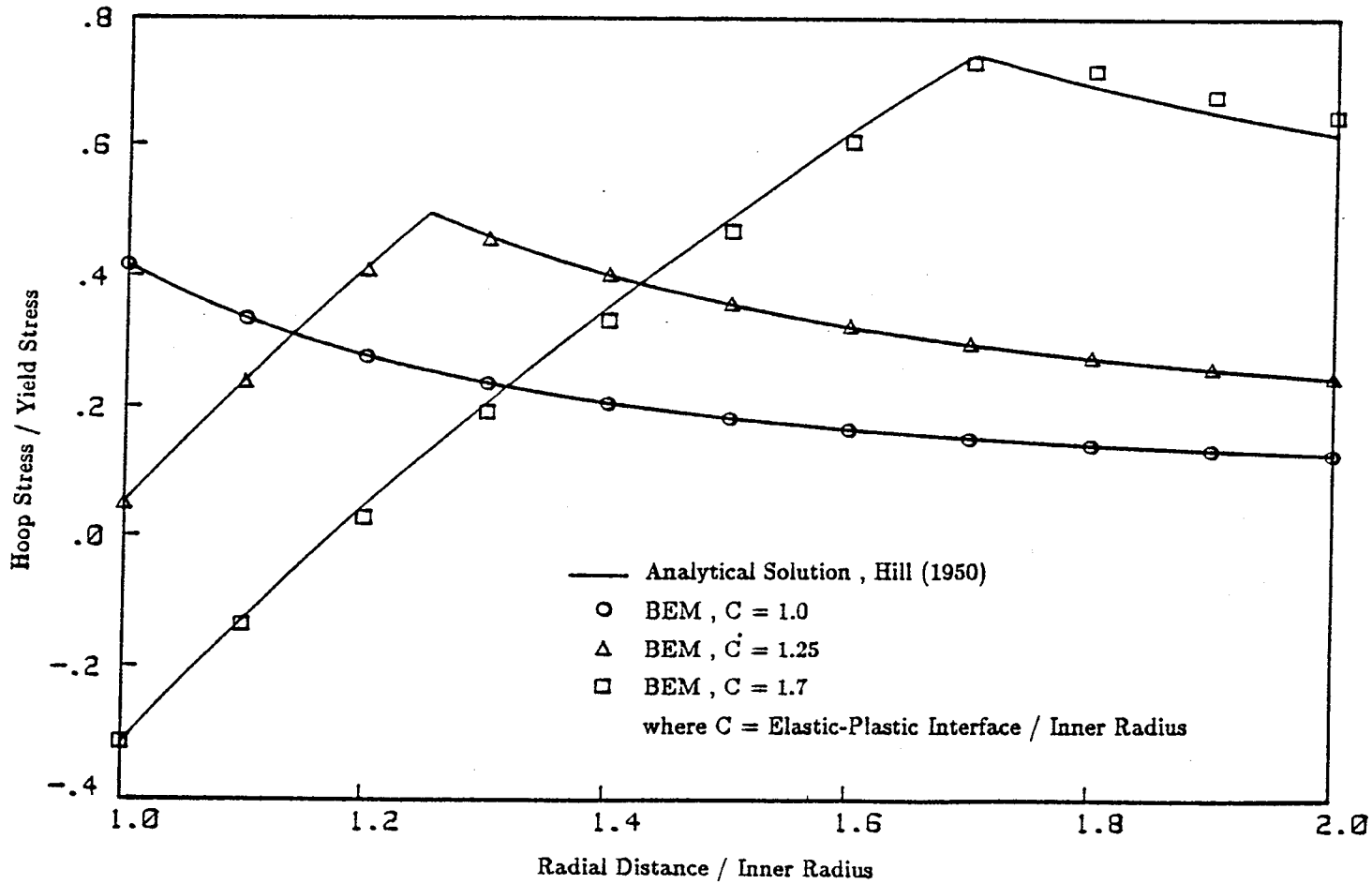

Figure 2.12
Hoop Stress in a Hollow Sphere subjected to Internal Pressure

CHAPTER 3

ELASTIC BOUNDARY ELEMENT FORMULATIONS BASED ON PARTICULAR INTEGRALS

CHAPTER THREE

ELASTIC BOUNDARY ELEMENT FORMULATIONS BASED ON PARTICULAR INTEGRALS

3.1 INTRODUCTION

In this chapter, a novel boundary element approach for the treatment of body forces is presented. The method is unique since no volume integration or additional surface integration is required as in earlier formulations. The method is based on the well known concept of developing the solution of an inhomogeneous differential equation by means of a complementary function and particular integral.

In the first section, the particular integral formulation for a general inhomogeneous differential equation is developed and the boundary element solution procedure is presented. The method is then applied to gravitational and centrifugal body force analyses. Finally, particular integrals are developed for thermal body forces according to the uncoupled theory of thermoelasticity. In this theory the heat conduction problem is independent of stress, and therefore, will not be considered here. Instead, the temperature distribution is assumed to be a known (or previously solved) function.

The axisymmetric, two-, and three-dimensional formulations are implemented in a general purpose, multi-region system, and examples are presented to demonstrate the accuracy of the method.

3.2 BOUNDARY ELEMENT FORMULATION USING PARTICULAR INTEGRALS

3.2.1 General Theory

A solution satisfying a linear, inhomogeneous, differential equation and boundary conditions can be found using the method of particular integrals if the complete solution of the corresponding homogeneous equation is known, provided, of course, a particular solution can be found. The procedure is described below:

A linear inhomogeneous differential equation for a vector variable u_i can be expressed in operator notation as

$$L(u_i) + f_i = 0 \tag{3.1}$$

where

$L(u_i)$ is a linear, self-adjoint, homogeneous, differential tensor operator, and

f_i is the inhomogeneous function.

The solution of the above equation can be represented as the sum of a complementary function u_i^c satisfying the homogeneous equation

$$L(u_i^c) = 0 \tag{3.2}$$

and a particular integral u_i^p satisfying the inhomogeneous equation

$$L(u_i^p) = f_i \tag{3.3}$$

The total solution u_i is expressed as

$$u_i = u_i^c + u_i^p \tag{3.4}$$

In the theory of linear, inhomogeneous, differential equations, it is understood that the particular integral is not unique, and any expression satisfying equation (3.3) is a particular integral, regardless of boundary conditions or how it was obtained.

Particular Integral - The particular integral is classically found via the method of undetermined coefficients, the method of variation of parameters, or obtained by inspection of the inhomogeneous differential equation. When these techniques fail to produce a particular integral, a general procedure can be used. Here, the singular solution satisfying the homogeneous differential equation is multiplied by the inhomogeneous quantity, and the product is integrated over an infinite domain. The final result is a particular integral of the inhomogeneous equation. This can be expressed mathematically as

$$u_i^p(\xi) = \int_{-\infty}^{\infty} G_{ij}(x,\xi)\, f_j(x)\, dV(x) \qquad (3.5)$$

where $G_{ij}(x,\xi)$ is the fundamental singular solution of the homogeneous differential equation. The use of a polar coordinate system will simplify the integration.

Once a particular integral is found, it is added to the complementary function to form the total solution. The parameters of the complementary function are adjusted to insure that the total solution satisfies the boundary condition, and hence, produces a unique solution to the boundary value problem.

3.2.2 BEM Solution Based on Particular Integrals

The use of particular integrals in BEM was tentatively discussed by Watson (1979) and Banerjee and Butterfield (1981). In 1986, Ahmad and Banerjee (1986) successfully employed the idea in a two-dimensional eigenvalue analysis. Gravitational and centrifugal formulations have been presented in axisymmetry (Henry, Pape, Banerjee, 1987) and two-dimensional (Pape, Banerjee, 1987) analysis.

Equation (3.1) can be defined for an elastostatic stress analysis with gravitational, centrifugal or thermal body force as

$$L(u_i) + f_i = 0 \tag{3.6}$$

where

$L(u_i) = (\lambda+\mu)\, u_{j,ij} + \mu u_{i,jj}$,

u_i represents the displacement vector,

$f_i = -\rho g e_3$ for gravity loading in the z direction,

$f_i = \rho\omega^2(x_1 e_1 + x_2 e_2)$ for centrifugal loading about the z axis, and

$f_i = -\beta T_{,i}$ for thermoelastic loading

When more than one type of body force is present, the net body force is the summation of the individual body forces.

Complementary Function - The boundary integral equation satisfying the homogeneous part of the differential equation is the complementary function in this procedure. The complementary function for displacement at point ξ, is expressed as

$$C_{ij}(\xi)\, u_i^c(\xi) = \int_S [G_{ij}(x,\xi)\, t_i^c(x) - F_{ij}(x,\xi)\, u_i^c(x)]\, dS(x) \tag{3.7}$$

where the u_i^c and t_i^c are the complementary functions for displacement and traction, respectively. The total solution for displacement u_i

and traction t_i are

$$u_i = u_i^c + u_i^p$$
$$t_i = t_i^c + t_i^p \qquad (3.8)$$

where u_i^p and t_i^p are the particular integrals for displacement and traction, respectively.

Explicit expressions for u_i^p and t_i^p will be derived for gravitational, centrifugal and thermal body forces in subsequent sections, but before proceeding to the formulation of these particular integrals, a brief overview of the particular integral based BEM procedure is presented.

Method of Solution - The boundary integral equation (3.7) is discretized and integrated for a system of boundary nodes in the manner described in Chapter 2. The resulting equations can be expressed in matrix form as

$$\mathbf{G}\,\mathbf{t}^c - \mathbf{F}\,\mathbf{u}^c = \mathbf{0} \qquad (3.9)$$

By introducing equation (3.8) into equation (3.9), the complementary function can be eliminated:

$$\mathbf{G}\,\mathbf{t} - \mathbf{F}\,\mathbf{u} = \mathbf{G}\,\mathbf{t}^p - \mathbf{F}\,\mathbf{u}^p \qquad (3.10)$$

The particular integral terms on the right hand side of this equation are functions of known body forces.

In a multi-region system, a set of (complementary) equations, similar to equation (3.9) are generated independently for each region. Likewise, the particular integrals of each region are derived independently, leading to a set of equations for each region similar

in form to equation (3.10). Interface conditions, expressing the interaction of real quantities between region, are applied, and after assembling the unknown boundary quantities and corresponding coefficients on the left hand side, and the known boundary conditions on the right, the final system can be written as

$$\mathbf{A}^{b}\mathbf{x} = \mathbf{b}^{b} + \mathbf{b}^{p} \qquad (3.11)$$

where $\mathbf{A}^{b}$ is a fully populated matrix, vector $\mathbf{x}$ represents the unknown boundary conditions, vector $\mathbf{b}^{b}$ is the contribution of the known boundary conditions and vector $\mathbf{b}^{p}$ is the contribution of the particular integral. This equation system can be solved for the unknown vector $\mathbf{x}$ by standard numerical techniques.

A Note on Multi-region Programming - The most efficient solution procedure for a single region BEM system utilizes equation (3.9) instead of equation (3.10) since equation (3.10) requires additional matrix multiplication. In this procedure the particular integrals u_i^p and t_i^p are calculated and the complementary functions corresponding to the known boundary conditions are determined using

$$u_i^c = U_i(x) - u_i^p \quad \text{and} \quad t_i^c = T_i(x) - t_i^p$$

where $U_i(x)$ and $T_i(x)$ represent the imposed displacement and traction boundary conditions, respectively. The solution to equation (3.9) yields the unknown complementary functions, and when added to the corresponding particular integral the correct solution is obtained.

This procedure is not as straight forward for multi-region implementations, since interface conditions relate real quantities of displacement and tractions, not the complementary quantities. In a large, multi-region system with a complex assembly for local

definition of boundary conditions, sliding between interface elements, etc., it may be beneficial to use equation (3.10) in spite of the extra matrix multiplications rather than equation (3.9), since the latter would require extensive modifications of interface conditions.

3.3 PARTICULAR INTEGRALS FOR GRAVITATIONAL AND CENTRIFUGAL BODY FORCES

In the previous section, a boundary element formulation utilizing particular integrals was described. Application of this procedure requires the determination of the particular solution for displacement and traction at all boundary nodes. Particular integrals for gravitational and centrifugal body force loadings, applicable to two-dimensional, three-dimensional and axisymmetry boundary element analysis, are presented in this section.

The two- and three-dimensional particular integrals are most readily obtained (Sokolnikoff, 1956) by the method of undetermined coefficients. Using tensor transformations, the axisymmetric particular integrals can be obtained from the three-dimensional form (Henry, Pape, and Banerjee, 1987). For pure axisymmetry, i.e., axisymmetric bodies under axisymmetric loads these transformations simplify to the following:

Coordinates:
$$x_1 = r$$
$$x_2 = 0 \qquad (3.12)$$
$$x_3 = z$$

Displacement:
$$u_r = u_1$$
$$u_\theta = 0 \qquad (3.13)$$
$$u_z = u_3$$

Stress:
$$\sigma_{rr} = \sigma_{11}$$
$$\sigma_{\theta\theta} = \sigma_{22}$$
$$\sigma_{zz} = \sigma_{33} \qquad (3.14)$$
$$\sigma_{rz} = \sigma_{13}$$
$$\sigma_{r\theta} = \sigma_{rz} = 0$$

and tractions are found using the Cauchy traction relation

$$t_i = \sigma_{ij}\, n_j \qquad i,j = r,z \qquad (3.15)$$

The application of the above transformation are straight forward and therefore only the two-, and three-dimensional particular integrals will be defined.

The following two-dimensional particular integrals assume the plane strain conditions.

The two-dimensional particular integrals for the plane stress condition are obtained from the plane strain conditions replacing the material constants ν and λ by a modified constants $\bar{\nu}$ and $\bar{\lambda}$

$$\bar{\nu} = \nu/(1+\nu) \qquad (3.16)$$

$$\bar{\lambda} = \frac{2\mu\lambda}{\lambda+2\mu} \qquad (3.17)$$

The shear modulus μ remains unchanged.

3.3.1 Particular Integrals for Gravitational Body Forces

Two-dimension (plain strain) - The body force in a two-dimensional solid of density ρ under gravitational acceleration g directed along the $-x_2$ axis is expressed as

$$f_1 = 0$$

$$f_2 = -\rho g \tag{3.18}$$

The particular integral for displacement under this body force is

$$u_1^p = \frac{\rho g}{4\mu(\lambda+\mu)} \lambda x_1 x_2$$

$$u_2^p = \frac{-\rho g}{8\mu(\lambda+\mu)} [(\lambda + 2\mu)x_2^2 + \lambda x_1^2] \tag{3.19}$$

and the corresponding particular integral for stress is

$$\sigma_{22}^p = -\rho g \, x_2$$

$$\sigma_{11}^p = \sigma_{12}^p = 0 \tag{3.20}$$

and the particular integrals for tractions is

$$t_1^p = 0$$

$$t_2^p = -\rho g \, x_2 \, n_2 \tag{3.21}$$

Three-dimension - The body force in a three-dimensional solid of density ρ under gravitational acceleration g directed along the $-x_3$ axis is expressed as

$$f_1 = f_2 = 0$$

$$f_3 = -\rho g \tag{3.22}$$

The particular integral for displacement under this body force is

$$u_1^p = \frac{\lambda \rho g}{2\mu(3\lambda+2\mu)} x_1 x_3$$

$$u_2^p = \frac{\lambda\rho g}{2\mu(3\lambda+2\mu)}\, x_2 x_3 \tag{3.23}$$

$$u_3^p = \frac{-(\lambda+\mu)\rho g}{2\mu(3\lambda+2\mu)}\, x_3^2 - \frac{\lambda\rho g}{4\mu(3\lambda+2\mu)}\,(x_1^2 + x_2^2)$$

and the corresponding particular integral for stress is

$$\sigma_{33}^p = -\rho g\, x_3$$

$$\sigma_{11}^p = \sigma_{22}^p = \sigma_{12}^p + \sigma_{13}^p = \sigma_{23}^p = 0 \tag{3.24}$$

and the particular integral for traction is

$$t_1^p = t_2^p = 0$$

$$t_3 = -\rho g\, x_3\, n_3 \tag{3.25}$$

3.3.2. Particular Integral for Centrifugal Body Forces

Two-dimension (plain strain) - The centrifugal body force in a two-dimensional solid of density ρ rotating at a speed ω about an axis parallel to the x_3 axis and centered at a reference coordinate ξ_i is expressed in indicial notation as

$$f_i = \rho\omega^2\, y_i \tag{3.26}$$

where

$$y_i = x_i - \xi_i$$

The particular integral for displacement under this body force is

$$u_i^p = \frac{-\rho\omega^2}{8(\lambda+2\mu)}\,(y_k y_k)\, x_i \tag{3.27}$$

where summation is implied over k.

The corresponding particular integral for stress and traction is, respectively

$$\sigma_{ij}^{p} = \frac{-\rho\omega^2}{4(\lambda+2\mu)} \left[(2\lambda+\mu)\ y_k y_k \delta_{ij} + 2\mu\ y_i y_j\right] \tag{3.28}$$

$$t_i^{p} = \frac{-\rho\omega^2}{4(\lambda+2\mu)} \left[(2\lambda+\mu)\ y_k\ y_k\ n_i + 2\mu\ y_i y_k\ n_k\right] \tag{3.29}$$

where

n_i is the boundary normal at x_i, and

δ_{ij} is the Kronecker delta.

Three-dimension - The centrifugal body force in a three-dimension solid of density ρ rotating at a speed ω about an axis parallel to the x_3 axis and centered at a reference coordinate ξ_i is expressed as

$$\begin{aligned} f_1 &= \rho\omega^2 y_1 \\ f_2 &= \rho\omega^2 y_2 \\ f_3 &= 0 \end{aligned} \tag{3.30}$$

where

$$y_i = x_i - \xi_i$$

Note, $\xi_i = 0$ in axisymmetry.

The particular integral for displacement under this body force is

$$u_1^{p} = \frac{-\rho\omega^2}{8(\lambda+2\mu)} \left[\ \frac{5\lambda+4\mu}{4(\lambda+\mu)}\ (y_1^2+y_2^2) + \frac{\mu}{\lambda+\mu}\ y_3^2\ \right] y_1$$

$$u_2^{p} = \frac{-\rho\omega^2}{8(\lambda+2\mu)} \left[\ \frac{5\lambda+4\mu}{4(\lambda+\mu)}\ (y_1^2+y_2^2) + \frac{\mu}{\lambda+\mu}\ y_3^2\ \right] y_2$$

$$u_3^p = \frac{-\rho\omega^2}{8(\lambda+2\mu)} (y_1^2 + y_2^2)\, y_3 \qquad (3.31)$$

The corresponding particular integral for stress is

$$\begin{aligned}
\sigma_{11}^p &= -\rho\omega^2 [c_1 x_1^2 + c_2 x_2^2 + c_3 x_3^2] \\
\sigma_{22}^p &= -\rho\omega^2 [c_2 x_1^2 + c_1 x_2^2 + c_3 x_3^2] \\
\sigma_{33}^p &= -\rho\omega^2 [c_4 x_1^2 + c_4 x_2^2 + c_5 x_3^2] \\
\sigma_{12}^p &= \rho\omega^2 c_6 x_1 x_2 \qquad (3.32) \\
\sigma_{13}^p &= \rho\omega^2 c_5 x_1 x_3 \\
\sigma_{23}^p &= \rho\omega^2 c_5 x_2 x_3
\end{aligned}$$

where

$$c_1 = \frac{6-3\nu-2\nu^2}{16(1-\nu)} \qquad c_3 = \frac{(1-2\nu)}{8(1-\nu)} \qquad c_5 = \frac{\nu(1-2\nu)}{4(1-\nu)}$$

$$c_2 = \frac{2+3\nu+2\nu^2}{16(1-\nu)} \qquad c_4 = \frac{-1+5\nu+2\nu^2}{8(1-\nu)} \qquad c_6 = \frac{-(2+\nu)(1-2\nu)}{8(1-\nu)}$$

and the particular integral for traction is obtained using the Cauchy traction relation

$$t_i = \sigma_{ij}\, n_j \qquad i,j = 1,2,3 \qquad (3.33)$$

3.4 PARTICULAR INTEGRALS FOR THERMAL ANALYSIS

The gravitational and centrifugal particular integrals, presented in the previous section, were relatively straight forward since their body forces had specific distributions that were represented by elementary functions. In thermal stress analysis this is not the case, since thermal body force can exhibit general temperature

distributions. So consequently, thermal particular integrals are more difficult to obtain.

In this section, the aim is to develop a particular integral applicable to any temperature distribution. This distribution is expressed by nodal temperatures specified at random point through the domain of the body.

The present formulation starts with the assumption that the particular integral for displacement can be expressed as a gradient of a thermoelastic displacement potential h(x) in accordance with the development of linear quasi-static thermoelastic theory (Nowacki, 1962):

$$u_i^p(x) = k\, h_{,i}(x) \tag{3.34}$$

where

$$k = \frac{\alpha(3\lambda+2\mu)}{(\lambda+2\mu)} \tag{3.35}$$

Substituting equation (3.34) into equation (3.6) and simplifying yields

$$h_{,jj}(x) = T(x) \tag{3.36}$$

Hence, an implicit relation between u_i^p and T is derived with the use of a potential function h(x). The irrotational form of the particular integral in equation (3.34) does not imply a loss of generality in the total solution since the balance of the temperature effect is incorporated into the complementary function.

The particular integral of equation (3.34) is of little interest unless a suitable function h(x) can be found to accurately represent a general temperature distribution in equation (3.36). This is achieved using a device, first introduced in the context of finite elements, called the global shape function.

3.4.1 Particular Integrals for Two- and Three-dimensional Analysis

Assuming the function h(x) can be represented by an infinite series, an expression relating h(x) to a set of fictitious scalar densities $\emptyset(\xi_n)$ via a global shape function $C(x,\xi_n)$ can be written as

$$h(x) = \sum_{n=1}^{\infty} C(x,\xi_n)\emptyset(\xi_n) \qquad (3.37)$$

where $C(x,\xi_n)$ = a suitable function of spatial coordinates x and ξ_n.

Several functions were considered for this purpose, however, the best results were obtained with the following expression:

$$C(x,\xi_n) = A_o^2 \, [\rho^2 - b_n \, \rho^3] \qquad (3.38)$$

where

A_o is a characteristic length,

ρ is the euclidean distance between the field point x and the source point ξ_n, and

b_n is a suitably chosen constant to be discussed later. For the present discussion, assume $b_n = 1$.

All distances are nondimensionalized by a characteristic length A_o.

Using equations (3.34) and (3.37), the particular integral for displacement is found:

$$u_i^p(x) = \sum_{n=1}^{\infty} D_i(x,\xi_n)\emptyset(\xi_n) \qquad (3.39)$$

$i = 1,2$ for two-dimensions

$i = 1,2,3$ for three-dimensions

where

$$D_i(x,\xi_n) = kC,_i(x,\xi_n) = kA_o[2 - 3b_n\ \rho]y_i$$

$$y_i = [x_i - (\xi_n)_i]$$

and

$d = 3$ for three-dimensional or $d = 2$ for two-dimensional (plane strain) analysis.

Applying the Laplacian operator on equation (3.37), an expression for the temperature distribution is derived

$$T(x) = \sum_{n=1}^{\infty} K(x,\xi_n)\emptyset(\xi_n) \qquad (3.40)$$

where

$$K(x,\xi_n) = C,_{ii}(x,\xi_n)$$
$$= [2d - 3(1+d)\ b_n\ \rho]$$

A particular integral for strain can be found upon substitution of equation (3.39) into the strain-displacement relation.

$$\varepsilon_{kl}^p(x) = \sum_{n=1}^{\infty} E_{kl}(x,\xi_n)\emptyset(\xi_n) \qquad (3.41)$$

where

$$E_{kl}(x,\xi_n) = kC,_{kl}(x,\xi_n)$$
$$= k\ [2\delta_{kl} - 3b_n\ (\delta_{kl}\rho + \frac{y_k y_l}{\rho})]$$

This result introduced into the stress-strain law of thermoelasticity produces the particular integral for stress:

$$\sigma^p_{ij}(x) = \sum_{n=1}^{\infty} S_{ij}(x,\xi_n)\emptyset(\xi_n) \qquad (3.42)$$

where

$$S_{ij}(x,\xi_n) = D^e_{ijkl}\, E_{kl}(x,\xi_n) - \delta_{ij}\, \beta K(x,\xi_n), \text{ and}$$

$$D^e_{ijkl} = \lambda\, \delta_{ij}\, \delta_{kl} + 2\mu\, \delta_{ik}\, \delta_{jl}\,, \quad \beta = \alpha(3\lambda+2\mu)$$

Finally a particular integral for traction is derived by multiplying the above equation by appropriate normals

$$t^p_i(x) = \sum_{n=1}^{\infty} H_i(x,\xi_n)\emptyset(\xi_n) \qquad (3.43)$$

where

$H_i(x,\xi_n) = S_{ij}(x,\xi_n)n_j(x)$, and

$n_j(x)$ = unit normal at x in the j^{th} direction.

Once again, the plane stress formulation can be obtained from the plane strain case by substituting the modified material constants $\bar{\alpha}$ and $\bar{\lambda}$ into the plane strain equation in place of α and λ, respectively, where

$$\bar{\alpha} = \frac{\alpha(3\lambda+2\mu)}{2(2\lambda+\mu)}$$

and $\bar{\lambda}$ is defined in equation (3.17)

3.4.2 Particular Integrals for Axisymmetric Analysis

The axisymmetric particular integrals can be derived in one of the two ways described below:

1. Direct Derivation - The particular integrals in equations (3.34) and (3.36) are expressed independent of coordinate systems using operator notation. Upon choosing a suitable, cylindrical form of a global shape function $C(x,\xi)$, the axisymmetric particular integrals are then obtained by applying the axisymmetric form of the differential operators. Note, a suitable shape function must render a **K** matrix that is well-conditioned and will admit to an inversion (see equation 3.53).

2. Indirect Derivation - The three-dimension particular integrals, given in equations (3.39) through (3.43), are rewritten in cylindrical coordinates. Upon application of appropriate tensor transformations and analytic integration in the angular (θ) direction, a suitable set of axisymmetric particular integrals are obtained.

The resulting particular integrals should exhibit axisymmetric behavior and satisfy the physical conditions at the origin ($u_r^p=0$, $\varepsilon_{rz}^p=0$, $\varepsilon_{rr}^p=\varepsilon_{\theta\theta}^p$). Choosing a global shape function for the direct derivation that will satisfy these conditions and still admit to an inversion is a difficult task. Nevertheless, the axisymmetric particular integrals derived from the three-dimensional functions using the indirect derivation should inherently satisfy these conditions. For this reason, the indirect derivation has been adopted in this dissertation. The resulting axisymmetric particular integrals are given below.

The particular integral for displacement, temperature and strain are, respectively:

$$u_i^p(x) = \sum_{n=1}^{\infty} D_i(x,\xi_n)\ \phi(\xi_n) \qquad i = r,z \tag{3.45}$$

$$T(x) = \sum_{n=1}^{\infty} K(x,\xi_n)\ \phi(\xi_n) \tag{3.46}$$

$$\varepsilon_{ij}^p(x) = \sum_{n=1}^{\infty} E_{ij}(x,\xi_n)\ \phi(\xi_n) \qquad ij = rr,zz,rz,\theta\theta \tag{3.47}$$

where $D_i(x,\xi_n)$, $K(x,\xi_n)$, $E_{ij}(x,\xi_n)$ are subsequently defined.

In the present formulation, strain is derived from displacement where differentiation (with respect to the field point x) is performed prior to the analytic integration (with respect to the source point ξ_n) in the angular direction.

The particular integral for stress and traction are derived directly from strain in the usual manner employing the following relations

$$\sigma_{ij}^p = D_{ijkl}^e\ \varepsilon_{kl}^p - \delta_{ij}\ \beta\ T \tag{3.48}$$

$$t_i^p = \sigma_{ij}^p\ n_j$$

The following notation is used in defining the axisymmetric particular integrals.

$r_x = x_r$ radial coordinate of the field point

$z_x = x_z$ axial coordinate of the field point

$r_\xi = (\xi_r)_n$ radial coordinate of the fictitious density node n

$z_\xi = (\xi_z)_n$ axial coordinate of the fictitious density node n

Note, the subscript n is dropped for simplicity. All coordinates are nondimensionalized by a characteristic length A_o.

$$z = z_x - z_\xi$$

$$R = [(r_x + r_\xi)^2 + z^2]^{1/2}$$

$$k = \frac{\alpha(1+\nu)}{(1-\nu)}$$

$$m = 4r_x r_\xi / R^2$$

$$m_1 = m-1$$

K = K(m) is the complete Elliptic Integral of the first kind

E = E(m) is the complete Elliptic Integral of the second kind

E and K are defined in Appendix III.D

General Form ($r_x \neq r_\xi$ and/or $z_x \neq z_\xi$):

$$c_1 = K$$

$$c_2 = (E-m_1K)/m$$

$$c_3 = [2E(2m-1)+m_1K(2-3m)]/3m^2$$

$$F_1 = 4c_1/R$$

$$F_2 = -4(2c_2-c_1)/R$$

$$F_3 = 4(4c_3-4c_2+c_1)/R$$

$$G_1 = 4RE$$

$$G_2 = 4mR(c_3-c_2)$$

If $r_x=0$ and/or $r_\xi=0$ and $z_x \neq z_\xi$, then the following substitutions should be made for F_α and G_α

$$F_1 = 2\pi/R$$

$$F_2 = 0$$

$$F_3 = F_1/2$$

$$G_1 = 2\pi R$$

$$G_2 = 0$$

Particular Integral for Temperature:

$$K(x,\xi_n) = 2\pi - 3b_n G_1$$

Particular Integral for Displacement:

$$D_r(x,\xi_n) = kA_o \left[\frac{2\pi}{3} r_x - \frac{3}{4} b_n(r_x G_1 - r_\xi G_2)\right]$$

$$D_z(x,\xi_n) = kA_o z \left[\frac{2\pi}{3} - \frac{3}{4} b_n G_1\right]$$

Particular Integral for Strain:

$$E_{rr}(x,\xi_n) = k \left[\frac{2\pi}{3} - \frac{3}{4} b_n (G_1 + r_x^2 F_1 - 2r_x r_\xi F_2 + r_\xi^2 F_3)\right]$$

$$E_{zz}(x,\xi_n) = k \left[\frac{2\pi}{3} - \frac{3}{4} b_n (G_1 + z^2 F_1)\right]$$

$$E_{rz}(x,\xi_n) = kz \left[-\frac{3}{4} b_n (r_x F_1 - r_\xi F_2)\right]$$

$$E_{\theta\theta}(x,\xi_n) = D_r(x,\xi_n)/(r_x A_o)$$

If $r_x=0$, then

$$E_{\theta\theta}(x,\xi_n) = E_{rr}(x,\xi_n)$$

Singular Form ($r_x = r_\xi$ and $z_x = z_\xi$):

The general form of the axisymmetric particular integrals are singular when $r_x = r_\xi$ and $z_x = z_\xi$. In this circumstance, the limiting form of these functions, given below, should be used.

Particular Integral for Temperature:

$$K(x,\xi_n) = 2\pi\text{-}24\ b_n\ r_x$$

Particular Integral for Displacement:

$$D_r(x,\xi_n) = kA_o r_x\ [\frac{2\pi}{3} - 8\ b_n r_x]$$

$$D_z(x,\xi_n) = 0$$

Particular Integral for Strain:

$$E_{rr}(x,\xi_n) = k\ [\frac{2\pi}{3} - 10\ b_n r_x]$$

$$E_{zz}(x,\xi_n) = k\ [\frac{2\pi}{3} - 6\ b_n r_x]$$

$$E_{rz}(x,\xi_n) = 0$$

$$E_{\theta\theta}(x,\xi_n) = k\ [\frac{2\pi}{3} - 8\ b_n r_x]$$

3.4.3 Numerical Implementations

The particular integral for displacement $u_i^p(x)$ and traction $t_i^p(x)$ must be evaluated at each boundary node before a solution to the governing equation (3.6) can be achieved. For the purpose of numerical evaluation, the infinite series representations of the particular integrals are truncated at a finite number of N terms. (The choice of N will be discussed later.) The particular integrals for displacement, traction, and temperature distribution can be rewritten for N number of terms as follows:

$$u_i^p(x) = \sum_{n=1}^{N} D_i(x,\xi_n)\emptyset(\xi_n) \tag{3.49}$$

$$t_i^p(x) = \sum_{n=1}^{N} H_i(x,\xi_n)\emptyset(\xi_n) \tag{3.50}$$

$$T(x) = \sum_{n=1}^{N} K(x,\xi_n)\emptyset(\xi_n) \tag{3.51}$$

The particular integrals are derived for each region, independent of the other regions. Hence a set of (the above) equations are written for each region where a temperature change is prescribed.

The evaluation of the u_i^p and t_i^p in the first two equations requires the determination of N fictitious nodal densities $\emptyset(\xi_n)$, n = 1 to N. For this reason N temperature equations (3.40) or (3.46) are written at each ξ_n node. These equations are expressed in matrix form, independently for each region, as

$$\mathbf{T} = \mathbf{K}\,\boldsymbol{\emptyset} \tag{3.52}$$

where $\mathbf{K}$ is a N x N matrix. Since the increment of temperature distribution is known, the fictitious nodal values $\phi(\xi_n)$ can be determined:

$$\phi = \mathbf{K}^{-1}\ \mathbf{T} \tag{3.53}$$

A back substitution of the quantities $\phi(\xi_n)$ in the particular integrals for displacement and traction allows for their evaluation at any point. Hence, u_i^p and t_i^p can be determined at all boundary nodes, and the boundary value problem can be solved as discussed in section 3.2.2.

Displacements, Stresses, and Strains at Interior Points- The solution for the interior quantities consist of a complementary and a particular part:

$$\begin{aligned} u_i &= u_i^c + u_i^p \\ \varepsilon_{ij} &= \varepsilon_{ij}^c + \varepsilon_{ij}^p \\ \sigma_{ij} &= \sigma_{ij}^c + \sigma_{ij}^p \end{aligned} \tag{3.54}$$

The particular integrals of the above quantities are defined in two- and three-dimensions by equations (3.39), (3.41) and (3.42) and the complementary functions are inferred from equation (3.7). The boundary stress calculation discussed in section 2.3.2 is used in place of the integral equation to represent the complementary function of stress for a point on the boundary. This avoids strong singularities in the integral equation associated with a boundary point.

Selection of Parameters - The formulation presented thus far is relatively straight forward, however, the following areas demand special attention to guarantee high accuracy in the results.

The boundary mesh chosen for a specific problem should be fine enough to produce satisfactory results for elastostatic analysis. Fictitious function nodes ξ_n should be introduced at all boundary collocation nodes and at points where interior quantities are to be evaluated since the interpolation of the global shape function is most accurate at these locations. Additional (fictitious function) nodes may be used through the interior of the body for a better representation of the particular integrals. A pattern of interior nodes consistent with the fineness of the boundary mesh is recommended, however, the number of additional points is dictated by the complexity of the temperature distribution. In any case, a uniform or neatly graded pattern is recommended for best results.

It is obvious from equation (3.40) that the largest term in each column of matrix **K** falls on the main diagonal (when symmetric node ordering is used). The magnitude of the off diagonal terms will not, in general, be strongly banded unless special attention is paid in ordering the nodes according to their proximity. In any case, errors may show up when a large number of fictitious nodes are used. To eliminate this problem, matrix **K** can be optimized by the choice of the constants b_n. These constants are dynamically calculated (independently for each n) to scale each column of matrix **K** so that the lowest value is forced to zero. This optimization and the use of double pivoting will reduce error in the solution of equation (3.53), however, a price is paid for this matrix conditioning, since **K** will be rendered nonsymmetric.

Still greater precision can be achieved by adding a constant term to the function in equation (3.40). This is accomplished by setting

one of the constants b_n to zero in one specific column (here, for simplicity, we choose the last column; n = N). The benefits gained are seen when equation (3.40) is expanded out. For a field point x, we have

$$T(x) = 2dC + 3(1+d)\left[b_1\rho_1\phi(\xi_1) + \ldots + b_n\rho_n\phi(\xi_n) + \ldots + b_{N-1}\,\rho_{N-1}\,\phi(\xi_{N-1})\right] + 2d\phi(\xi_N) \qquad (3.55)$$

where

$C = \phi(\xi_1) + \phi(\xi_2) + \ldots + \phi(\xi_n) + \ldots + \phi(\xi_{N-1})$

ρ_n = the euclidean distance between x and ξ_n, and

$2d\phi(\xi_N)$ is the (self-adjusting) constant term

For a given temperature distribution, C is constant (independent of x), whereas the term in brackets depends on the spatial varying function ρ_n, and therefore, the term in the brackets dictates the shape of the function. Note, the last term containing $\phi(\xi_n)$ (for n=N) is independent of coordinates and therefore is seen as a constant term that can adjust according to the value of $\phi(\xi_N)$.

The values of the nodal densities $\phi(\xi_n)$ must adjust to satisfy the temperature $T(x_m)$ in N nodal equations. In the presence of the last term, C is seen as arbitrary, since the last term $\phi(\xi_N)$ can adjust to accommodate any value of C produced by the other N-1 $\phi(\xi_n)$ values. This allows the ϕ's for the terms in brackets to adjust to satisfy the temperature distribution in a free, relaxed manner. In the absence of the last term, C is no longer arbitrary and the $\phi(\xi_n)$'s

must take on values that force the term in brackets to balance C so that the temperature distribution is satisfied at nodal points. In essence, without the last terms, the global shape function may be forced to behave in a unnatural manner between the nodal points.

3.5 EXAMPLES

In this section three problems are presented to demonstrate the particular integral based, body force analysis.

3.5.1 Gravity Stresses Around a Vertical Shaft

The axisymmetric, gravity body force analysis is used to determine the stress distribution in the soil near a vertical shaft in a halfspace due to its own weight. Eight quadratic elements (two for each side of a square region) with a total of sixteen nodes are used to model this geometry. In addition, stresses are calculated at four interior points. In figure 3.1, the BEM results are compared with the analytical solution (Terzaghi, 1943). Excellent agreement is obtained, even for this crude mesh.

3.5.2 Stresses in a Rotating Sphere

The axisymmetric centrifugal body force analysis is used to determine stresses in a solid sphere rotating about the vertical axis. Due to symmetry, only half of the body is modelled as shown in figure 3.2. Four elements with a total of nine nodes are used. Note that the centerline is not discretized. The nodes along the r axis are constrained against displacement in the z direction. The only loading applied is that due to a rotation about the z axis. The BEM results are compared to theoretical and finite element

(Zienkiewicz, 1977) results in figure 3.3 and 3.4. Again, excellent agreement is obtained.

3.5.3 Thick Cylinder Subjected to Thermal Load

The axisymmetric, two- and three-dimensional thermoelastic analysis by particular integrals is tested on a thick cylinder under plane strain conditions. The boundary element discretizations for the problem are shown in figure 3.5. The thick cylinder, with an inner radius of 10 inches and an outer radius of 20 inches, is assumed to have the following material properties:

$$E = 2600 \text{ lb/in}^2$$

$$\nu = 0.3$$

$$\alpha = 0.001 \text{ in/in/deg F}$$

The temperature distribution

$$T(r) = 1{,}000 \frac{r^i}{r} - 70 \qquad \text{(deg F)}$$

is applied to the cylinder where r^i is the inner radius and r is the radial distance. The resulting BEM solutions for displacement and stress are given in Figures 3.6 and 3.7, respectively. These results are compared with the analytical solution by Boley and Weiner (1960), and once again, excellent agreement is observed.

3.6 CONCLUDING REMARKS

A new boundary element procedure, based on particular integrals, was introduced for the treatment of body forces. A range of problems was solved and shown to correlate favorably with existing results.

The particular integrals satisfy the inhomogeneous differential equation exactly, and therefore, the need for a volume integral or additional surface integrals is eliminated. The (homogeneous) boundary integral equation together with the particular integral represents an exact statement of the problem, and any error in the BEM solution is the result of approximations and errors introduced in the numerical implementation and solution.

The general particular integral formulation introduced in this chapter can be applied in other BEM analyses which involve inhomogeneous differential equations. One such area, inelastic stress analysis, will be taken up in the next chapter.

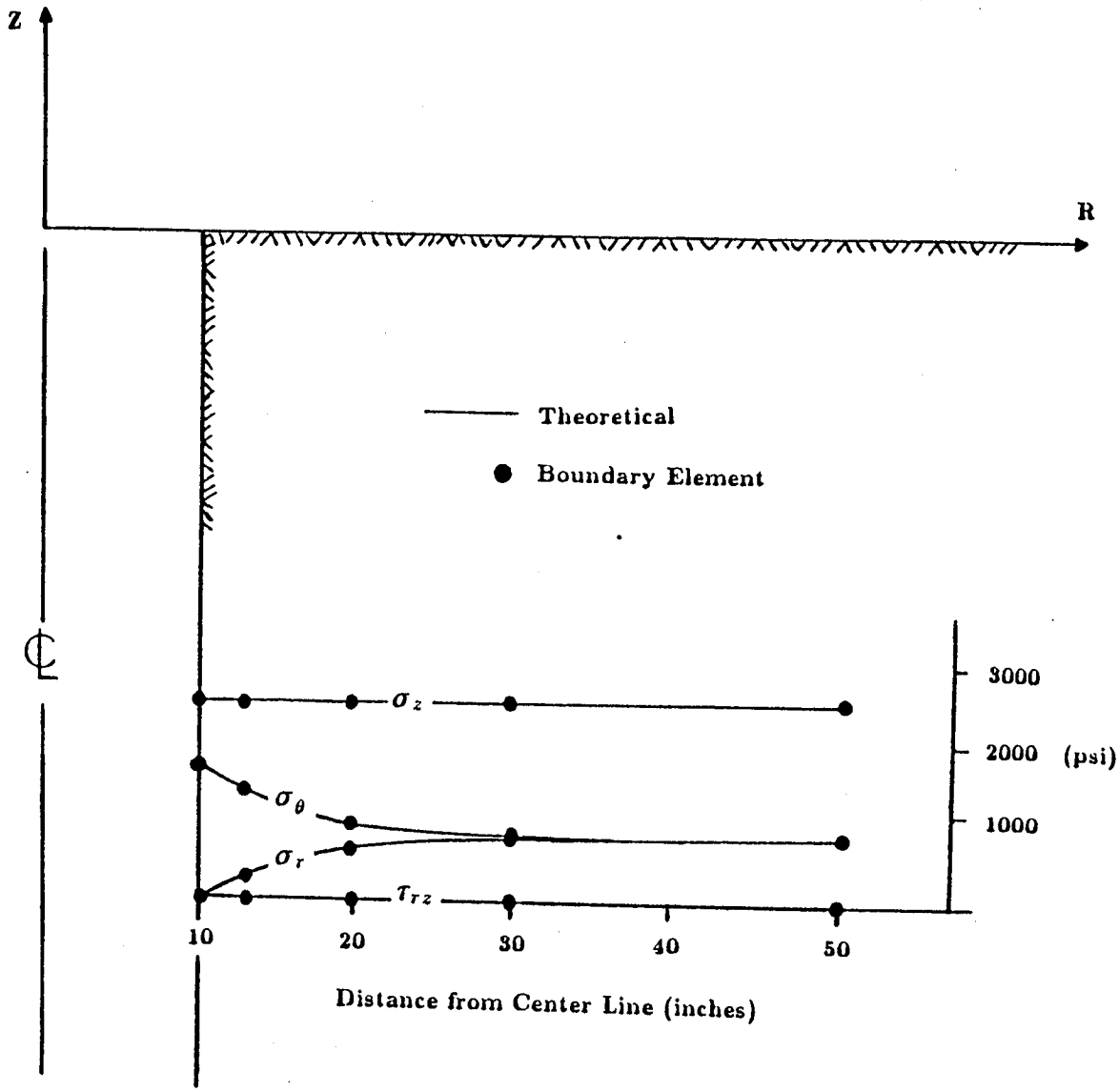

Figure 3.1
Stress Distribution near a Vertical Shaft due to Self-weight

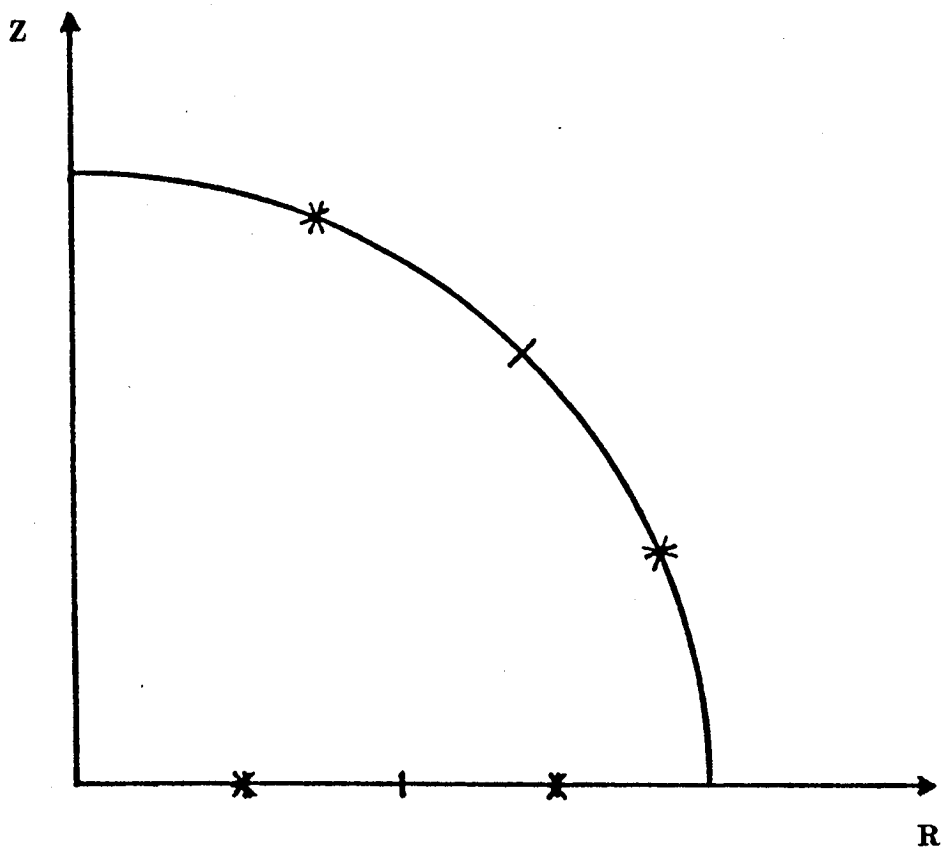

Figure 3.2
Axisymmetric Mesh of a Solid Sphere

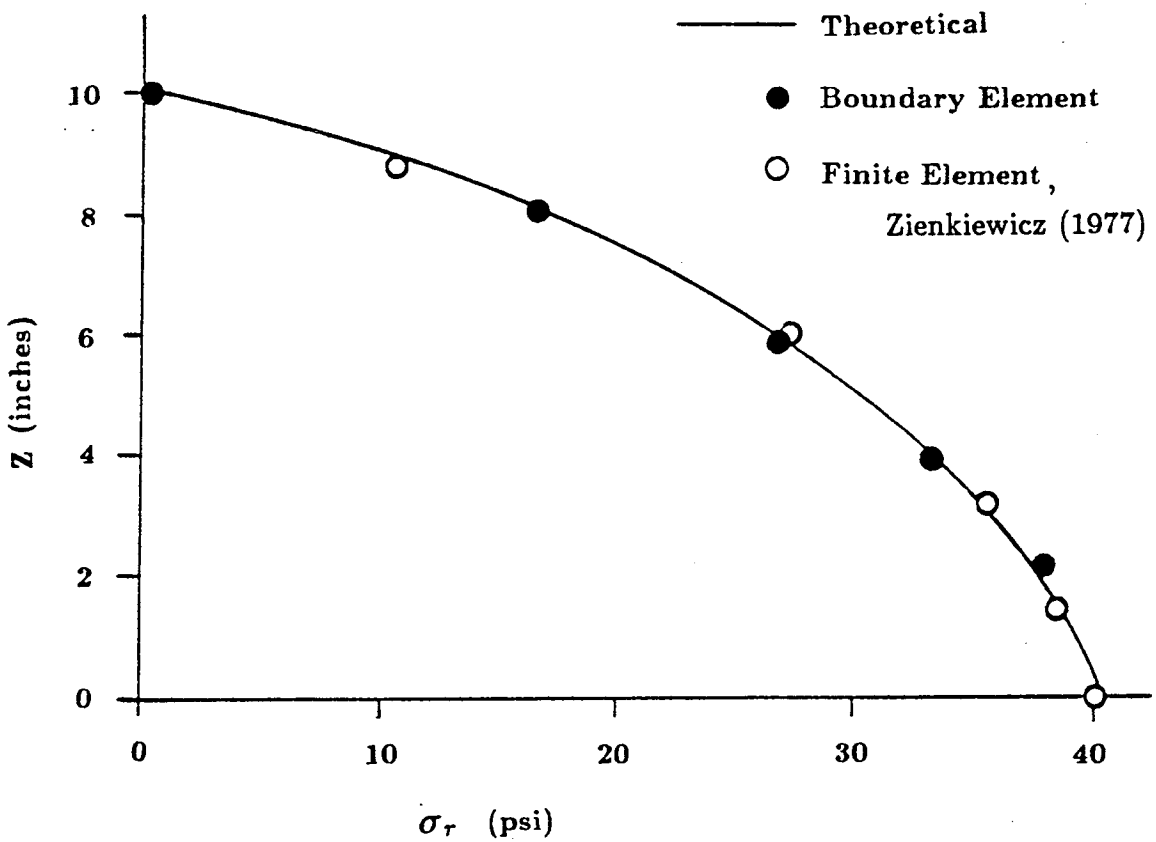

Figure 3.3
Radial Stress through a Rotating Sphere at R=0

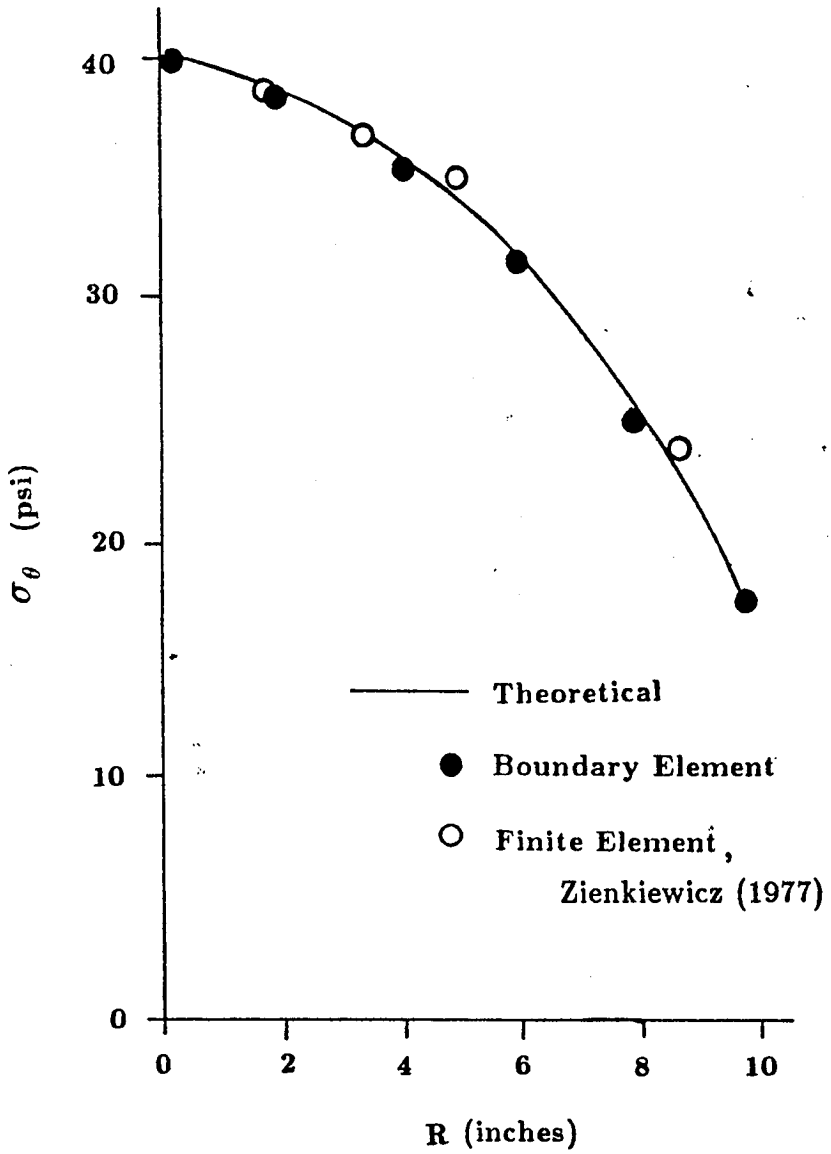

Figure 3.4
Tangential Stress through a Rotating Sphere at Z=0

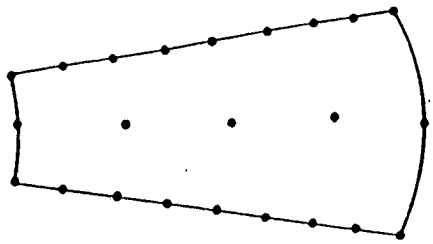

Figure 3.5a
Two-dimensional Mesh of a Thick Cylinder (Diameter Ratio 1:2)

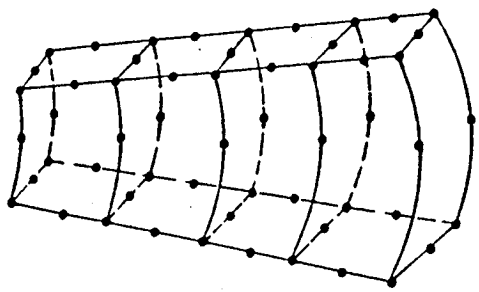

Figure 3.5b
Three-dimensional Mesh of a Thick Cylinder (Diameter Ratio 1:2)

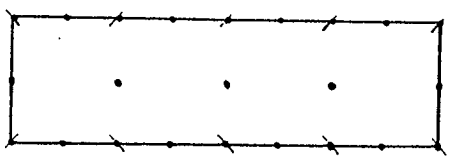

Figure 3.5c
Axisymmetry Mesh of a Thick Cylinder (Diameter Ratio 1:2)

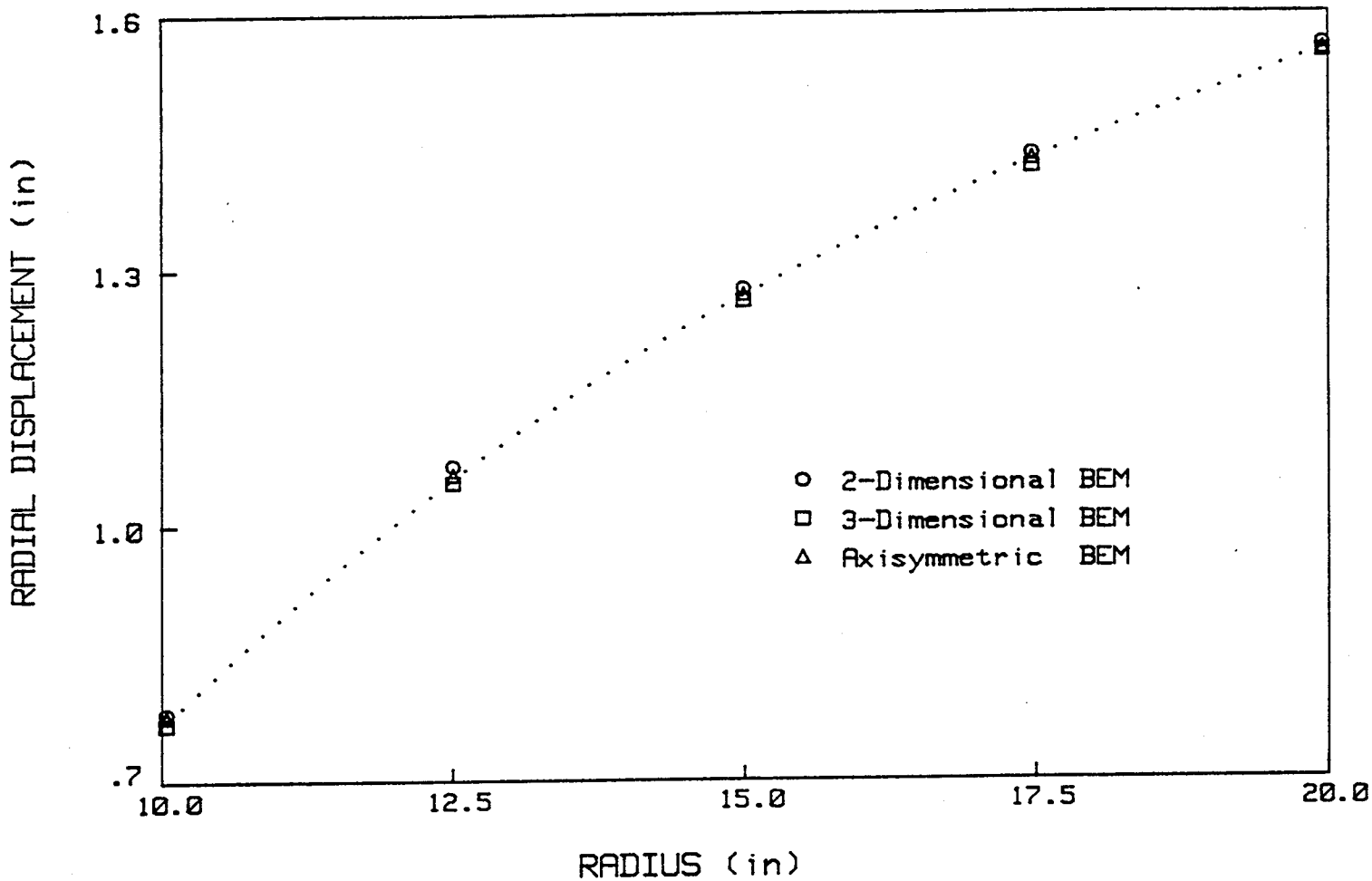

Figure 3.6
Radial Displacement through a Thermally Loaded Thick Cylinder (Plane Strain)

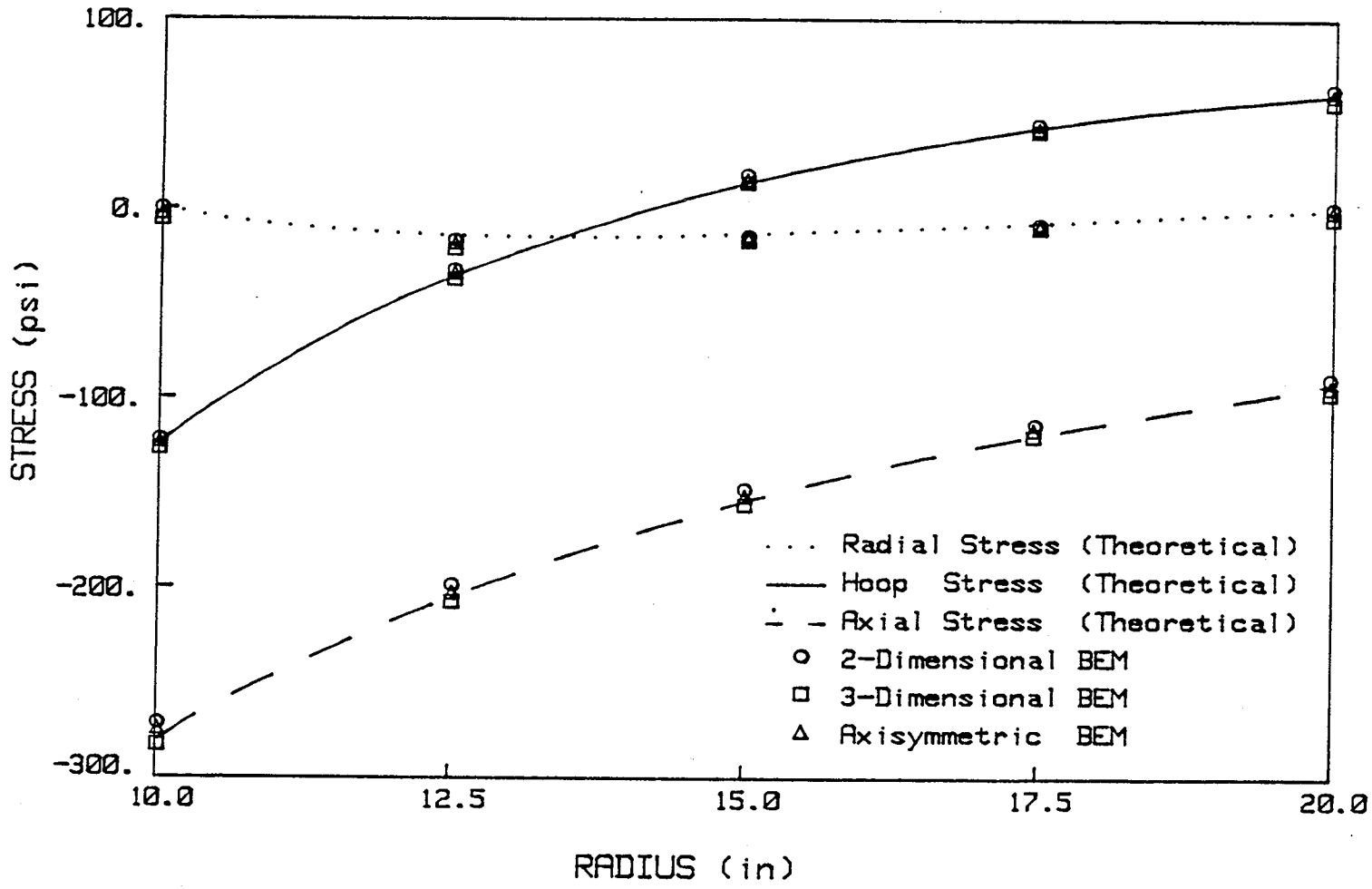

Figure 3.7
Stress through a Thermally Loaded Thick Cylinder (Plane Strain)

CHAPTER 4

INELASTIC BOUNDARY ELEMENT FORMULATION BASED ON PARTICULAR INTEGRALS

CHAPTER FOUR

INELASTIC BOUNDARY ELEMENT FORMULATION BASED ON PARTICULAR INTEGRALS

4.1 INTRODUCTION

In the previous chapter, a general boundary element formulation based on particular integrals was presented and applied to gravitational, centrifugal and thermoelastic analysis. The next logical step is the extension of the technique to other areas of BEM analysis. In the present chapter, the formulation is extended to problems where the body forces are generated by the initial stress gradient; specifically elastoplastic analysis.

Two- and three-dimensional particular integrals, as well as axisymmetric particular integrals are developed and implemented in a general purpose BEM computer code. The final BEM equation system produced by this formulation is similar in form to that generated by volume integration. This allows the iterative and variable stiffness algorithms developed in earlier works (Raveendra, 1984) to be incorporated with this new particular integral formulation without modification. Furthermore, the formulations developed in the next chapter for elastic and inelastic inhomogeneous media will employ the present procedure.

4.2 PARTICULAR INTEGRALS FOR INITIAL STRESS BODY FORCES

The governing differential equation for a body subjected to an initial stress body force is expressed in terms of displacement u_i as

$$(\lambda+\mu)u_{j,ji} + \mu\, u_{i,jj} = \sigma^{o}_{ij,j} \tag{4.1}$$

where λ and μ are Lamé constants.

The initial stress σ^{o}_{ij} may be induced by a 'lack of fit' stress, temperature change, inhomogeneities, inelastic effects, or a combination of these. In this chapter a boundary element formulation using particular integrals is derived for the solution of the above equation, and from this formulation, the incremental formulation for plasticity is inferred.

The total solution of the above equation can be decomposed into a particular integral and a complementary function:

$$\begin{aligned} u_i &= u_i^c + u_i^p \\ t_i &= t_i^c + t_i^p \\ \sigma_{ij} &= \sigma_{ij}^c + \sigma_{ij}^p \end{aligned} \tag{4.2}$$

The boundary integral derived in Chapter 2 for elasticity represents the complementary function since it satisfies the homogeneous centerpart of equation (4.1). Hence, equations for the boundary system, displacement, and stress can be expressed in matrix form as

$$\mathbf{F}\mathbf{u}^c = \mathbf{G}\mathbf{t}^c \tag{4.3a}$$

$$\boldsymbol{\sigma}^c = \mathbf{G}^{\sigma}\mathbf{t}^c - \mathbf{F}^{\sigma}\mathbf{u}^c \tag{4.3b}$$

Using equation (4.2), these equations can be rewritten as

$$\mathbf{F}\mathbf{u} = \mathbf{G}\mathbf{t} + [\mathbf{F}\mathbf{u}^p - \mathbf{G}\mathbf{t}^p] \tag{4.4a}$$

$$\boldsymbol{\sigma} = \mathbf{G}^{\sigma}\mathbf{t} - \mathbf{F}^{\sigma}\mathbf{u} + [\mathbf{F}^{\sigma}\mathbf{u}^p - \mathbf{G}^{\sigma}\mathbf{t}^p + \boldsymbol{\sigma}^p] \tag{4.4b}$$

The particular integral vectors u^p, t^p, and σ^p of the above equations are related to the initial stress by virtue of equation (4.1). Once explicit relations are known, these functions are evaluated at nodal points allowing equation (4.4) to be solved in the conventional manner for a set of well-posed boundary conditions.

Effort is now turned toward deriving explicit expressions for the particular integrals.

4.2.1 Two- and Three-Dimensional Particular Integrals

The two- and three-dimensional particular integrals for displacement are related to the Galerkin vector F_i via

$$u_i^p = \frac{(1-\nu)}{\mu} F_{i,kk} - \frac{1}{2\mu} F_{k,ki} \tag{4.5}$$

where ν is Poisson's ratio.

Substituting this equation into equation (4.1) renders a relationship between the Galerkin vector and the initial stress function:

$$F_{i,kkjj} = \frac{1}{(1-\nu)} \sigma^o_{ij,j} \tag{4.6}$$

In subsequent steps of this derivation, it will be advantageous for the implicit expression of equations (4.5) and (4.6) to be related by a second order tensor, rather than a vector. Therefore, a tensor function h_{ij} is introduced where

$$h_{ij,mmnn} = \sigma^o_{ij} \tag{4.7}$$

Substitution of this equation into equation (4.6) and simplifying yields an expression for the Galerkin vector in terms of this new function:

$$F_i = \frac{1}{(1-\nu)} h_{ij,j} \tag{4.8}$$

Finally, substituting this expression into equation (4.5) yields the desired particular integral for displacement

$$u_i^p = \frac{1}{\mu} h_{il,lkk} - \frac{1}{2\mu(1-\nu)} h_{lm,ilm} \tag{4.9}$$

The particular integral for strain, stress and tractions are found using the following relations

$$\varepsilon_{ij}^p = \frac{1}{2} (u_{i,j}^p + u_{j,i}^p) \tag{4.10a}$$

$$\sigma_{ij}^p = D_{ijkl}^e \varepsilon_{kl}^p - \sigma_{ij}^o \tag{4.10b}$$

$$t_i^p = \sigma_{ij}^p n_j \tag{4.10c}$$

where D_{ijkl}^e is the elastic constitutive relation given by equation (2.7a). It is important to note that the initial stress must be subtracted out of equation (4.10b) in order to produce the correct particular integral for stress. The complementary function for stress and strain, on the other hand, are related directly by D_{ijkl}^e, i.e., $\sigma_{ij}^c = D_{ijkl}^e \varepsilon_{kl}^c$.

Employing equations (4.10), the following expressions are obtained for the particular integral for strain and stress:

$$\varepsilon_{ij}^p = \frac{1}{2\mu} (h_{il,lkkj} + h_{jl,lkki} - \frac{1}{(1-\nu)} h_{lm,ijlm}) \tag{4.11}$$

$$\sigma_{ij}^p = \frac{(\nu)}{(1-\nu)} h_{ml,mlkk} \delta_{ij} + h_{il,jlkk} + h_{jl,ilkk}$$

$$- \frac{1}{(1-\nu)} h_{lk,ijkl} - h_{ij,llkk} \tag{4.12}$$

In passing we note the above relations for particular integral are derived in terms of initial stress, which is consistent with Chapter 2. An initial strain ε^{o}_{ij} formulation is possible assuming

$$h_{ij,mmnn} = \varepsilon^{o}_{ij} \tag{4.13}$$

where the associate particular integral for displacement is

$$u^{p}_{i} = \frac{(\nu)}{(1-\nu)} h_{kk,ijj} + 2\, h_{ij,jkk} - \frac{1}{(1-\nu)} h_{kj,ikj} \tag{4.14}$$

The particular integrals given by equations (4.7), (4.9), (4.11) and (4.12) have little practical use in this implicit form. However, by applying the global shape function concept of the previous chapter, an explicit formulation can be developed for analysis of problems with general initial stress distributions.

Global Shape Function - Tensor $h_{ij}(x)$ can be expressed in terms of a fictitious tensor density $\emptyset_{ij}(\xi)$ as an infinite series using a suitable global shape function $C(x,\xi)$:

$$h_{ml}(x) = \sum_{n=1}^{\infty} C(x,\xi_n)\ \emptyset_{ml}(\xi_n) \tag{4.15}$$

m,l = 1,2 for two-dimensions
m,l = 1,2,3 for three dimensions

Several functions were considered, however, the best results were obtained with the following expression.

$$C(x,\xi_n) = A_o^4\ [\rho^4 - b_n\ \rho^5] \tag{4.16}$$

where

A_o is a characteristic length,

ρ is the euclidean distance between the field point x and the source point ξ_n,

b_n is a constant, chosen in a manner described in section 3.4.3. For the present discussion b_n can assume the value of unity.

All distances are non-dimensionalized by a characteristic length A_o.

The unknown fictitious densities are related to the initial stress through equation (4.7). Substituting equation (4.15) into equation (4.7) leads to

$$\sigma^o_{lm} = \sum_{n=1}^{\infty} K(x,\xi_n)\ \emptyset_{lm}(\xi_n) \qquad (4.17)$$

where

$$K(x,\xi_n) = C_{,mmnn}(x,\xi_n) = a - b\rho$$

$$a = 8d(d+2)\ , \qquad b = b_n 15(d+3)(d+1)$$

d = 3; for three-dimensional analysis, and

d = 2; for two-dimensional (plane strain) analysis.

The particular integral for displacement can be found by substituting equation (4.15) into equation (4.9).

$$u^p_i(x) = \sum_{n=1}^{\infty} D_{iml}(x,\xi_n)\ \emptyset_{lm}(\xi_n) \qquad (4.18)$$

where

$$D_{iml}(x,\xi_n) = A_o \left[(c_1+d_1\rho)\ (y_i\delta_{lm}+y_m\delta_{il}) + (c_2+d_2\rho)y_l\delta_{im} + \frac{d_1}{\rho}\ y_i y_l y_m\right]$$

$$y_i = [x_i - (\xi_n)_i]$$

$$c_1 = \frac{-8}{2\mu(1-\nu)} \qquad d_1 = \frac{b_n 15}{2\mu(1-\nu)}$$

$$c_2 = c_1 + \frac{8(d+2)}{\mu} \qquad d_2 = d_1 - \frac{b_n 15(d+3)}{\mu}$$

The particular integral for strain and stress can be found by substituting equation (4.18) into equation (4.10). Alternatively, these functions can be found directly by a substitution of equation (4.15) into equations (4.11) and (4.12). Employing the latter method, the particular integral for stress can be written as

$$\sigma^p_{ij} = \sum_{n=1}^{\infty} S_{ijlm}(x,\xi_n)\emptyset_{lm}(\xi_n) \qquad (4.19)$$

where

$$S_{ijlm}(x,\xi_n) = (e_2+f_2\rho)\delta_{jm}\delta_{il} + (e_3+f_3\rho)\delta_{ij}\delta_{lm} + (e_4+f_4\rho)\delta_{im}\delta_{jl}$$
$$+ \frac{f_1}{\rho}(y_j y_m \delta_{il} + y_i y_j \delta_{lm} + y_i y_m \delta_{jl})$$
$$+ \frac{f_2}{\rho}(y_i y_l \delta_{jm} + y_j y_l \delta_{im}) + \frac{f_3}{\rho} y_l y_m \delta_{ij} + \frac{f_5}{\rho^3} y_i y_j y_l y_m$$

$$e_1 = 2\mu c_1 \qquad f_1 = -f_5 = 2\mu d_1$$

$$e_2 = \mu(c_1+c_2) \qquad f_2 = \mu(d_1+d_2)$$

$$e_3 = e_1+\lambda[c_1(d+1)+c_2] \qquad f_3 = f_1 + \lambda[d_1(d+2)+d_2]$$

$$e_4 = e_2 - a \qquad f_4 = f_2 + b$$

Finally, the particular integrals for traction are found using equations (4.10c) and (4.19).

Once again the plane stress formulation is derived from the two-dimensional plane strain formulation by substituting the modified material constants defined in equations (3.16) and (3.17) into the plane strain equations.

4.2.2 Axisymmetric Particular Integrals

Although the methodology for axisymmetric BEM analysis by particular integrals is similar to that of two- and three-dimensions, the functions, of course, are different. In this section, an axisymmetric form of particular integrals is presented for axisymmetric initial stress body forces.

The axisymmetric particular integrals can be derived by one of the two methods described in Section 3.4.2.

These methods are:

1. A direct derivation utilizing the axisymmetric form of the differential operators in equations (4.7) and (4.9), and a suitable axisymmetric shape function.

2. A derivation from the three-dimensional particular integral utilizing appropriate cylindrical coordinate and tensor transformations, and an analytic integration in the angular (θ) direction.

The second method has been adopted in this dissertation, and the resulting axisymmetric particular integrals for initial stress, displacement, and strain are given below.

$$\begin{Bmatrix} \sigma^{o}_{rr}(x) \\ \sigma^{o}_{zz}(x) \\ \sigma^{o}_{rz}(x) \\ \sigma^{o}_{\theta\theta}(x) \end{Bmatrix} = \sum_{n=1}^{\infty} \begin{bmatrix} K^{n}_{11} & 0 & 0 & K^{n}_{14} \\ 0 & K^{n}_{22} & 0 & 0 \\ 0 & 0 & K^{n}_{33} & 0 \\ K^{n}_{41} & 0 & 0 & K^{n}_{44} \end{bmatrix} \begin{Bmatrix} \phi_{rr}(\xi_n) \\ \phi_{zz}(\xi_n) \\ \phi_{rz}(\xi_n) \\ \phi_{\theta\theta}(\xi_n) \end{Bmatrix} \tag{4.20}$$

$$\begin{Bmatrix} u^{p}_{r}(x) \\ u^{p}_{z}(x) \end{Bmatrix} = \sum_{n=1}^{\infty} \begin{bmatrix} D^{n}_{11} & D^{n}_{12} & D^{n}_{13} & D^{n}_{14} \\ D^{n}_{21} & D^{n}_{22} & D^{n}_{23} & D^{n}_{24} \end{bmatrix} \begin{Bmatrix} \phi_{rr}(\xi_n) \\ \phi_{zz}(\xi_n) \\ \phi_{rz}(\xi_n) \\ \phi_{\theta\theta}(\xi_n) \end{Bmatrix} \tag{4.21}$$

$$\begin{Bmatrix} \varepsilon^{p}_{rr}(x) \\ \varepsilon^{p}_{zz}(x) \\ \varepsilon^{p}_{rz}(x) \\ \varepsilon^{p}_{\theta\theta}(x) \end{Bmatrix} = \sum_{n=1}^{\infty} \begin{bmatrix} E^{n}_{11} & E^{n}_{12} & E^{n}_{13} & E^{n}_{14} \\ E^{n}_{21} & E^{n}_{22} & E^{n}_{23} & E^{n}_{24} \\ E^{n}_{31} & E^{n}_{32} & E^{n}_{33} & E^{n}_{34} \\ E^{n}_{41} & E^{n}_{42} & E^{n}_{43} & E^{n}_{44} \end{bmatrix} \begin{Bmatrix} \phi_{rr}(\xi_n) \\ \phi_{zz}(\xi_n) \\ \phi_{rz}(\xi_n) \\ \phi_{\theta\theta}(\xi_n) \end{Bmatrix} \tag{4.22}$$

where K^{n}_{ij}, D^{n}_{ij} and E^{n}_{ij} are subsequently defined.

The particular integral expression for stress and traction are derived from equations (4.20) and (4.22) using equations (4.10b) and (4.10c). In the present implementation, $\varepsilon^{p}_{ij}(x)$ is evaluated using equation (4.22) and the resulting values are substituted in equations (4.10b) and (4.10c) for the numerical determination of for the $\sigma^{p}_{ij}(x)$ and $t^{p}_{ij}(x)$.

The following notation is used in defining the axisymmetric particular integrals.

$r_x = x_r$ radial coordinate of field point

$z_x = x_z$ axial coordinate of field point

$r_\xi = (\xi_r)_n$ radial coordinate of the fictitious density node n

$z_\xi = (\xi_z)_n$ axial coordinate of the fictitious density node n

Note, the subscript n will be dropped for simplicity. All coordinates are nondimensionalized by a characteristic length A_o.

$$z = z_x - z_\xi$$

$$R = [(r_x + r_\xi)^2 + z^2]^{1/2}$$

$$m = 4r_x r_\xi / R^2$$

$$m_1 = m-1$$

K = K(m) is the complete Elliptic Integral of the first kind

E = E(m) is the complete Elliptic Integral of the second kind

E and K are defined in Appendix III.D

$$h_1 = 0$$

$$h_2 = \frac{1}{\mu}$$

$$h_3 = \frac{-1}{2\mu(1-\nu)}$$

$$a_1 = h_3/15$$

$$a_2 = h_3/15$$

$$a_3 = h_2/3 + a_1$$

$$b_1 = h_3/8$$

$$b_2 = h_3/8$$

$$b_3 = 3h_2/4 + b_1$$

$$b_4 = -b_1$$

General Form ($r_x \neq r_\xi$ and/or $z_x \neq z_\xi$):

$$c_1 = K$$

$$c_2 = (E-m_1K)/m$$

$$c_3 = [2E(2m-1) + m_1K(2-3m)]/3m^2$$

$$c_4 = [4(2m-1)c_3 + 3m_1c_2]/5m$$

$$c_5 = [6(2m-1)c_4 + 5m_1c_3]/7m$$

$$c_6 = [8(2m-1)c_5 + 7m_1c_4]/9m$$

$$e_1 = [2(1+m_1)E - m_1K]/3$$

$$e_2 = [4(1 + m_1)e_1 - 3m_1E]/5$$

$$d_1 = E/m_1$$

$$d_2 = (K-E)/m$$

$$d_3 = [E(1+m_1) - 2m_1K]/m^2$$

$$d_4 = [E(2-7m_1 - 3m_1^2) + K(9m_1-1)m_1]/3m^3$$

$$d_5 = [e_2 + 6m_1^2E - 4m_1e_1 - 4m_1^3 K + m_1^4 d_1]/m^4$$

$$F_1 = 4c_1/R$$

$$F_2 = -4(2c_2 - c_1)/R$$

$$F_3 = 4(4c_3 - 4c_2 + c_1)/R$$

$$F_4 = -4(8c_4 - 12c_3 + 6c_2 - c_1)/R$$

$$G_1 = 4RE$$

$$G_2 = 4mR\ (c_3 - c_2)$$

$$G_3 = 2R\ [E-m\ (2c_4 - 3c_3 + c_2)]$$

$$T_1 = 4d_1/R^3$$

$$T_2 = -4(2d_2 - d_1)/R^3$$

$$T_3 = 4(4d_3 - 4d_2 + d_1)/R^3$$

$$T_4 = -4(8d_4 - 12d_3 + 6d_2 - d_1)/R^3$$

$$T_5 = 4(16d_5 - 32d_4 + 24d_3 - 8d_2 + d_1)/R^3$$

If $r_x = 0$ and/or $r_\xi = 0$ and $z_x \neq z_\xi$, then the following substitutions should be made for F_α, G_α and T_α

$$F_1 = 2\pi/R$$

$$F_2 = 0$$

$$F_3 = F_1/2$$

$$F_4 = 0$$

$$G_1 = 2\pi R$$

$$G_2 = 0$$

$$G_3 = \pi R$$

$$T_1 = 2\pi/R^3$$

$$T_2 = 0$$

$$T_3 = T_1/2$$

$$T_4 = 0$$

$$T_5 = 3T_3/4$$

Particular Integral for Initial Stress:

$$K_{11}(x,\xi) = \pi - 3G_3$$

$$K_{14}(x,\xi) = \pi - 3(G_1-G_3)$$

$$K_{22}(x,\xi) = 2\pi - 3G_1$$

$$K_{33}(x,\xi) = -3G_2$$

$$K_{41}(x,\xi) = \pi - 3(G_1-G_3)$$

$$K_{44}(x,\xi) = \pi - 3G_3$$

Particular Integral for Displacement:

$$D_{11}(x,\xi) = A_o \{ \pi(2a_1+a_2+a_3)r_x - b_1(r_xG_1-r_\xi G_2)$$

$$- (b_2+b_3)(r_xG_3-r_\xi G_2) - b_2 [r_x(r_x^2+ 2r_\xi^2)F_3 - r_x^2 r_\xi F_4$$

$$- r_\xi(2r_x^2+r_\xi^2)F_2 + r_x r_\xi^2 F_1] \}$$

$$D_{12}(x,\xi) = A_o \{ 2\pi a_1 r_x - b_1(r_xG_1-r_\xi G_2) - b_2(r_xF_1-r_\xi F_2)z^2 \}$$

$$D_{13}(x,\xi) = -A_o z \{ 2b_2 [(r_x^2+r_\xi^2)F_2 - r_x r_\xi(F_1+F_3)] + (b_2+b_3)G_2] \}$$

$$D_{14}(x,\xi) = A_o \{ \pi(2a_1+a_2+a_3)r_x - (b_2+b_3)\ (G_1-G_3)r_x$$

$$- b_1(r_xG_1-r_\xi G_2) - b_2 r_x^2 [r_x(F_1-F_3) - r_\xi(F_2-F_4)] \}$$

$$D_{21}(x,\xi) = A_o z \{ 2\pi a_1 - b_1G_1 - b_2 (r_x^2F_3-2r_x r_\xi F_2+r_\xi^2 F_1) \}$$

$$D_{22}(x,\xi) = A_o z \{ 2\pi(a_1+a_2+a_3) - (b_1+b_2+b_3)G_1 - b_2 z^2 F_1 \}$$

$$D_{23}(x,\xi) = -A_o \{ 2\pi(a_2+a_3) r_\xi + (b_2+b_3)\ (r_xG_2-r_\xi G_1)$$

$$+ 2b_2 z^2 (r_xF_2-r_\xi F_1) \}$$

$$D_{24}(x,\xi) = A_o z \{ 2\pi a_1 - b_1G_1 - b_2 r_x^2\ (F_1-F_3) \}$$

Particular Integral for Strain:

$$E_{11}(x,\xi) = \pi(2a_1+a_2+a_3) - b_1G_1 - (b_2+b_3)G_3$$

$$+ (3b_2+b_3)r_x r_\xi F_4 - [b_1 r_\xi^2+b_2(4r_x^2+3r_\xi^2) + b_3(r_x^2+r_\xi^2)]F_3$$

$$+ r_x r_\xi\ (2b_1+5b_2+b_3)F_2 - [b_1 r_x^2+b_2 r_\xi^2]F_1$$

$$+ b_2 [r_x^2 r_\xi^2(T_1+T_5) - 2r_x r_\xi(r_x^2+r_\xi^2)(T_2+T_4) + (r_x^4+4r_x^2 r_\xi^2+r_\xi^4)T_3]$$

$$E_{12}(x,\xi) = 2\pi a_1 - b_1 G_1 - b_1(r_x^2 F_1 - 2r_x r_\xi F_2 + r_\xi^2 F_3) - b_2 z^2 F_1$$

$$+ b_2 z^2 (r_x^2 T_1 - 2r_x r_\xi T_2 + r_\xi^2 T_3)$$

$$E_{13}(x,\xi) = (3b_2+b_3) r_\xi z F_3 - (5b_2+b_3) r_x z F_2 + 2b_2 z r_\xi F_1$$

$$+ 2b_2 z \left[r_x r_\xi^2 T_4 - r_\xi (2r_x^2 + r_\xi^2) T_3 + r_x (r_x^2 + 2r_\xi^2) T_2 - r_x^2 r_\xi T_1 \right]$$

$$E_{14}(x,\xi) = \pi(2a_1+a_2+a_3) - b_1 G_1 - (b_2+b_3)(G_1 - G_3)$$

$$- b_1 (r_x^2 F_1 - 2r_x r_\xi F_2 + r_\xi^2 F_3) - (b_2+b_3)(r_x^2 F_1 - r_x r_\xi F_2 - r_x^2 F_3 + r_x r_\xi F_4)$$

$$- b_2 r_x \left[3r_x (F_1 - F_3) - 2r_\xi (F_2 - F_4) \right]$$

$$+ b_2 r_x^2 \left[r_x^2 (T_1 - T_3) - 2r_x r_\xi (T_2 - T_4) + r_\xi^2 (T_3 - T_5) \right]$$

$$E_{21}(x,\xi) = 2\pi a_1 - b_1 G_1 + b_2 z^2 (r_x^2 T_3 - 2r_x r_\xi T_2 + r_\xi^2 T_1)$$

$$- b_1 z^2 F_1 - b_2 (r_x^2 F_3 - 2r_x r_\xi F_2 + r_\xi^2 F_1)$$

$$E_{22}(x,\xi) = 2\pi(a_1+a_2+a_3) - (b_1+b_2+b_3) G_1 - [b_1+4b_2+b_3]\, z^2 F_1 + b_2 z^4 T_1$$

$$E_{23}(x,\xi) = -z(b_3+5b_2)(r_x F_2 - r_\xi F_1) + 2b_2 z^3 (r_x T_2 - r_\xi T_1)$$

$$E_{24}(x,\xi) = 2\pi a_1 - b_1 G_1 - b_1 z^2 F_1 - b_2 r_x^2 (F_1 - F_3) + b_2 z^2 r_x^2 (T_1 - T_3)$$

$$E_{31}(x,\xi) = \frac{1}{2} \{ -z \left[(3b_2+b_3) r_x F_3 - (2b_1+3b_2+b_3) r_\xi F_2 + 2b_1 r_x F_1 \right]$$

$$+ 2b_2 z \left[-r_x^2 r_\xi T_4 + r_x (r_x^2 + 2r_\xi^2) T_3 - r_\xi (2r_x^2 + r_\xi^2) T_2 + r_x r_\xi^2 T_1 \right] \}$$

$$E_{32}(x,\xi) = \frac{1}{2} \{ -z \left[(2b_1+3b_2+b_3)(r_x F_1 - r_\xi F_2) \right] + 2b_2 z^3 (r_x T_1 - r_\xi T_2) \}$$

$$E_{33}(x,\xi) = \frac{1}{2}\{ -2(b_2+b_3)G_2 + (3b_2+b_3)[(r_x r_\xi(F_1+F_3) - (r_x^2+r_\xi^2+z^2)F_2]$$

$$- 4b_2 z^2 [r_x r_\xi(T_1+T_3) - (r_x^2+r_\xi^2)T_2] \}$$

$$E_{34}(x,\xi) = \frac{1}{2}\{ -2z\, b_1(r_x F_1 - r_\xi F_2) - z(3b_2+b_3)r_x(F_1-F_3)$$

$$+ 2b_2 z\, r_x^2 [r_x(T_1-T_3) - r_\xi(T_2-T_4)] \}$$

$$E_{41}(x,\xi) = D_{11}(x,\xi)/A_o r_x$$

$$E_{42}(x,\xi) = D_{12}(x,\xi)/A_o r_x$$

$$E_{43}(x,\xi) = D_{13}(x,\xi)/A_o r_x$$

$$E_{44}(x,\xi) = D_{14}(x,\xi)/A_o r_x$$

If $r_x = 0$, then

$$E_{41}(x,\xi) = E_{11}(x,\xi)$$

$$E_{42}(x,\xi) = E_{12}(x,\xi)$$

$$E_{43}(x,\xi) = E_{13}(x,\xi)$$

$$E_{44}(x,\xi) = E_{14}(x,\xi)$$

Singular Form ($r_x = r_\xi$ and $z_x = z_\xi$):

The general form of the axisymmetric particular integrals are singular when $r_x = r_\xi$ and $z_x = z_\xi$. In this circumstance, the limiting form of these functions, given below, should be used.

$$G_1 = 8r_x$$

$$G_2 = -G_1/3$$

$$G_3 = 7G_1/15$$

$$T_1 = 4$$

$$T_2 = -4/3$$

$$T_3 = 28/15$$

Particular Integral for Initial Stress:

$$K_{11}(x,\xi) = \pi - 3G_3$$

$$K_{14}(x,\xi) = \pi - 3(G_1-G_3)$$

$$K_{22}(x,\xi) = 2\pi - 3G_1$$

$$K_{33}(x,\xi) = -3G_2$$

$$K_{41}(x,\xi) = \pi - 3(G_1-G_3)$$

$$K_{44}(x,\xi) = \pi - 3G_3$$

Particular Integral for Displacement:

$$D_{11}(x,\xi) = A_o r_x \{ 2\pi a_1 + \pi(a_2+a_3) - b_1(G_1-G_2)$$

$$- (b_2+b_3)(G_3-G_2) - b_2 r_x (T_1-2T_2+T_3) \}$$

$$D_{12}(x,\xi) = A_o r_x \{ 2\pi a_1 - b_1 (G_1-G_2) \}$$

$$D_{13}(x,\xi) = 0$$

$$D_{14}(x,\xi) = A_o r_x \{ 2\pi a_1 - b_1(G_1-G_2) - b_2 r_x(T_1-T_3) + [(a_2+a_3)\pi - (b_2+b_3)(G_1-G_3)] \}$$

$$D_{21}(x,\xi) = 0$$

$$D_{22}(x,\xi) = 0$$

$$D_{23}(x,\xi) = -A_o r_x \{ 2\pi(a_2+a_3) + (b_2+b_3)(G_2-G_1) \}$$

$$D_{24}(x,\xi) = 0$$

Particular Integral for Strain:

$$E_{11}(x,\xi) = \pi(2a_1+a_2+a_3) - b_1G_1 - (b_2+b_3)G_3 + r_x [(3b_2+b_3)(T_2-T_3) - (b_1+b_2)(T_1-T_2) + \frac{1}{2} b_2 (T_1-2T_2+T_3)]$$

$$E_{12}(x,\xi) = 2\pi a_1 - b_1G_1 - b_1 r_x(T_1-T_2)$$

$$E_{13}(x,\xi) = 0$$

$$E_{14}(x,\xi) = \pi(2a_1+a_2+a_3) - b_1G_1 - (b_2+b_3)(G_1-G_3) - r_x\{b_1(T_1-T_2) + (\frac{1}{2} b_2+b_3)(T_1-T_3) + b_2[3(T_1+T_2) - 2(T_2+T_3)]\}$$

$$E_{21}(x,\xi) = 2\pi a_1 - b_1G_1 - b_2 r_x(T_1-T_2)$$

$$E_{22}(x,\xi) = 2\pi(a_1+a_2+a_3) - (b_1+b_2+b_3)G_1$$

$$E_{23}(x,\xi) = 0$$

$$E_{24}(x,\xi) = 2\pi a_1 - b_1G_1 - b_2 r_x(T_1+T_2)$$

$$E_{31}(x,\xi) = 0$$

$$E_{32}(x,\xi) = 0$$

$$E_{33}(x,\xi) = -(b_2+b_3)G_2 + (\frac{3}{2}b_2 + \frac{1}{2}b_3)r_x(T_1-T_2)$$

$$E_{34}(x,\xi) = 0$$

$$E_{41}(x,\xi) = D_{11}(x,\xi)/A_o r_x$$

$$E_{42}(x,\xi) = D_{12}(x,\xi)/A_o r_x$$

$$E_{43}(x,\xi) = 0$$

$$E_{44}(x,\xi) = D_{14}(x,\xi)/A_o r_x$$

If $r_x = 0$, then

$$E_{41}(x,\xi) = E_{11}(x,\xi)$$

$$E_{42}(x,\xi) = E_{12}(x,\xi)$$

$$E_{43}(x,\xi) = 0$$

$$E_{44}(x,\xi) = E_{14}(x,\xi)$$

4.3 NUMERICAL IMPLEMENTATION

The present formulation is implemented in a manner analogous to Chapter 3. Essentially, the procedure consists of evaluating the relevant particular integrals at nodal points and solving equation (4.4) for these values and a set of appropriate boundary conditions. The particular integrals are a function of initial stress. However, the initial stress of an inelastic analysis is unknown and must be determined as part of the solution process. Therefore, it is necessary to assemble the equation system in a manner that will admit

to an inelastic solution algorithm. Both the iterative and the variable stiffness algorithms of Chapter 2 can be employed without modification if the assembly process presented below is utilized.

For the purpose of numerical evaluation, the particular integral series solutions of the previous section are truncated to a finite number of terms. Note, the particular integrals of each region are evaluated independent of the other regions, and calculated only in regions where inelastic effects are anticipated.

Equations for u_i^p and t_i^p are written for the boundary nodes and are expressed in matrix form for each region as

$$\begin{aligned} u^p &= D\,\emptyset \\ t^p &= T\,\emptyset \end{aligned} \qquad (4.23)$$

in which D and T are matrices of the order (f*M) by (g*N) where M is the number of boundary nodes, N is the number of terms in the series, f is the number of degrees of freedom of the analysis, and g is the number of independent stress components.

The initial stress, evaluated at the N nodal points, is expressed as

$$\sigma^o = K\,\emptyset \qquad (4.24)$$

in which K is a well conditioned (g*N) by (g*N) matrix. Post-multiplying equations (4.24) by K^{-1} yields

$$\emptyset = K^{-1}\,\sigma^o \qquad (4.25)$$

Back substituting this equation into equation (4.23) renders

$$\begin{aligned} u^p &= D\,K^{-1}\,\sigma^o \\ t^p &= T\,K^{-1}\,\sigma^o \end{aligned} \qquad (4.26)$$

Similar particular integral expressions can be written for displacement and stress at interior points of interest. The particular integral solution for stress, corresponding to nodes of equation (4.4b), is written in matrix form as

$$\sigma^p = S\, K^{-1}\, \sigma^o \tag{4.27}$$

Substituting equations (4.26) and (4.27) into equation (4.4) and rearranging yields

$$\begin{aligned} Gt - Fu + B\sigma^o &= 0 \\ \sigma = G^\sigma t - F^\sigma u + B^\sigma \sigma^o & \end{aligned} \tag{4.28}$$

where

$$B = -[GT - FD]K^{-1}$$

$$B^\sigma = -[G^\sigma T - F^\sigma D]K^{-1}$$

The equations of (4.28) are in the same form as those obtained by conventional volume integration. After the above equations are generated for all regions in a problem, they are assembled in a manner described in Chapter 2. The final system equations are expressed as

$$\begin{aligned} A^b x &= B^b y + C^b \sigma^o \\ \sigma = A^\sigma x + B^\sigma y + C^\sigma \sigma^o & \end{aligned} \tag{4.29}$$

A solution for the inelastic, incremental form of this equation is obtained using one of the two algorithms presented in Chapter 2.

Finally we note, two time-saving features that are employed in the present implementation.

First, careful observation of equation (4.15) reveals that the **K** matrix (equation 4.25), in two- and three-dimensions, consists of N^2 diagonal matrix blocks. All diagonal terms of a particular diagonal matrix block are the same value. By reducing each diagonal matrix block to a single term, the overall reduced matrix is inverted at a fraction of the cost of the whole. Expanding each term of the inverted matrix back to a diagonal matrix block produces the correct $\mathbf{K}^{-1}$.

Second, the stress for a boundary point is directly (and efficiently) calculated by the method described in section 2.3.2, instead of using the formal particular integral procedure of this chapter.

4.4 EXAMPLES

In this section, three examples are presented to demonstrate the particular integral based, inelastic analysis.

4.4.1 Three-Dimensional Analysis of a Cube with Hardening

The three-dimensional, inelastic particular integrals are tested on a unit cube in tension with plastic strain hardening. The material constants are (in consistent units): $E = 100$, $\nu = 0.3$ and $h = 50.0$. The surface of the cube is discretized (figure 4.1) using six (eight-noded) boundary elements. The particular integrals are defined using the twenty boundary nodes and one interior node located at the center of the cube. The displacement in the axial direction on a face opposite the fixed end is shown in figure 4.2 for increasing tension. The particular integral based results are in excellent agreement with the analytical solution.

4.4.2 Axisymmetric Analysis of a Thick Cylinder

A thick cylinder (1:2 ratio) subjected to interior pressure is analyzed using the axisymmetric, inelastic particular integral formulation under the plane strain condition. The axisymmetric mesh, shown in figure 4.3, has ten quadratic boundary elements. Twenty-three nodes are used to define the particular integral domain representation. The load-displacement response at the outer surface is in good agreement with the analytical solution (Hill, 1950) as shown in figure 4.4. The hoop strain at the inner and outer surface is shown in figure 4.5 for increasing pressure. Once again, the results are in good agreement with the analytical solution.

4.5 CONCLUDING REMARKS

The particular integral based boundary element formulation introduced in Chapter 3 was successfully extended to inelastic analysis in the present chapter. The system matrices produced by this method were assembled in the same form as those created using the volume integral based method, and therefore, the two inelastic solution algorithms, presented in Chapter 2, could be applied without any modifications.

The method was demonstrated for a number of problems and excellent agreement was obtained in comparison with existing results. Practical applications of the present analysis will be presented in Chapter 6.

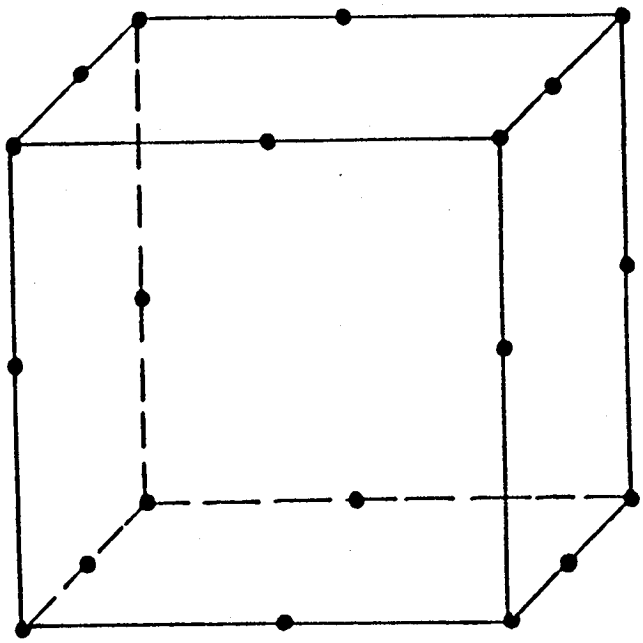

Figure 4.1
Three-dimensional Mesh of a Cube

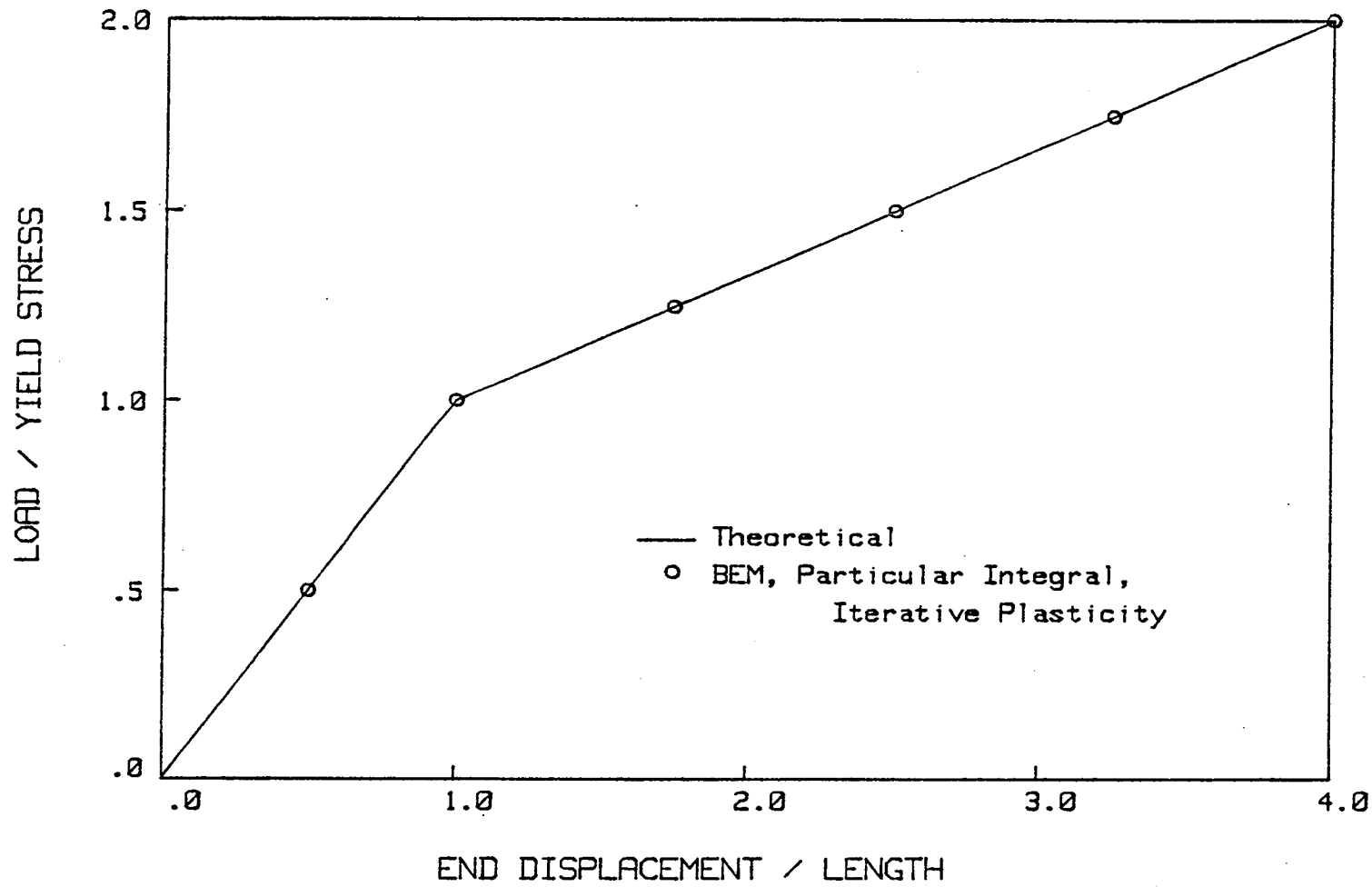

Figure 4.2
End Displacement of a Cube (with Strain Hardening) under Tension

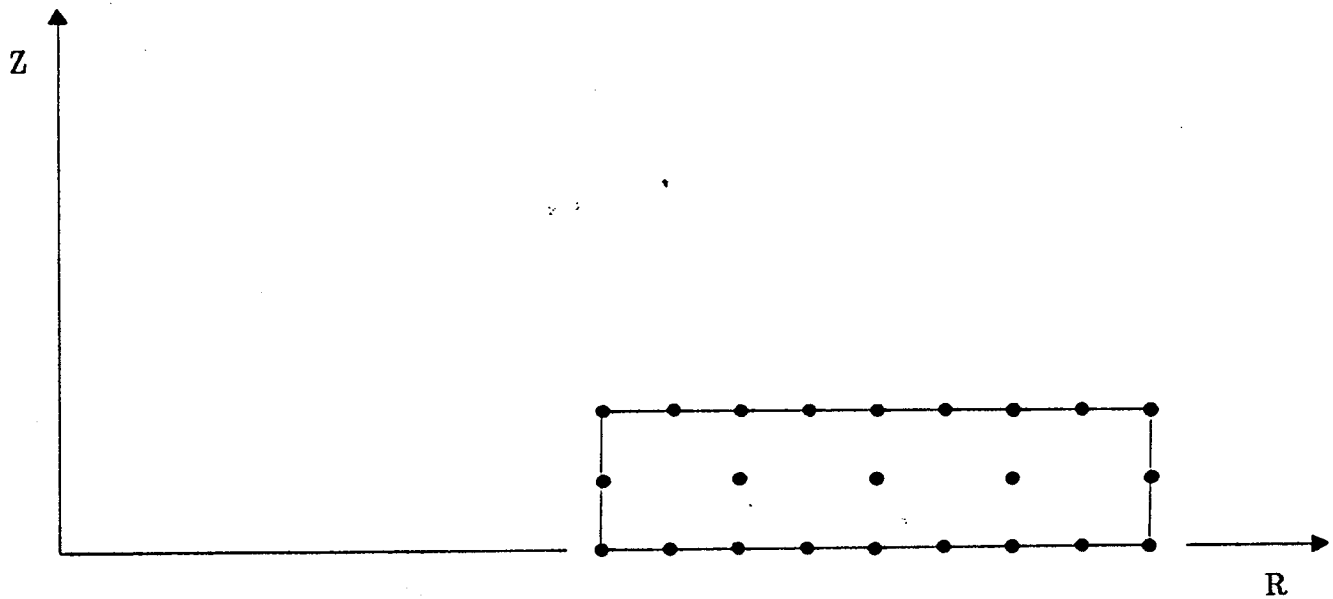

Figure 4.3
Axisymmetric Mesh of a Thick Cylinder for a Particular Integral based Plasticity Analysis (Diameter Ratio 1:2)

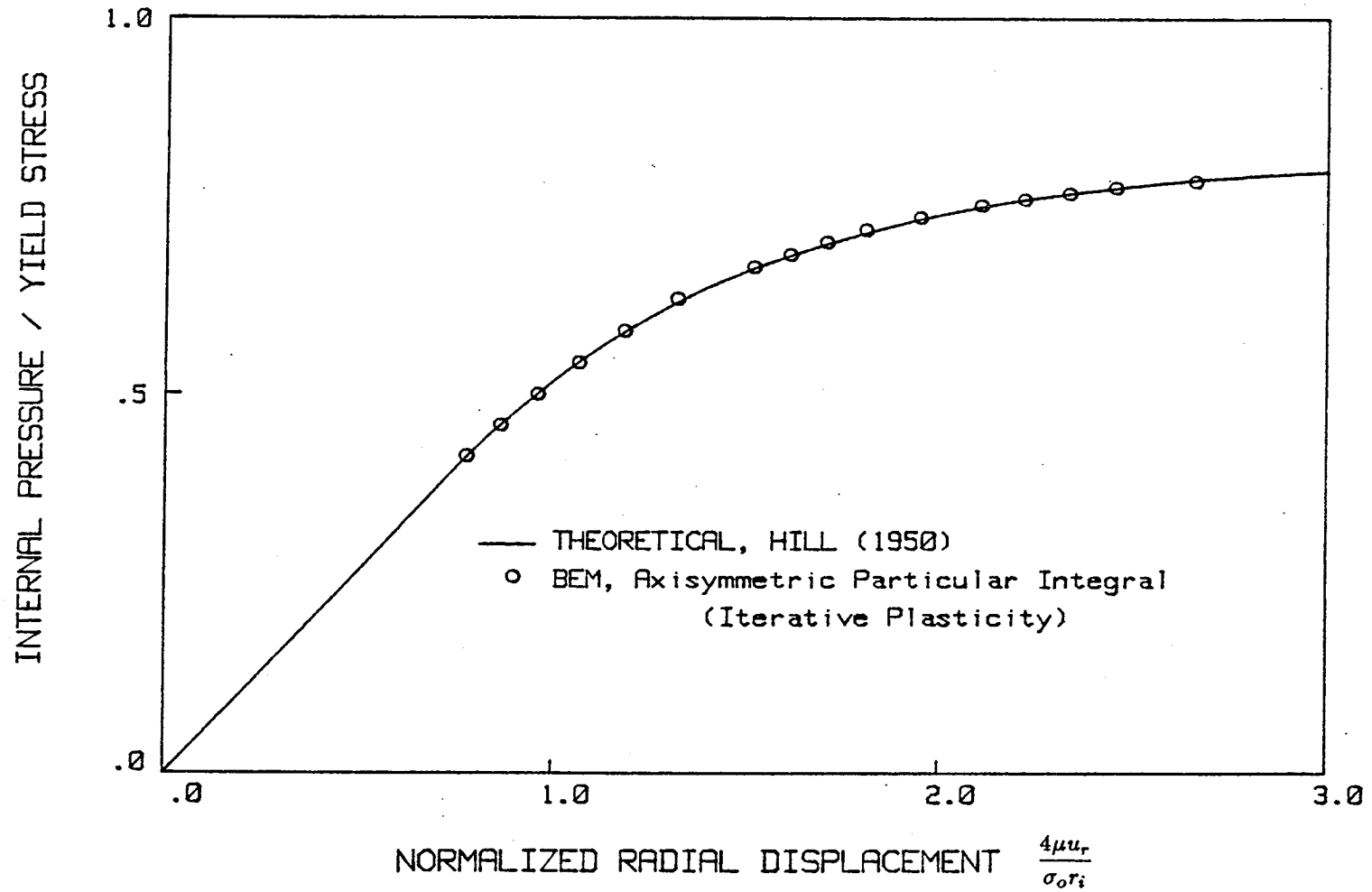

Figure 4.4
Radial Displacement of the Outer Surface of a Thick Cylinder under Internal Pressure (Plane Strain)

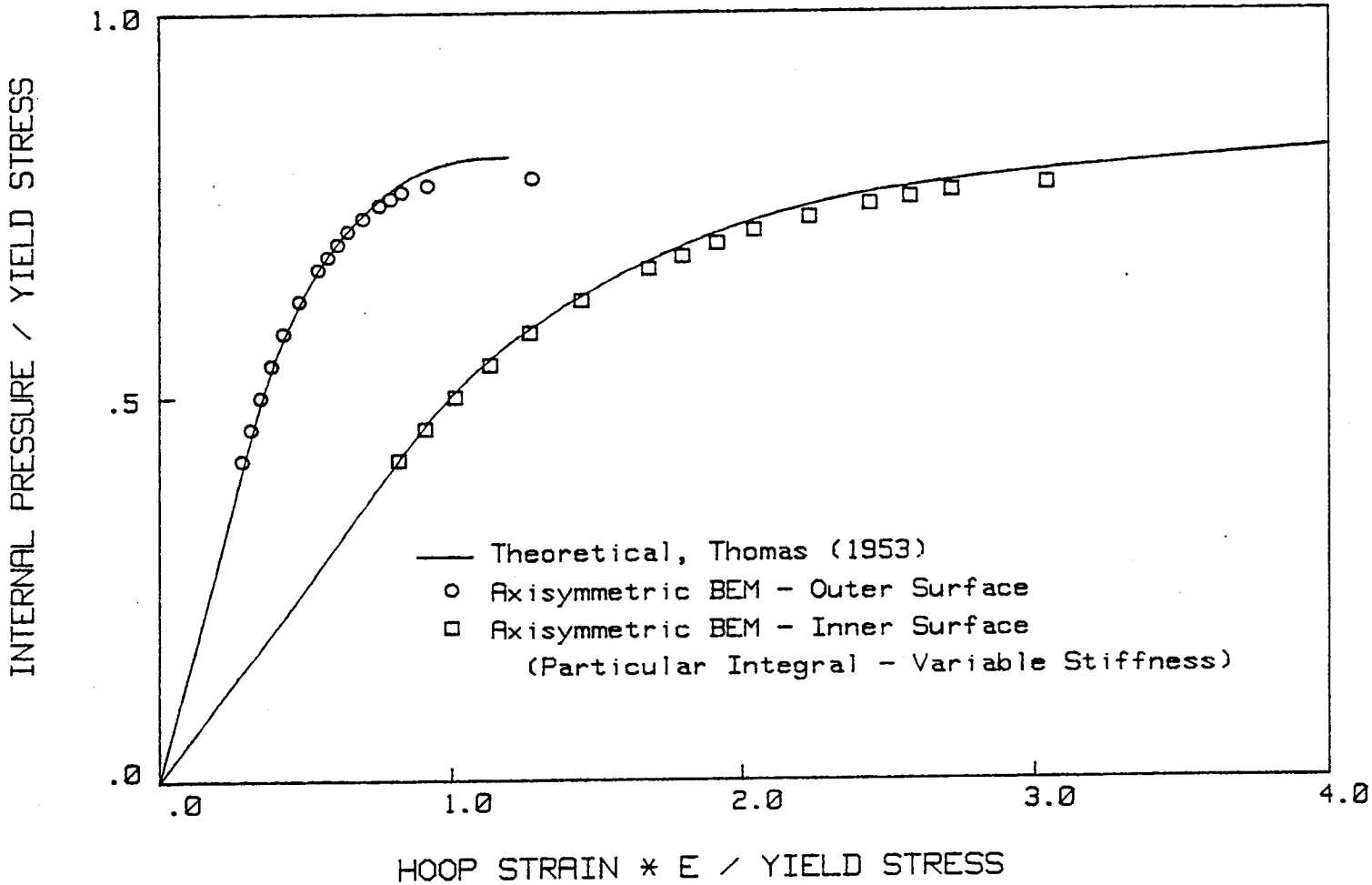

Figure 4.5
Hoop Strain in a Thick Cylinder (Plane Stress)

CHAPTER 5

BOUNDARY ELEMENT FORMULATION FOR INHOMOGENEOUS MEDIA

CHAPTER FIVE

BOUNDARY ELEMENT FORMULATION FOR INHOMOGENEOUS MEDIA

5.1 INTRODUCTION

One deficiency of the boundary element method is its inability to readily handle continuous material inhomogeneities. However, a method analogous to the plasticity procedure can be employed to overcome this difficulty. In this procedure, the effects of the inhomogeneities in the material are incorporated in the boundary element system through an initial stress body force.

In this chapter, formulations for elastic and inelastic analysis of inhomogeneous media are presented. The inhomogeneities may occur as a result of spatial variation in material parameters, or may be thermally induced when material parameters are assumed to be temperature dependent.

Successful inhomogeneous BEM formulations have been implemented by Butterfield (1978) for potential flow problems and by Ghosh and Mukherjee (1984) for thermoelastic bodies. Both of these linear analyses were based on iterative procedures. The present analysis is a direct implementation which incorporates the inhomogeneous effects into the system without iteration. This leads to a direct solution procedure for elastic inhomogeneous problems and a single iteration process for plasticity analysis. The formulations are implemented in a two-dimensional and axisymmetric, multiregion, general purpose

system. Since the procedure involves an initial stress body force, the volume must be appropriately represented in both elastic and inelastic analysis. Either the conventional volume integral or the new particular integral representation may be used for this purpose.

5.2 BEM FORMULATION FOR ELASTIC INHOMOGENEOUS MEDIA

In Chapter 2, the boundary integral equations are derived via the Betti reciprocal work theorem. Although, this theorem is valid for continuums of general material, the adoption of the Kelvin point force solution renders the resulting integral equations valid only in homogeneous, isotropic material. Nevertheless, material inhomogeneities can be incorporated in the standard boundary integral equations through a volume integral or the particular integral equivalent.

The differential equation expressed in terms of stress (equation 2.1) is independent of material, and therefore, valid for inhomogeneous material.

$$\sigma_{ij,j} + f_i = 0 \tag{5.1}$$

The strain in an elastic, inhomogeneous, isotropic body is related to stress via

$$\sigma_{ij} = D^{e,L}_{ijkl}\ \varepsilon^{m}_{kl} \tag{5.2a}$$

or

$$\varepsilon^{m}_{kl} = C^{e,L}_{ijkl}\ \sigma_{ij} \tag{5.2b}$$

where:

the superscript L indicates the use of a (local) constitutive relation that varies with position, i.e.,

$D^{e,L}_{ijkl} = \lambda(x)\ \delta_{ij}\ \delta_{kl} + 2\mu(x)\ \delta_{ik}\ \delta_{jl}$, and

mechanical strain ε^{m}_{kl} is defined in terms of total strain

$$\varepsilon^{m}_{kl} = \varepsilon_{kl} - \delta_{kl}\ \alpha(x)\ T \tag{5.3}$$

Substituting the strain-displacement equation (2.4) and equation (5.2) into equation (5.1) yields the displacement form of the equilibrium equation. Since material parameters are a function of position, the resulting expression will include spatial derivitives of these parameters. These derivitives can be avoided, however, by recasting the constitutive relation in an alternate form as described below:

The mechanical strain ε^{m}_{ij} is divided into two parts; a homogeneous strain ε^{h}_{ij} and an inhomogeneous strain ε^{i}_{ij}.

$$\varepsilon^{m}_{ij} = \varepsilon^{h}_{ij} + \varepsilon^{i}_{ij} \tag{5.4}$$

The homogeneous strain is defined with respect to global reference material parameters λ^{G} and μ^{G} that do not vary with position.

$$\varepsilon^{h}_{ij} = C^{e,G}_{ijkl}\ \sigma_{kl} \tag{5.5}$$

or

$$\sigma_{ij} = D^{e,G}_{ijkl}\ \varepsilon^{h}_{kl} \tag{5.6}$$

where $C^{e,G}_{ijkl}$, $D^{e,G}_{ijkl}$ are the global compliance tensors. The inhomogeneous strain is simply the supplement part

$$\varepsilon^{i}_{ij} = \varepsilon^{m}_{ij} - \varepsilon^{h}_{ij} \tag{5.7}$$

Using equation (5.4) in equation (5.6) yields an expression for stress in terms of the global compliance tensor:

$$\sigma_{ij} = D^{e,G}_{ijkl}\ \varepsilon^{m}_{kl} - \sigma^{i}_{kl} \tag{5.8}$$

where

$$\sigma^{i}_{kl} = D^{e,G}_{ijkl}\ \varepsilon^{i}_{kl} \tag{5.9}$$

or using the definition of mechanical strain, a relation between stress and total strain can be expressed as

$$\sigma_{ij} = D^{e,G}_{ijkl}\ \varepsilon_{kl} - \sigma^{t}_{kl} - \sigma^{i}_{kl} \tag{5.10}$$

where

$$\sigma^{t}_{kl} = D^{e,G}_{ijkl}\ \delta_{kl}\ \alpha(x)\ T \tag{5.11}$$

Note in this calculation the local value $\alpha(x)$ is assumed, but the constitutive relation is with respect to global reference parameters.

Substitution of equation (5.10) and the strain-displacement relation into equation (5.1) leads to the displacement equilibrium equation expressed in terms global material parameters:

$$(\lambda^{G}+\mu^{G})\ u_{j,ij} + \mu^{G}\ u_{i,jj} + f_i = \sigma^{o}_{ij,j} \tag{5.12}$$

where

$$\sigma^{o}_{ij} = \sigma^{t}_{ij} + \sigma^{i}_{ij}$$

Note, since λ^{G} and μ^{G} are not a function of position, they are removed from within the differential operators.

Equation (5.12) is the extended form of the Navier equation, expressed in terms of the global reference parameters. The boundary integral equations satisfying equation (5.12) were presented in Chapter 2. The expression for displacement (neglecting body forces) is repeated here.

$$C_{ij}(\xi)u_i(\xi) = \int_S [G_{ij}(x,\xi)t_i(x) - F_{ij}(x,\xi)u_i(x)]\, dS(x)$$

$$+ \int_V B_{ikj}(x,\xi)\ \sigma^{o}_{ik}(x)\ dV(x) \qquad (5.13)$$

where the kernel functions assume the global reference parameters. Similar expressions for stress and strain can be written. Alternatively, a solution satisfying equation (5.12) also can be formulated using the particular integral procedure presented in the previous chapter. Regardless of the formulation employed, the final form of the system equations are the same for both the volume integral and the particular integral based procedures. The solution to the boundary value problem requires the knowledge of the inhomogeneous part of the initial stress. To this end, equation (5.2) is set equal to equation (5.8), and upon rearranging, the following relation is obtained.

$$\sigma^{i}_{ij} = (D^{e,G}_{ijkl} - D^{e,L}_{ijkl})\ \varepsilon^{m}_{kl} \qquad (5.14)$$

This expression is analogous to equation (2.52c) of the plasticity formulation and it plays a similar role in the iterative procedure for inhomogeneous problem. However, unlike plasticity, the elastic, inhomogeneous analysis is not incremental.

The inhomogeneous problem can be solved using the following iterative procedure. The integral equations for the boundary system and interior stresses are integrated and assembled in the usual manner (Chapters 2 and 4). σ^i_{ij} is initially assumed to be zero. The boundary problem is solved under this condition and the resulting stresses (and strains) are determined at cell nodes (or particular integral nodes). Using equation (5.14), the inhomogeneous part of the initial stresses are determined at these same nodes. In addition to the external loading, the calculated values for the inhomogeneous (initial) stress are applied to the system. The problem is resolved and new values for σ^i_{ij} are determined. This process is repeated until a convergenced solution is obtained.

The rate of convergence is dependent on the degree of inhomogeneity, the choice of global reference parameters, and the geometry and loading of the problem. In some cases the convergence may be slow or may not converge at all. For this reason, a direct algorithm, analogous to the variable stiffness plasticity method of Chapter 2, is developed. In this procedure, the unknown, inhomogeneous part of the initial stress is eliminated from the boundary system permitting a direct solution.

The present formulation is implemented on a nodal basis, and therefore, the subsequent derivation is carried out on the discrete nodal equations rather than on the (continuous) integral equation. First, the integral equations are integrated for a system of nodal equations and assembled in a manner described in Chapter 2 or Chapter 4. Since the assembled form of the boundary equations are similar for both the volume integral base method and the particular integral

formulation, no distinction is necessary in the present derivation. These assembled equations are repeated here in matrix form:

$$A^b x = B^b y + C^b{}_\sigma t + C^b{}_\sigma i \tag{5.15a}$$

$$\sigma = A^\sigma x + B^\sigma y + C^\sigma{}_\sigma t + C^\sigma{}_\sigma i \tag{5.15b}$$

where a stress equation is written for every node where the unknown σ^i_{ij} exist. Therefore, C^σ is a square matrix.

Substituting equation (5.2b) into equation (5.14) we arrive at the nodal relation

$$\sigma^i_{ij} = (D^{e,G}_{ijkl} - D^{e,L}_{ijkl})\ C^{e,L}_{klmn}\ \sigma_{mn} \tag{5.16}$$

In the present work, we will assume the modulus of elasticity may vary with position, but Poisson's ratio is constant over the domain. This is a realistic assumption for most materials. Upon invoking this assumption, the following simplification is possible.

$$(D^{e,G}_{ijkl} - D^{e,L}_{ijkl})\ C^{e,L}_{klmn} = \frac{E^G - E^L}{E^L}\ \delta_{im}\ \delta_{jn} \tag{5.17}$$

where E^G and E^L are global and local moduli of elasticity, respectively. Substituting this result in equation (5.16) and rearranging yields

$$\sigma_{ij} = H\ \sigma^i_{ij} \tag{5.18a}$$

where

$$H = \frac{E^L}{E^G - E^L} \tag{5.18b}$$

Applying this relation to the nodes of equation (5.15), a matrix expression can be written:

$$\sigma = Ih\sigma^i \tag{5.19}$$

where I represents the identify matrix and h represents a nodal vector of corresponding nodal values of H.

Substituting equation (5.19) into equation (5.15b) yields

$$Ih\sigma^i = A^\sigma x + B^\sigma y + C^\sigma\sigma^t + C^\sigma\sigma^i \tag{5.20}$$

and upon rearranging equations (5.15a) and (5.20) we have

$$A^b x = b^b + C^b\sigma^i \tag{5.21a}$$

$$D\sigma^i = A^\sigma x + b^\sigma \tag{5.21b}$$

where

$$b^b = B^b y + C^b\sigma^t$$

$$b^\sigma = B^\sigma y + C^\sigma\sigma^t$$

$$D = Ih - C^\sigma$$

Equation (5.21b) can then be recast as:

$$\sigma^i = D^{-1}\,(A^\sigma x + b^\sigma) \tag{5.22}$$

Substituting the above equation into equation (5.21a) results in the final system equation:

$$A^* x = b^* \tag{5.23}$$

where

$$A^* = A^b - EA^\sigma,$$

$$\mathbf{b}^* = \mathbf{b}^b + \mathbf{E}\mathbf{b}^\sigma, \text{ and}$$

$$\mathbf{E} = \mathbf{C}^b\mathbf{D}^{-1}$$

This equation can be solved for the unknown vector $\mathbf{x}$ using standard numerical techniques. Once $\mathbf{x}$ is found, equation (5.22) is used to calculate the inhomogeneous part of the initial stress, and equation (5.19) is used to evaluate the corresponding stress at these nodes. With vector $\mathbf{x}$ and σ^i determined, the displacement, stress or strain can be found at any point.

In a multi-region system, the matrices of the above equations are block-banded. When the above formulation is efficiently implemented, this property leads to a reduction of work in the matrix multiplication. Furthermore, the inversion of matrix $\mathbf{D}$ is carried out one region at a time in a substructured analysis.

5.3 BEM FORMULATION FOR INELASTIC INHOMOGENEOUS MEDIA

The total inelastic strain increment is comprised of an elastic, plastic and thermal strain rate components:

$$\dot{\varepsilon}_{ij} = \dot{\varepsilon}^e_{ij} + \dot{\varepsilon}^p_{ij} + \dot{\varepsilon}^t_{ij} \tag{5.24}$$

The elastic strain rate can be unceremoniously divided into two parts: a homogeneous strain rate $\dot{\varepsilon}^h_{ij}$; and a inhomogeneous strain rate $\dot{\varepsilon}^i_{ij}$.

$$\dot{\varepsilon}^e_{ij} = \dot{\varepsilon}^i_{ij} + \dot{\varepsilon}^h_{ij} \tag{5.25}$$

using global material constants, $\dot{\varepsilon}^h_{ij}$ can arbitrarily be defined as

$$\dot{\varepsilon}^h_{ij} = D^{e,G}_{ijkl}\,\dot{\sigma}_{kl} \tag{5.26a}$$

or $$\dot{\sigma}_{ij} = D^{e,G}_{ijkl}\ \dot{\varepsilon}^{h}_{kl} \tag{5.26b}$$

and $\dot{\varepsilon}^{i}_{ij}$ is defined as the difference between $\dot{\varepsilon}^{e}_{ij}$ and $\dot{\varepsilon}^{h}_{ij}$

In light of equation (5.25), equation (5.24) can be rewritten as

$$\dot{\varepsilon}^{h}_{ij} = \dot{\varepsilon}_{ij} - \dot{\varepsilon}^{t}_{ij} - \dot{\varepsilon}^{i}_{ij} - \dot{\varepsilon}^{p}_{ij} \tag{5.27}$$

and substituting this result in equation (5.26b) leads to the following relation for stress rates.

$$\dot{\sigma}_{ij} = D^{e,G}_{ijkl}\ \dot{\varepsilon}_{kl} - D^{e,G}_{ijkl}\ \dot{\varepsilon}^{t}_{kl} - D^{e,G}_{ijkl}\ \dot{\varepsilon}^{i}_{kl} - D^{e,G}_{ijkl}\ \dot{\varepsilon}^{p}_{ij} \tag{5.28}$$

Rewriting the above equation in simpler form yields a global constitutive relation for inhomogeneous plastic media.

$$\dot{\sigma}_{ij} = D^{e,G}_{ijkl}\ \dot{\varepsilon}_{kl} - \dot{\sigma}^{o}_{ij} \tag{5.29}$$

where

$$\dot{\sigma}^{o}_{ij} = \dot{\sigma}^{t}_{ij} + \dot{\sigma}^{i}_{ij} + \dot{\sigma}^{p}_{ij} \tag{5.30a}$$

$$\dot{\sigma}^{t}_{ij} = D^{e,G}_{ijkl}\ \dot{\varepsilon}^{t}_{kl} \tag{5.30b}$$

$$\dot{\sigma}^{i}_{ij} = D^{e,G}_{ijkl}\ \dot{\varepsilon}^{i}_{kl} \tag{5.30c}$$

$$\dot{\sigma}^{p}_{ij} = D^{e,G}_{ijkl}\ \dot{\varepsilon}^{p}_{kl} \tag{5.30d}$$

The displacement rate formulation of the equilibrium equation for inhomogeneous media is derived by substituting the above constitutive relation and the strain-displacement relation into the stress rate equilibrium equation. The resulting equilibrium equation is

$$(\lambda^G + \mu^G)\, \dot{u}_{j,ij} + \mu^G\, \dot{u}_{i,jj} + \dot{f}_i = \dot{\sigma}^o_{ij,j} \qquad (5.31)$$

where λ^G, μ^G are the global material constants, and the initial stress rates are defined by equation (5.30).

Once again, it is apparent that the boundary integral equation derived in Chapter 2 or the alternate particular integral formulation of Chapter 4, satisfies the above equilibrium equation. The thermal (initial) stress rates are calculated from the known temperature distribution, however, the initial stress rates for the plastic and inhomogeneous effects, are unknown and must be determined as part of the solution procedure. Therefore, it is necessary to derive a relation between these initial stress rates and the current rate of stress.

A relation for the inhomogeneous (initial) stress $\dot{\sigma}^i_{ij}$ will be derived first. In both the elastic and plastic regions, the elastic strain rate is related to the stress rate via the local elastic constitutive relation.

$$\dot{\sigma}_{ij} = D^{e,L}_{ijkl}\, \dot{\varepsilon}^e_{kl} \qquad (5.32a)$$

or

$$\dot{\sigma}_{ij} = D^{e,L}_{ijkl}\, (\dot{\varepsilon}^m_{kl} - \dot{\varepsilon}^p_{kl}) \qquad (5.32b)$$

where

$$\dot{\varepsilon}^m_{kl} = \dot{\varepsilon}_{kl} - \dot{\varepsilon}^t_{kl}\ , \text{ and}$$

$$\dot{\varepsilon}^p_{kl} = 0 \qquad \text{in the elastic region}$$

(This equation is analogous to equation (5.2) of the previous section.) Equating this with equation (5.28) and rearranging leads to

the desired relation

$$\dot{\sigma}^{i}_{ij} = (D^{e,G}_{ijkl} - D^{e,L}_{ijkl})\ (\dot{\varepsilon}^{m}_{kl} - \dot{\varepsilon}^{p}_{kl}) \qquad (5.33a)$$

or

$$\dot{\sigma}^{i}_{ij} = (D^{e,G}_{ijkl} - D^{e,L}_{ijkl})\ (\dot{\varepsilon}^{m}_{kl}) \quad \text{for the elastic region} \qquad (5.33b)$$

Next a relation involving the plastic (initial) stress is derived using the local elastoplastic constitutive relation (equation (2.50)):

$$\dot{\sigma}_{ij} = D^{ep,L}_{ijkl}\ \dot{\varepsilon}^{m}_{kl} \qquad (5.34)$$

Equating this to equation (5.29) yields

$$\dot{\sigma}^{i}_{ij} + \dot{\sigma}^{p}_{ij} = (D^{e,G}_{ijkl} - D^{ep,L}_{ijkl})\dot{\varepsilon}^{m}_{kl} \quad \text{for the plastic region.} \qquad (5.35)$$

The equations above suggest the use of a single iterative procedure in which the effects of the inhomogeneity and plasticity are treated together. In an iterative algorithm (similar to the one in Chapter 2) a small load increment is applied to the system, and the resulting elastic stress state is determined. Theoretically, this stress state is checked at nodal points through the domain and depending whether or not the yield condition is violated, either equation (5.33b) or equation (5.35) is employed. However, when inhomogeneities exist in the body, the boundary integral equations will yield a fictitious state of stress that is dependent on the global reference parameters, and therefore, the choice of equation (5.33b) or (5.35) is not clear. The proper choice, however, is critical since plastic deformation is irrecoverable and the use of the wrong equation will ultimately result in error. So, before the effect of plasticity can be accounted for, the actual inhomogeneous elastic

stress state must be determined by its own initial stress correction. Hence, a double iterative procedure is necessary to account first, for the inhomogeneity effect, and second, the plasticity effect. More specifically, between each iterative step of the plasticity algorithm, it is implied that a converge inhomogeneous state is achieved through a separate iteration.

This double iteration is very costly and a scheme for accelerating the convergence (similar to that of Chapter 2) would be essential. Also, further study may reveal that additional savings can be obtained at later iterations, i.e., during initial iterations of each load step, a double iteration process is necessary, however, at later iterations, when the plastic regime is clearly defined, a single iterative procedure may prove viable.

Nevertheless, a semi-direct method, based on the direct formulation of the previous section, is possible. In this procedure, the inhomogeneous effects are directly incorporated in the boundary system through a back-substitution of the stress rate equations, and the plastic deformation is incorporated in the system through an iteration process. Hence, the method entails only a single iteration process in which inhomogeneity is satisfied at all times. In the present work this approach is adopted. Therefore, it is necessary to separate the plasticity and inhomogeneities effects of equation (5.35). This could be accomplished by subtracting equation (5.33a) from equation (5.35), resulting in

$$\dot{\sigma}^{p}_{ij} = (D^{e,L}_{ijkl} - D^{ep,L}_{ijkl})\dot{\varepsilon}^{m}_{kl} + (D^{e,G}_{ijkl} - D^{e,L}_{ijkl})\dot{\varepsilon}^{p}_{kl}$$

$$= D^{e,G}_{ijkl}\,\dot{\varepsilon}^{p}_{kl} \qquad (5.36)$$

This equation, however, is not an explicit relation between the plastic (initial) stress rate and the current rate of stress (or strain). Therefore, this equation is reformulated in an alternate manner consistent with Chapter 2. From equation (2.52c), the mechanical strain at a point in which yielding occurs is related to the plastic (initial) stress rate via

$$\dot{\bar{\sigma}}^{p}_{ij} = (D^{e,L}_{ijkl} - D^{ep,L}_{ijkl})\dot{\varepsilon}^{m}_{ijkl} \tag{5.37}$$

The bar indicates that the plastic stress rate is related to the plastic strain rate through the local constitutive relations as follows

$$\dot{\varepsilon}^{p}_{ij} = C^{e,L}_{ijkl}\ (D^{e,L}_{klmn} - D^{ep,L}_{klmn})\dot{\varepsilon}^{m}_{mn} \tag{5.38}$$

Substitution of this result into equation (5.30d) yields the desired form of the relation:

$$\dot{\sigma}^{p}_{ij} = D^{e,G}_{ijkl}\ C^{e,L}_{klmn}\ (D^{e,L}_{mnop} - D^{ep,L}_{mnop})\dot{\varepsilon}^{m}_{op} \tag{5.39}$$

(This is a restatement of equation (5.36)). With equations (5.33) and (5.39), the semi-direct BEM procedure for inelastic, inhomogeneous media can be formulated.

We begin with the system equations (from either Chapter 2 or 4) expressed in matrix form:

$$\mathbf{A}^{b}\dot{\mathbf{x}} = \mathbf{B}^{b}\dot{\mathbf{y}} + \mathbf{C}^{b}_{\sigma}\dot{\mathbf{t}} + \mathbf{C}^{b}_{\sigma}\dot{\mathbf{i}} + \mathbf{C}_{\sigma}\dot{\mathbf{p}} \tag{5.40a}$$

$$\dot{\boldsymbol{\sigma}} = \mathbf{A}^{\sigma}\dot{\mathbf{x}} + \mathbf{B}^{\sigma}\dot{\mathbf{y}} + \mathbf{C}^{\sigma}_{\sigma}\dot{\mathbf{t}} + \mathbf{C}^{\sigma}_{\sigma}\dot{\mathbf{i}} + \mathbf{C}^{\sigma}_{\sigma}\dot{\mathbf{p}} \tag{5.40b}$$

Once again, the Poisson ratio is assumed not to vary spatially within a substructured region. Therefore, the following relation between the stress rate and the inhomogeneous (initial) stress rate can be written:

$$\dot{\sigma}^{i}_{ij} = \frac{1}{H}\,\dot{\sigma}_{ij} \tag{5.41}$$

where

$$H = \frac{E^{L}}{E^{G}-E^{L}}$$

or expressed in matrix form for the nodes of equation (4.40b)

$$\dot{\sigma} = Ih\,\dot{\sigma}^{i} \tag{5.42}$$

Substituting this into equation (4.40b) leads to

$$Ih\,\dot{\sigma}^{i} = A^{\sigma}\dot{x} + B^{\sigma}\dot{\sigma}^{t} + C^{\sigma}\dot{\sigma}^{t} + C^{\sigma}\dot{\sigma}^{i} + C^{\sigma}\dot{\sigma}^{p} \tag{5.43}$$

and rearranging equations (5.40a) and (5.43) yields.

$$A^{b}\dot{x} = \dot{b}^{b} + C^{b}\dot{\sigma}^{i} + C^{b}\dot{\sigma}^{p} \tag{5.44a}$$

$$\dot{\sigma}^{i} = D^{-1}\,(A^{\sigma}\dot{x} + \dot{b}^{\sigma} + C^{\sigma}\dot{\sigma}^{p}) \tag{5.44b}$$

where

$$\dot{b}^{b} = B^{b}\dot{y} + C^{b}\dot{\sigma}^{t}$$

$$\dot{b}^{\sigma} = B^{\sigma}\dot{y} + C^{\sigma}\dot{\sigma}^{t}$$

$$D = Ih - C^{\sigma}$$

Substituting equation (5.44b) into (5.44a) results in the final system equation:

$$\mathbf{A}^{*}\dot{\mathbf{x}} = \dot{\mathbf{b}}^{*} + \mathbf{C}^{*}\dot{\boldsymbol{\sigma}}^{p} \tag{5.45}$$

where

$$\mathbf{A}^{*} = \mathbf{A}^{b} - \mathbf{E}\mathbf{A}^{\sigma}$$

$$\dot{\mathbf{b}}^{*} = \dot{\mathbf{b}}^{b} + \mathbf{E}\dot{\mathbf{b}}^{\sigma}$$

$$\mathbf{C}^{*} = \mathbf{C}^{b} + \mathbf{E}\mathbf{C}^{\sigma}$$

$$\mathbf{E} = \mathbf{C}^{b}\mathbf{D}^{-1}$$

This equation system for inhomogeneous inelastic material takes on the same form as the homogeneous, inelastic equation (see eq. 2.54), and can be solved in a similar fashion using the iterative plasticity method. The stress at cell nodes (or particular integral nodes) can be found using equation (5.42) where the corresponding inhomogeneous (initial) stress $\dot{\boldsymbol{\sigma}}^{i}$ is defined by equation (5.44b). After the unknowns on the boundary have been determined, the displacement and stress at any point in the body can be found with the appropriate discretized integral equation.

A few comments are in order. First, when the inhomogeneities are caused by a prescribed variation in material parameters, the inhomogeneities remain constant and the boundary system need only be constructed once. However, thermally induced inhomogeneities vary with change of temperature and the boundary system should, in principle, be reconstructed at every load increment. Thermally induced inhomogeneities are, however, very mild and reconstruction is not necessary at every load step. Instead, reconstruction can be

delayed until the resulting error surpasses a prescribed tolerance.

This brings us to the second point; efficiency. Although it is necessary to explicitly construct the $\mathbf{A}^*$ matrix (and in the process construct the $\mathbf{D}^{-1}$ and $\mathbf{E}$ matrices), other matrix manipulations associated with the right hand side of equation (5.45) are unnecessary and can be handled more efficiently through a series of matrix/vector multiplications. More specifically, equation (5.45) should be set up in the following manner.

$$\mathbf{A}^*\dot{\mathbf{x}} = \dot{\mathbf{b}}^1 + \dot{\mathbf{b}}^2 \tag{5.46}$$

where

$$\dot{\mathbf{b}}^1 = \dot{\mathbf{b}}^b + \mathbf{C}^b{}_\sigma \dot{\mathbf{p}}$$

$$\dot{\mathbf{b}}^2 = \mathbf{E}\dot{\mathbf{b}}^3$$

$$\dot{\mathbf{b}}^3 = \dot{\mathbf{b}}^\sigma + \mathbf{C}^\sigma{}_\sigma \dot{\mathbf{p}}$$

Note vector $\mathbf{b}^3$ can be used a second time during the calculation of the inhomogeneous (initial) stress rates (equation (5.44b)) and subsequent calculation of the real stress rate (equation (5.42)).

Finally, it is possible to formulate an entirely direct approach, for the analysis of inelastic, inhomogeneous media, by employing the variable stiffness plasticity technique together with the direct formulation for inhomogeneities. However, this approach is very costly and inefficient due to the large amount of matrix manipulations involved. For instance, the matrix multiplications in equation (5.44b) and (5.42) has to be carried out explicitly in order to form the inhomogeneous stress rate equation. And, in addition to the

construction of matrix $\mathbf{A}^*$ of equation (5.45), the $\mathbf{C}^*$ matrix also has to be explicitly constructed. Finally, once the inhomogeneous operations are complete, the matrix operations associated with the variable stiffness method must still be carried out. Therefore, the overhead involved in the setup of the completely direct procedure will inhibit its chance of becoming a viable alternative. This is particularly true for thermally induced inhomogeneities since it requires repeated construction of the inhomogeneous system.

5.4 EXAMPLES

In this section, three examples are presented to demonstrate the inhomogeneous formulations. Inhomogeneous variation is usually relatively mild in most problems. However, for purpose of demonstration, severe variations are assumed in these examples.

5.4.1 Elastic Rod with Spatially Varying Modulus

An elastic cylindrical rod shown in figure 5.1a has an elastic modulus that varies through the length. A uniform traction is applied to top, and the bottom surface is fixed in the axial direction. An axisymmetric discretization, shown in figure 5.1b, has three boundary elements and one volume cell. The material properties of the rod are (in consistent units):

$$E(z) = \frac{100}{1+z}$$

$$\nu = 0.3$$

The global reference modulus is assumed to be unity $E^G = 1.0$. The axial strain through the cube is shown in figure 5.2 for an applied traction of $t_z = 100$. Good agreement is obtained with the analytical

solution $\varepsilon_z = (1+z)$.

5.4.2 Elastic Cube with Temperature Dependent Modulus

An elastic cube with a temperature dependent elastic modulus is analyzed under plane strain conditions. For a cube in plane strain with boundary conditions shown in 5.3a and subjected only to thermal loading, the following relations are obtained

$$\varepsilon_x = \frac{(1+\nu)}{(1-\nu)} \alpha T$$

$$\varepsilon_y = \varepsilon_z = \varepsilon_{xy} = 0$$

$$\sigma_x = \sigma_{xy} = 0$$

$$\sigma_y = \sigma_z = -E \frac{\alpha T}{(1-\nu)}$$

In most materials, the modulus is usually assumed to vary as a linear function of temperature within a prescribed temperature range. In terms of temperature T this can be expressed as

$$E(t) = E_o + k(T-T_o)$$

where E_o is the elastic modulus at the reference temperature T_o. The change in modulus in most real materials is usually quite small, and therefore, k is usually a very small value. However, in this example a severe variation of elastic modulus (k=1) is assumed for demonstration purposes. The assumed temperature distribution and material properties are (in consistent units):

$$T(x) = 100x$$

$$\alpha = 0.7 \times 10^{-3}$$

$\nu = 0.3$

$E_o = 100.0 \quad \text{at} \quad T_o = 0.0$

$k = 1.0$

Therefore,

$$E(T) = 100 + T$$

or

$$E = 100\ (1+x)$$

Substituting these values in the expression for stress and strain yield

$$\varepsilon_x = 0.13x$$

$$\sigma_y = -10x(1+x)$$

and integrating the strain across the length yields an expression for displacement:

$$u_x = 0.065x^2$$

The discretization of the cube, shown in figure 5.3b, has four boundary elements and nine particular integral nodes. The displacement and stress profile obtained from the analysis is shown in figures 5.4 and 5.5, respectively. Good agreement is obtained in comparison to the analytical solutions.

5.4.3 Plastic Analysis of a Cube with Spatially Varying Modulus

The plastic deformation of an inhomogeneous cube (figure 5.6a) in tension is analyzed under plane strain conditions. The discretization, shown in figure 5.6b, consists of four boundary elements and one volume cell. The material properties, described

below, assume a modulus of elasticity that varies as a function of x. Given in consistent units:

$E = 100/(1+x)$

$\nu = 0.3$

$\sigma_o = 100.0$

$h = 50.0$

$E^G = 1.0$

In figure 5.7, the displacement rate profile through the cube in the x direction (at y = 0) is given for loads: $t_x = 100.$ (yield), $t_x = 110.$, $t_x = 120.$, and $t_x = 130.$ Good agreement is found in comparison with the analytical solution. A similar graph is given for the lateral displacement rate (at y = 0.5) in figure 5.8. Once again, good agreement, with the analytical solution, is obtained.

5.5 CONCLUDING REMARKS

An axisymmetric and two-dimensional, boundary element formulations were derived for elastic and inelastic, thermal, inhomogeneous media. The elastic formulation employed a direct solution procedure. The inelastic formulation used a semi-direct procedure based on the iterative plasticity algorithm presented in Chapter 2. The results obtained by this method for the example problems were in excellent agreement with analytical solutions.

The present formulation can be extended to three-dimensional analysis without difficulty.

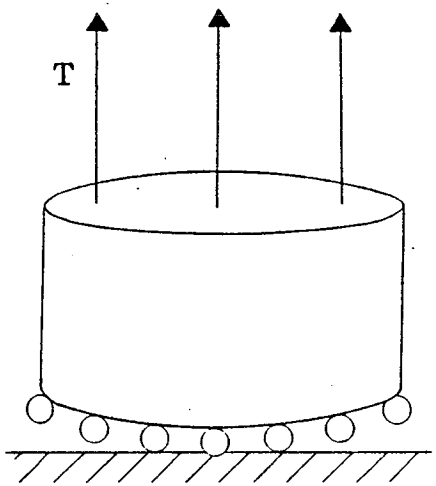

Figure 5.1a
Inhomogeneous Cylindrical Rod in Axial Tension

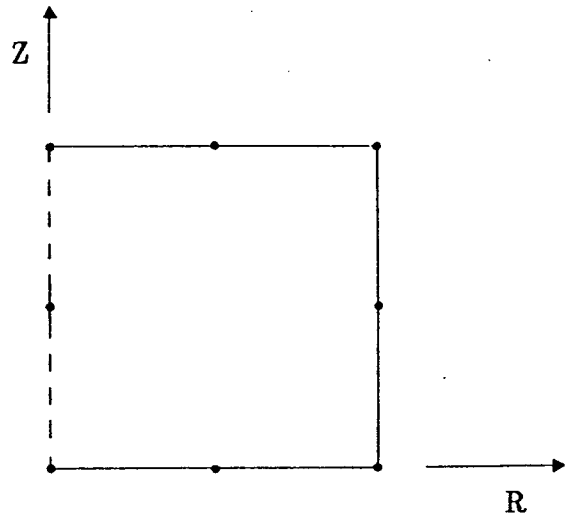

Figure 5.1b
Axisymmetric Mesh of a Cylindrical Rod with One Volume Cell

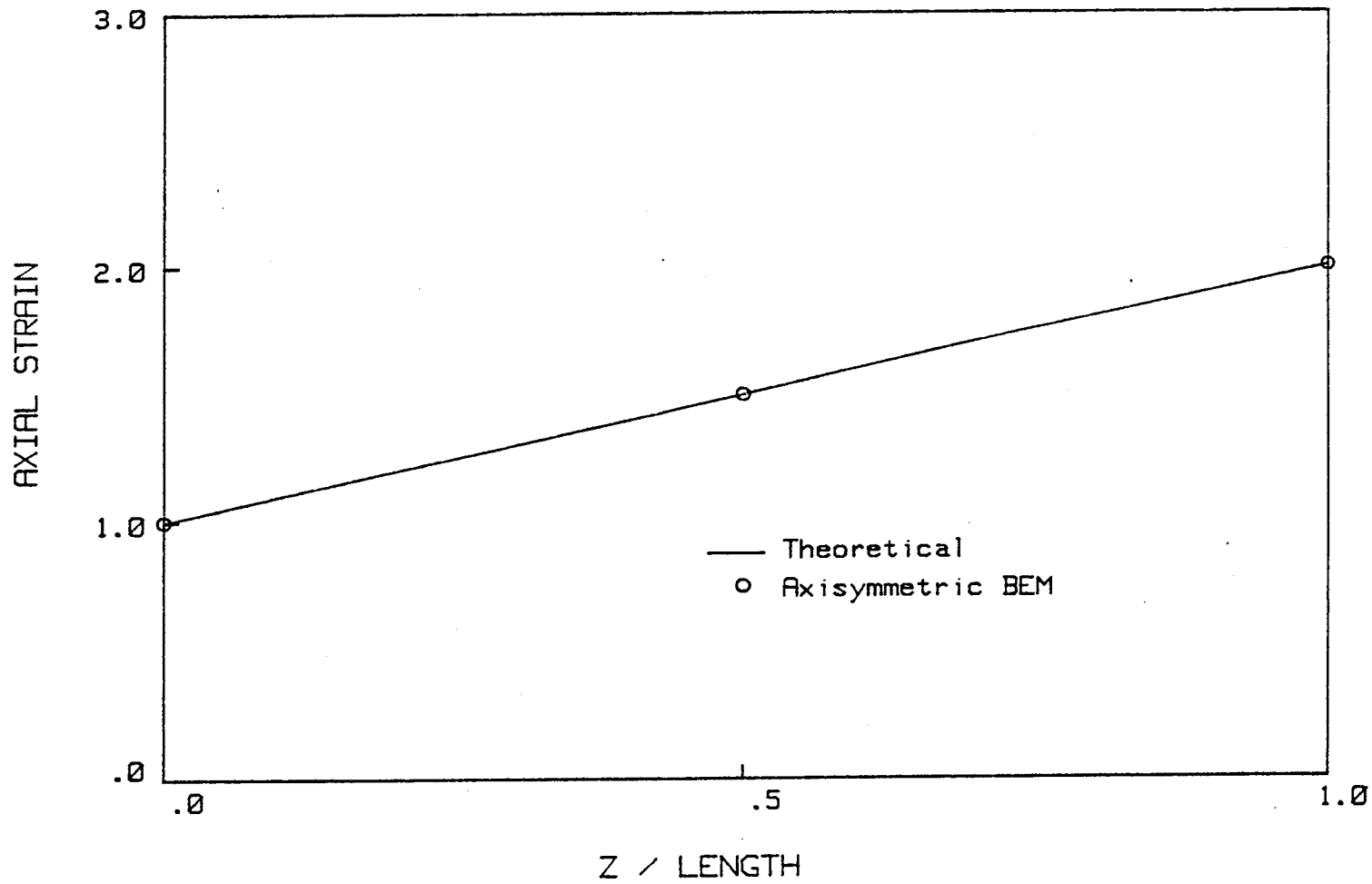

Figure 5.2
Axial Strain through an Inhomogeneous Cylindrical Rod in Tension

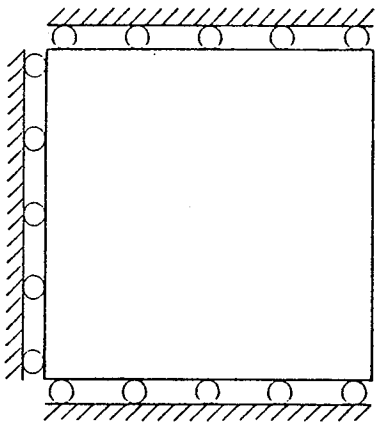

Figure 5.3a
A Cube of Thermal-sensitive Material (Plane Strain)

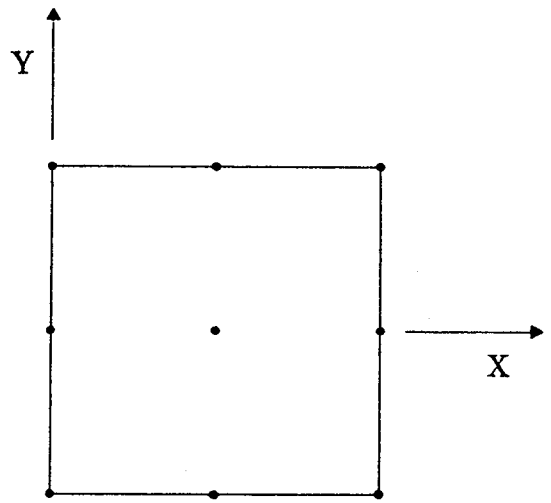

Figure 5.3b
Discretiztion of a 2-D Cube using a
Particular Integral Domain Reprsentation

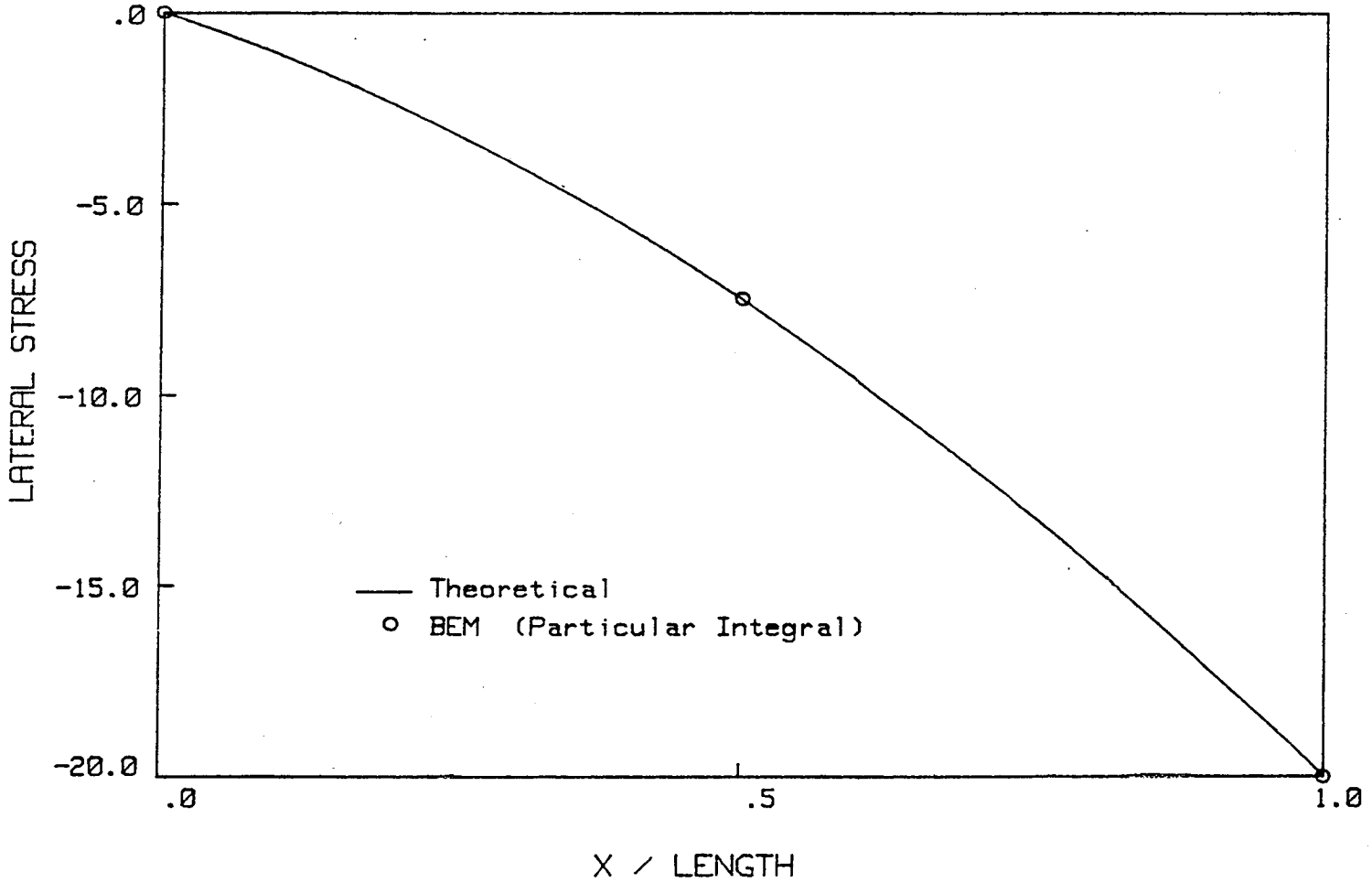

Figure 5.5
Thermally Induced Inhomogeneous Lateral Stress (σ_y and σ_z)
in a Cube (Plane Strain)

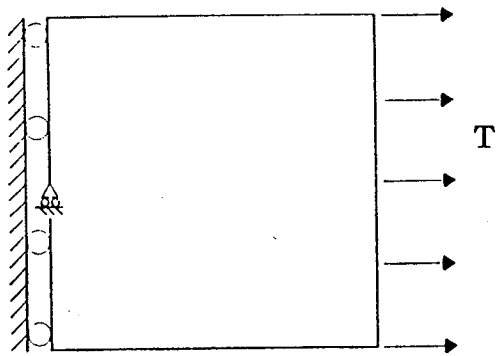

Figure 5.6a
Inhomogeneous Cube in Axial Tension

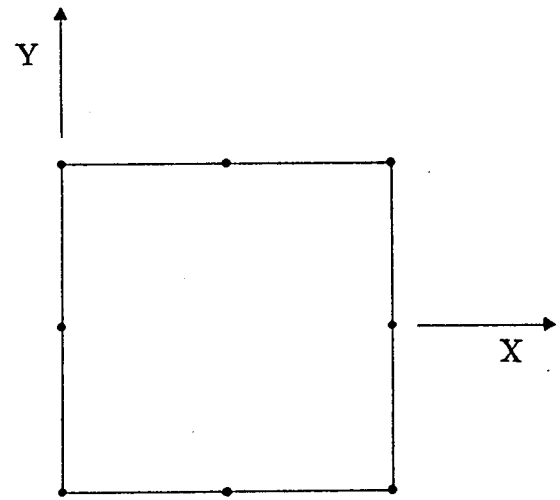

Figure 5.6b
Discretization of a 2-D Cube with One Volume Cell

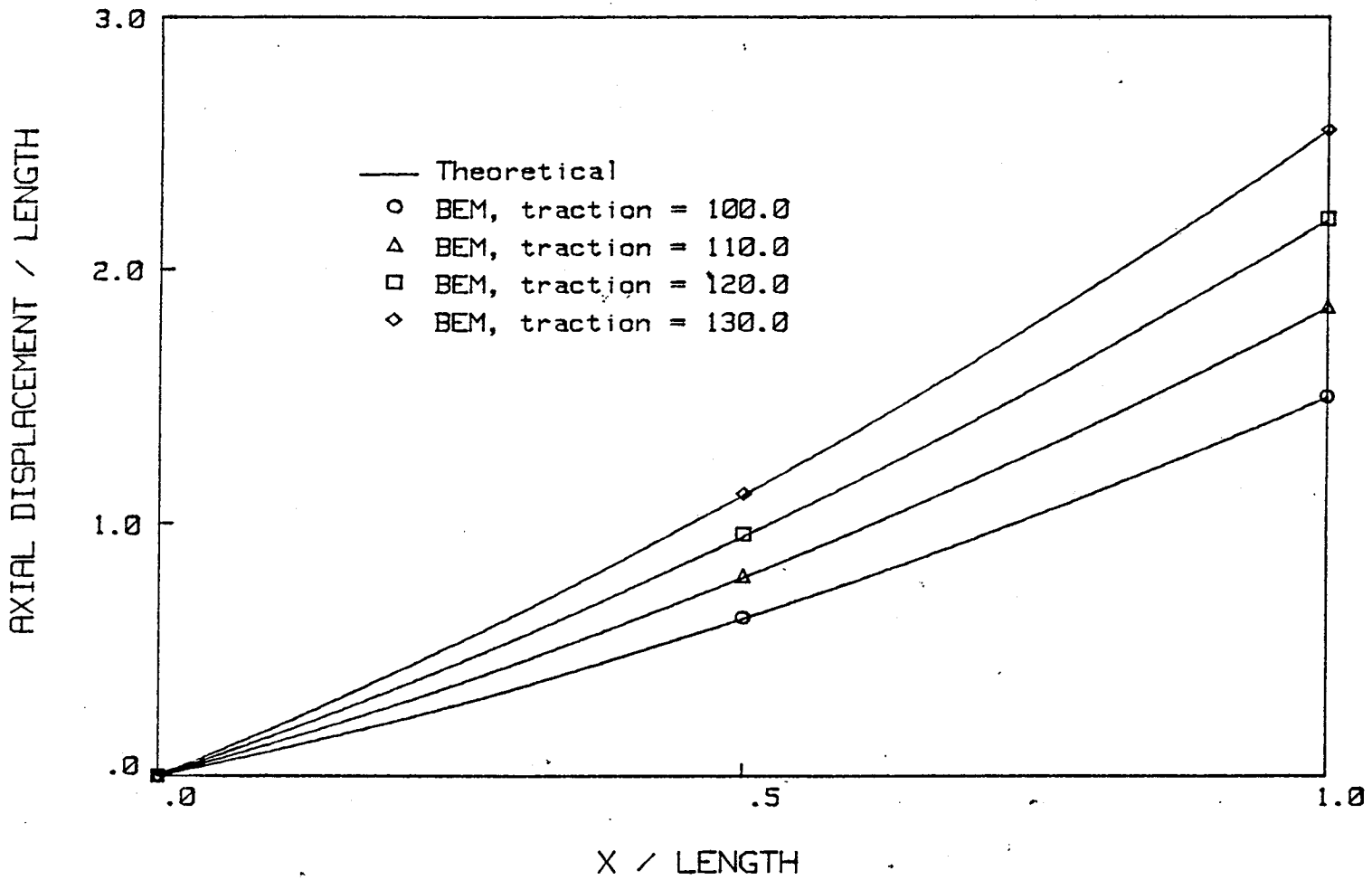

Figure 5.7
Inhomogeneous Plastic (Axial) Displacement in a Cube in Tension

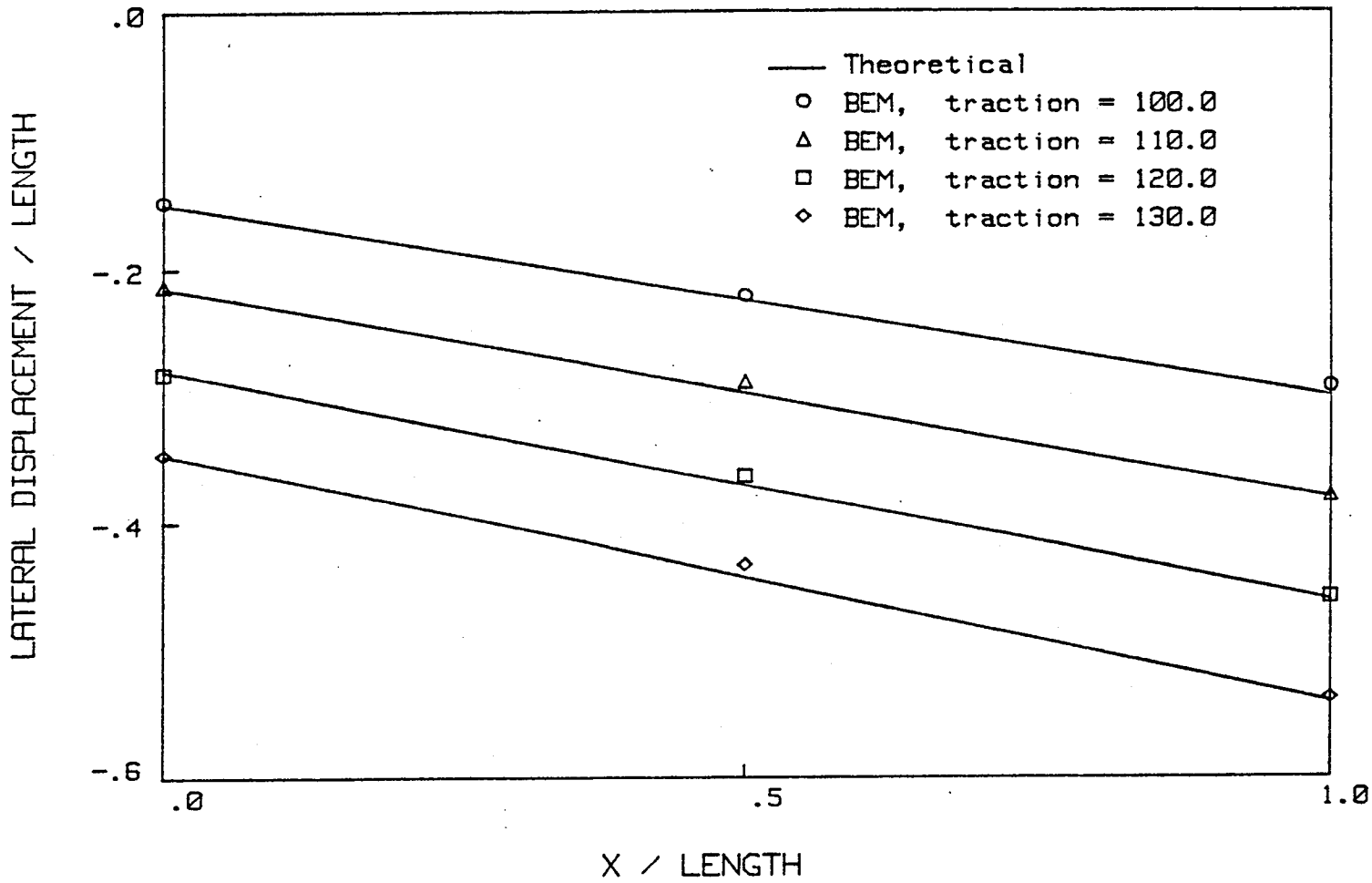

Figure 5.8
Inhomogeneous Plastic (Lateral) Displacement in a Cube in Tension

CHAPTER 6

ADVANCED ENGINEERING APPLICATIONS

CHAPTER SIX

ADVANCED ENGINEERING APPLICATIONS

6.1 INTRODUCTION

In previous chapters, elementary examples such as cubes, spheres and cylinders are used to verify the accuracy and convergence of proposed formulations. These problems were chosen since their simplicity gave way to analytical solutions.

In this chapter, more challenging problems of practical interest are considered.

6.2 ELASTIC ANALYSIS

6.2.1 Bending of a Circular Plate

A clamped, circular plate subjected to a uniformly distributed, circular, patch load is shown in figure 6.1a. The plate is modeled by a five region, axisymmetric mesh shown in figure 6.1b. The modulus of elasticity is E = 210,000, the Poisson's ration is ν = 0.3, and a/b = 10.

In figures 2 and 3, the radial, tangential, and shear stresses obtained using the present axisymmetric BEM analysis is compared with Reisner's plate theory and a boundary element solution based on Reisner's plate theory (Van der Weeën, 1982). General agreement is exhibited by the various analyses. The BEM solution of the present analysis, deviates slightly from the plate theory results under the

origin and near the support. However, this is expected, since plate theory is invalid near such conditions.

The same problem was analyzed with a single region mesh. Results were unchanged from those shown.

6.2.2 Conical Water Tank

A BEM analysis of a water tank shown in Figure 6.4 is carried out using the axisymmetric gravitational particular integrals presented in Chapter 3. The hoop stress on the inside surface of the tank subjected to hydrostatic pressure is shown in Figure 6.4 along with the result from Zienkiewicz (1977). The two results are similar although an exact comparison is not possible since geometry data and material constants are not given for the later case. In Figure 6.5, a comparison of BEM solutions are presented for the hoop stress, on both the inner and outer surface (along A-B) of the tank, for two different loadings. The first loading is hydrostatic pressure only, and the second is a combination of the hydrostatic pressure and self-weight. Note that in the lower section the hoop stress at the outer surface is compressive, i.e. the bending effect is dominant there.

One hundred isoparametric quadratic boundary elements are used to model the body. The tank is assumed to be constructed of concrete with ρ = 4.65 lbm/ft.^{3}, E = 3.472x10^6 psi, and ν = 0.18. The thickness of the uniform section is taken to be 1 ft. The time required for integration is reduced by dividing the tank into six subregions. Two or more elements are used at every interface to insure an accurate representation of the variables across the interface. The computation time for a single region mesh is one and one-half that of the six subregion model, although the computed

results are almost identical. A solution to within 5% of the one shown is achievable with half the number of elements.

6.2.3 Rotating Hub

The axisymmetric BEM analysis of a rotating disk is carried out using the centrifugal particular integral discussed in Chapter 3. Fourteen boundary elements with twenty-nine nodes are used to model the axisymmetric hub (see Figure 6.6). In addition to the boundary nodes, stresses at eight internal points are determined. In Figures 6.6 and 6.7, the contours of tangential stress and equivalent stress are shown. Inadequate data is given in Zienkiewicz (1977) for a detailed comparison of the similar problem, however, the similarities are obvious.

6.3 INELASTIC ANALYSIS

6.3.1 Thick Cylinder of Two Materials (with Strain Hardening)

When a body consists of two or more materials a multi-region capability becomes a necessity. The axisymmetric representation of a thick cylinder of two materials is shown in Figure 6.8 and the variable strain hardening curve for each material is described in Table 6.1 below. The load-displacement behavior of the inner and outer surfaces is shown in Figure 6.9 for both the direct and iterative BEM algorithms based on volume integration. Once again excellent agreement is achieved between the two methods with the direct method producing a solution up to collapse whereas the iterative method does not. The load-displacement curve is initially straight while both materials are elastic and starts to bend as the inner material begins to yield. At this early stage at which only the

inner cylinder has yielded, the evidence of the nonlinearities are not appreciable. It is not until the outer material begins to yield that substantial nonlinearities develop.

The cpu times were essentially the same for both methods.

TABLE 6.1

Material 1 Yield Stress = 10,000 psi		Material 2 Yield Stress = 36,000 psi	
Stress (psi)	Plastic Strain	Stress (psi)	Plastic Strain
10,000	0.00	36,000	0.00
30,000	0.02	60,000	0.04
40,000	0.04	60,000	1.00
40,000	1.00		

6.3.2 Steel Pressure Vessel

An axisymmetric, elastoplastic analysis of a vessel subjected to internal pressure is shown in figure 6.10. The vessel, constructed of steel, has a modulus of elasticity, Poisson's ratio, and a yield stress of $E = 29.12 \times 10^6$ psi, $\nu = 0.3$, and $\sigma_o = 40{,}540$ psi, respectively. The Von Mises criterion is assumed with no strain hardening. Six regions, ninety-nine quadratic boundary elements, and twelve quadratic volume cells are used to model the body (Figure 6.11). Using engineering intuition, cells must be placed in areas where yielding is anticipated. The weld connection between the spherical shell and branch is of prime concern and it is in this region that the cells are situated. The other five regions are assumed to remain elastic, and at the end of the analysis it must be verified that the stresses in these regions have not violated the yield condition.

A plot of the vertical deflection of point A with increasing pressure obtained from both the variable stiffness and iterative plasticity algorithm by volume integration is shown in Figure 6.12 along with results obtained by Zienkiewicz (1977) using the finite element method and test results by Dinno and Gill. The BEM results are in excellent agreement with the results obtained by FEM. The numerical solutions slightly deviate from the experimental results. This variation is due to the idealizations in the numerical analysis, such as ideal plasticity and the adoption of Von Mises criterion. More importantly, the body is assumed homogeneous when in reality the weld and the surrounding region will exhibit greater stiffness.

It should be noted that the variable stiffness method proceeds farther along the curve than the iterative procedure which does not converge at these load levels. The cpu times of the two BEM analysis were about equal, although on a virtual memory computer (HP9000) the real time of the direct plasticity method was greater than the iterative procedure due to excessive page faulting. The use of a multiregion system in both BEM analysis reduces the computational time dramatically, since each nodal equation need only be integrated over the surface in which it is contained. Furthermore, the volume integration need only be performed over the region containing cells.

In the past it has been said that BEM analysis should not be used on bodies of narrow cross-section, but through sophisticated numerical integration and the utilization of a fine mesh, excellent results are obtained.

6.3.3 Residual Stresses in a Cylindrical Rod

An axisymmetric, thermoplastic problem of practical interest shown in figure 6.13, regards the residual stresses in a long cylindrical rod induced by cooling. In this problem the temperature of a rod constructed of 1060 steel is raised gradually to 1250^{o}F and then quenched in a brine spray, quickly lowering the temperature to 80^{o}F. Experimental results obtained by Carman and Hess at Frankford Arsenal are given in Boley and Weiner (1960) for the residual stresses through the cross-section on the midplane of the rod. The Von Mises yield criterion is assumed with a yield value that varies with temperature

$$\sigma_o(t) = \begin{cases} -14.3\ t + 48710.0 & \text{for } t < 400 \\ -18.7\ t + 50470.0 & \text{for } 400 \leq t \leq 775 \\ -46.3\ t + 71900.0 & \text{for } t > 775 \end{cases}$$

where σ_o = yield stress (psi) and t is current temperature (F^{o}). An assumed Biot number of 10 is used in determining the rate in which heat is diffused through the rod.

Utilizing the iterative plasticity algorithm, ten quadratic boundary elements and twelve quadratic volume cells were enough to produce excellent results for this rather complex problem. Symmetry was utilized by the introduction of a roller boundary condition on the horizontal bottom face. The residual stresses along this face are given in figures 6.14, 6.15 and 6.16.

6.3.4 Flexible Circular Footing

This problem concerns a flexible circular footing on an elastic-ideally plastic half space which has a modulus of elasticity of E =

10,000 kN/m^2, Poisson's ratio of $\nu = 0.25$ and a yield stress of σ_o = 173.2 kN/m^2 ($Cu = \sigma_o/\sqrt{3}$). A Von Mises criterion and associated flow rule is assumed.

For this axisymmetric analysis, two modeling regions are used. One region encloses the anticipated plastic zone and the other defines the remainder of the half space which is assumed to remain elastic. In Figure 6.17, elements modeling the infinite half space are shown starting at the axis of symmetry and continuing along the surface up to a finite distance where it is assumed that additional elements (modeling the infinite boundary) do not affect the functions in the area of interest. (In an argument similar to the three-dimensional proof described by Watson (1979), this assumption can be shown to hold valid for axisymmetry.) When calculating the coefficients for the singular node of the F_{ij} (traction) kernel via the 'inflation mode technique', the modeled region must be completely bounded by a surface. Keeping in mind that these coefficients are dependent only on the geometry of their respective boundary element, the open region can be artificially closed with an arbitrary surface. This arbitrary surface is defined with so called 'enclosing elements' and their only role is in the calculation of the singular boundary coefficients. It is to be understood that the nodal points of the enclosing elements do not become part of the boundary system.

In order to find the convergence of the correct solution, a number of cell patterns were constructed for the plastic region. Two of these meshes that were fine enough to produce satisfactory results are shown in Figure 6.18a and 6.18b. The load-displacement behavior at the center of the footing is shown in Figure 6.19 along side the

results obtained by Cathie and Banerjee (1980) where the exact analytical collapse load for this problem is $6C_u$. The results of Cathie and Banerjee (1980) are stiffer than the results of the present paper. The reason for this is the original analysis utilized cells with constant variations of initial stress rates in contrast to the quadratic shape functions used in the present analysis. More importantly, the first investigators calculated stress rates via a linear shape function representation for displacement rates (as in the finite element method), whereas the present analysis uses an accurate integral representation for this. In Figures 6.20 and 6.21 the vertical stress and horizontal stress along the axis of symmetry is shown.

It is important to point out a complication associated with the idealization of the flexible footing. Any applied loading discontinuity can be accurately represented by the boundary element discretization since tractions are described on a per element basis. However, the boundary stress rates do not as easily admit to a discontinuity. In the present analysis the stress rates are calculated individually at the node on each adjoining elements using the boundary stress calculation and the average value is assumed. Therefore, the stress rates are smoothed out across the discontinuity. Alternative ways to handle this difficulty are to model the edge of the footing as a ramp function across a single element and thus avoiding the discontinuity, or a double node can be introduced at this point (one for each adjoining cell) and stress averaging eliminated. In any case the element(s) containing the troubled point should be kept small to better approximate the stress across the discontinuity.

6.3.5 Three-dimensional Analysis of a Notch Plate

The plastic deformation of a notch plate subjected to tension is analyzed under plane stress conditions. Four combinations of analyses are considered:

Particular Integral - Iterative

Particular Integral - Variable Stiffness

Volume Integral - Iterative

Volume Integral - Variable Stiffness

The material properties for the plate are:

$E = 7000\ kg/mm^2$

$\nu = 0.2$

$\sigma_o = 24.3\ kg/mm^2$ (Von Mises yield criterion)

$h = 0.0$

A 90^o notch is cut out of the sides of the plate. The maximum to minimum width ratio is 2 and the thickness is 6/10 of the maximum width. A quarter of the plate is discretized in two subregions as shown in figure 6.22. The region, containing the notch, has thirty quadratic boundary elements. The inset in this figure shows six (twenty-node) isoparametric cells (with sixty-eight distinct cell nodes) which are used in the volume integral based analysis. In the particular integral analysis, particular integrals are defined using the boundary nodes and three interior nodes (corresponding to the mid-side nodes of the cells) for a total of ninety-two particular integral nodes. The second region has sixteen quadratic boundary elements. Boundary conditions on the front and back faces are assumed traction free.

In figure 6.23, the stress-strain response on the mid-plane of the root is given for the four (3-D) BEM analyses and compared with the two-dimensional plane stress and plane strain BEM solutions obtained by Raveendra (1984). The three-dimensional results are in good agreement with one another, and fall between the two-dimensional solutions, closer to the plane stress result, as one would expect. For solutions above the load level $2\sigma_m/\sigma_o = 1.0$ requires a finer mesh around the notch, particularly in the volume cell discretization.

Figure 6.24, shows another notch plate mesh for a particular integral analysis. The boundary discretization is the same, but ten additional particular integral nodes are added in the interior (101 particular integral nodes, total). The bottom face becomes a plane of symmetry by applying a roller boundary condition. In order to keep the dimension of the plate proportional to the first analysis, the thickness of the mesh must be reduced by one-half, since symmetry is assumed by virtue of the additional roller boundary condition. The stress-strain response at the root, obtained for this mesh using the variable stiffness algorithm, is shown in figure 6.25. Results for the three nodes across the thickness of the root are compared with the two-dimensional solution (Raveendra, 1984). Once again, the three-dimensional results lie between the plane stress and plane strain solution.

6.3.6 Three-dimensional Analysis of a Perforated Plate

The plastic deformation of a perforated plate in tension is analyzed under plane stress conditions. The volume distribution of initial stress is represented using either twenty-noded isoparametric volume cells or the point based particular integral. Each

representation is coupled with either the iterative or the variable stiffness solution process, leading to a total of four distinct algorithms. The material properties for the plate are:

$E = 7000 \text{ kg/mm}^2$

$\nu = 0.2$

$\sigma_o = 24.3 \text{ kg/mm}^2$ (Von Mises yield criterion)

$h = 224.0 \text{ kg/mm}^2$

The diameter of the circular hole, at the center of the plate, is one-half the width, and the thickness is one-fifth the width. A quarter of the plate is discretized in two subregions, as shown in figure 6.26. The first region, containing the root of the plate, has thirty quadratic boundary elements. For the volume integral based analysis the domain of this region is discretized using nine (twenty-node) isoparametric cells. In the particular integral analysis, particular integrals are defined at points corresponding to the cell nodes used in the volume integral analysis. The second region has twenty-three boundary elements. No volume discretization or definition of particular integrals is required in this region since it remains elastic throughout the analysis. Boundary conditions on both the front and back faces are assumed traction free.

This problem was previously analyzed experimentally by Theocaris and Marketos (1964) and by Zienkiewicz (1977) using the finite element method. The results obtained by the boundary element analysis is compared to these results in figures 6.27 and 6.28. The stress-strain response at the root of the plate is shown in figure 6.27. The results obtained using the various BEM algorithms show good agreement

with one another and with the variable stiffness FEM analysis. Differences between the iterative and variable stiffness BEM formulations are much less significant than the difference in the two FEM algorithms. The volume integral base BEM procedure exhibits greater stiffness than the particular integral method. In figure 6.28, the stress distribution between the root and the free surface of the specimen is shown for a load of $2\sigma_m/\sigma_o = 0.91$. Once again, excellent agreement is obtained among the four boundary element analysis. In order to evaluate the degree of convergence of the results, a mesh with sixteen volume cells (or the particular integral equivalent) was studied. The results were unchanged from those shown.

The present analysis was carried out on the Cray-1 computer. The CPU times for the four algorithms were:

Particular Integral/Iterative	= 254 sec.
Particular Integral/Variable Stiffness	= 358 sec.
Volume Integral/Iterative	= 272 sec.
Volume Integral/Variable Stiffness	= 361 sec.

6.3.7 Two-dimensional Analysis of a Perforated Plate

The perforated plate of the previous problem is analyzed using the particular integral based, inelastic, two-dimensional, plane stress analysis. Three discretizations, shown in figure 6.29, are used to model the plate. Each mesh is divided into two subregions. The initial stress distribution in the inelastic region is defined using the particular integral representation. Twenty, forty-one and sixty-five nodes are used, respectively, in these discretizations to define the particular integrals.

A solution is obtained using the variable stiffness method, and the results are compared with the particular integral based, variable stiffness results of the previous three-dimensional analysis. The stress-strain response at the root of the plate is shown in figure 6.30. The results obtained for the two-dimensional discretizations are in good agreement with the three-dimensional solution. The results of the more refined (65 particular integral nodes) mesh, however, exhibits a smoother response and follows the three-dimensional solution more closely than the other two-dimensional results. The axial stress distribution across the plate, from the root to the free edge, is shown in figure 6.31. All two-dimensional results vary from the three-dimension solution, however, overall agreement is observed.

6.4 CONCLUDING REMARKS

In this chapter, a range of problems of practical interest have been analyzed using the axisymmetric, two- and three-dimensional, thermal, elastic and inelastic boundary element formulations of previous chapters. In addition to displacement and traction boundary loads, body forces due to self-weight, centrifugal, and thermal loads are considered. The solutions obtained in the analyses were compared to known solutions when they exist, and good agreement was found in most cases. Many of the problems were analyzed using various alternative procedures to illustrate the relative accuracy of these methods. Also demonstrated was the multi-region capability of the computer code which enables one to model a body in substructured parts; thus dramatically reducing the cost of the analysis.

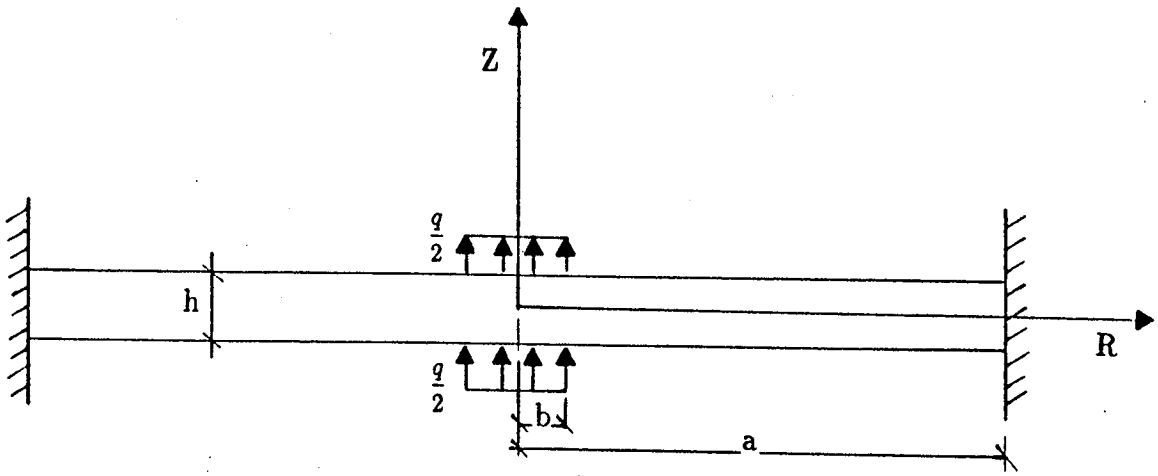

Figure 6.1a
Clamped Circular Plate

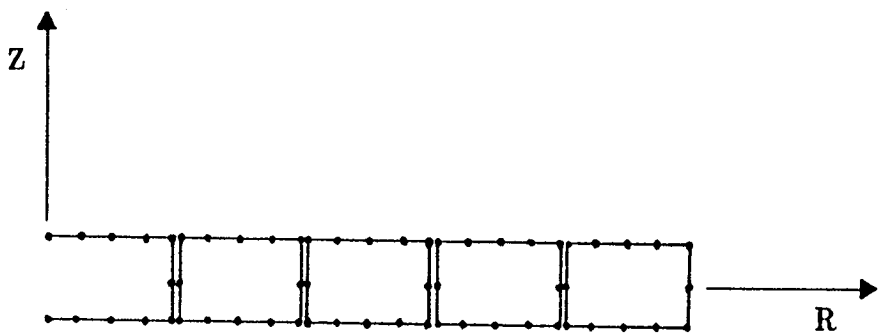

Figure 6.1b
Axisymmetric Mesh of a Circular Plate

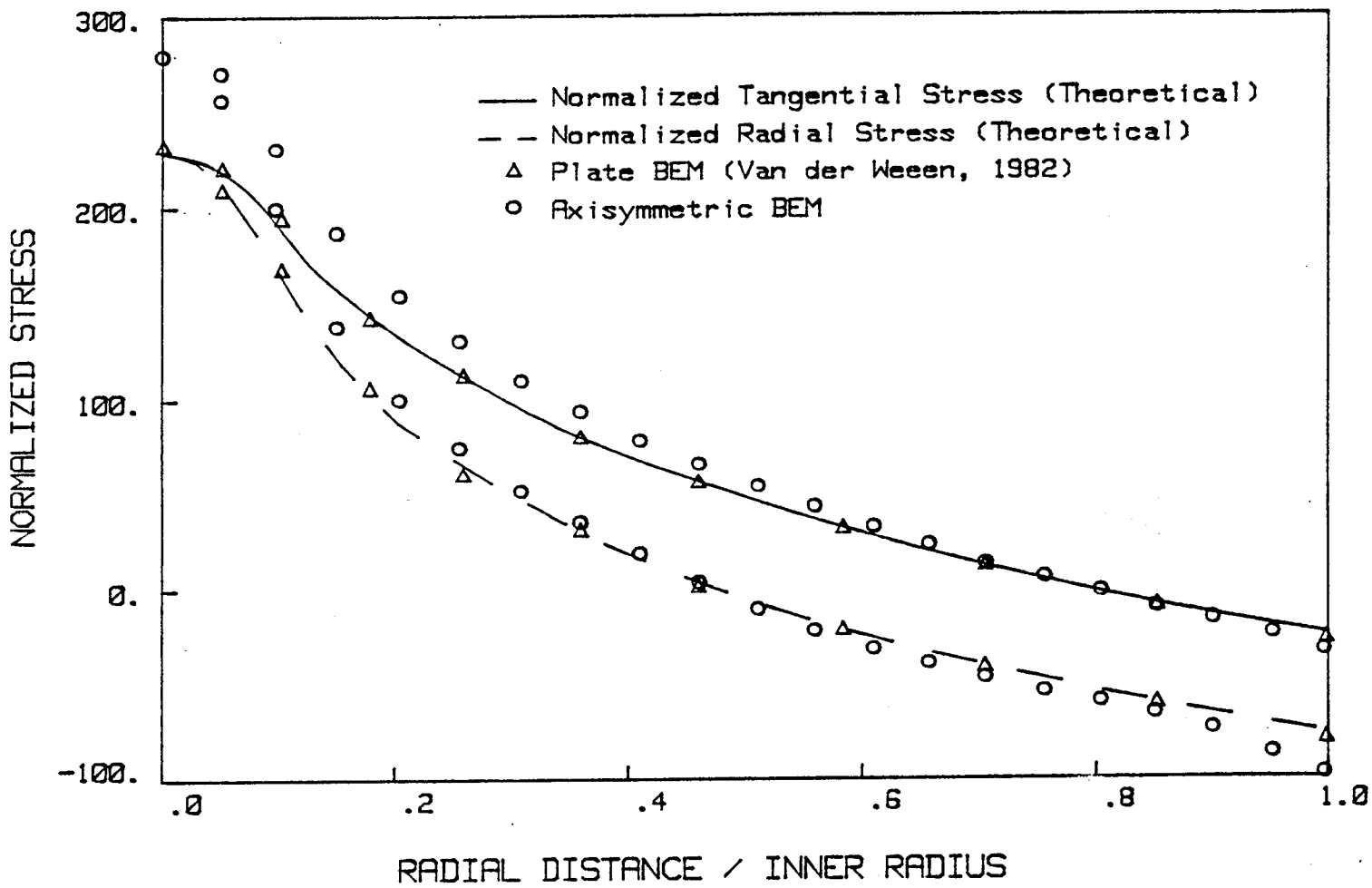

Figure 6.2
Radial and Tangential Stress through a Circular Plate

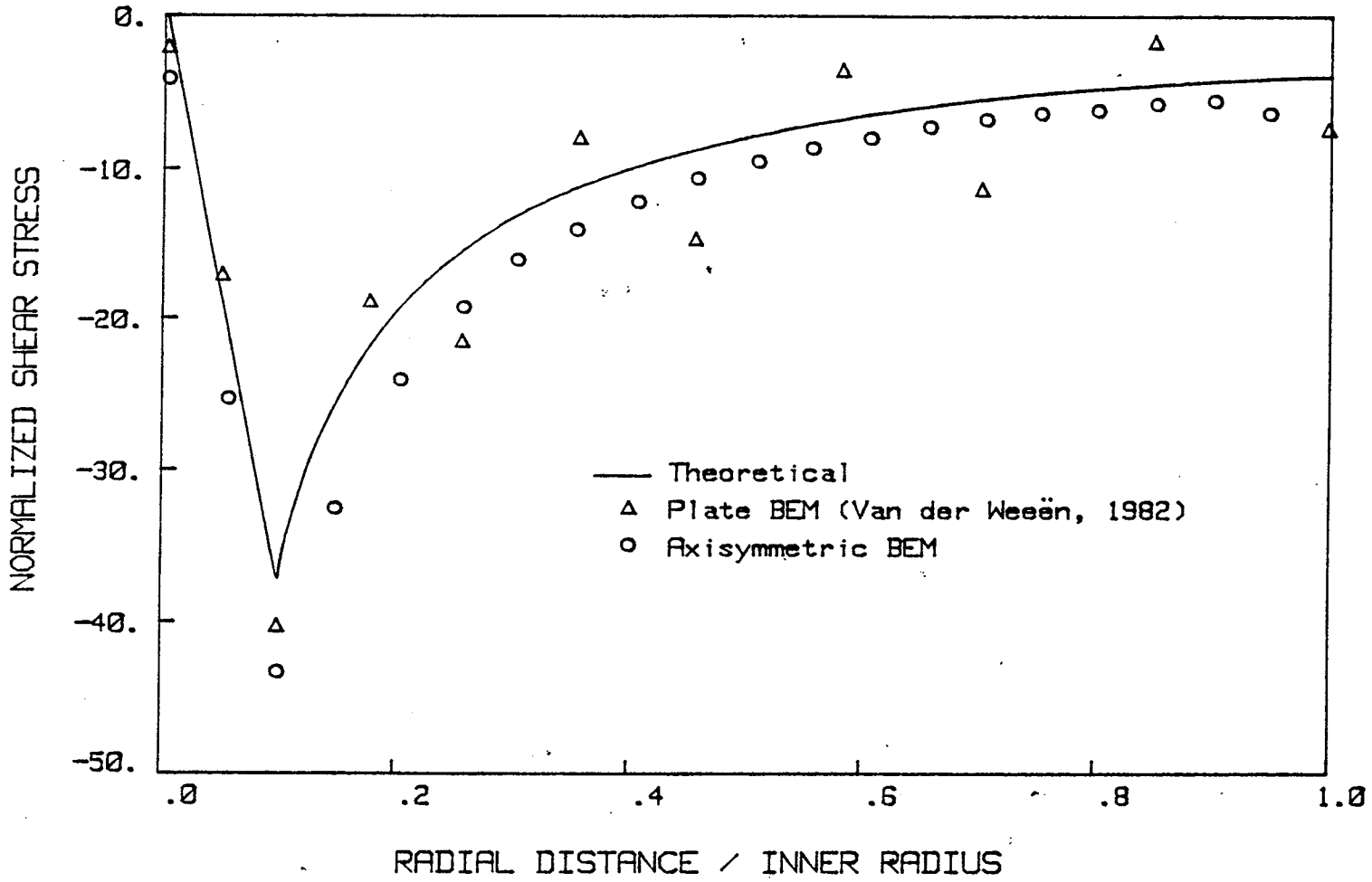

Figure 6.3
Shear Stress though a Circular Plate

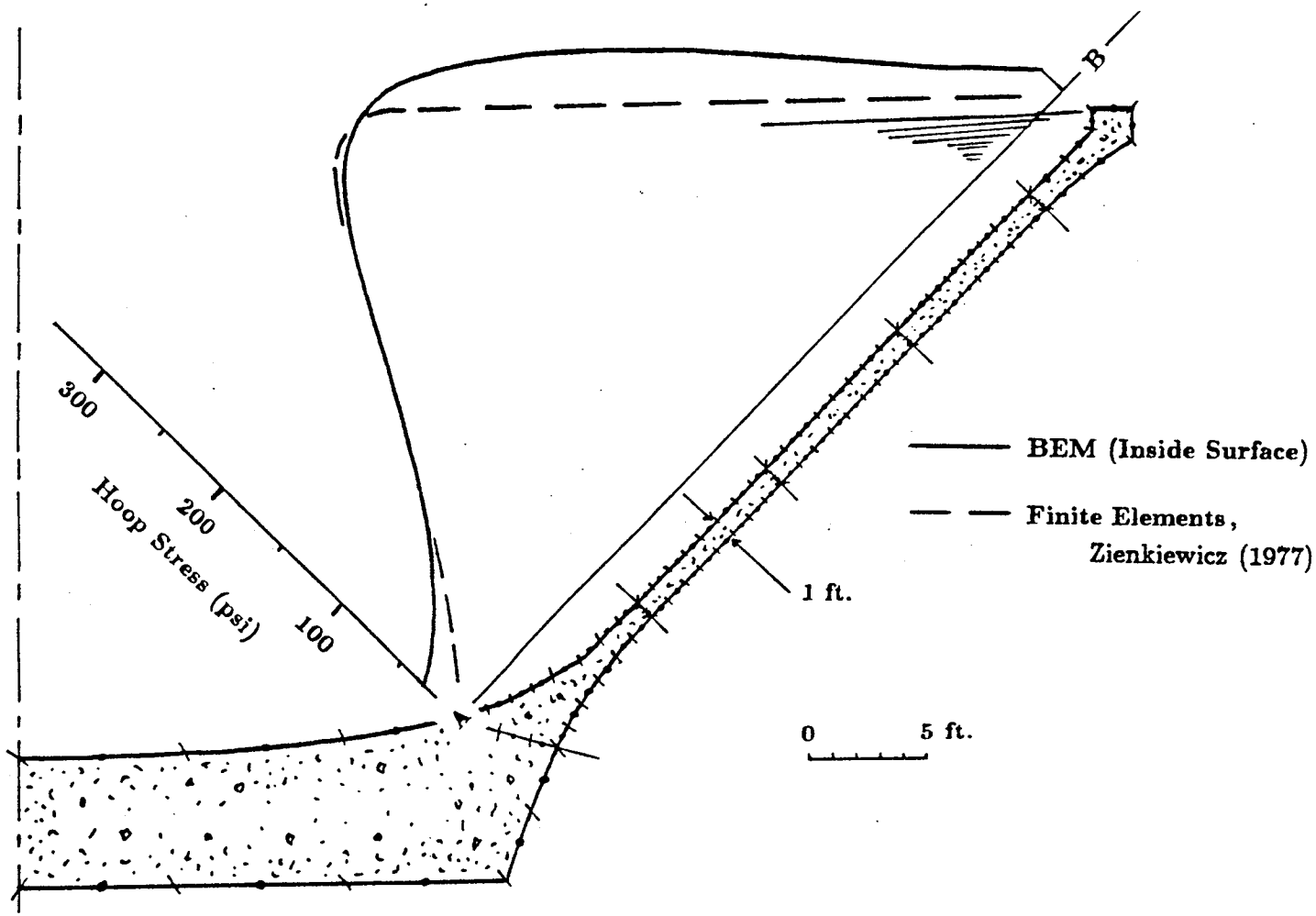

Figure 6.4
Conical Water Tank subjected to Hydrostatic Pressure

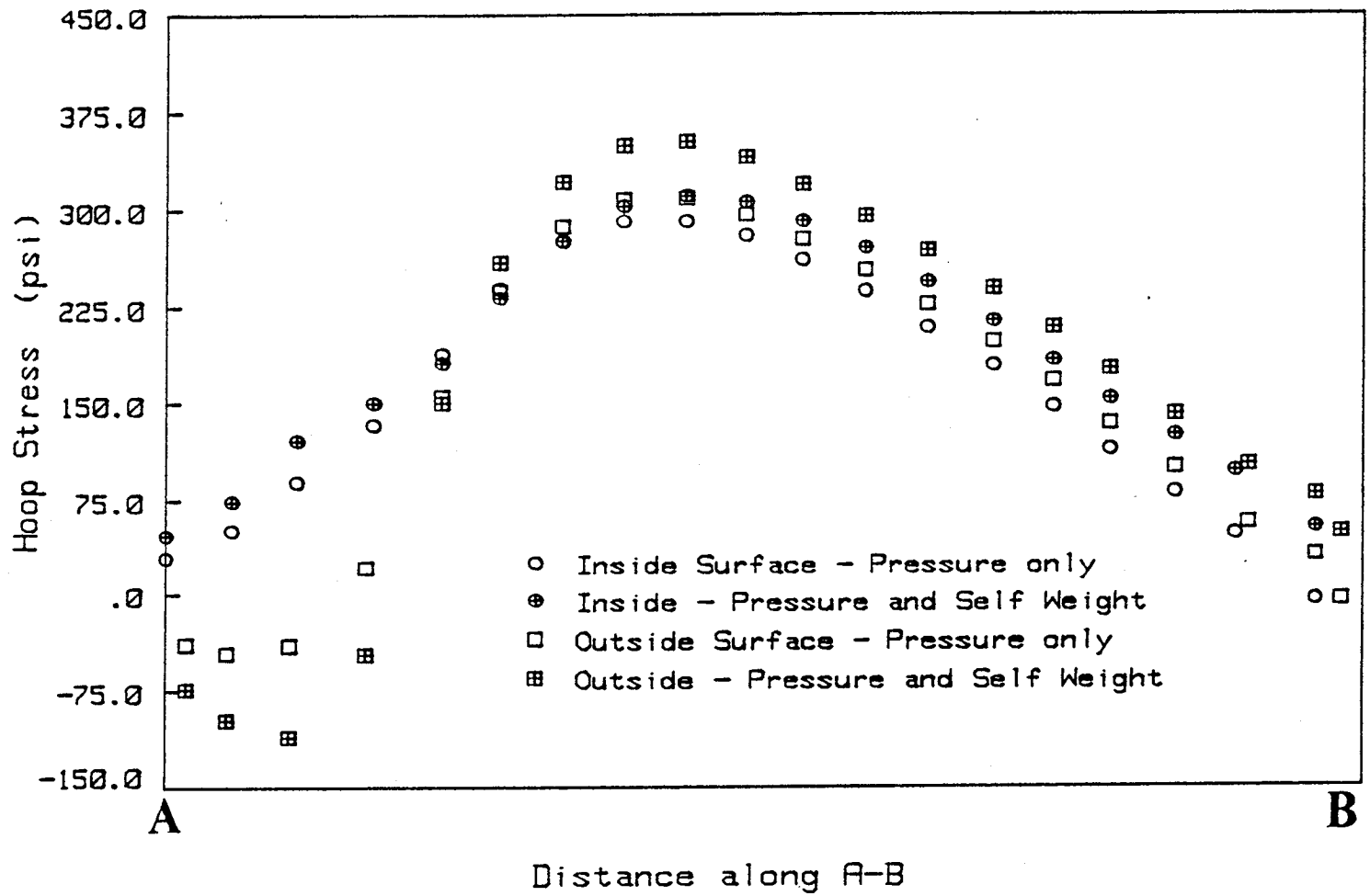

Figure 6.5
Hoop Stress in a Conical Tank due to Hydrostatic Pressure and Self-weight

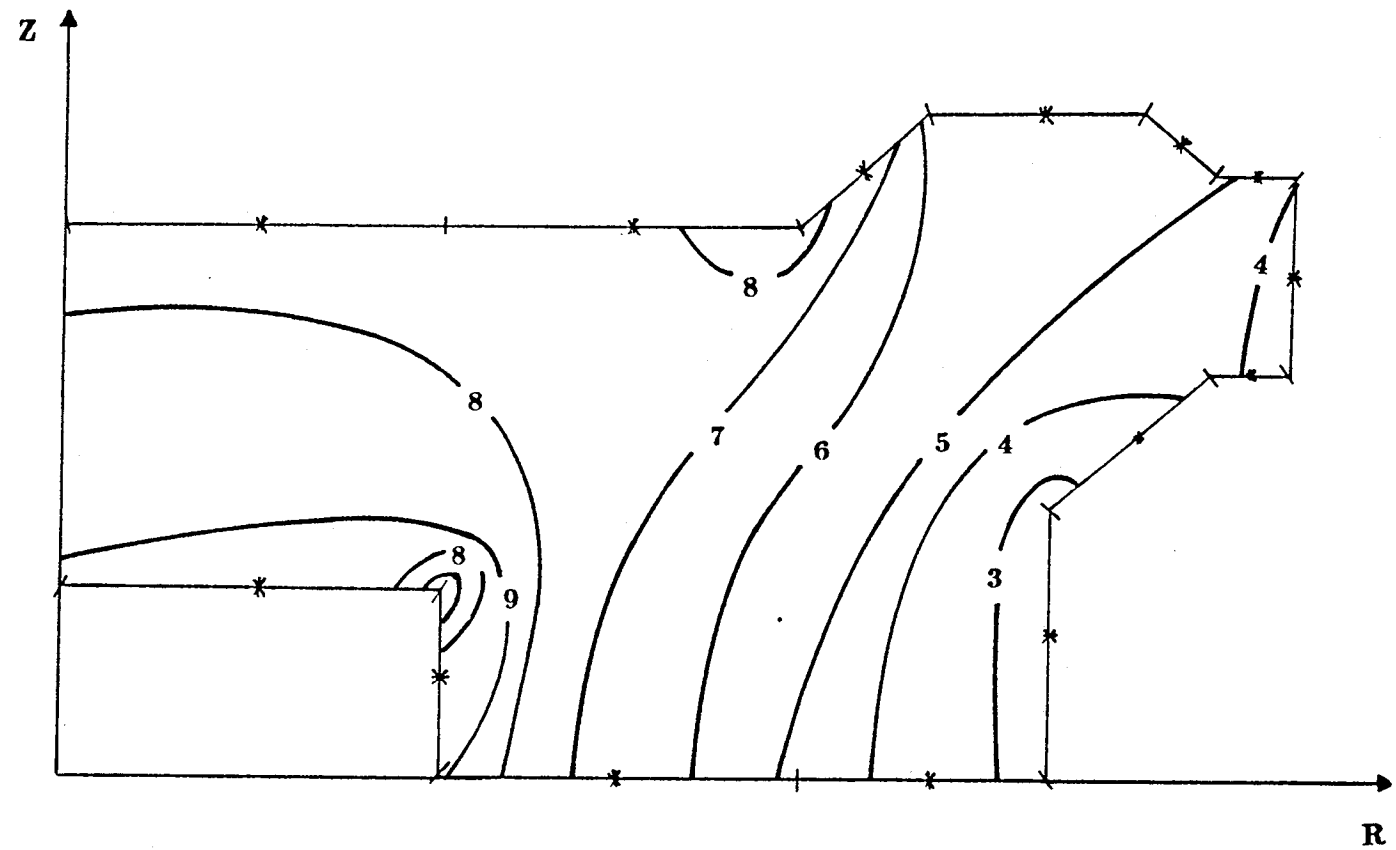

Figure 6.6
Contours of Tangential Stress in a Rotating Hub

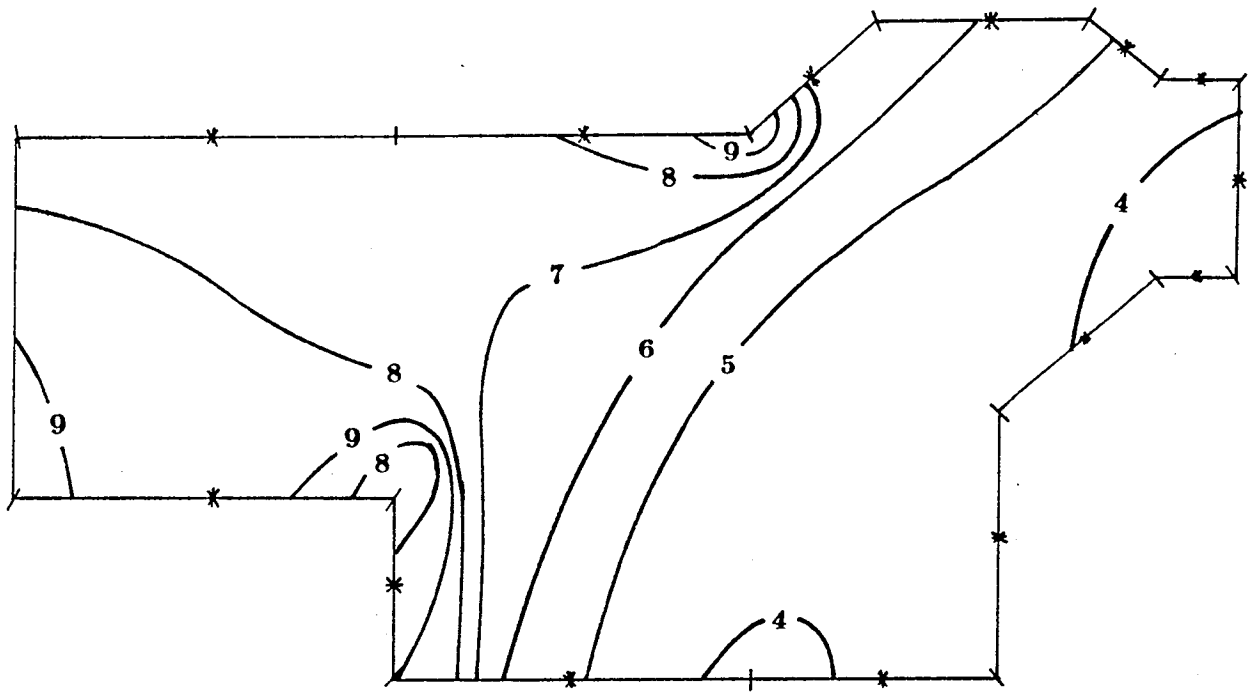

Figure 6.7
Contours of Equivalent Stress in a Rotating Hub

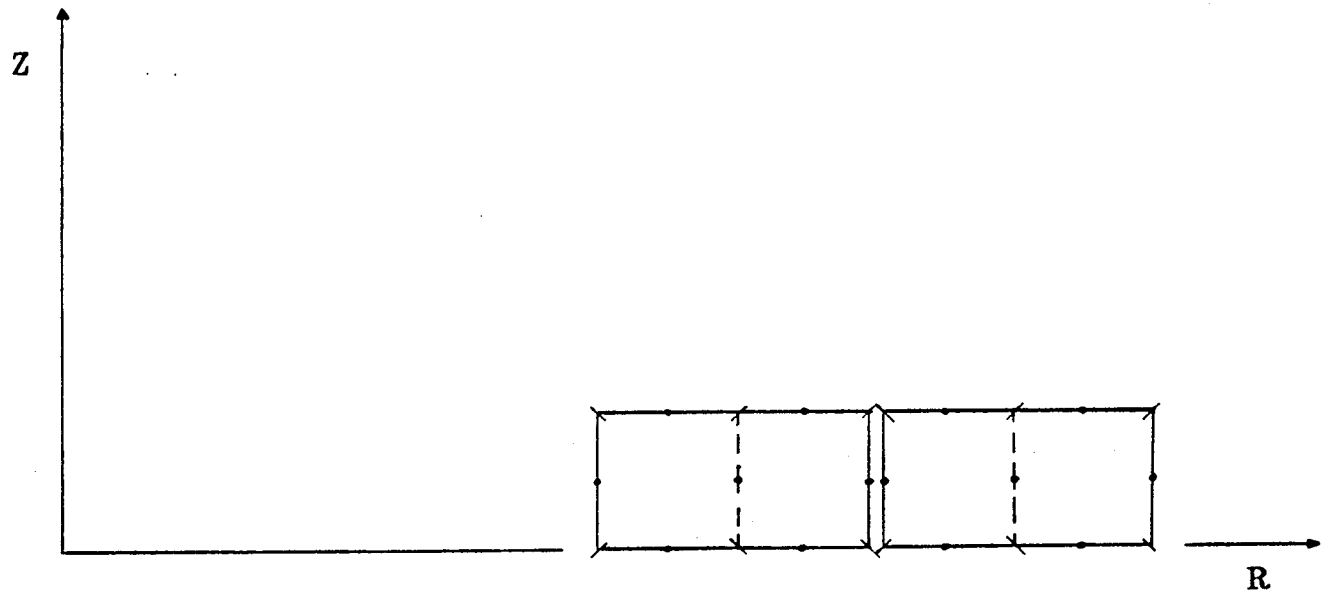

Figure 6.8
Axisymmetric Mesh of a Thick Cylinder of Two Materials

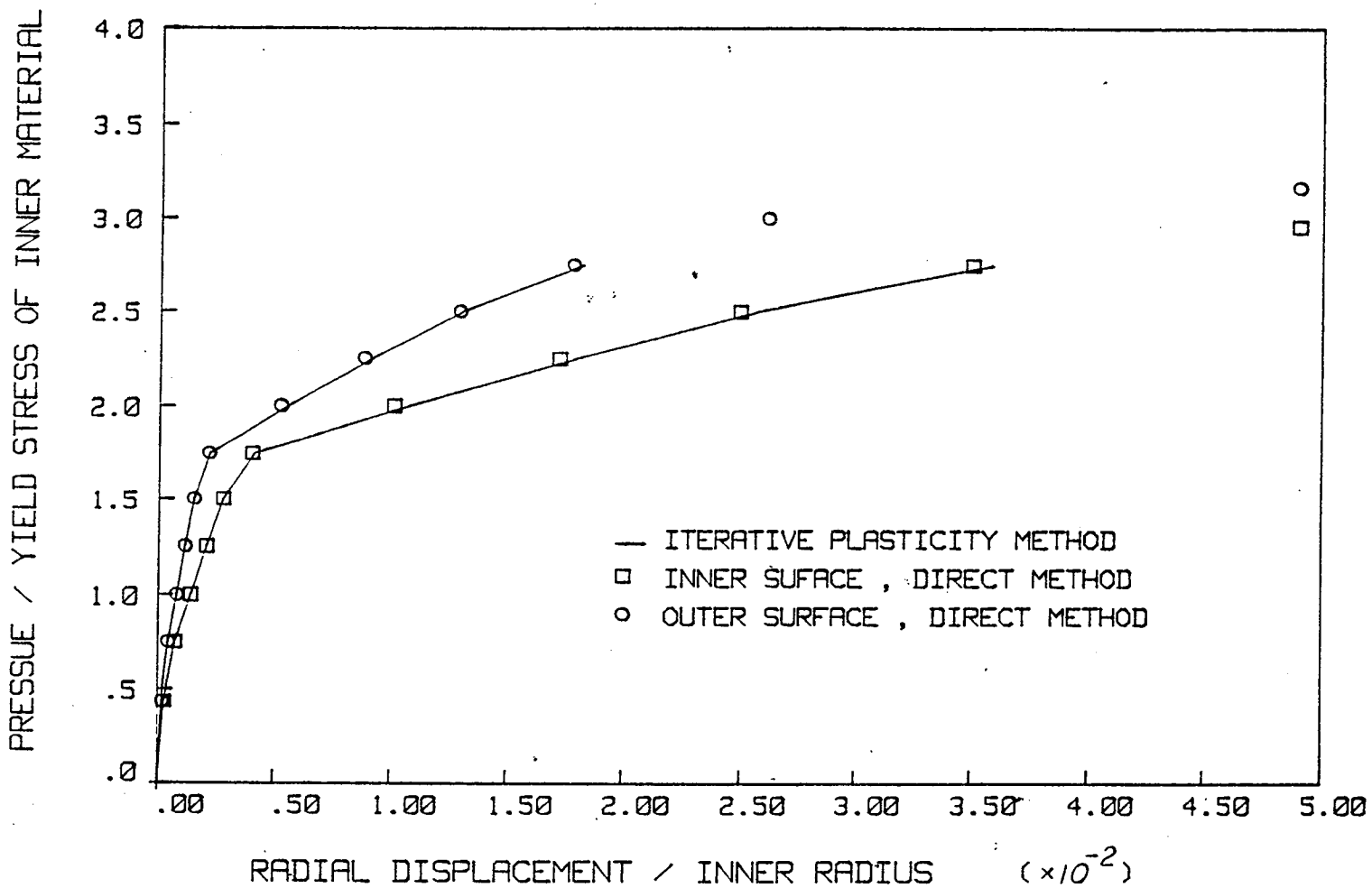

Figure 6.9
Radial Displacement of a Two-Material Thick Cylinder under Internal Pressure (Plane Strain)

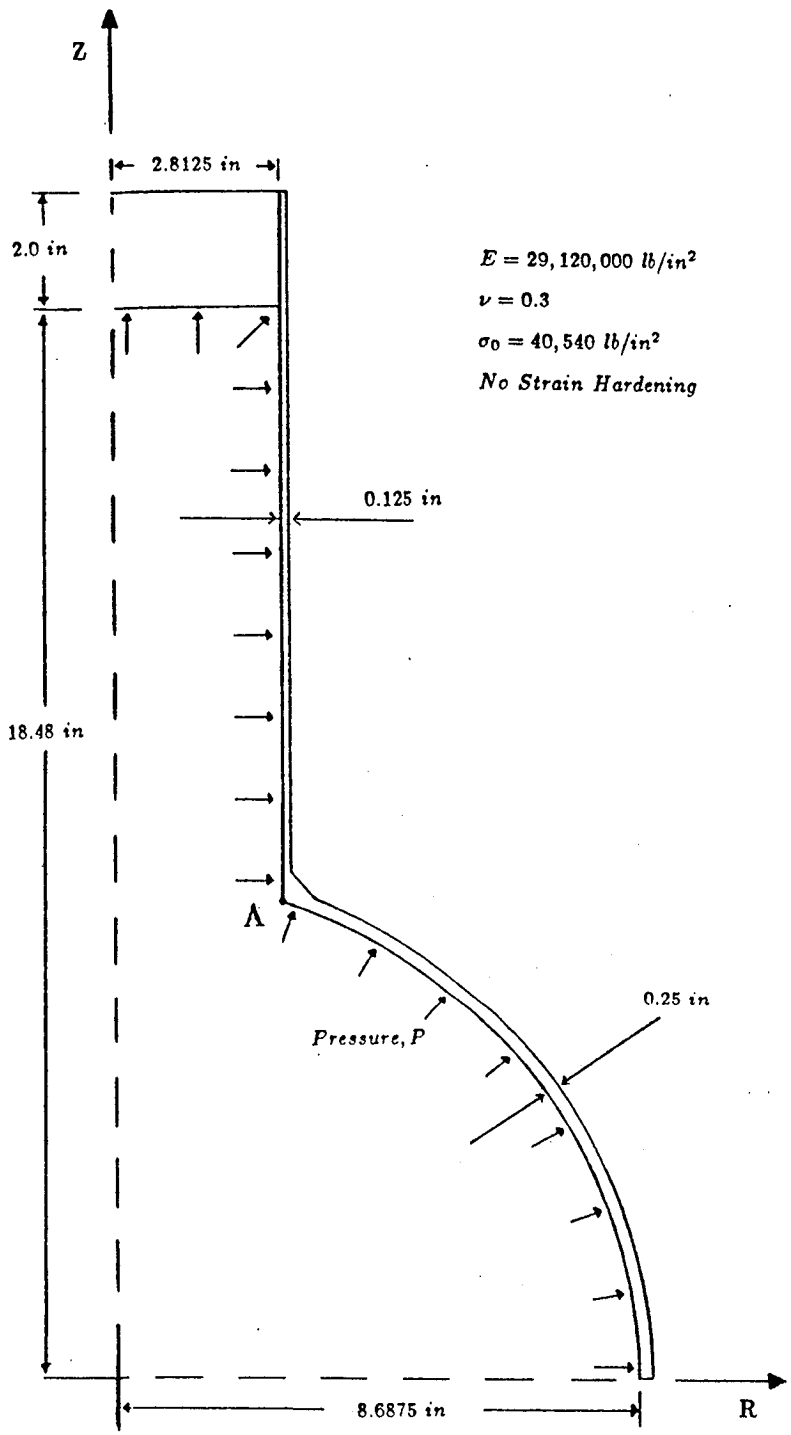

Figure 6.10
Axisymmetric Steel Pressure Vessel

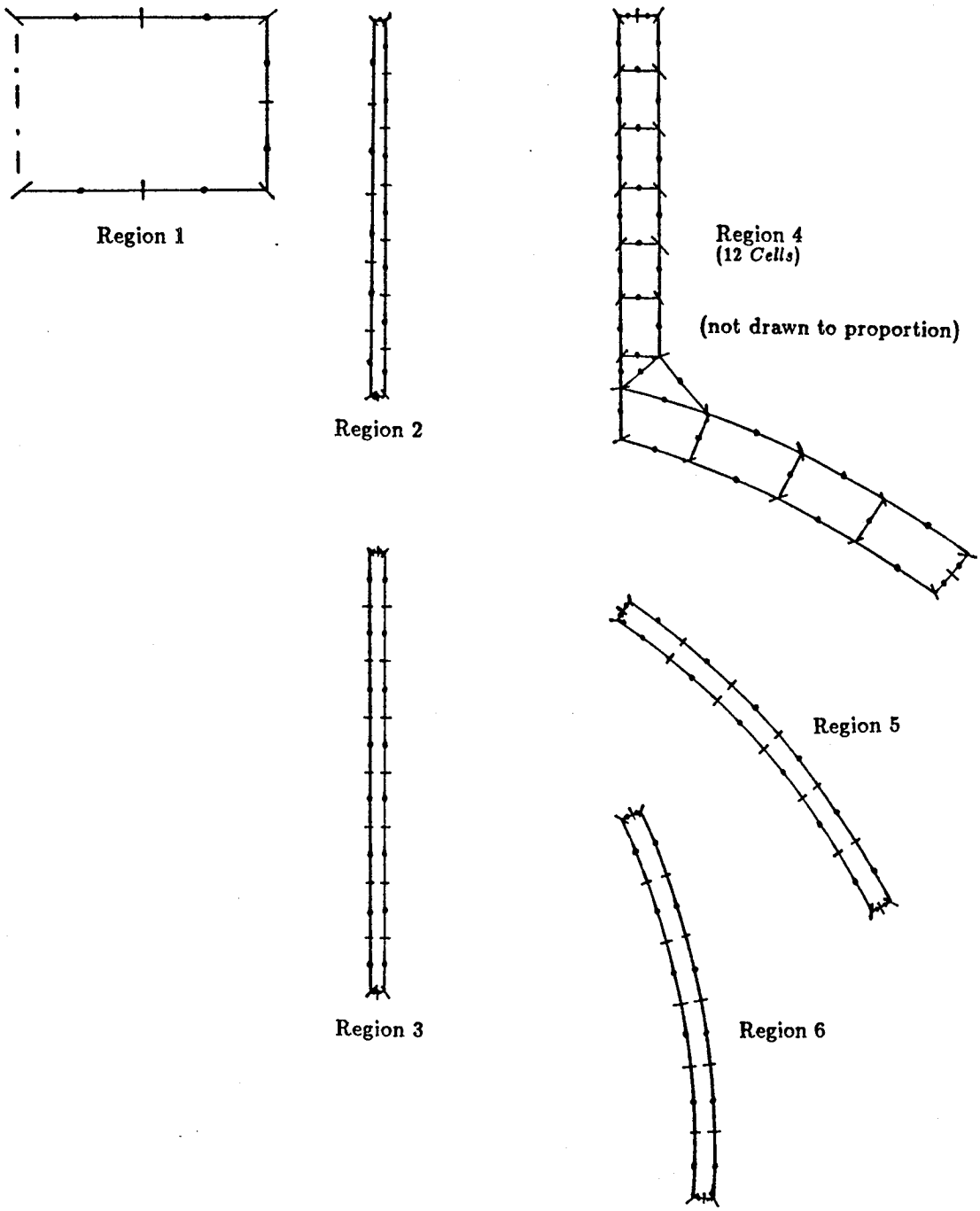

Figure 6.11
Discretization of Pressure Vessel Mesh by Region

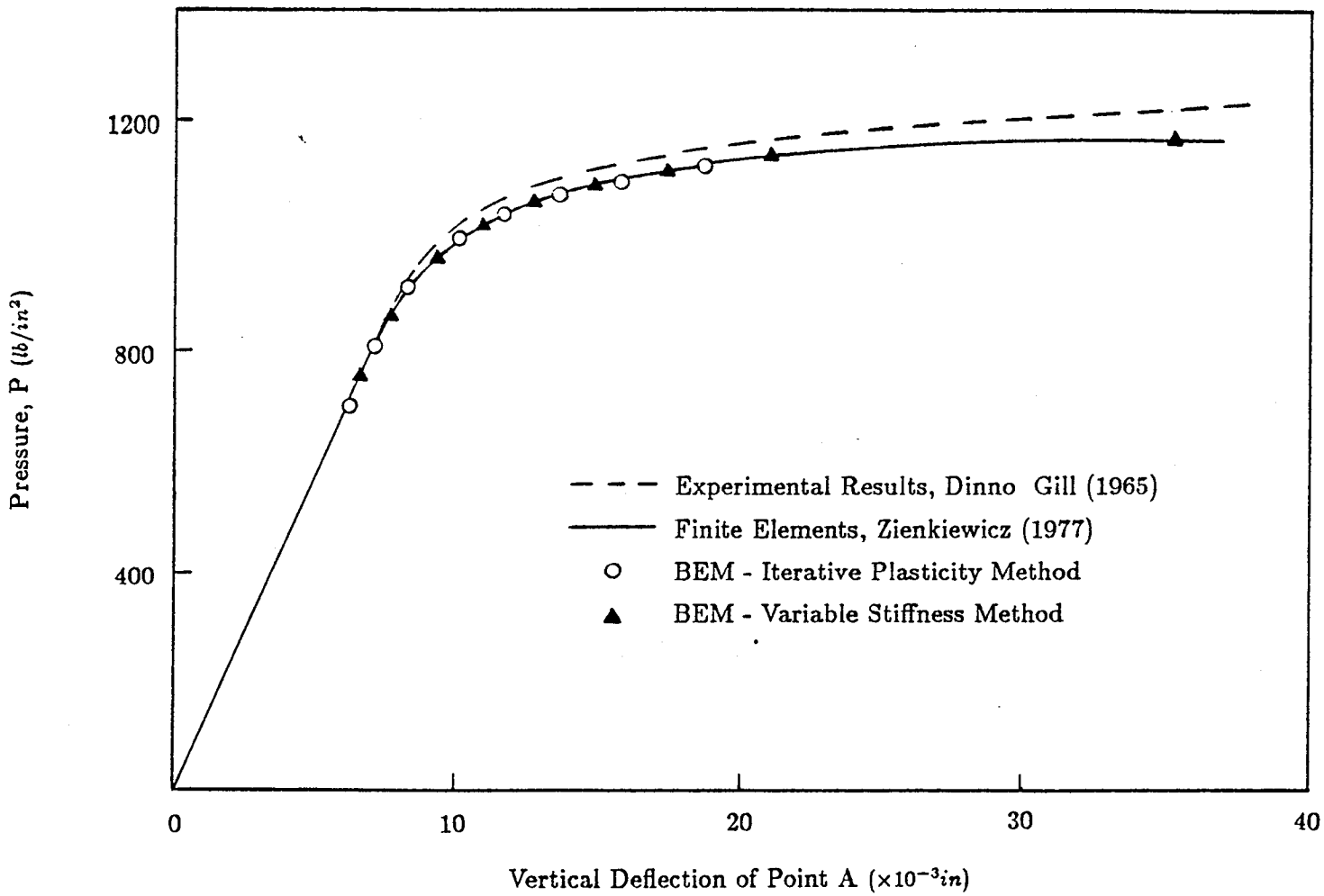

Figure 6.12
Vertical Deflection of Point A of the Pressure Vessel with Increasing Pressure

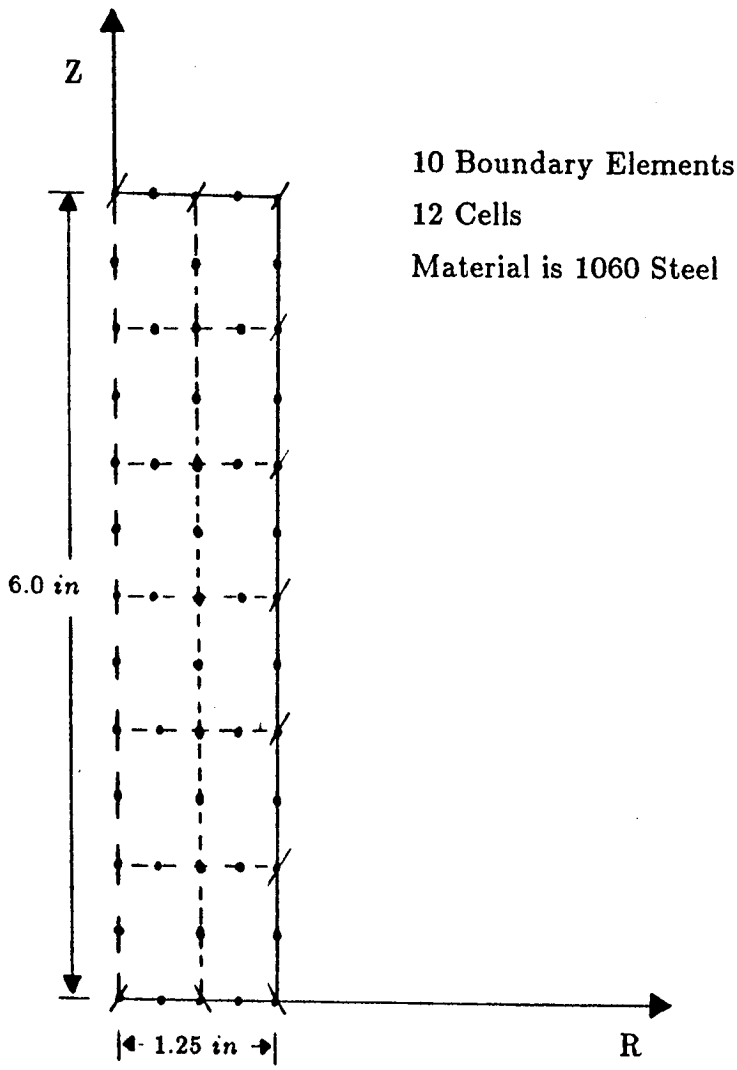

Figure 6.13
Axisymmetric Mesh of a Cylindrical Rod

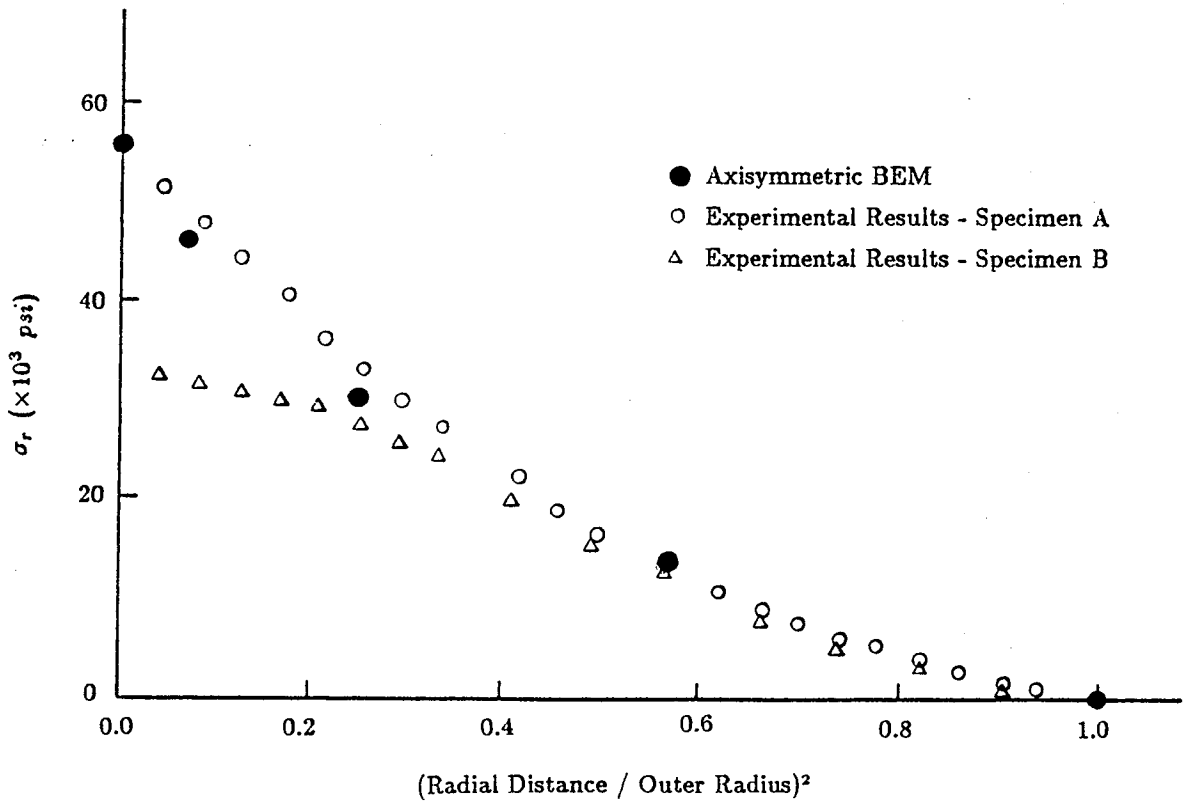

Figure 6.14

Residual Radial Stress in a Cylindrical Rod

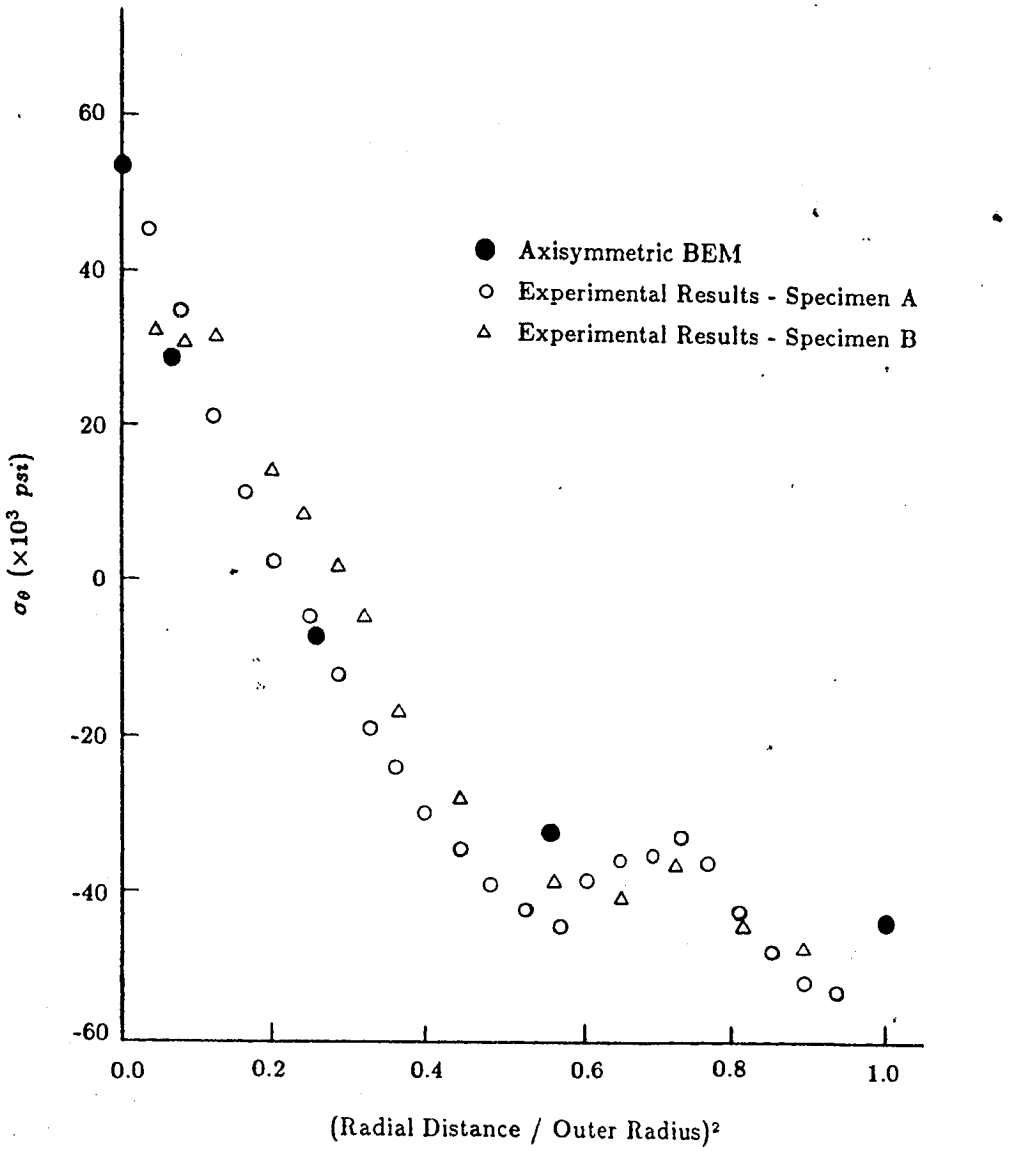

Figure 6.15
Residual Tangential Stress in a Cylindrical Rod

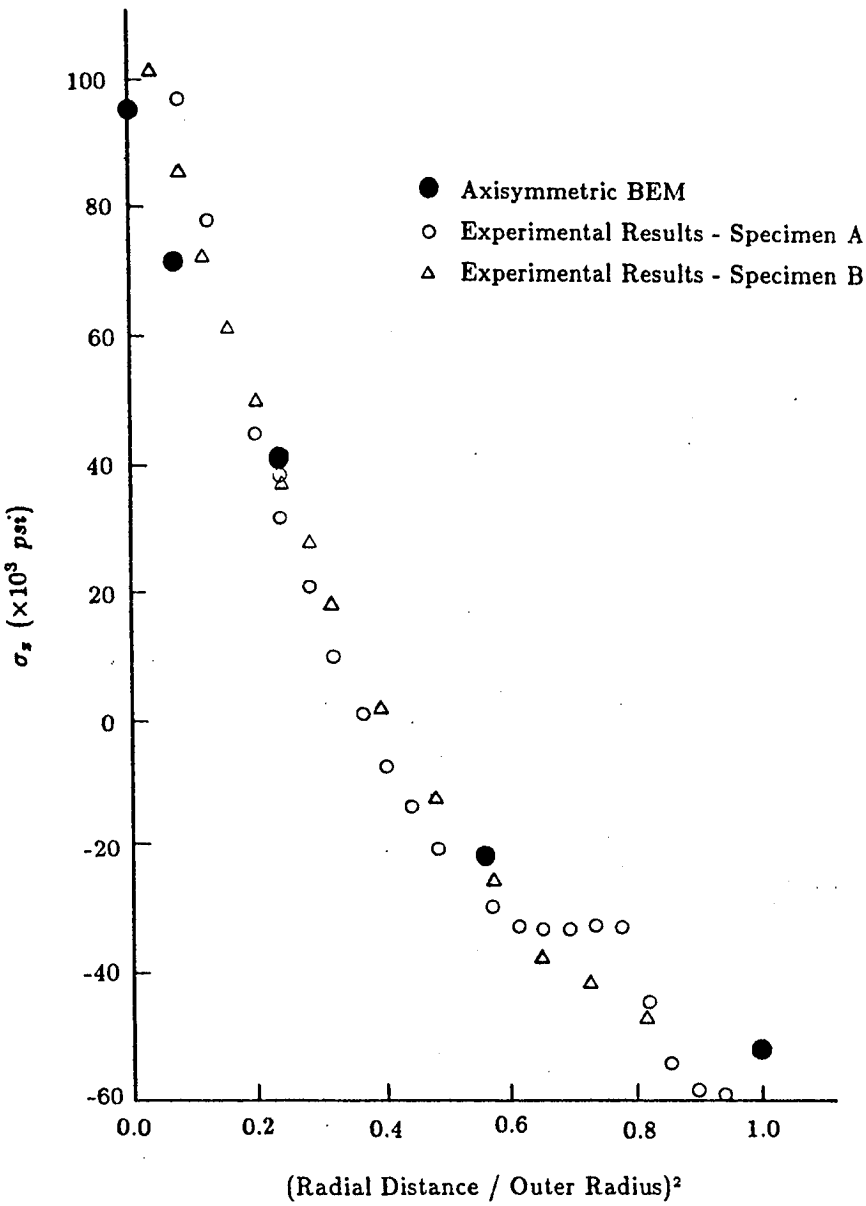

Figure 6.16
Residual Axial Stress in a Cylindrical Rod

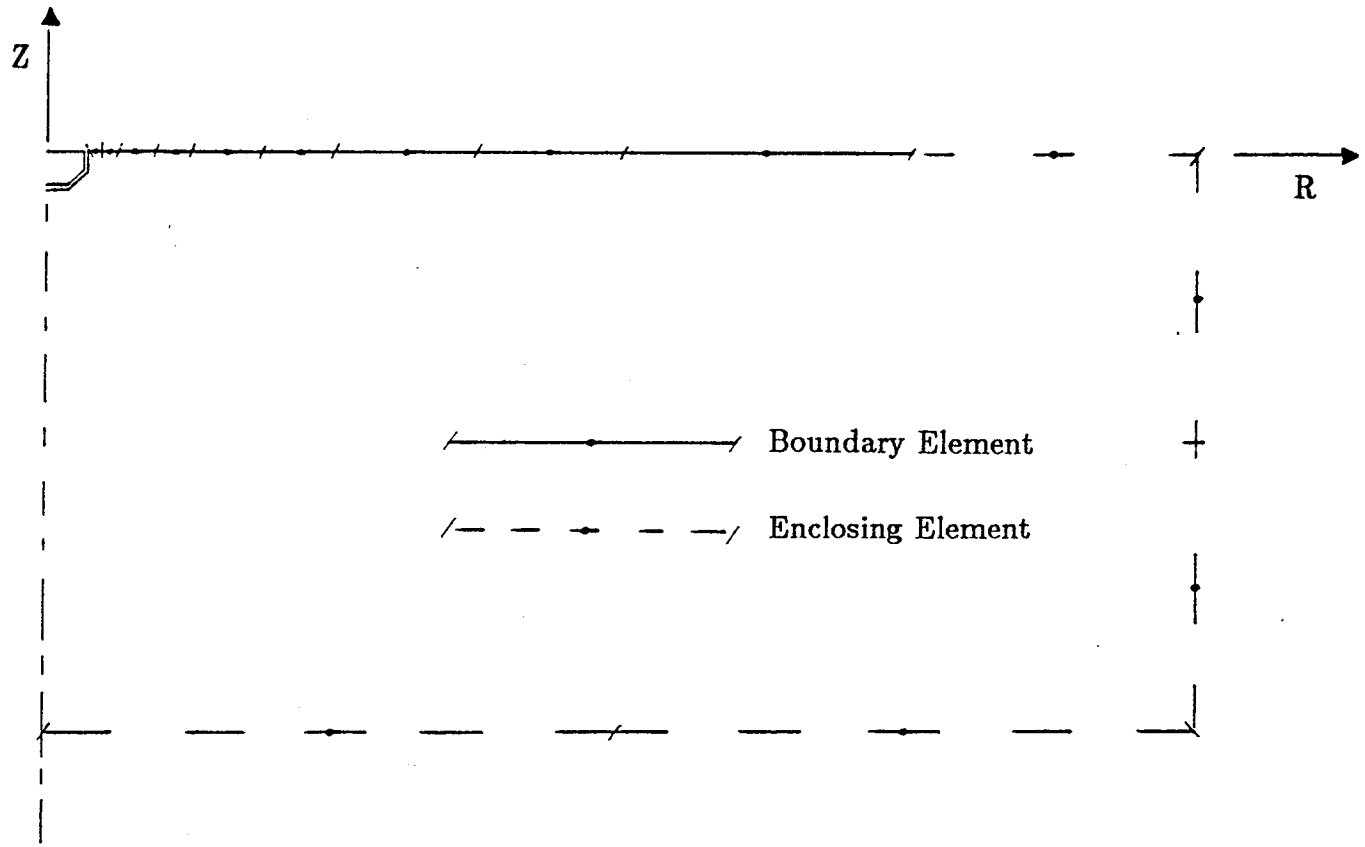

Figure 6.17
Boundary Discretization of an Axisymmetric Halfspace under a Flexible Circular Footing

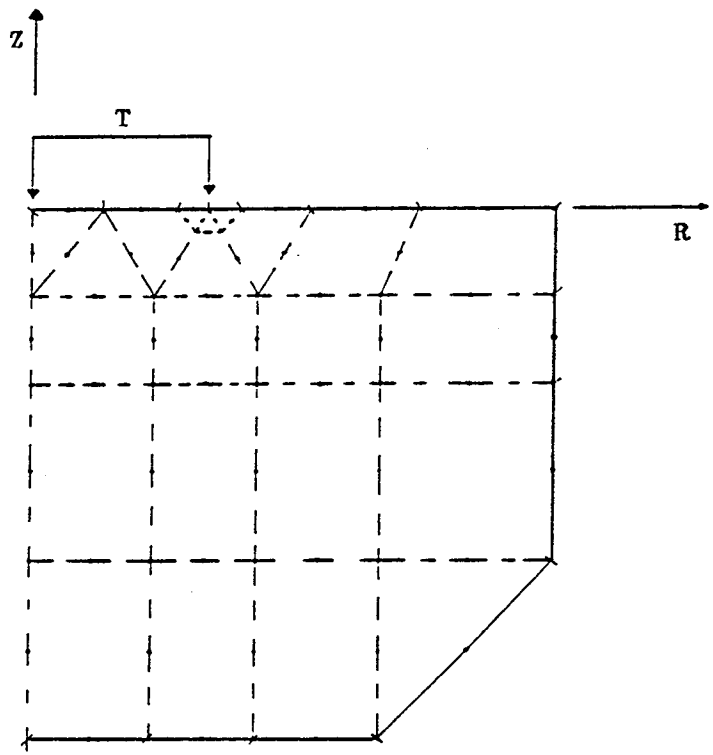

Figure 6.18a
Mesh 1: Volume Discretization of the Plastic Region under a Circular Footing

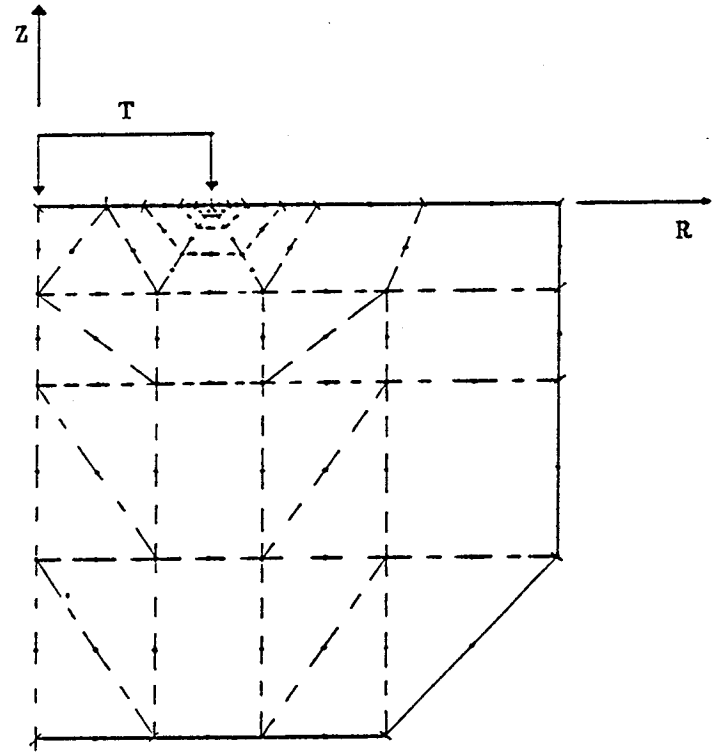

Figure 6.18b
Mesh 2: Refine Mesh of the Plastic Region under a Circular Footing

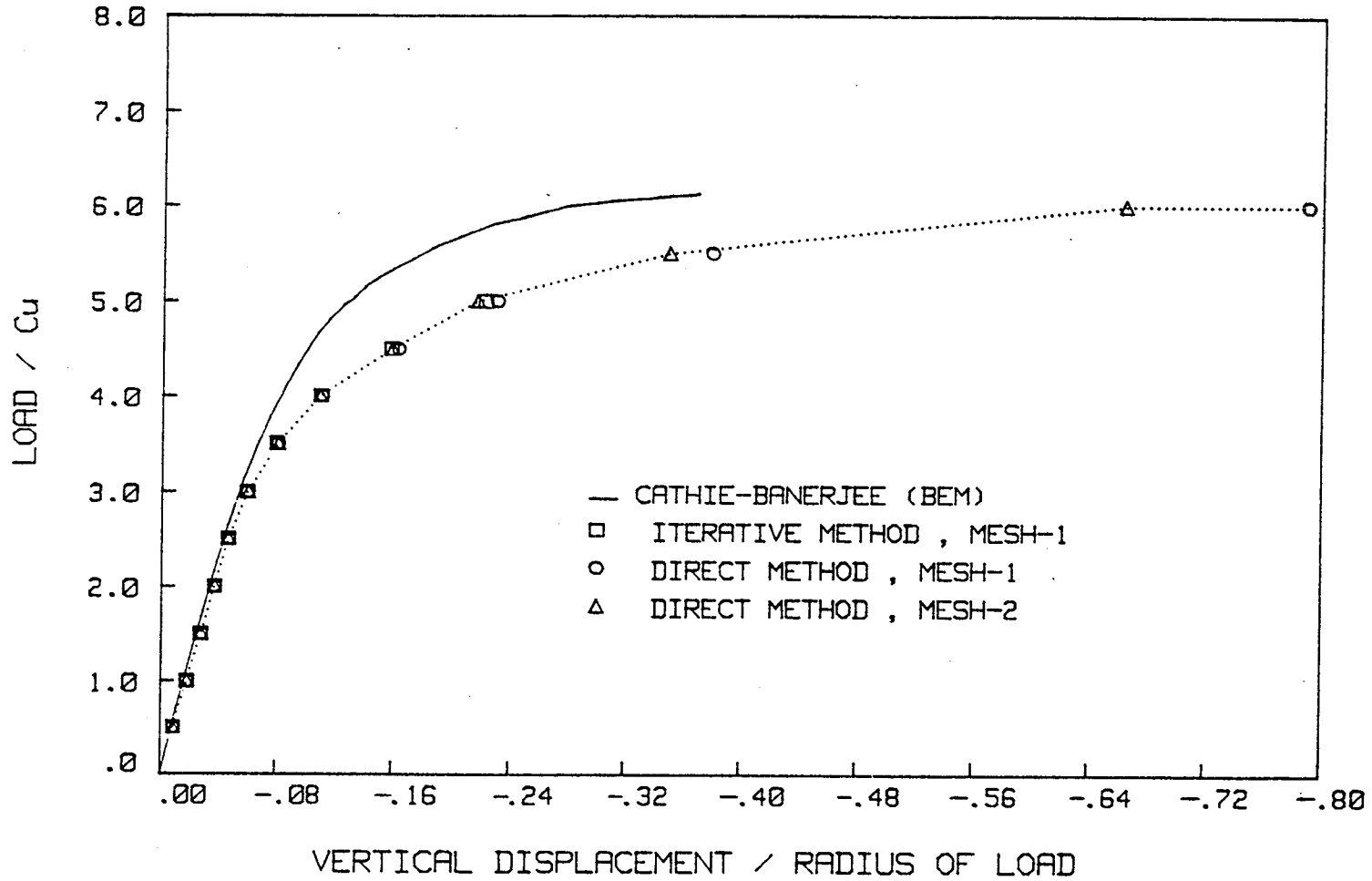

Figure 6.19
Load-Displacement Behavior under a Circular Footing

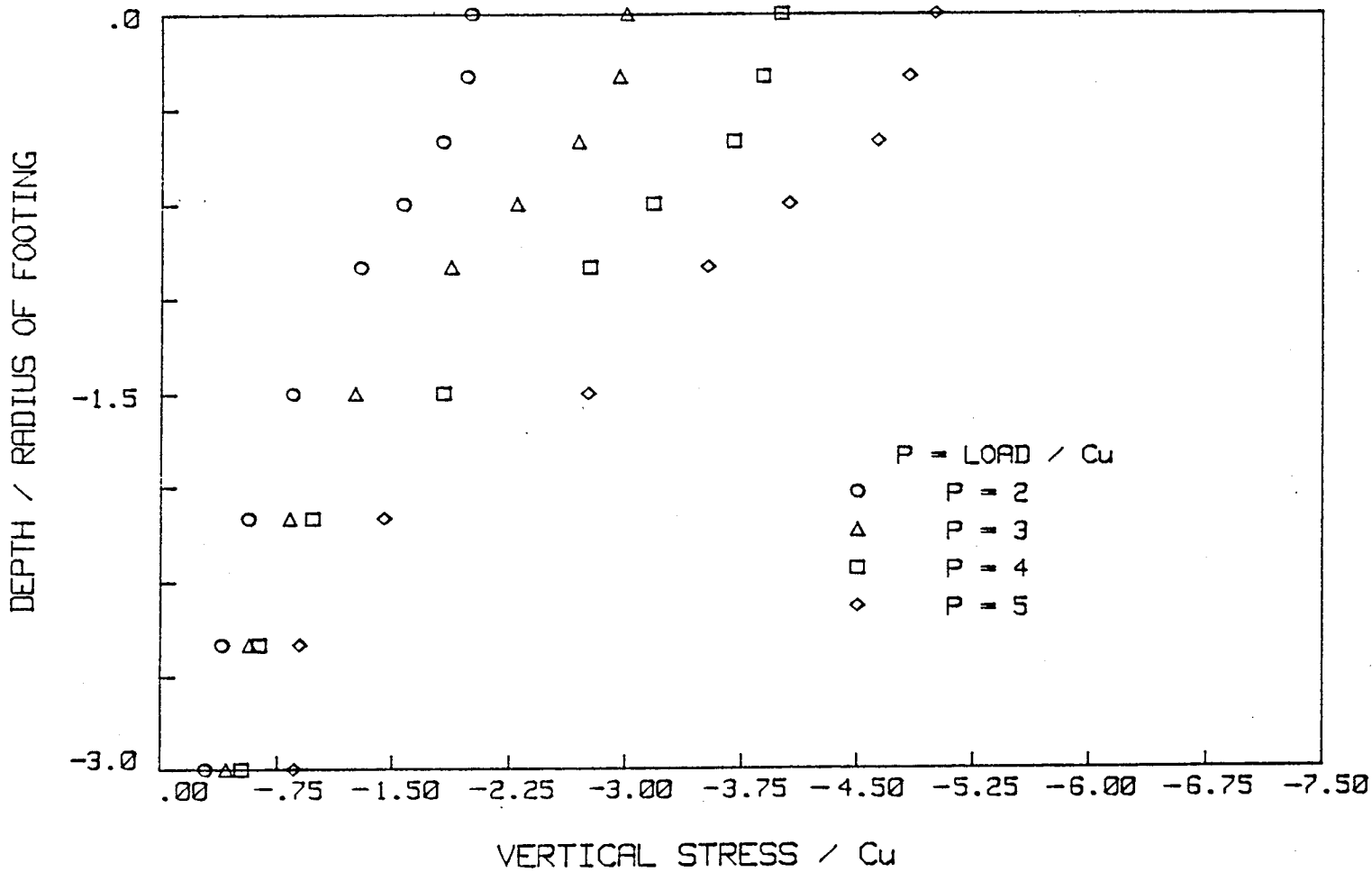

Figure 6.20
Vertical Stress at the Origin under a Circular Footing

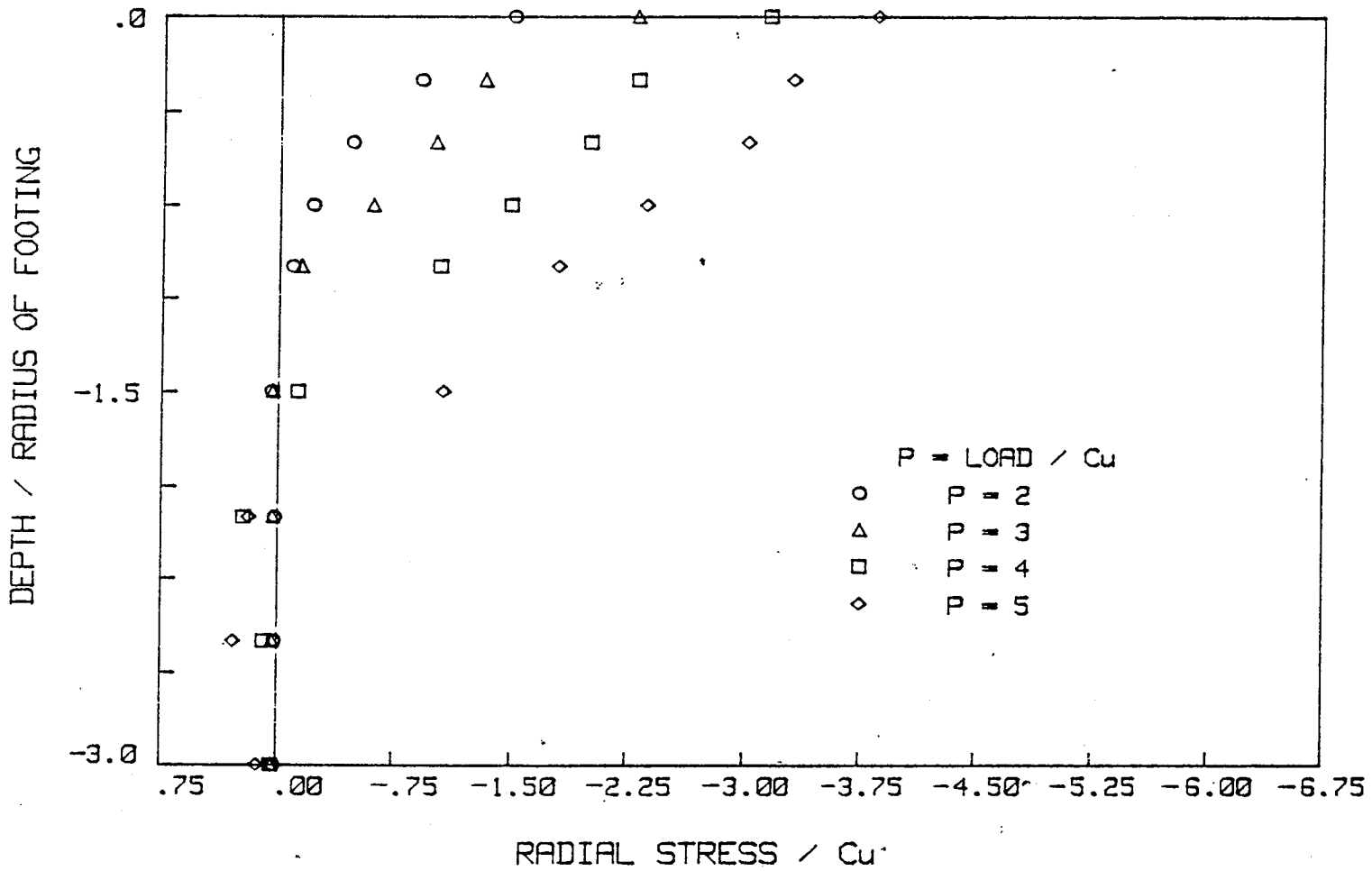

Figure 6.21
Radial Stress at the Origin under a Circular Footing

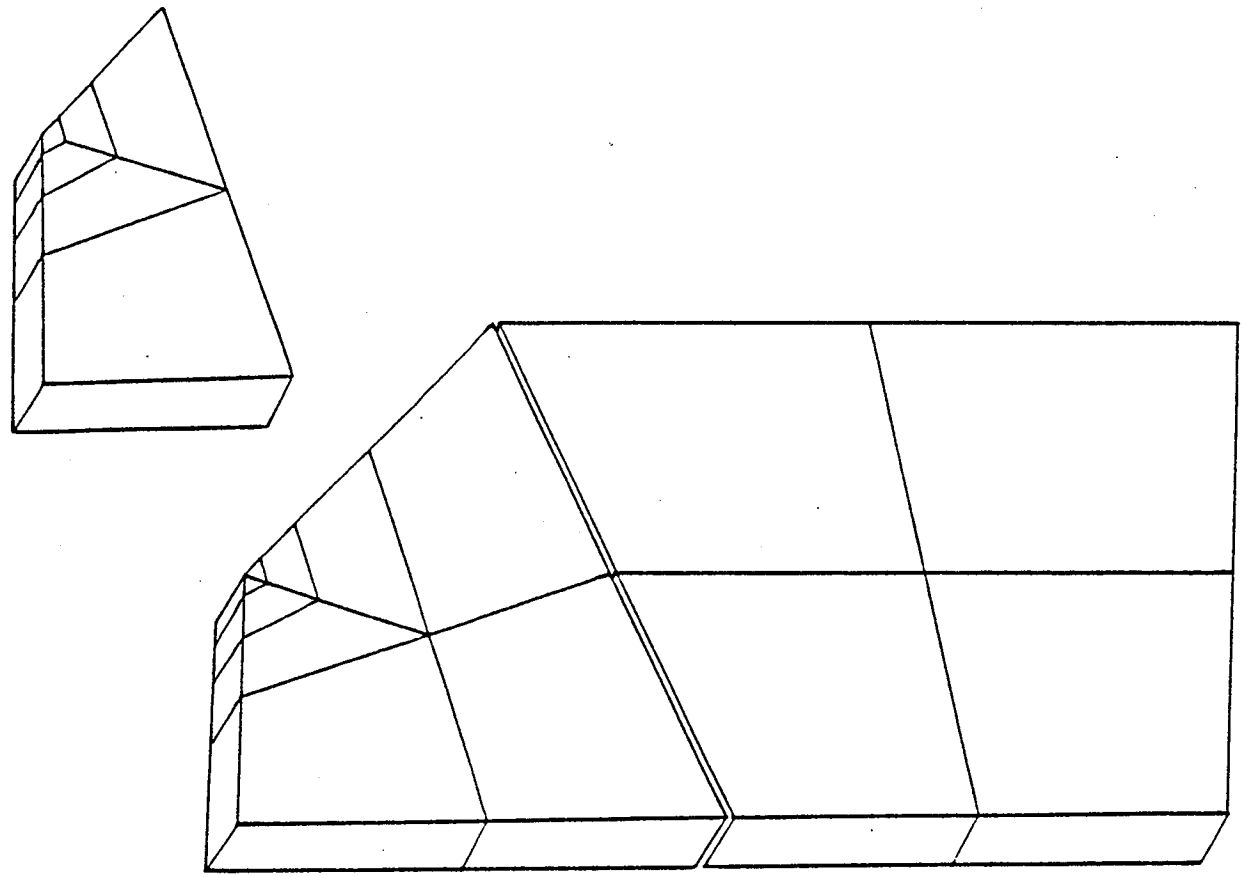

Figure 6.22
Boundary and Volume Discretization of a Three-dimensional Notch Plate

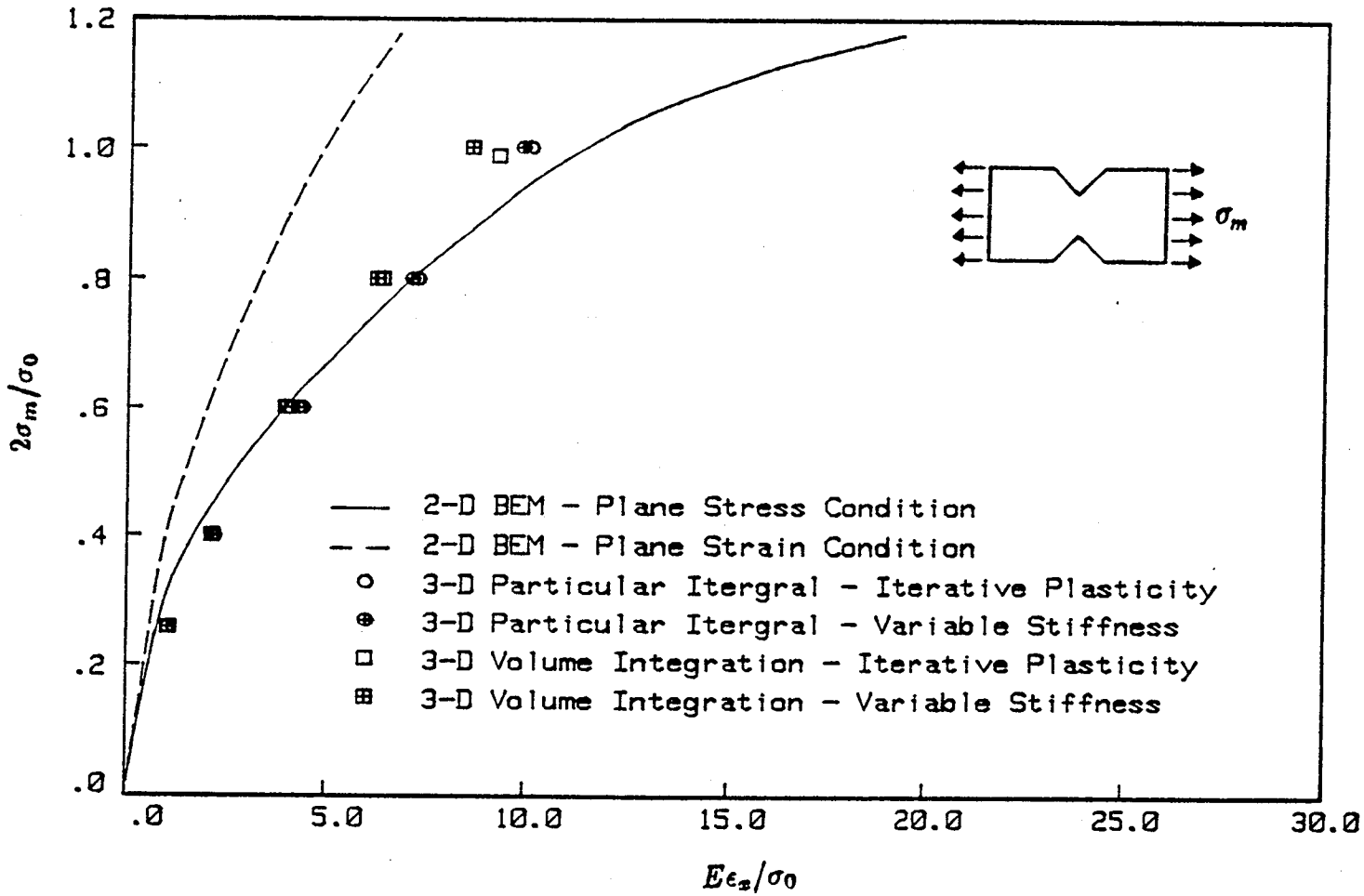

Figure 6.23
Stress-Strain Response (on the Mid-plane) at the Root of a
Three-dimensional Notch Plate

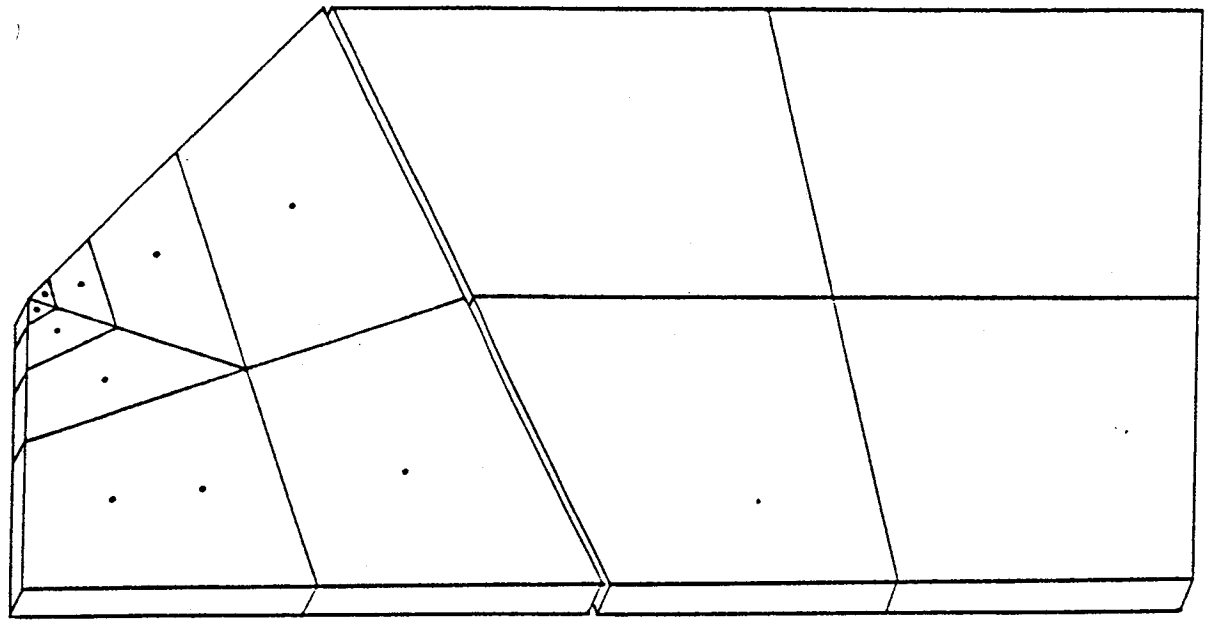

Figure 6.24
Three-dimensional Discretization of a Notch Plate for Particular Integral Analysis

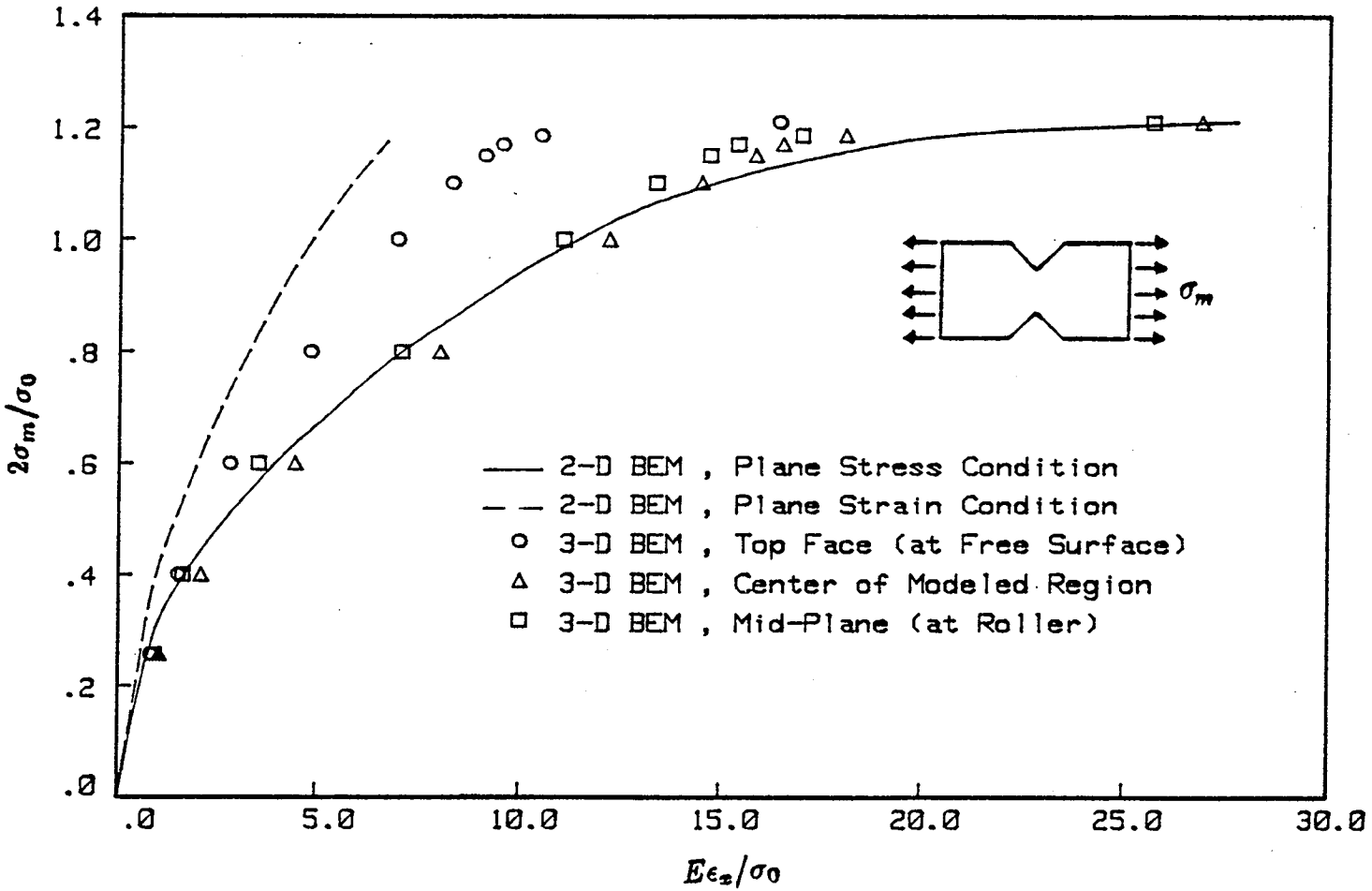

Figure 6.25
Stress-Strain Response at the Root of a Notch Plate,
Particular Integral - Variable Stiffness (Plane Stress) Analysis

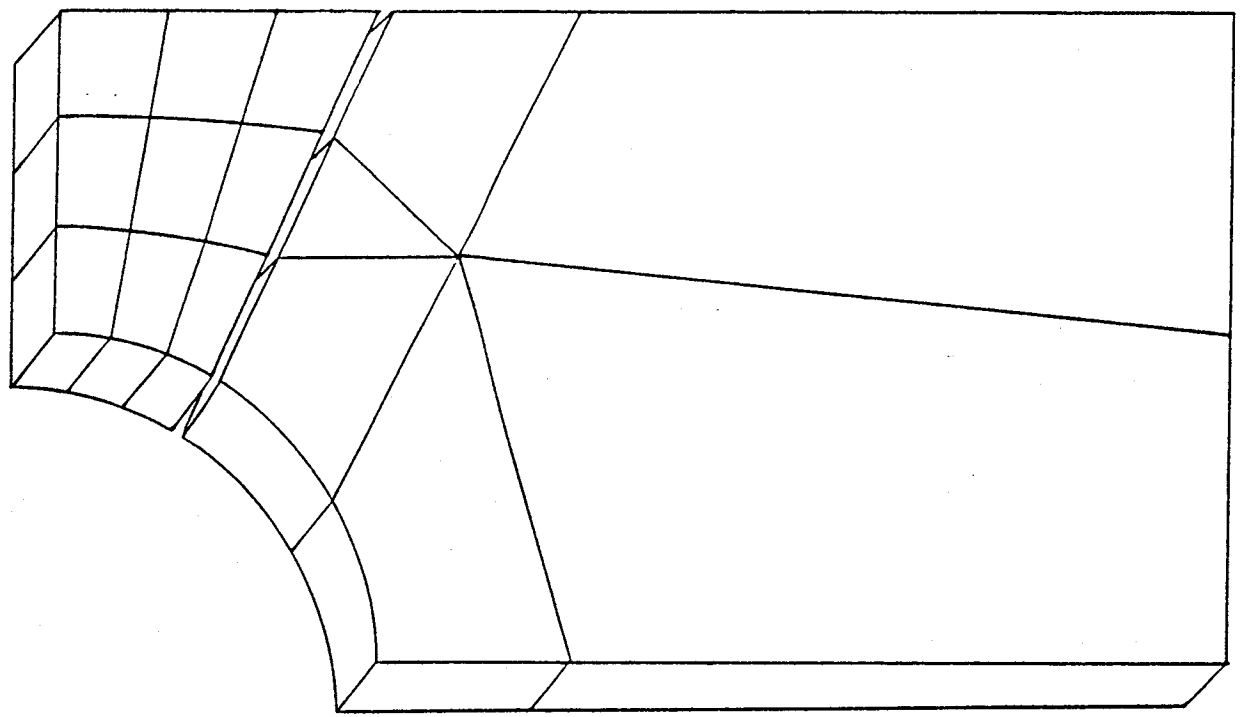

(2 Regions, 9 cells)

Figure 6.26
Three-Dimensional Mesh of a Perforated Plate

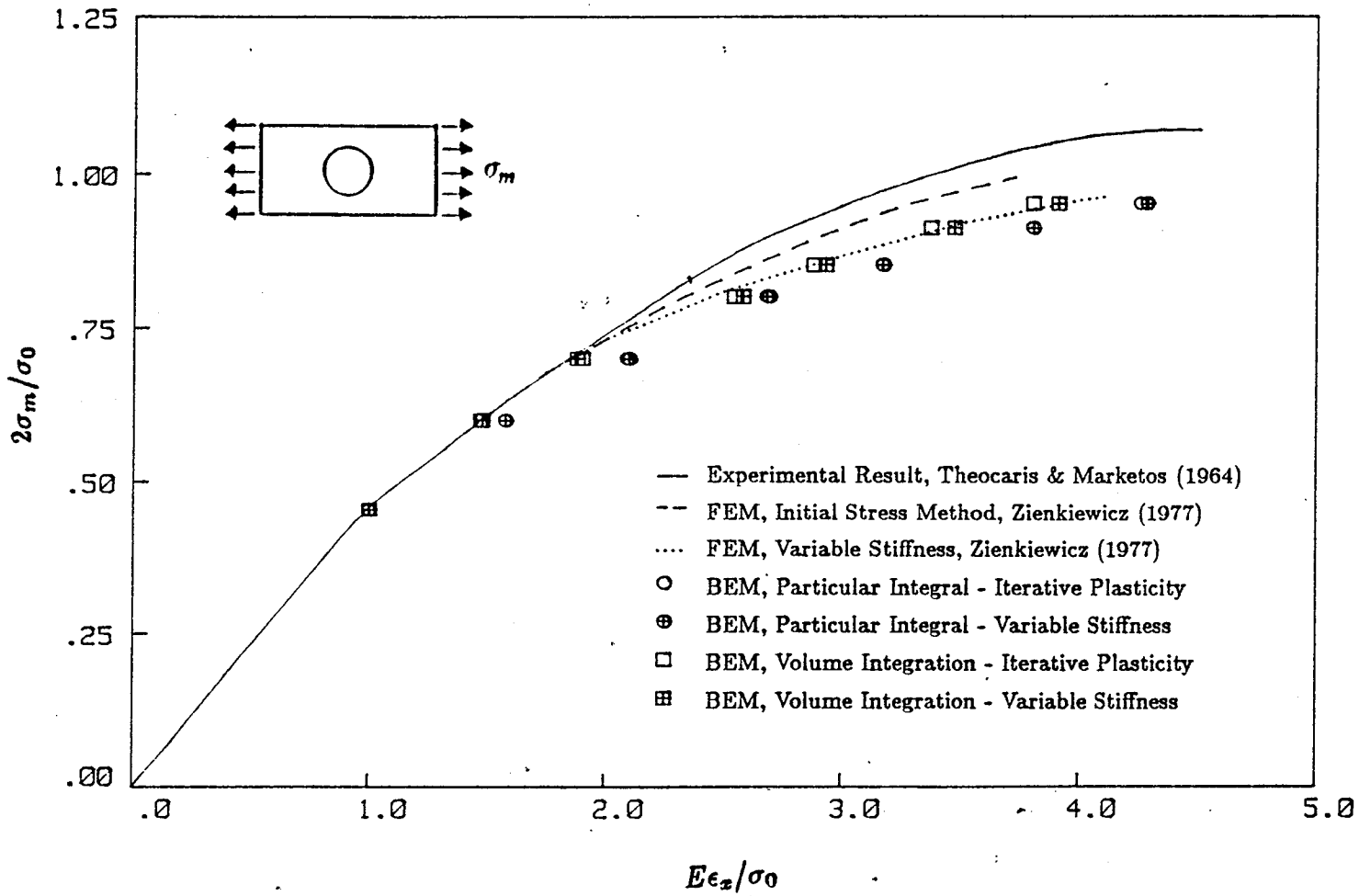

Figure 6.27

Stress-Strain Response at the Root of a 3-D Perforated Plate

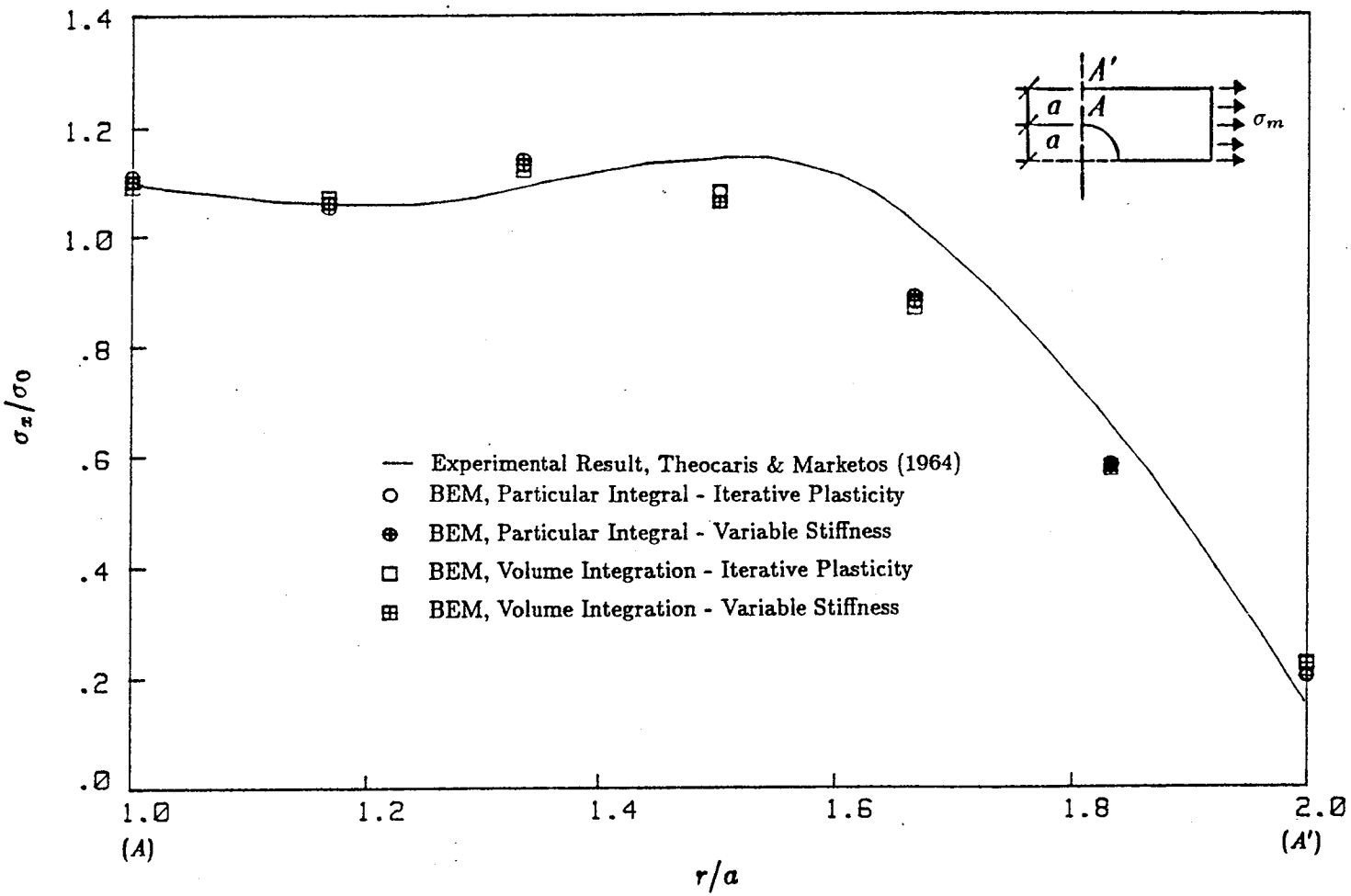

Figure 6.28
Stress Distribution across a 3-D Perforated Plate near Collapse Load (at $2\sigma_m/\sigma_0 = 0.91$)

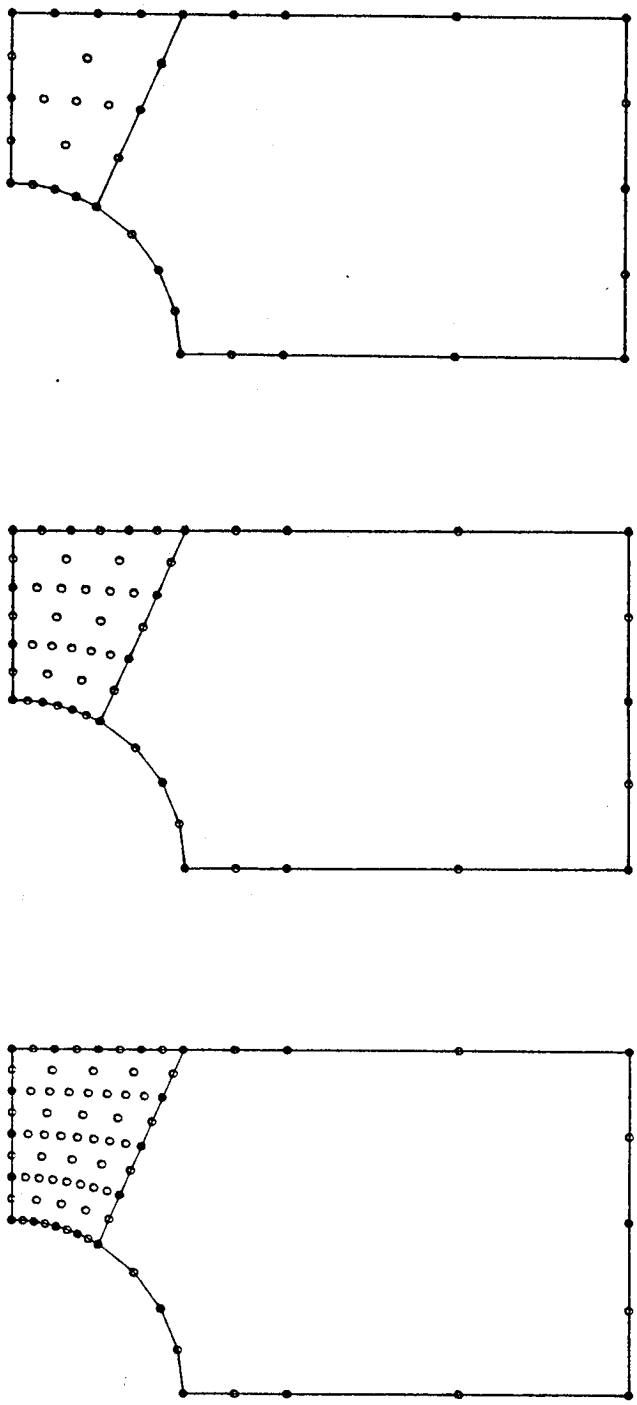

Figure 6.29
Discretization of a Two-dimensional Perforated Plate

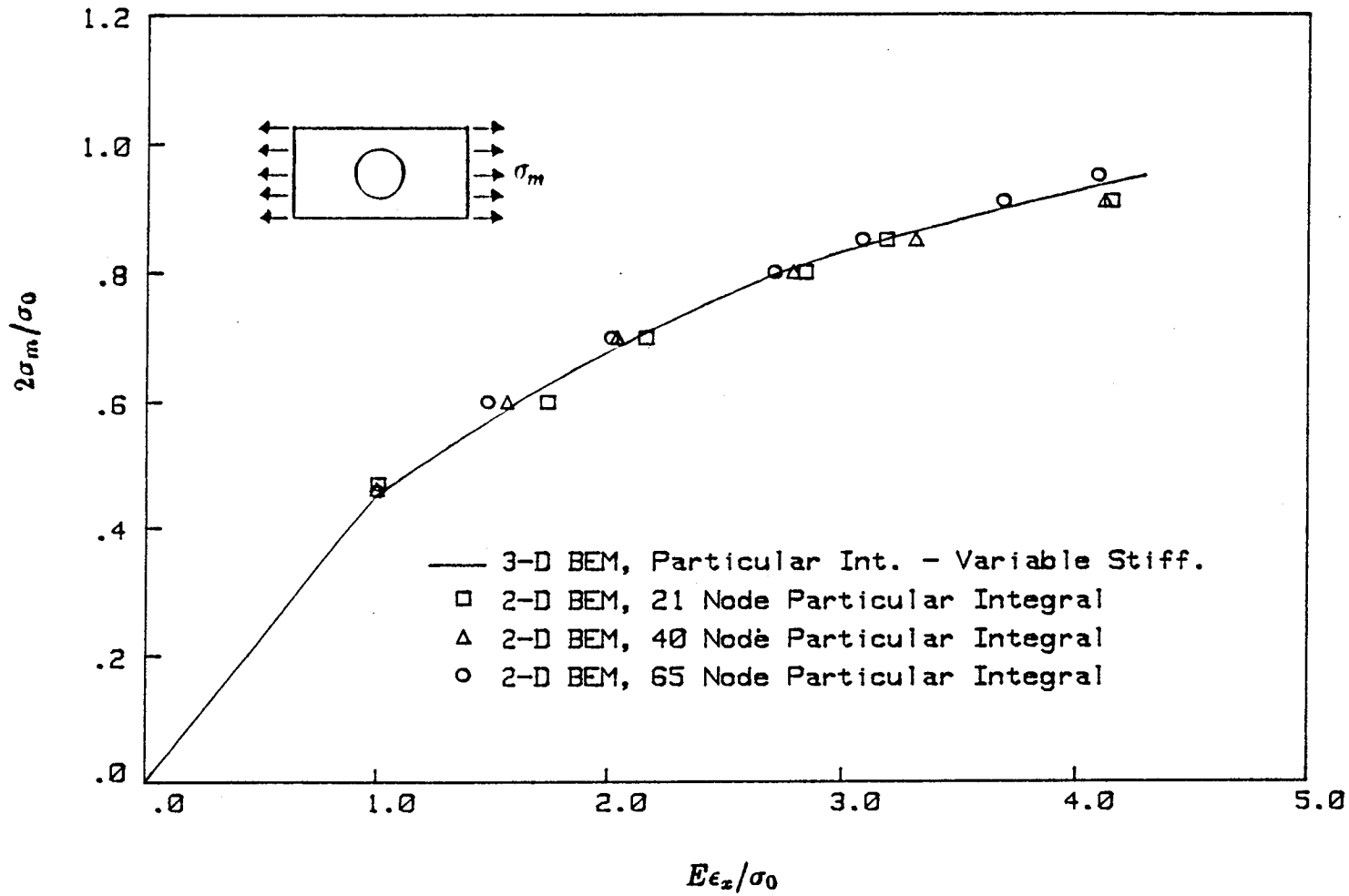

Figure 6.30
Stress-Strain Response at the Root of a Perforated Plate (Plane Stress)

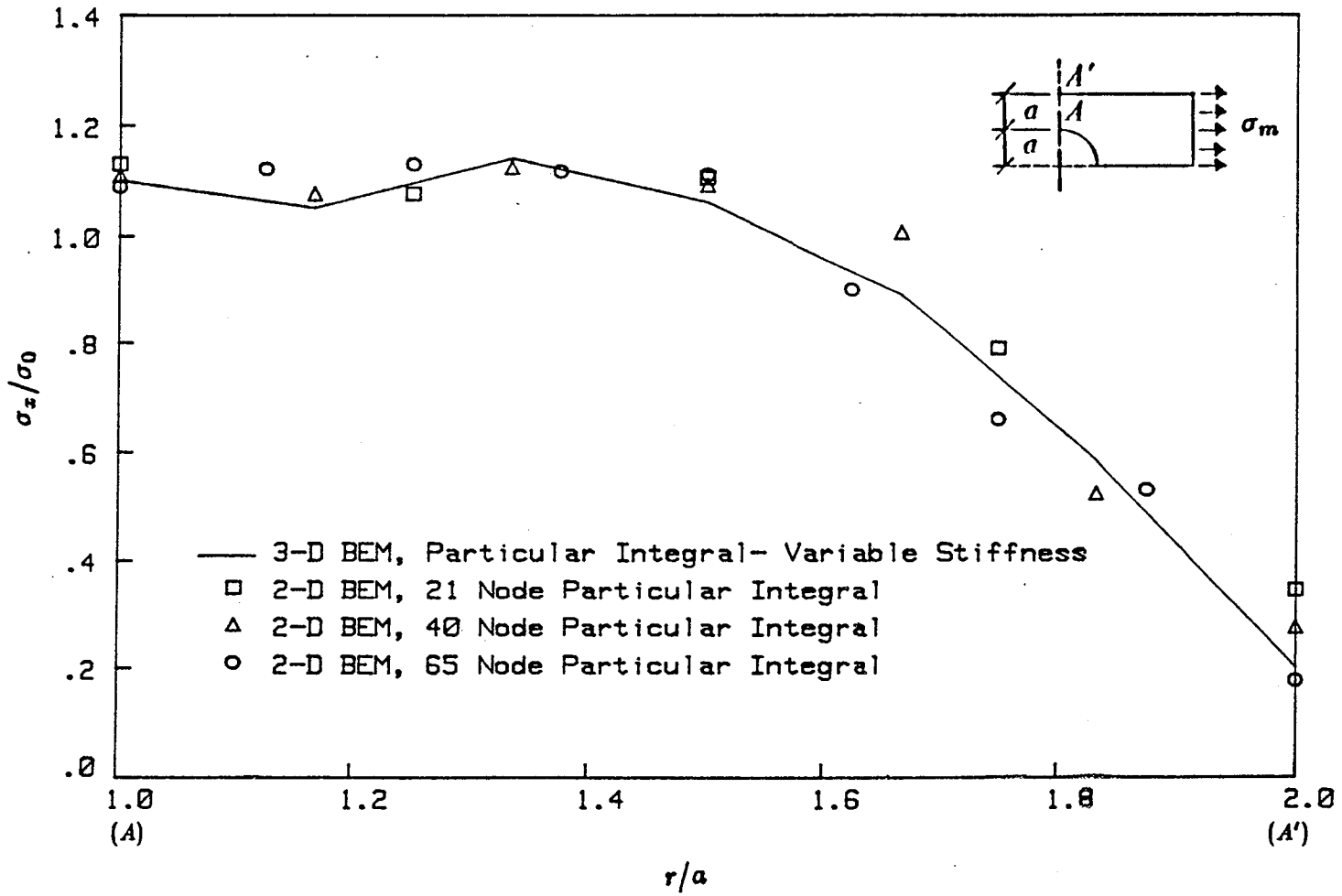

Figure 6.31
Stress-Distribution across a Perforated Plate (Plane Stress)

CHAPTER 7

CONCLUSIONS AND RECOMMENDATIONS

7.1 GENERAL CONCLUSIONS

7.2 RECOMMENDATIONS FOR FUTURE WORK

CHAPTER SEVEN

CONCLUSIONS AND RECOMMENDATIONS

7.1 GENERAL CONCLUSIONS

Considerable effort was aimed at extending all formulations presented in this dissertation to their axisymmetric form. The inelastic axisymmetric BEM analysis of this work represents the most advanced implementation of its kind. The initial stress expansion technique was particularly helpful in axisymmetry to overcome the difficulty in calculating the coefficient of a singular point near the origin.

A direct, variable stiffness type inelastic solution algorithm was, for the first time, implemented in a general purpose, multiregion computer code. Although the computational time of analysis for this method is greater than that of the conventional iterative procedure, a distinct advantage of the variable stiffness method is its ability to produce a solution close to the collapse state of stress.

New boundary element formulations, based on particular integrals, were introduced for the treatment of body forces and nonlinear effects. The method eliminated the need for volume integrals or extra surface integrals to account for these effects. Furthermore, the method is applicable to other BEM analysis which involve an inhomogeneous differential equation.

Finally, inhomogeneous formulations were presented for elastic and (for the first time) inelastic media. The formulations accounted

for thermally induced inhomogeneities and those resulting from natural variation in material parameters. The equation system of this analysis is arranged in the same form as the homogeneous-material system. This allowed existing inelastic solution algorithms to be employed without modification.

7.2 RECOMMENDATIONS FOR FUTURE WORK

In order to facilitate future research based on the findings of the present work, the following recommendations are presented:

1. The axisymmetric analysis of the present work is capable of handling axisymmetric (boundary and body force) loading only. Although the axisymmetric elastic analysis for arbitrary loading exists, to date, the inelastic formulation does not, and therefore, should be developed.

2. Further refinement for efficiency is needed in the variable stiffness inelastic solution algorithm. At present, a solution of a new system matrix is required at every load step. A new strategy, utilizing a re-solution of the previous increment's decomposed matrix system at alternate load steps, may be possible.

3. The variable stiffness method is more stable than the iterative algorithm near the collapse state of stress, however, the iterative method is capable of plastic strain softening where the present variable stiffness implementation is not. It is conceivable that a hybrid method could be developed that would incorporate the best features of both methods.

4. The present work has been more concerned with the development of BEM as an instrument for solving inelastic problems than with the development of inelastic models for BEM. This was obvious since only the Von Mises yield criterion (with hardening) was employed. Now with the present inelastic BEM analysis refined to such an advanced stage, more realistic material models need to be included for the study of more complex materials.

5. The analyses in this dissertation are limited to problems of material nonlinearities. Problems such as metal forming require the modeling of geometric nonlinearities associated with finite displacement theory. BEM formulations should be developed based on this theory. An extended form of the particular integral based method can be derived for this purpose or the conventional volume integral approach can be used.

6. Although the present functional form of the global shape function, chosen for the approximation of the particular integrals, produced satisfactory results, further research still should be devoted to the discovery of new functions.

7. The axisymmetric and two-dimensional inhomogeneous formulations developed in this dissertation should be extended to three-dimensional analysis. However, the extension to three-dimensions greatly increases the overhead of the analysis, and therefore, an efficiency study should be carried out to determine its feasibility.

8. The variable stiffness algorithm, the particular integral formulation, and the inhomogeneity formulation all have one thing in common. All involve a large amount of matrix manipulations. Therefore, to maximize the efficiency of these new methods, the computer code should be vectorized to exploit the state-of-the-art computer technology.

REFERENCES

REFERENCES

Abramowitz, M. and Stegun, I.E. (1974). Handbook of Mathematical Dover, New York.

Ahmad, S. (1986). 'Linear and Nonlinear Dynamic Analysis by the Boundary Element Method,' Ph.D. Thesis, State University of New York at Buffalo.

Ahmad, S. and Banerjee, P.K. (1986). 'Free Vibration Analysis by BEM Using Particular Integrals,' Jour. of Eng. Mech., ASCE, 112, pp. 682-695.

Bakr. A.A. and Fenner, R.T. (1983). 'Boundary Integral Equation Analysis of Axisymmetric Thermoelastic Problems,' Journal of Strain Analysis, Vol. 18, No. 4, pp. 239-251.

Banerjee, P.K. (1969). 'A Contribution to the Study of Axially Loaded Pile Foundation,' Ph.D Thesis, Faculty of Applied Science, University of Southampton.

Banerjee, P.K. (1976). 'Integral Equation Methods for Analysis of Piece-wise Nonhomogeneous Three-dimensional Elastic Solids of Arbitrary Shape,' Int. J. Mech. Sci., 8, pp. 293-303.

Banerjee, P.K. and Ahmad, S. (1985). 'Advanced Three-dimensional Dynamic Analysis by Boundary Element Method,' Pro. of ASCE Conf. on Advanced Topics in Boundary Element Analysis, AMD-Vol. 72.

Banerjee, P.K. and Butterfield, R. (1976). 'Boundary Element Methods in Geomechanics,' Num. Methd. in Soil and Rock Mechanics, Chap. 16, Ed. Gudehus, G, Wiley.

Banerjee, P.K. and Butterfield, R. (1979). Developments in Boundary Element Methods I, Applied Sci. Publishers, Barking, Essex, UK.

Banerjee, P.K. and Butterfield, R. (1981). Boundary Element Methods in Engineering Science, McGraw-Hill, London, UK.

Banerjee, P.K., Cathie, D.N. and Davies, T.G. (1979). 'Two and Three-dimensional Problems of Elastoplasticity,' Chapter IV in Developments in Boundary Element Methods I, Ed. Banerjee, P.K. and Butterfield, R., Applied Science Publishers, Barking, Essex, UK.

Banerjee, P.K. and Cathie, D.N. (1980). 'A Direct Formulation and Numerical Implementation of the Boundary Element Method for Two-dimensional Problems of Elastoplasticity,' Int. J. Mech. Sci., 22, pp. 233-245.

Banerjee, P.K. and Mukherjee, S. (1984). Developments in Boundary Element Methods III, Applied Sci. Publishers, Barking, Essex, UK.

Banerjee, P.K. and Mustoe, G.G.W. (1978). 'Boundary Element Methods in Two-dimensional Problems of Elasto-plasticity,' Proc. Int. Conf. on Recent Developments in BEM, pp. 283-300, Southampton University.

Banerjee, P.K. and Raveendra, S.T. (1986). 'Advanced Boundary Element Analysis of Two and Three-dimensional Problems of Elastoplasticity,' International Journal for Numerical Methods in Engineering, Vol. 23, pp. 985-1002.

Banerjee, P.K. and Raveendra, S.T. (1987). 'A New Boundary Element Formulation for Two-dimensional Elastoplastic Analysis,' Journal of Engineering Mechanics, ASCE, Vol. 113, No. 2, pp. 252-265.

Banerjee, P.K. and Shaw, R.P. (1982). Developments in Boundary Element Methods II, Applied Sci. Publishers, Barking, Essex, UK.

Banerjee, P.K. and Watson, J.O. (1986). Developments in Boundary Element Methods - IV, Applied Sci. Publishers, UK.

Banerjee, P.K., Wilson, R.B. and Miller, N. (1985). 'Development of a Large BEM System for Three-dimensional Inelastic Analysis,' Proc. of ASME Conf. on Advanced Topics in Boundary Element Analysis, AMD-Vol. 72.

Boley, B.A. and Weiner (1960). J.H., Theory of Thermal Stresses, New York, Wiley.

Brebbia, C.A. Telles, J.C. and Wrobel, L.C. (1984). Boundary Element Techniques - Theory and Application in Engineering, Springer-Verlag, Berlin and New York.

Bui, H.D. (1978). 'Some Remarks About the Formulation of Three Dimensional Thermoelastoplastic Problems by Integral Equations,' Int. J. Solids Structures, 14, pp. 935-939.

Butterfield, R. (1978). 'An Application of the Boundary Element Method to Potential Flow Problems in Generally Inhomogeneous Bodies,' Recent Advances in the Boundary Element Method, Ed. Brebbia, C.A., p. 123, Pentech. Press, London, UK.

Butterfield, R. and Banerjee, P.K. (1971). 'The Problems of Pile Cap, Pile Groups Interaction,' Geotech., 21(2), pp. 135-141.

Cathie, D.N. and Banerjee, P.K. (1980). 'Boundary Element Methods in Axisymmetric Plasticity,' Innovative Numerical Analysis for the Applied Engineering Sciences, Ed. R.P. Shaw et al, University of Virginia Press.

Cathie, D.N. and Banerjee, P.K. (1982). 'Boundary Element Methods for Plasticity and Creep Including a Viscoplastic Approach,' Res. Mechanica, 4, pp. 3-22.

Chaudonneret, M. (1977). 'Methode des Equations Integrales Appliquees a la Resolution de Problemes de Viscoplasticite,' J. Mecanique Appliquee, 1:113-132.

Chaudouet, A. and Loubignac, G. (1981). 'Boundary Integral Equations Used to Solve Thermoelastic Problems: Application to Standard and Incompressible Materials,' in Numerical Methods in Heat Transfer, Ed., by R.W. Lewis, K. Morgan and O.C. Zienkiewicz, John Wiley and Sons, London-New York, pp. 115-133.

Chen, W.F. (1975). Limit Analysis and Soil Plasticity, Elsevier, New York.

Chiu, Y.P. (1977). 'On the Stress Field Due to Initial Strains in a Cuboid Surrounded by an Infinite Elastic Space,' Jour. of App. Mech., ASME, pp. 587-590.

Cruse, T.A. (1967). Transient Problems in Classical Elastodynamics Solved by Integral Equation, Ph.D Thesis, University of Washington.

Cruse, T.A. (1969). 'Numerical Solutions in Three Dimensional Elastostatics,' Int. J. Sol. Struct., No. 5, pp. 1259-1274.

Cruse, T.A. (1972). 'Application of the Boundary Integral Solution Method in Solid Mechanics, Var. Meth. in Engng. II, Proc. of Conf. Var. Meth. in Engng., Southampton.

Cruse, T.A. (1973). 'Application of the Boundary Integral Equation Method to 3-D Stress Analysis,' J. Comp. Struct. 3, pp. 509-527.

Cruse, T.A. (1974). 'An Improved Boundary Integral Equation Method for Three-dimensional Elastic Stress Analysis,' Int. Jour. Computers and Structures, 4, pp. 741-757.

Cruse, T.A. and Rizzo, F.J. (1968). 'A Direct Formulation and Numerical Solution of the General Transient Elastodynamic Problem,' Part I and II, J. Math. and Appl. 22, pp. 244-259 and 241-358.

Cruse, T.A., Snow, D.W. and Wilson, R.B. (1977). 'Numerical Solutions in Axisymmetric Elasticity,' Comp. and Struct., 7, pp. 445-451.

Cruse, T.A. and Wilson, R.B. (1979). 'Advanced Applications of Boundary Integral Equation Methods,' Nucl. Eng. Des., 46, pp. 223-234.

Danson, D.J. (1981). 'A Boundary Element Formulation of Problems in Linear Isotropic Elasticity with Body Forces,' Proc. 3rd Int. Seminar on Recent Advances in Boundary Element Methods, Irvine, California, pp. 105-122.

Dinno, K.S. and Gill, S.S. (1965). 'An Experimental Investigation into the Plastic Behavior of Flush Nozzles in Spherical Pressure Vessels,' International Journal of Mechanical Sciences,' Vol. 7, pp. 817.

Dongarra, J.J., et al, (1979). Linpack User's Guide, SIAM, Philadelphia, PA.

Drucker, D.C. (1951). 'A More Fundamental Approach to Plastic Stress-Strain Relations,' Proc. 1st U.S. Nat. Cong. Appl. Mech., ASME, pp. 487-491.

Drucker, D.C. (1956). 'On Uniqueness in the Theory of Plasticity,' Quart. Appl. Math., 14, pp. 35-42.

Drucker, D.C. (1959). 'A Definition of Stable Inelastic Materials,' J. Appl. Mech. Trans. ASME, 26, No. 1, pp. 101-106.

Eshelby, J.D. (1961) 'Elastic Inclusions and Inhomogeneities,' Progress in Solid Mechanics, Vol. 2, Eds., Sneddon, I.N. and Hill, R., North-Holland Publishing Col, pp. 89-139.

Ford, H. and Alexander, J.M. (1977). Advanced Mechanics of Materials, 2nd Edition, Ellis Horwood, Chichester.

Fredholm, I. (1903). 'Sur une Classe d'equations Fonctionelles,' Acta Math., Vol. 27, pp. 365-390.

Fredholm, I. (1905). 'Solution d'un Probleme Fondamental de la Theorie de l'elasticite,' Arkiv Mat. Astron. Fys., pp. 1-8.

Fung, Y.C. (1965). Foundations of Solid Mechanics, Prentice Hall.

Ghosh, S. and Mukherjee (1984). 'Boundary Element Method Analysis of Thermoelastic Deformation in Nonhomogeneous Media,' Int. J. Solid Structures, Vol. 20, No. 9/10, pp. 829-843.

Henry, D.P., Pape, D.A. and Banerjee, P.K. (1987). 'New Axisymmetric BEM Formulation for Body Forces Using Particular Integrals, Jour. of Eng. Mech., ASCE, Vol. 113, No. 5, pp. 671-688.

Henry, D.P. and Banerjee, P.K. (1987). 'A Thermoplastic BEM Analysis of Substructured Axisymmetric Bodies,' Jour. of Eng. Mech., ASCE, to appear.

Hill, R. (1950). The Mathematical Theory of Plasticity, Clarendon Press, Oxford.

Hodge, P.G. Jr. and White, G.N. Jr. (1950). 'A Quantitative Comparison of Flow and Deformation Theories of Plasticity,' J. Appl. Mech., 17, pp. 180-184.

Jaswon, M.A. and Ponter, A.R. (1963). 'An Integral Equation Solution of the Torsion Problem,' Proc. Roy. Soc. Ser. A., 273, pp. 237-246.

Kamiya, N. and Sawaki, Y. (1985). 'An Efficient BEM for Some Inhomogeneous and Nonlinear Problems,' Proc. 7th Int. Conf. on BEM, Italy, pp. 13-59 to 13-68.

Kellog, O.D. (1929). Foundations of Potential Theory, Dover Publ., New York, 1953.

Kermanidis, T. (1975). 'A Numerical Solution for Axially Symmetrical Elasticity Problems,' Int. Jour. Solids Struct., 11, pp. 493-500.

Kobayashi, S. and Nishimura, N. (1980). 'Elastoplastic Analysis by the Integral Equation Method,' Mem. Fac. Eng., Kyoto Univ., pp. 324-334.

Kumar, V. and Mukerjee, S. (1977). 'A Boundary Integral Equation Formuation for Time Dependent Inelastic Deformation in Metals,' Int. J. Mech. Sci., 19, No. 12, pp. 713-724.

Kupradze, V.D. (1964). 'Dynamic Problem in Elasticity,' Progress in Solid Mech., 3rd Ed., Sneddon, I.N. and Hill, R., North Holland.

Lachat, J.C. (1975). 'Further Development of Boundary Integral Techniques for Elastostatics,' Ph.D. Thesis, Southampton University, UK.

Lachat, J.C. and Watson, J.O. (1976). 'Effective Numerical Treatment of Boundary Integral Equations: A Formulation for Three-dimensional Elastostatics,' Int. J. Num. Meth. Engng.,.10, pp. 991-1005.

Lamb, H. (1932). Hydrodynamics, 6th Ed., Dover, New York.

Love, A.E.H. (1944). A Treatise on the Mathematical Theory of Elasticity, Dover, New York.

Masinda, J. (1984). Application of the Boundary Element Method to 3D Problems of Non-stationary Thermoelasticity,' Eng. Anal., Vol. 1, No. 2, pp. 66-69.

Mayer, M., Drexler, W. and Kuhn, G. (1980). 'A Semi-analytical Boundary Integral Approach for Axisymmetric Elastic Bodies with Arbitrary Boundary Conditions,' Int. J. Solids β Struct., 16, pp. 863-871.

Mendelson, A. (1968). Plasticity, Theory and Application, Macmillan, New York.

Mendelson, A. and Albers, L.V. (1975). 'Application of Boundary Integral Equation Method to Elastoplastic Problems,' Proc. ASME Conf. on Boundary Integral Equation Methods, AMD, 11, Eds. Cruse, T.A. and Rizzo, F.J., New York.

Mikhlin, S.G. (1957). Integral Equations, Pergamon Press, London.

Mikhlin, S.G. (1962). 'Singular Integral Equations,' Amer. Math. Soc. Trans. Series 1, 10, pp. 84-197.

Mikhlin, S.G. (1964). Variational Methods in Mathematical Physics, Macmillan, New York.

Mikhlin, S.G. (1965). Multidimensional Singular Integrals and Integral Equations. Pergamon Press. Mindlin, R.D. (1936). 'Force at a Point in the Interior of a Semi-infinite Solid,' Physics.

Morjaria, M. and Mukherjee, S. (1980). 'Improved Boundary Integral Equation Method for Time Dependent Inelastic Deformation in Metals,' Int. J. Num. Meth. Engng., 15, pp. 97-111.

Morjaria, M. and Mukherjee, S. (1981). 'Numerical Analysis of Planar Time Dependent Inelastic Deformation of Plates with Cracks by Boundary Element Method,' Int. J. Solids Struct., 17, pp. 127-143.

Mukherjee, S. (1977). 'Corrected Boundary Integral Equations in Planar Thermoelastoplasticity,' Int. J. Solid and Struct., 13, No. 4, pp. 331-336.

Mukherjee, S. (1982). Boundary Elements in Creep and Fracture, Applied Science Publishers, London, UK.

Mukherjee, S. and Kumar, V. (1978). 'Numerical Analysis of Time Dependent Inelastic Deformation in Metallic Media Using Boundary Integral Equation Method,' J. Appl. Mech., ASME, 45, No. 4, pp.785-790.

Muskhelishvili, N.I. (1953). Singular Integral Equations, Noordoff, Gronigen.

Mustoe, G.G.W. (1980). 'Symmetric Variational Boundary Integral Equation Procedures in Continuum Mechanics,' Ph.D. Thesis, University of Wales, Swansea, UK.

Mustoe, G.G. (1984). 'Advanced Integration Schemes Over Boundary Elements and Volume Cells for Two and Three-dimensional Nonlinear Analysis,' Chapter IX of Developments in BEM - IV, Applied Science Publishers, UK.

Nardini, D. and Brebbia, C.A. (1982). 'A New Approach to Free Vibration Analysis Using Boundary Elements,' Proc. of the Fourth Int. Conf. in BEM, Springer-Verlag, pp. 313-326.

Nayak, G.C. and Zienkiewicz, O.D. (1972). 'Elasto-plastic Stress Analysis, Generalization for Various Constitutive Relations Including Strain Softening,' Int. J. Num. Meth. Engng., 11, pp. 53-64.

Nigam, R.K. (1979). 'The Boundary Integral Equation Method for Elastostatics Problems Involving Axisymmetric Geometry and Arbitrary Boundary Conditions,' M.S. Thesis, University of Kentucky.

Nowacki, W. (1962). Thermoelasticity, Addison-Wesley, London, UK.

Pape, D.A. and Banerjee, P.K. (1987). 'Treatment of Body Forces in 2D Elastostatic BEM Using Particular Integrals,' Journ. Applied Mech., ASME, to appear.

Prager, W. (1955). 'Theory of Plasticity - A Survey of Recent Achievement,' (James Clayton Lecture), Proc. First Mech. Eng., 169, pp. 41-57.

Prager, W. and Hodge, P.G. (1968). Theory of Perfectly Plastic Solids, Dover, New York.

Raveendra, S.T. (1984). 'Advanced Development of BEM for Two and Three-dimensional Nonlinear Analysis,' Ph.D Thesis, State University of New York at Buffalo.

Reisner, H. (1931). 'Initial Stresses and Sources of Initial Stresses,' (In German), Z. Agnew, Math. Mech., 11, pp. 1-8.

Riccardella, P. (1973). 'An Implementation of the Boundary Integral Technique for Planar Problems of Elasticity and Elastoplasticity,' Ph.D. Thesis, Carnegie Mellon University, Pittsburgh, USA.

Rizzo, F.J. (1967). 'An Integral Equation Approach to Boundary Value Problems of Classical Elastostatics,' Quart. Appl. Math., 25, No. 1, pp. 83-85.

Rizzo, F.J. (1968). 'A Formulation and Solution Procedure for the General Non-homogeneous Elastic Inclusion Problem,' Int. J. Solids and Struct., 4.

Rizzo, F.J. and Shippy, D.J. (1968). 'A Formulation and Solution Procedure for the General Non-Homogeneous Elastic Inclusion Problem,' Int. J. Solids Struct., 4, pp. 1161-1179.

Rizzo, F.J. and Shippy, D.J. (1977). 'An Advanced Boundary Integral Equation Method for Three-dimensional Thermo-elasticity,' Int. J. Num. Meth. in Engng., Vol. 11, pp. 1753-1768.

Rizzo, F.J. and Shippy, D.J. (1986). 'A Boundary Element Method for Axisymmetric Elastic Bodies,' Chapter 3 in Developments in Boundary Element Methods, Vol. 4, pp. 67-90, Eds. Banerjee, P.K. and Watson, J.O., Applied Science Publishers, London, UK.

Rzasnicki, W. and Mendelson, A. (1975). 'Application of the Boundary Integral Equation Method to the Elasto-plastic Analysis of V-notched Beams,' NASA Tech. Report, TMX-71472.

Sarihan, V. and Mukherjee, S. (1982). 'Axisymmetric Viscoplastic Deformation by the Boundary Element Method,' Int. J. Solids Structures, 18, pp. 1113-1128.

Shield, R.T. and Ziegler, H. (1958) 'On Prager's Hardening Rule,' ZAMP., 9A, pp. 260-276.

Smirnov, V.J. (1964). 'Integral Equations and Partial Differential Equations,' A Course in Higher Mathematics, Vol. IV, Addison-Wesley, London, UK.

Sokolinikoff (1956). 'Mathematical Theory of Elasticity,' McGraw-Hill.

Somigliana, C. (1885). 'Sopra L'equllibrio di un Corpo Elastico Isotropo.'

Somigliana, C. (1892). Atti Reale Accad. Linc. Roma, Series 5, Vol. 1, p. 111.

Stroud, A.H. and Secrest, D. (1966). Gaussian Quadrature Formulas, Prentice Hall.

Swedlow, J.L. (1973). 'A Procedure for Solving Problems of Elasto-plastic Flow,' Comp. and Struct., 3, pp. 879-898.

Swedlow, J.L. Cruse, T.A. (1971). 'Formulation of Boundary Integral Equations for Three Dimensional Elasto-plastic Flow,' Int. J. Solids and Struct. 7, pp. 1673-1683.

Tan, C.T. (1984). 'Interior Point Solution for Boundary Integral Equation Axisymmetric Stress Analysis,' Appl. Math. Modelling, Vol. 8, pp. 57-60.

Tanaka, M. and Tanaka, K. (1980). 'On Numerical Scheme for Thermoelastic Problems in Inhomogeneous Media Discretized by Means of Boundary Volume Element, ZAMM, 60, 719.

Terzaghi, K. (1943). Theoretical Soil Mechanics, John Wiley and Sons, New York.

Theocaris, P.S. and Marketos, E. (1964). 'Elasto-plastic Analysis of Perforated Thin Strips of a Strain Hardening Material,' J. Mech. Phys. Solids, 12, pp. 377-390.

Telles, J.C.F. (1983). Lecture Notes in Engineering: The Boundary Element Method Applied to Inelastic Problems, Eds. C.A. Brebbia and S.A. Orszag, Springer-Verlag.

Telles, J.C.F. and Brebbia, C.A. (1979). 'On the Application of the Boundary Element Method to Plasticity,' Appl. Math. Modelling, 3, pp. 466-470.

Telles, J.C.F. and Brebbia, C.A. (1981). 'Boundary Elements: New Developments in Elastoplastic Analysis,' Appl. Math. Modeling, 5, 376-382.

Telles, J.C.F. and Brebbia, C.A. (1981). 'The Boundary Element Method in Plasticity,' Appl. Math. Modeling, 5, 275-281.

Thomas, D.G.B. (1953). J. Mech. Phy. Solids, Vol. 1 and Vol. 2 (Corrigendum).

Timoshenko, S.P. and Goodier, J.N. (1970). Theory of Elasticity, 3rd Edition, McGraw Hill.

Tomlin, G.R. (1973). 'Numerical Analysis of Continuum Problems in Zoned Anistropic Media,' Ph.D Thesis, Southampton University, UK.

Van der Weeën, F. (1982). 'Application of the Direct Boundary Element Method to Reissner's Plate Model,' Proceedings at the Fourth International Seminar, Ed. Brebbia, C.A., Southampton, UK.

Watson, J.O. (1973). 'Analysis of Thick Shells with Holes by Using Integral Equation Method,' Ph.D Thesis, Southampton, University, UK.

Watson, J.O. (1979). 'Advanced Implementation of the Boundary Element Method for Two and Three Dimensional Elastostatics,' Chapter 3 in Developments in Boundary Element Methods I, Applied Science Publishers, UK, pp. 31-64.

Wilson, R.B. and Cruse, T.A. (1978). 'Efficient Implementation of Anisotropic Three-dimensional Boundary Integral Equation Stress Analysis,' Int. J. Num. Meth. Eng., 12, pp. 1383-1397.

Ziegler, H. (1959). 'A Modification of Prager's Hardening Rule,' Quart. Appl. Math., 17, pp. 55-65.

Zienkiewicz, O.C. (1977). The Finite Element Method, 3rd Edition, McGraw Hill.

APPENDICES

APPENDICES

APPENDIX I - NUMERICAL INTEGRATION

I.A Shape Functions

When a body is discretized, as described in Chapter 2, shape functions are used to describe the geometry and field variables across the boundary element (or cell) in terms of nodal variables. Geometry coordinates; displacements, tractions, and initial stresses are expressed in terms of shape functions as

$$x_i = N^{\alpha}(\xi)\ \bar{x}_i^{\alpha}$$

$$u_i = N^{\alpha}(\xi)\ \bar{u}_i^{\alpha}$$

$$t_i = N^{\alpha}(\xi)\ \bar{t}_i^{\alpha}$$

$$\sigma_{ij}^{o} = M^{\beta}(\eta_1,\eta_2)\cdot(\bar{\sigma}_{ij}^{o})^{\beta}$$

where

N^{α} and M^{β} represent the shape function,

α and β the order of the shape function,

ξ, η_1 and η_2 are intrinsic (local) coordinates, and

the bar indicates the nodal values.

Some common shape functions used in this dissertation are given below. Additional shape functions can be found in text books, (e.g. Banerjee and Butterfield, 1981).

Three-noded, one-dimensional shape functions (Figure A.1):

$$M^1(\eta) = \frac{1}{2}\,\eta(1+\eta)$$

$$M^2(\eta) = -\frac{1}{2}\,\eta(1-\eta)$$

$$M^3(\eta) = (1+\eta)(1-\eta)$$

Eight-noded, two-dimensional shape function (Figure A.2):

$$M^{\alpha}(\eta_1,\eta_2) = \frac{1}{4}(1+s_{\alpha 1}\eta_1)(1+s_{\alpha 2}\eta_2)(s_{\alpha 1}\eta_1+s_{\alpha 2}\eta_2-1) \quad \alpha = 1,2,3,4$$

$$M^{\alpha}(\eta_1) = \frac{1}{2}(1+s_{\alpha 2}\eta_2)(1-\eta_1^2) \qquad \alpha = 5,7$$

$$M^{\alpha}(\eta_1) = \frac{1}{2}(1+s_{\alpha 1}\eta_1)(1-\eta_2^2) \qquad \alpha = 6,8$$

where $s_{\alpha 1}$ takes the sign of η_1 coordinates. The shape functions for six-noded triangular elements can be obtained by collapsing the quadrilateral to triangle.

Twenty-noded, three-dimensional shape function (Figure A.3):

$$M^{\alpha}(\eta_1,\eta_2,\eta_3) = \frac{1}{8}\,(1+s_{\alpha 1}\eta_1)(1+s_{\alpha 2}\eta_2)(1+s_{\alpha 3}\eta_3)(s_{\alpha 1}\eta_1+s_{\alpha 2}\eta_2+s_{\alpha 3}\eta_3-2) \qquad \alpha=1..8$$

$$M^{\alpha}(\eta_1) = \frac{1}{4}(1-\eta_1^2)(1+s_{\alpha 2}\eta_2)(1+s_{\alpha 3}\eta_3) \qquad \alpha=9..12$$

$$M^{\alpha}(\eta_1) = \frac{1}{4}(1-\eta_2^2)(1+s_{\alpha 1}\eta_1)(1+s_{\alpha 3}\eta_3) \qquad \alpha=13..16$$

$$M^{\alpha}(\eta_1) = \frac{1}{4}(1-\eta_3^2)(1+s_{\alpha 1}\eta_1)(1+s_{\alpha 2}\eta_2) \qquad \alpha=17..20$$

where $s_{\alpha 1}$ assumes the sign of η_1 coordinates.

I.B Jacobian Transformations

Boundary element mapping:

A curvilinear (2-D) line element can be mapped into one-dimensional space using the following Jacobian transformation

$$dC(x) = J_L(\eta)d\eta$$

where

$$J_L(\eta) = \left[\frac{\partial x_i}{\partial \eta} \frac{\partial x_i}{\partial \eta} \right]^{1/2}$$

i = 1,2 for a two-dimensional curvilinear element

Similarly, a curvilinear (3-D) surface element can be mapped into two-dimensional space using the following Jacobian transformations

$$dS(x) = J_s(\eta_1,\eta_2)d\eta_1 d\eta_2$$

where

$$J_s(\eta_1,\eta_2) = [d_1^2 + d_2^2 + d_3^2]^{1/2}$$

$$d_1 = \left(\frac{\partial x_2}{\partial \eta_1} \frac{\partial x_3}{\partial \eta_2} - \frac{\partial x_2}{\partial \eta_2} \frac{\partial x_3}{\partial \eta_1} \right)$$

$$d_2 = \left(\frac{\partial x_1}{\partial \eta_1} \frac{\partial x_3}{\partial \eta_2} - \frac{\partial x_1}{\partial \eta_2} \frac{\partial x_3}{\partial \eta_1} \right)$$

$$d_3 = \left(\frac{\partial x_1}{\partial \eta_1} \frac{\partial x_2}{\partial \eta_2} - \frac{\partial x_1}{\partial \eta_2} \frac{\partial x_2}{\partial \eta_1} \right)$$

Volume cell mapping:

Two- and three-dimensional volume cells can be mapped into two- and three-dimensional space, respectively, using the following Jacobian transformations

$$dA(x) = J(\eta_1,\eta_2)\, d\eta_1 d\eta_2$$

$$dV(x) = J(\eta_1,\eta_2,\eta_3)\, d\eta_1 d\eta_2 \eta_3$$

where

$$J(\eta_i) = \left|\left|\frac{\partial x_i}{\partial \eta_j}\right|\right|$$

i,j = 1,2 for two-dimensions
i,j = 1,2,3 for three-dimensions

I.C Gauss-Legendre Formula

In one dimension, the application of Gauss-Legendre formula (Stroud and Secrest, 1966) is expressed as

$$\int_{-1}^{1} f(x)dx = \sum_{a=1}^{A} w^a f(x^a)$$

where

$f(x)$ is the prescribed function,

w^a is the weight at sampling point a,

s^a is the abscissae of the sampling point, and

A is the order of the integration rule.

Two- and three-dimensional integrals are evaluated through repeated application of the above formula:

$$\int_{-1}^{1}\int_{-1}^{1} f(x,y)dxdy = \sum_{a=1}^{A}\sum_{b=1}^{B} w^a w^b f(x^a,x^b)$$

and

$$\int_{-1}^{1}\int_{-1}^{1}\int_{-1}^{1} f(x,y,z)dxdydz = \sum_{a=1}^{A}\sum_{b=1}^{B}\sum_{c=1}^{C} w^a w^b w^c f(x^a,y^b,z^c)$$

APPENDIX II - TWO- AND THREE-DIMENSIONAL KERNEL FUNCTIONS

The kernel functions for the two- and three-dimensional boundary integral equations for displacement and stress are presented below. In these definitions the parameter d=2 is used for two-dimensions (plane strain) and d=3 for three-dimensions. The indicial notation ranges from 1 to 2 for two-dimensions, and from 1 to 3 for three-dimensions. The two-dimensional plane stress kernel functions are derived from the plain strain function by using a modified material parameter $\bar{\nu} = \quad /(1+\nu)$.

II.A Displacement Equation

$$u_j(\xi) = \int_s [G_{ij}(x,\xi)t_i(x) - F_{ij}(x,\xi)u_i(x)]ds(x)$$

$$+ \int_v [G_{ij}(x,\xi)f_i(x) + B_{ikj}(x,\xi)\sigma^o_{ik}(x)]dv(x)$$

in which G_{ij} is the fundamental point force solution due to Kelvin (Love, 1944)

$$G_{ij}(x,\xi) = \frac{C_1}{(d-1)r^{(d-2)}}\left[C_2\delta_{ij}\,[(d-2) + (d-3)\ln(r)] + z_i z_j\right]$$

where

$$C_1 = \frac{1}{8\pi\mu(1-\nu)}$$

$$C_2 = (3-4\,\nu)$$

$$y_i = x_i - \xi_i$$

$$r^2 = y_i y_i$$

$$z_i = y_i/r$$

and d is the dimensionality of the problem.

G_{ij} represents the displacement $u_i(x)$ at x in direction i due to a point force $e_j(\xi)$ at ξ in direction j,

i.e. $$u_i(x) = G_{ij}(x,\xi)e_j(\xi)$$

It should be noted that the two-dimensional solution includes an arbitrary constant term A_{ij} in addition to the expressions provided by the above equations since, unlike the three-dimensional case where G_{ij} vanishes as $r\to\infty$, the expression for G_{ij} does not vanish as $r\to\infty$ for two-dimensional problems.

The B_{ijk} kernel represents the strains corresponding to the fundamental displacement solution and is given as

$$B_{ijk}(x,\xi) = -\frac{C_1}{(d-1)r^{(d-1)}}\left[C_4(\delta_{jk}z_i + \delta_{ik}z_j) - \delta_{ij}z_k + dz_iz_jz_k\right]$$

where

$$C_4 = (1-2\nu)$$

The F_{ij} kernel represents the tractions on an incline normal $n_k(x)$ due to a point force:

$$F_{ij}(x,\xi) = \frac{C_3}{(d-1)r^{(d-1)}}\left[C_4(n_jz_i - n_iz_j) + (C_4\delta_{ij} + dz_iz_j)z_mn_m\right]$$

II.B Stress Equation

$$\sigma_{ij}(\xi) = \int_s [G^{\sigma}_{ijk}(x,\xi)t_i(x) - F^{\sigma}_{ijk}(x,\xi)u_i(x)]ds(x)$$

$$+ \int_v [G^{\sigma}_{ijk}(x,\xi)f_i(x) + B^{\sigma}_{ipjk}(x,\xi)\sigma^{o}_{ip}]dv$$

where

$$G^{\sigma}_{ijk}(x,\xi) = -\frac{C_3}{(d-1)r^{(d-1)}}\left[C_4(\delta_{ij}z_k + \delta_{ik}z_j - \delta_{jk}z_i) + dz_iz_jz_k\right]$$

and

$$F^{\sigma}_{ijk}(x,\xi) = \frac{C_5}{(d-1)r^d}\,[n_i(C_6\delta_{jk} - dC_4 z_j z_k) - n_j(C_4\delta_{ik} + d(\nu)z_i z_k)$$

$$- n_k(C_4\delta_{ij} + d(\nu)z_i z_j) - dz_m n_m\,[C_4\delta_{jk}z_i + (\nu)\delta_{ik}z_j$$

$$- (\nu)\,\delta_{ij}z_k - (d+2)z_i z_j z_k]]$$

$$B^{\sigma}_{ipjk}(z,\xi) = \frac{C_3}{(d-1)r^d}\,[C_4(\delta_{ip}\delta_{jk} - \delta_{ij}\delta_{kp} - \delta_{ik}\delta_{jp} - d\delta_{jk}z_i z_p)$$

$$- d\delta_{ip}z_j z_k - d(\nu)(\delta_{ij}z_k z_p + \delta_{jp}z_i z_k + \delta_{kp}z_i z_j + \delta_{ik}z_j z_p)$$

$$+ d(d+2)z_i z_j z_k z_p]$$

$$C_3 = \frac{-1}{4\pi(1-\nu)}$$

$$C_5 = \frac{-\mu}{2\pi(1-\nu)}$$

$$C_6 = (1-4\nu)$$

The integration of the B^{σ}_{ijkl} kernel is strongly singular and must be treated as a Lebesgue integral. This term can be decomposed into Cauchy principle-value integral and a free term $J^{\sigma}_{ijkl}(\xi)$:

$$\int_v B^{\sigma}_{ijkl}(x,\xi)dv(x) = \int_v \bar{B}^{\sigma}_{ijkl}(x,\xi)dv(x) + J^{\sigma}_{ijkl}(\xi)$$

where

$$J^{\sigma}_{ipjk} = \frac{C_8}{d(d+2)}\left[[(d^2-2) - (\nu)(d^2-4)]\delta_{ij}\delta_{kp} + [1-(\nu)(d+2)\delta_{ip}\delta_{jk}]\right]$$

$$C_8 = \frac{-1}{(1-\nu)}$$

APPENDIX III - AXISYMMETRIC KERNEL FUNCTIONS

Here, the displacement and stress kernel functions used in the axisymmetric boundary element analysis of bodies subjected to axisymmetric boundary loads and initial stress body forces are given.

The G_{ij} kernel of equation (III.2) is the ring source solution, first derived by Kermanidis (1975) and Cruse et. al. (1977). Other authors Baker and Fenner (1983) and Tan (1984) have defined G_{ij} as the transpose of the ring solution. In the following r and z correspond to the field point, and R and Z are the integration (Gauss) points. Note, although $\frac{\partial}{\partial z} = -\frac{\partial}{\partial Z}$ holds true for axial (z) direction in axisymmetric kernels, such is not the case for the radial (r) direction, i.e. $\frac{\partial}{\partial r} \neq -\frac{\partial}{\partial R}$.

A $2\pi R$ term, which appears after integration in the θ direction, has been absorbed in the kernel; therefore, the numerical integration is performed over a curve dC. Some other authors Bakr and Fenner (1983) and Cruse et. al. (1977) do not absorb this term in their kernels.

III.A Displacement Equations

$$\begin{Bmatrix} u_r(r,z) \\ u_z(r,z) \end{Bmatrix} = \int_C \left\{ \begin{bmatrix} G_{rr} & G_{zr} \\ G_{rz} & G_{zz} \end{bmatrix} \begin{Bmatrix} t_r \\ t_z \end{Bmatrix} - \begin{bmatrix} F_{rr} & F_{zr} \\ F_{rz} & F_{zz} \end{bmatrix} \begin{Bmatrix} u_r \\ u_z \end{Bmatrix} \right\} dC(R,Z)$$

$$+ \int_A \begin{bmatrix} B_{11} & B_{21} & B_{31} & B_{41} \\ B_{12} & B_{22} & B_{32} & B_{42} \end{bmatrix} \begin{Bmatrix} \sigma^o_{rr} \\ \sigma^o_{zz} \\ \sigma^o_{rz} \\ \sigma^o_{\theta\theta} \end{Bmatrix} dA(R,Z) \qquad \text{(III.1)}$$

in which

$$G_{ij} = A_{ij}K + B_{ij}E \qquad i,j = r,z \tag{III.2}$$

G_{ij} being the displacement vector u_i due to a ring load intensity e_j, i.e., $u_i(x) = G_{ij}(x,\xi)e_j$

$K = K(m)$ is the complete Elliptic Integral of the first kind, and

$E = E(m)$ is the complete Elliptic Integral of the second kind.

$$F_{ri} = \left[c_1 \frac{\partial G_{ri}}{\partial R} + c_2\left(\frac{G_{ri}}{R} + \frac{\partial G_{zi}}{\partial Z}\right)\right] n_r + \mu \left[\frac{\partial G_{ri}}{\partial Z} + \frac{\partial G_{zi}}{\partial R}\right] n_z$$

$$F_{zi} = \left[c_1 \frac{\partial G_{zi}}{\partial Z} + c_2\left(\frac{G_{ri}}{R} + \frac{\partial G_{ri}}{\partial R}\right)\right] n_z + \mu \left[\frac{\partial G_{ri}}{\partial Z} + \frac{\partial G_{zi}}{\partial R}\right] n_r \qquad i=r,z$$

$$B_{11} = \frac{\partial G_{rr}}{\partial R} \qquad B_{21} = \frac{\partial G_{zr}}{\partial Z} \qquad B_{31} = \frac{\partial G_{rr}}{\partial Z} + \frac{\partial G_{zr}}{\partial R} \qquad B_{41} = \frac{G_{rr}}{R}$$

$$B_{12} = \frac{\partial G_{rz}}{\partial R} \qquad B_{22} = \frac{\partial G_{zz}}{\partial Z} \qquad B_{32} = \frac{\partial G_{rz}}{\partial Z} + \frac{\partial G_{zz}}{\partial R} \qquad B_{42} = \frac{G_{rz}}{R}$$

where

$$\frac{\partial G_{ij}}{\partial R} = \frac{\partial A_{ij}}{\partial R} K + \frac{\partial B_{ij}}{\partial R} E + A_{ij} \frac{\partial K}{\partial R} + B_{ij} \frac{\partial E}{\partial R}$$

$$\frac{\partial G_{ij}}{\partial Z} = \frac{\partial A_{ij}}{\partial Z} K + \frac{\partial B_{ij}}{\partial Z} E + A_{ij} \frac{\partial K}{\partial Z} + B_{ij} \frac{\partial E}{\partial Z} \qquad i,j = r,z$$

$n_r = n_r(R,Z)$ is the normal in r direction

$n_z = n_z(R,Z)$ is the normal in z direction

$$A_{rr} = \frac{a}{r\bar{R}H}\,(c_3M + \bar{Z}^2) \qquad B_{rr} = -\frac{a}{r\bar{R}H}\,(c_3H^2 + \frac{M\bar{Z}^2}{\rho^2})$$

$$A_{rz} = \frac{a\bar{Z}}{\bar{R}H} \qquad B_{rz} = -\frac{a\bar{Z}}{R\rho^2H}\,(M - 2R^2)$$

$$A_{zr} = -\frac{a\bar{Z}}{rH} \qquad B_{zr} = \frac{a\bar{Z}}{r\rho^2H}\,N$$

$$A_{zz} = \frac{2a}{H}\,c_3 \qquad B_{zz} = \frac{2a\bar{Z}^2}{\rho^2H}$$

$$\frac{\partial A_{rr}}{\partial R} = \frac{2ac_3}{rH} - d_1A_{rr} \qquad \frac{\partial B_{rr}}{\partial R} = -\frac{2as_1}{RrH} - d_1B_{rr}$$

$$\frac{\partial A_{rz}}{\partial R} = -d_1A_{rz} \qquad \frac{\partial B_{rz}}{\partial R} = \frac{2a\bar{Z}}{\rho^2H} - (\frac{1}{R} + d_2)\,B_{rz}$$

$$\frac{\partial A_{zr}}{\partial R} = -p_1A_{zr} \qquad \frac{\partial B_{zr}}{\partial R} = \frac{2aR\bar{Z}}{r\rho^2H} - d_2B_{zr}$$

$$\frac{\partial A_{zz}}{\partial R} = -p_1A_{zz} \qquad \frac{\partial B_{zz}}{\partial R} = -d_2B_{zz}$$

$$\frac{\partial A_{rr}}{\partial Z} = \frac{a8(1-\nu)\bar{Z}}{r\bar{R}H} - \frac{\bar{Z}}{A^2}\,A_{rr} \qquad \frac{\partial B_{rr}}{\partial Z} = -\frac{2a\bar{Z}}{RrH}\,s_2 - \frac{\bar{Z}}{H^2}\,B_{rr}$$

$$\frac{\partial A_{rz}}{\partial Z} = \frac{a}{\bar{R}H} - \frac{\bar{Z}}{H^2}\,A_{rz} \qquad \frac{\partial B_{rz}}{\partial Z} = \frac{a}{R\rho^2H}\,d_4 - d_3B_{rz}$$

$$\frac{\partial A_{zr}}{\partial Z} = -\frac{a}{rH} - \frac{\bar{Z}}{H^2}\,A_{zr} \qquad \frac{\partial B_{zr}}{\partial Z} = \frac{a}{r\rho^2H}\,d_5 - d_3B_{zr}$$

$$\frac{\partial A_{zz}}{\partial Z} = -\frac{\bar{Z}}{H^2} A_{zz}$$

$$\frac{\partial B_{zz}}{\partial Z} = \frac{4\alpha\bar{Z}}{\rho^2 H} - d_3 B_{zz}$$

$$H = \left[(R + r)^2 + \bar{Z}^2\right]^{1/2}$$

λ, μ = Lamé constants

$$\bar{Z} = (Z - z)$$

ν = Poisson's ratio

$$\rho^2 = \left[(R - r)^2 + \bar{Z}^2\right]$$

$$\left.\begin{matrix} r \\ z \end{matrix}\right] = \text{field points}$$

$$\alpha = \frac{R}{8\pi\mu(1-\nu)}$$

$$\left.\begin{matrix} R \\ Z \end{matrix}\right] = \text{integration (Gauss) points}$$

$$c_1 = \lambda + 2\mu$$

$$c_2 = \lambda$$

$$c_3 = 3 - 4\nu$$

$$M = R^2 + r^2 + \bar{Z}^2$$

$$N = R^2 - r^2 + \bar{Z}^2$$

$$p_1 = \frac{R + r}{H^2}$$

$$d_1 = \frac{1}{R} + p_1$$

$$d_2 = p_1 + \frac{2(R-r)}{\rho^2}$$

$$d_3 = \bar{Z}\left(\frac{2}{\rho^2} + \frac{1}{H^2}\right)$$

$$d_4 = N - 4\bar{Z}^2$$

$$d_5 = N + 2\bar{Z}^2$$

$$s_1 = c_3(R + r) + \frac{\bar{Z}^2 r}{\rho^4}(M - 2R^2)$$

$$s_2 = c_3 - \frac{2\bar{Z}^2 Rr}{\rho^4} + \frac{M}{\rho^2}$$

III.B Stress Equation

$$\begin{Bmatrix} \sigma_{rr}(r,z) \\ \sigma_{zz}(r,z) \\ \sigma_{rz}(r,z) \\ \sigma_{\theta\theta}(r,z) \end{Bmatrix} = \int_C \left\{ \begin{bmatrix} G^\sigma_{r1} & G^\sigma_{z1} \\ G^\sigma_{r2} & G^\sigma_{z2} \\ G^\sigma_{r3} & G^\sigma_{z3} \\ G^\sigma_{r4} & G^\sigma_{z4} \end{bmatrix} \begin{Bmatrix} t_r \\ t_z \end{Bmatrix} - \begin{bmatrix} F^\sigma_{r1} & F^\sigma_{z1} \\ F^\sigma_{r2} & F^\sigma_{z2} \\ F^\sigma_{r3} & F^\sigma_{z3} \\ F^\sigma_{r4} & F^\sigma_{z4} \end{bmatrix} \begin{Bmatrix} u_r \\ u_z \end{Bmatrix} \right\} dC(R,Z)$$

$$+ \int_A \begin{bmatrix} B^\sigma_{11} & B^\sigma_{21} & B^\sigma_{31} & B^\sigma_{41} \\ B^\sigma_{12} & B^\sigma_{22} & B^\sigma_{32} & B^\sigma_{42} \\ B^\sigma_{13} & B^\sigma_{23} & B^\sigma_{33} & B^\sigma_{43} \\ B^\sigma_{14} & B^\sigma_{24} & B^\sigma_{34} & B^\sigma_{44} \end{bmatrix} \begin{Bmatrix} \sigma^o_{rr} \\ \sigma^o_{zz} \\ \sigma^o_{rz} \\ \sigma^o_{\theta\theta} \end{Bmatrix} dA(R,Z) \qquad \text{(III.3)}$$

in which

$$G^\sigma_{i1} = c_1 \frac{\partial G_{ir}}{\partial r} + c_2\left(\frac{G_{ir}}{r} + \frac{\partial G_{iz}}{\partial z}\right)$$

$$G^\sigma_{i2} = c_1 \frac{\partial G_{iz}}{\partial z} + c_2\left(\frac{G_{ir}}{r} + \frac{\partial G_{ir}}{\partial r}\right)$$

$$G^\sigma_{i3} = \mu \left(\frac{\partial G_{iz}}{\partial r} + \frac{\partial G_{ir}}{\partial z}\right)$$

$$G^\sigma_{i4} = c_1 \frac{G_{ir}}{r} + c_2\left(\frac{\partial G_{ir}}{\partial r} + \frac{\partial G_{iz}}{\partial z}\right) \qquad i = r,z$$

$$F^{\sigma}_{i1} = c_1 \frac{\partial F_{ir}}{\partial r} + c_2\left(\frac{F_{ir}}{r} + \frac{\partial F_{iz}}{\partial z}\right)$$

$$F^{\sigma}_{i2} = c_1 \frac{\partial F_{iz}}{\partial z} + c_2\left(\frac{F_{ir}}{r} + \frac{\partial F_{ir}}{\partial r}\right)$$

$$F^{\sigma}_{i3} = \mu \left(\frac{\partial F_{iz}}{\partial r} + \frac{\partial F_{ir}}{\partial z}\right)$$

$$F^{\sigma}_{i4} = c_1 \frac{F_{ir}}{r} + c_2\left(\frac{\partial F_{ir}}{\partial r} + \frac{\partial F_{iz}}{\partial z}\right) \qquad i = r,z$$

$$\frac{\partial G_{ij}}{\partial r} = \frac{\partial A_{ij}}{\partial r} K + \frac{\partial B_{ij}}{\partial r} E + A_{ij} \frac{\partial K}{\partial r} + B_{ij} \frac{\partial E}{\partial r}$$

$$\frac{\partial G_{ij}}{\partial z} = - \frac{\partial G_{ij}}{\partial Z} \qquad i,j = r,z$$

$$\frac{\partial F_{ri}}{\partial r} = \left[c_1 \frac{\partial^2 G_{ri}}{\partial R \partial r} + c_2\left(\frac{1}{R} \frac{\partial G_{ri}}{\partial r} + \frac{\partial^2 G_{zi}}{\partial Z \partial r}\right)\right] n_r + \mu\left(\frac{\partial^2 G_{ri}}{\partial Z \partial r} + \frac{\partial^2 G_{zi}}{\partial R \partial r}\right) n_z$$

$$\frac{\partial F_{ri}}{\partial z} = \left[c_1 \frac{\partial^2 G_{ri}}{\partial R \partial z} + c_2\left(\frac{1}{R} \frac{\partial G_{ri}}{\partial z} + \frac{\partial^2 G_{zi}}{\partial Z \partial z}\right)\right] n_r + \mu\left(\frac{\partial^2 G_{ri}}{\partial Z \partial z} + \frac{\partial^2 G_{zi}}{\partial R \partial z}\right) n_z$$

$$\frac{\partial F_{zi}}{\partial r} = \left[c_1 \frac{\partial^2 G_{zi}}{\partial Z \partial r} + c_2\left(\frac{1}{R} \frac{\partial G_{ri}}{\partial r} + \frac{\partial^2 G_{ri}}{\partial R \partial r}\right)\right] n_z + \mu\left(\frac{\partial^2 G_{ri}}{\partial Z \partial r} + \frac{\partial^2 G_{zi}}{\partial R \partial r}\right) n_r$$

$$\frac{\partial F_{zi}}{\partial z} = \left[c_1 \frac{\partial^2 G_{zi}}{\partial Z \partial z} + c_2\left(\frac{1}{R} \frac{\partial G_{ri}}{\partial z} + \frac{\partial^2 G_{ri}}{\partial R \partial z}\right)\right] n_z + \mu\left(\frac{\partial^2 G_{ri}}{\partial Z \partial z} + \frac{\partial^2 G_{zi}}{\partial R \partial z}\right) n_r$$

$$i = r,z$$

$$B^{\sigma}_{11} = c_1 \frac{\partial^2 G_{rr}}{\partial R \partial r} + c_2\left(\frac{1}{r} \frac{\partial G_{rr}}{\partial R} + \frac{\partial^2 G_{rz}}{\partial R \partial z}\right)$$

$$B^{\sigma}_{21} = c_1 \frac{\partial^2 G_{zr}}{\partial Z \partial r} + c_2 \left(\frac{1}{r} \frac{\partial G_{zr}}{\partial Z} + \frac{\partial^2 G_{zz}}{\partial Z \partial z}\right)$$

$$B^{\sigma}_{31} = c_1 \left(\frac{\partial^2 G_{rr}}{\partial Z \partial r} + \frac{\partial^2 G_{zr}}{\partial R \partial r}\right) + c_2 \left[\frac{1}{r} \left(\frac{\partial G_{rr}}{\partial Z} + \frac{\partial G_{zr}}{\partial R}\right) + \left(\frac{\partial^2 G_{rz}}{\partial Z \partial z} + \frac{\partial^2 G_{zz}}{\partial R \partial z}\right)\right]$$

$$B^{\sigma}_{41} = c_1 \frac{1}{R} \frac{\partial G_{rr}}{\partial r} + c_2 \frac{1}{R} \left(\frac{1}{r} G_{rr} + \frac{\partial G_{rz}}{\partial z}\right)$$

$$B^{\sigma}_{12} = c_1 \frac{\partial^2 G_{rz}}{\partial R \partial z} + c_2 \left(\frac{1}{r} \frac{\partial G_{rr}}{\partial R} + \frac{\partial^2 G_{rr}}{\partial R \partial r}\right)$$

$$B^{\sigma}_{22} = c_1 \frac{\partial^2 G_{zz}}{\partial Z \partial z} + c_2 \left(\frac{1}{r} \frac{\partial G_{zr}}{\partial Z} + \frac{\partial^2 G_{zr}}{\partial Z \partial r}\right)$$

$$B^{\sigma}_{32} = c_1 \left(\frac{\partial^2 G_{rz}}{\partial Z \partial z} + \frac{\partial^2 G_{zz}}{\partial R \partial z}\right) + c_2 \left[\frac{1}{r} \left(\frac{\partial G_{rr}}{\partial Z} + \frac{\partial G_{zr}}{\partial R}\right) + \left(\frac{\partial^2 G_{rr}}{\partial Z \partial r} + \frac{\partial^2 G_{zr}}{\partial R \partial r}\right)\right]$$

$$B^{\sigma}_{42} = c_1 \frac{1}{R} \frac{\partial G_{rz}}{\partial z} + c_2 \frac{1}{R} \left(\frac{1}{r} G_{rr} + \frac{\partial G_{rr}}{\partial r}\right)$$

$$B^{\sigma}_{13} = \mu \left(\frac{\partial^2 G_{rz}}{\partial R \partial r} + \frac{\partial^2 G_{rr}}{\partial R \partial z}\right)$$

$$B^{\sigma}_{23} = \mu \left(\frac{\partial^2 G_{zz}}{\partial Z \partial r} + \frac{\partial^2 G_{zr}}{\partial Z \partial z}\right)$$

$$B^{\sigma}_{33} = \mu \left[\left(\frac{\partial^2 G_{rz}}{\partial Z \partial r} + \frac{\partial^2 G_{zz}}{\partial R \partial r}\right) + \left(\frac{\partial^2 G_{rr}}{\partial Z \partial z} + \frac{\partial^2 G_{zr}}{\partial R \partial z}\right)\right]$$

$$B^{\sigma}_{43} = \mu \frac{1}{R} \left(\frac{\partial G_{rz}}{\partial r} + \frac{\partial G_{rr}}{\partial z}\right)$$

$$B^{\sigma}_{14} = c_1 \frac{1}{r} \frac{\partial G_{rr}}{\partial R} + c_2 \left(\frac{\partial^2 G_{rr}}{\partial R \partial r} + \frac{\partial^2 G_{rz}}{\partial R \partial z}\right)$$

$$B^{\sigma}_{24} = c_1 \frac{1}{r} \frac{\partial G_{zr}}{\partial Z} + c_2 \left(\frac{\partial^2 G_{zr}}{\partial Z \partial r} + \frac{\partial^2 G_{zz}}{\partial Z \partial z}\right)$$

$$B^{\sigma}_{34} = c_1 \frac{1}{r} \left(\frac{\partial G_{rr}}{\partial Z} + \frac{\partial G_{zr}}{\partial R}\right) + c_2 \left[\left(\frac{\partial^2 G_{rr}}{\partial Z \partial r} + \frac{\partial^2 G_{zr}}{\partial R \partial r}\right) + \left(\frac{\partial^2 G_{rz}}{\partial Z \partial z} + \frac{\partial^2 G_{zz}}{\partial R \partial z}\right)\right]$$

$$B^{\sigma}_{44} = c_1 \frac{1}{rR} G_{rr} + c_2 \frac{1}{R} \left(\frac{\partial G_{rr}}{\partial r} + \frac{\partial G_{rz}}{\partial z}\right)$$

where

$$\frac{\partial^2 G_{ij}}{\partial R \partial r} = \frac{\partial^2 A_{ij}}{\partial R \partial r} K + \frac{\partial A_{ij}}{\partial R} \frac{\partial K}{\partial r} + \frac{\partial A_{ij}}{\partial r} \frac{\partial K}{\partial R} + A_{ij} \frac{\partial^2 K}{\partial R \partial r}$$

$$+ \frac{\partial^2 B_{ij}}{\partial R \partial r} E + \frac{\partial B_{ij}}{\partial R} \frac{\partial E}{\partial r} + \frac{\partial B_{ij}}{\partial r} \frac{\partial E}{\partial R} + B_{ij} \frac{\partial^2 E}{\partial R \partial r} \qquad i,j = r,z$$

Similar for $\frac{\partial^2 G_{ij}}{\partial R \partial z}$, $\frac{\partial^2 G_{ij}}{\partial Z \partial r}$ and $\frac{\partial^2 G_{ij}}{\partial Z \partial z}$

$$\frac{\partial A_{rr}}{\partial r} = \frac{2c_3 a}{RH} - e_1 A_{rr} \qquad \frac{\partial B_{rr}}{\partial r} = -\frac{2a}{RrH} s_3 - e_1 B_{rr}$$

$$\frac{\partial A_{rz}}{\partial r} = -p_1 A_{rz} \qquad \frac{\partial B_{rz}}{\partial r} = -\frac{2aZr}{R\rho^2 H} - e_2 B_{rz}$$

$$\frac{\partial A_{zr}}{\partial r} = -e_1 A_{zr} \qquad \frac{\partial B_{zr}}{\partial r} = -\frac{2aZ}{\rho^2 H} - e_3 B_{zr}$$

$$\frac{\partial A_{zz}}{\partial r} = - p_1 A_{zz} \qquad \frac{\partial B_{zz}}{\partial r} = - e_2 B_{zz}$$

$$\frac{\partial A_{ij}}{\partial z} = - \frac{\partial A_{ij}}{\partial Z} \qquad \frac{\partial B_{ij}}{\partial z} = - \frac{\partial B_{ij}}{\partial Z} \qquad i,j = r,z$$

$$\frac{\partial^2 A_{rr}}{\partial R \partial r} = - \frac{2c_3 \alpha e_1}{rH} - f_1 A_{rr} - d_1 \frac{\partial A_{rr}}{\partial r}$$

$$\frac{\partial^2 A_{rz}}{\partial R \partial r} = - f_1 A_{rz} - d_1 \frac{\partial A_{rz}}{\partial r}$$

$$\frac{\partial^2 A_{zr}}{\partial R \partial r} = - f_1 A_{zr} - p_1 \frac{\partial A_{zr}}{\partial r}$$

$$\frac{\partial^2 A_{zz}}{\partial R \partial r} = - f_1 A_{zz} - p_1 \frac{\partial A_{zz}}{\partial r}$$

$$\frac{\partial^2 B_{rr}}{\partial R \partial r} = \frac{2\alpha}{RrH} (s_1 e_1 - t_1) - f_1 B_{rr} - d_1 \frac{\partial B_{rr}}{\partial r}$$

$$\frac{\partial^2 B_{rz}}{\partial R \partial r} = - \frac{2\alpha \bar{Z}}{\rho^2 H} e_2 - f_2 B_{rz} - g_3 \frac{\partial B_{rz}}{\partial r}$$

$$\frac{\partial^2 B_{zr}}{\partial R \partial r} = - \frac{2\alpha R \bar{Z}}{r\rho^2 H} e_3 - f_2 B_{zr} - d_2 \frac{\partial B_{zr}}{\partial r}$$

$$\frac{\partial^2 B_{zz}}{\partial R \partial r} = - f_2 B_{zz} - d_2 \frac{\partial B_{zz}}{\partial r}$$

$$\frac{\partial^2 A_{rr}}{\partial R \partial z} = + \frac{2c_3 \alpha \bar{Z}}{rH^3} + f_3 A_{rr} - d_1 \frac{\partial A_{rr}}{\partial z}$$

$$\frac{\partial^2 A_{rz}}{\partial R \partial z} = + f_3 A_{rz} - d_1 \frac{\partial A_{rz}}{\partial z}$$

$$\frac{\partial^2 A_{zr}}{\partial R \partial z} = + f_3 A_{zr} - p_1 \frac{\partial A_{zr}}{\partial z}$$

$$\frac{\partial^2 A_{zz}}{\partial R \partial z} = + f_3 A_{zz} - p_1 \frac{\partial A_{zz}}{\partial z}$$

$$\frac{\partial^2 B_{rr}}{\partial R \partial z} = - \frac{2a}{r\bar{R}H} \left(\frac{\bar{Z}}{H^2} s_1 - t_3 \right) + f_3 B_{rr} - d_1 \frac{\partial B_{rr}}{\partial z}$$

$$\frac{\partial^2 B_{rz}}{\partial R \partial z} = - \frac{2a}{\rho^2 H} (1 - \bar{Z} d_3) + f_4 B_{rz} - g_3 \frac{\partial B_{rz}}{\partial z}$$

$$\frac{\partial^2 B_{zr}}{\partial R \partial z} = - \frac{2aR}{r\rho^2 H} (1 - \bar{Z} d_3) + f_4 B_{zr} - d_2 \frac{\partial B_{zr}}{\partial z}$$

$$\frac{\partial^2 B_{zz}}{\partial R \partial z} = + f_4 B_{zz} - d_2 \frac{\partial B_{zz}}{\partial z}$$

$$\frac{\partial^2 A_{rr}}{\partial Z \partial r} = - \frac{8(1-\nu)aZ}{RrH} e_1 + \frac{2Z}{H^2} p_1 A_{rr} - \frac{\bar{Z}}{H^2} \frac{\partial A_{rr}}{\partial r}$$

$$\frac{\partial^2 A_{rz}}{\partial Z \partial r} = \frac{a}{\bar{R}H} (g_1 - p_2 p_1)$$

$$\frac{\partial^2 A_{zr}}{\partial Z \partial r} = \frac{a}{rH} (e_1 p_2 - g_1)$$

$$\frac{\partial^2 A_{zz}}{\partial Z \partial r} = \frac{2\bar{Z}}{H^2} p_1 A_{zz} - \frac{\bar{Z}}{H^2} \frac{\partial A_{zz}}{\partial r}$$

$$\frac{\partial^2 B_{rr}}{\partial Z \partial r} = \frac{2aZ}{r\bar{R}H} (s_2 e_1 - t_2) + \frac{2\bar{Z}}{H^2} p_1 B_{rr} - \frac{\bar{Z}}{H^2} \frac{\partial B_{rr}}{\partial r}$$

$$\frac{\partial^2 B_{rz}}{\partial Z \partial r} = - \frac{a}{R\rho^2 H} (e_2 d_4 + 2r) - g_4 B_{rz} - d_3 \frac{\partial B_{rz}}{\partial r}$$

$$\frac{\partial^2 B_{zr}}{\partial Z \partial r} = -\frac{a}{r\rho^2 H}(e_3 d_5 + 2r) - g_4 B_{zr} - d_3 \frac{\partial B_{zr}}{\partial r}$$

$$\frac{\partial^2 B_{zz}}{\partial Z \partial r} = -\frac{4aZ}{\rho^2 H} e_2 - g_4 B_{zz} - d_3 \frac{\partial B_{zz}}{\partial r}$$

$$\frac{\partial^2 A_{rr}}{\partial Z \partial z} = -\frac{8(1-\nu)a}{rRH}\left(1 - \frac{Z^2}{H^2}\right) - \frac{p_3 A_{rr}}{H^2} - \frac{Z}{H^2}\frac{\partial A_{rr}}{\partial z}$$

$$\frac{\partial^2 A_{rz}}{\partial Z \partial z} = -\frac{3Z}{H^2}\frac{\partial A_{rz}}{\partial z}$$

$$\frac{\partial^2 A_{zr}}{\partial Z \partial z} = -\frac{3Z}{H^2}\frac{\partial A_{zr}}{\partial z}$$

$$\frac{\partial^2 A_{zz}}{\partial Z \partial z} = -\frac{p_3}{H^2} A_{zz} - \frac{Z}{H^2}\frac{\partial A_{zz}}{\partial z}$$

$$\frac{\partial^2 B_{rr}}{\partial Z \partial z} = +\frac{2a}{r\bar{R}H}\left[s_2\left(1 - \frac{Z^2}{H^2}\right) + t_4 Z\right] - \frac{p_3}{H^2} B_{rr} - \frac{Z}{H^2}\frac{\partial B_{rr}}{\partial z}$$

$$\frac{\partial^2 B_{rz}}{\partial Z \partial z} = +\frac{a}{R\rho^2 H}(d_3 d_4 + 6\bar{Z}) + g_5 B_{rz} - d_3 \frac{\partial B_{rz}}{\partial z}$$

$$\frac{\partial^2 B_{zr}}{\partial Z \partial z} = +\frac{a}{r\rho^2 H}(d_3 d_5 - 6\bar{Z}) + g_5 B_{zr} - d_3 \frac{\partial B_{zr}}{\partial z}$$

$$\frac{\partial^2 B_{zz}}{\partial Z \partial z} = -\frac{4a}{\rho^2 H}(1 - d_3 \bar{Z}) + g_5 B_{zz} - d_3 \frac{\partial B_{zz}}{\partial z}$$

$$e_1 = \frac{1}{r} + p_1 \qquad g_1 = f_1(R + r) + p_1$$

$$e_2 = p_1 - \frac{2(R-r)}{\rho^2} \qquad g_2 = f_3(R + r)$$

$$e_3 = \frac{1}{r} + e_2 \qquad g_3 = \frac{1}{R} + d_2$$

$$f_1 = \frac{1}{H^2} - 2(p_1)^2 \qquad g_4 = -2\bar{Z}\left[\frac{(R+r)}{H^4} - \frac{2(R-r)}{\rho^4}\right]$$

$$f_2 = -\frac{2}{\rho^2} + \left[\frac{2(R-r)}{\rho^2}\right]^2 + f_1 \qquad g_5 = \frac{2}{\rho^2} + \frac{1}{H^2} - 2\bar{Z}^2\left(\frac{2}{\rho^4} + \frac{1}{H^4}\right)$$

$$f_3 = -\frac{2p_1\bar{Z}}{H^2} \qquad p_2 = \left(\frac{R+r}{H}\right)^2$$

$$f_4 = f_3 - \frac{4\bar{Z}}{\rho^4}(R - r) \qquad p_3 = \left(\frac{2\bar{Z}^2}{H^2} - 1\right)$$

$$s_3 = c_3(R + r) + \frac{\bar{Z}^2}{\rho^4}(r\rho^2 + M(R - r))$$

$$t_1 = c_3 + 2\left(\frac{\bar{Z}r}{\rho^2}\right)^2 + \frac{\bar{Z}^2}{\rho^4}(M - 2R^2)[1 + 4r(R-r)/\rho^2]$$

$$t_2 = \frac{2R}{\rho^6}\left[\rho^2(R^2 - r^2) - 4\bar{Z}^2r(R-r)\right]$$

$$t_3 = \frac{2\bar{Z}r}{\rho^4}\left[(M - 2R^2)\left(1 - 2\frac{\bar{Z}^2}{\rho^2}\right) + \bar{Z}^2\right]$$

$$t_4 = -\frac{8rR\bar{Z}}{\rho^6}(R - r)^2$$

III.C Axisymmetric Jump Term Tensor, $J^{\sigma}_{ijkl}(\xi)$

The jump term (or free term) that is associated with the Lebesgue domain integral of the stress equation is given below. This jump term corresponds to the axisymmetric 'initial stress' formulation defined

in equation (III.3).

Using notation corresponding to equation (III.3)

$$[J]\{\sigma^o\} = \frac{-1}{8(1-\nu)} \begin{bmatrix} (3-4\nu) & (1-4\nu) & 0 & 0 \\ (1-4\nu) & (3-4\nu) & 0 & 0 \\ 0 & 0 & 2 & 0 \\ -4\nu & -4\nu & 0 & 8(1-\nu) \end{bmatrix} \begin{Bmatrix} \sigma^o_{rr} \\ \sigma^o_{zz} \\ \sigma^o_{rz} \\ \sigma^o_{\theta\theta} \end{Bmatrix}$$

When the field point falls at the origin the jump term tensor given above is no longer valid. For this situation the three-dimensional jump term tensor given below should be used.

$$[J]\{\sigma^o\} = \frac{-1}{15(1-\nu)} \begin{bmatrix} 2(4-5\nu) & (1-5\nu) & 0 & (1-5\nu) \\ (1-5\nu) & 2(3-4\nu) & 0 & (1-5\nu) \\ 0 & 0 & (7-5\nu) & 0 \\ (1-5\nu) & (1-5\nu) & 0 & 2(4-5\nu) \end{bmatrix} \begin{Bmatrix} \sigma^o_{rr} \\ \sigma^o_{zz} \\ \sigma^o_{rz} \\ \sigma^o_{\theta\theta} \end{Bmatrix}$$

III.D Elliptic Integrals

The complete elliptic integral of the first (K(m)) and second (E(m)) kind with modulus m can be defined as

$$K(m) = \int_0^{\pi/2} \frac{d\theta}{[1-m \sin^2\theta]^{1/2}}$$

$$E(m) = \int_0^{\pi/2} [1-m \sin^2\theta]^{1/2} d\theta$$

The modulus corresponding to the axisymmetric kernel is given as

$$m = \frac{4Rr}{H^2} \qquad m_1 = 1 - m$$

For numerical calculations, the integrals are approximated using the following polynominal approximation (Abramowitz and Stegun, 1974) for ($0 \leq m < 1$).

$$K = K(m) = \sum_{i=o}^{4} \left[a_i m_1^i + b_i m_1^i \ln\left(\frac{1}{m_1}\right) \right] + \varepsilon(m)$$

$$E = E(m) = 1 + \sum_{i=1}^{4} \left[c_i m_1^i + d_i m_1^i \ln\left(\frac{1}{m_1}\right) \right] + \varepsilon(m)$$

$|\varepsilon(m)|$ is $\leq 2 \times 10^{-8}$ and a_i, b_i, c_i and d_i are constants defined below:

$a_0 = 1.38629\ 436112$	$b_0 = .5$
$a_1 = .09666\ 344259$	$b_1 = .12498\ 593597$
$a_2 = .03590\ 092383$	$b_2 = .06880\ 248576$
$a_3 = .03742\ 563713$	$b_3 = .03328\ 355346$
$a_4 = .01451\ 196212$	$b_4 = .00441\ 787012$
$c_1 = .44325\ 141463$	$d_1 = .24998\ 368310$
$c_2 = .06260\ 601220$	$d_2 = .09200\ 180037$
$c_3 = .04757\ 383546$	$d_3 = .04069\ 697526$
$c_4 = .01736\ 506451$	$d_4 = .00526\ 449639$

III.E Derivative of Elliptic Integrals

$$\frac{\partial K}{\partial R} = h_1 P \qquad \frac{\partial E}{\partial R} = -\frac{h_1}{H^2} Q$$

$$\frac{\partial K}{\partial Z} = -Z P \qquad \frac{\partial E}{\partial Z} = \frac{Z}{H^2} Q$$

$$\frac{\partial K}{\partial r} = \frac{M-2r^2}{2r} P \qquad \frac{\partial E}{\partial r} = -\frac{M-2r^2}{2rH^2} Q$$

$$\frac{\partial K}{\partial z} = -\frac{\partial K}{\partial Z} \qquad \frac{\partial E}{\partial z} = -\frac{\partial E}{\partial Z}$$

$$\frac{\partial^2 K}{\partial R \partial r} = \frac{r}{R} P + h_1 h_2 \qquad \frac{\partial^2 E}{\partial R \partial r} = -\frac{1}{H^2}\left(\frac{r}{R} - 2h_1 p_1\right) Q - \frac{h_1}{H^2}\left[\frac{\partial K}{\partial r} - \frac{\partial E}{\partial r}\right]$$

$$\frac{\partial^2 K}{\partial R \partial z} = -\frac{\bar{Z}}{R} P - h_1 h_3 \qquad \frac{\partial^2 E}{\partial R \partial z} = -\left(\frac{2h_1 \bar{Z}}{H^2} - \frac{\bar{Z}}{R}\right) \frac{Q}{H^2} - \frac{h_1}{H^2}\left(\frac{\partial K}{\partial z} - \frac{\partial E}{\partial z}\right)$$

$$\frac{\partial^2 K}{\partial Z \partial r} = -h_2 \bar{Z} \qquad \frac{\partial^2 E}{\partial Z \partial r} = -\frac{2\bar{Z}}{H^2} p_1 Q + \frac{\bar{Z}}{H^2}\left[\frac{\partial K}{\partial r} - \frac{\partial E}{\partial r}\right]$$

$$\frac{\partial^2 K}{\partial Z \partial z} = +P + h_3 \bar{Z} \qquad \frac{\partial^2 E}{\partial Z \partial z} = -\frac{1}{H^2}\left(1 - 2\frac{\bar{Z}^2}{H^2}\right) Q + \frac{\bar{Z}}{H^2}\left[\frac{\partial K}{\partial z} - \frac{\partial E}{\partial z}\right]$$

where $P = \dfrac{E}{\rho^2} - \dfrac{K}{H^2}$ $\qquad Q = K - E$

$$h_1 = \frac{M - 2R^2}{2R}$$

$$h_2 = \frac{1}{\rho^2}\frac{\partial E}{\partial r} + \frac{2(R-r)}{\rho^4} E - \frac{1}{H^2}\frac{\partial K}{\partial r} + \frac{2p_1}{H^2} K$$

$$h_3 = -\frac{2\bar{Z}}{\rho^4} E - \frac{1}{\rho^2}\frac{\partial E}{\partial z} + \frac{1}{H^2}\frac{\partial K}{\partial z} + \frac{2\bar{Z}}{H^4} K$$

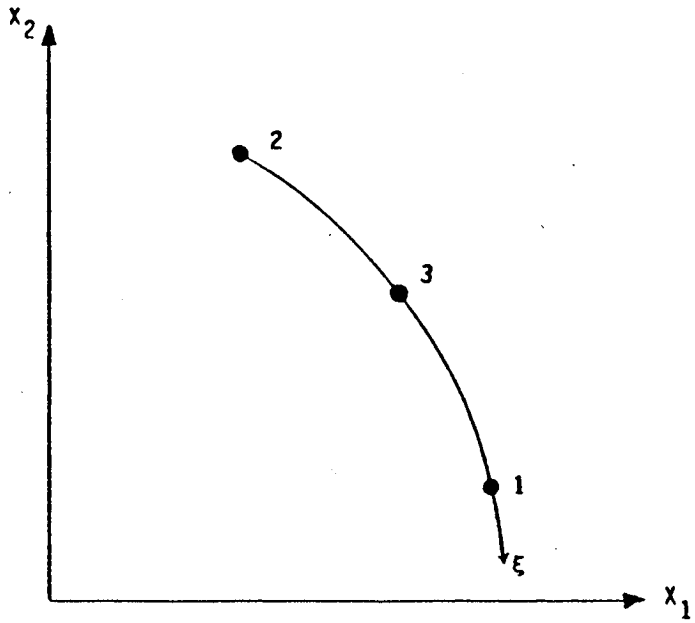

Figure A.1
Two-dimensional Boundary Element

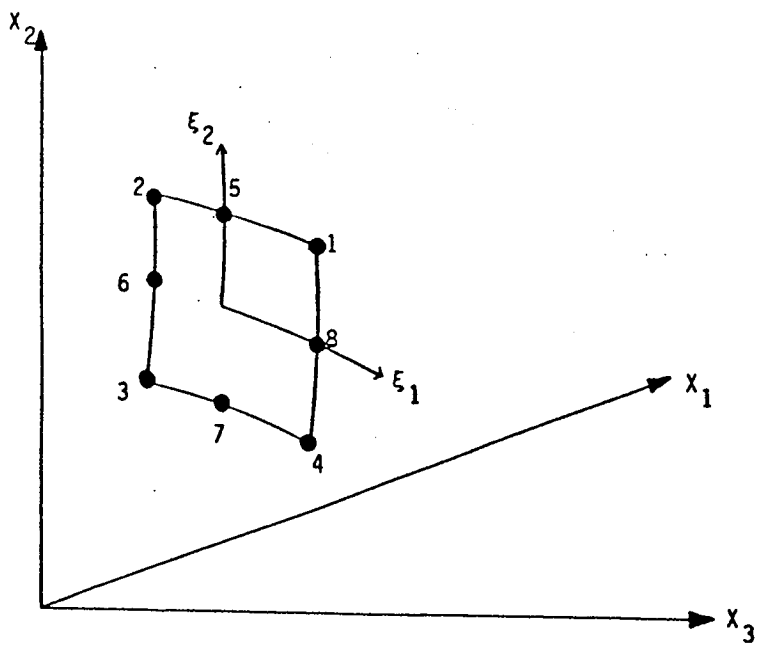

Figure A.2
Three-dimensional Boundary Element
(or Two-dimensional Volume Cell)

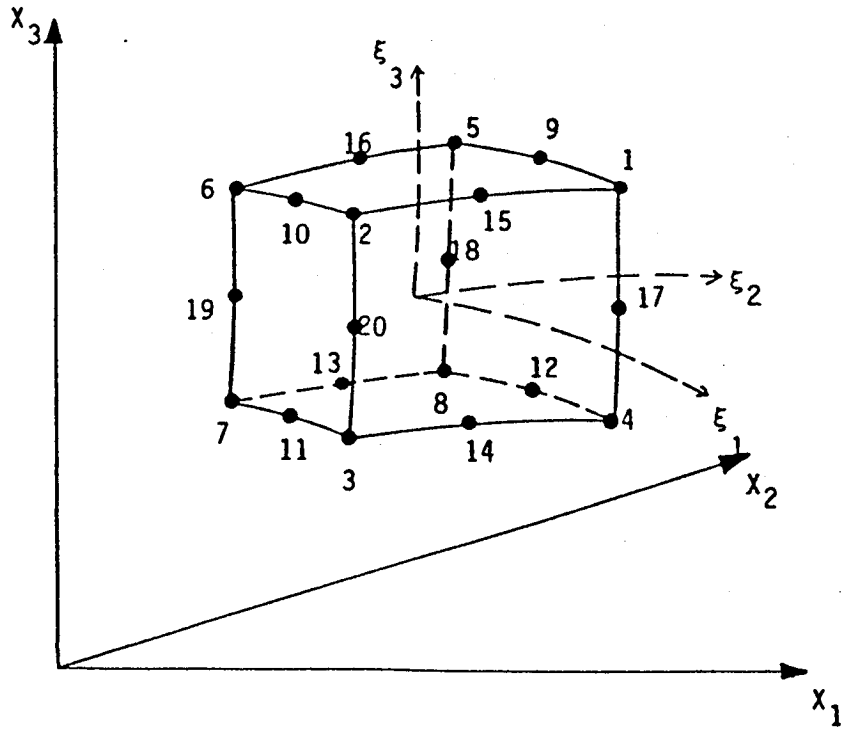

Figure A.3
Three-dimensional Volume Cell

REPORT DOCUMENTATION PAGE

Form Approved
OMB No. 0704-0188

1. AGENCY USE ONLY (*Leave blank*)	2. REPORT DATE	3. REPORT TYPE AND DATES COVERED
	December 1991	Final Contractor Report

4. TITLE AND SUBTITLE

Advanced Development of the Boundary Element Method for Elastic and Inelastic Thermal Stress Analysis

5. FUNDING NUMBERS

WU-553-13-00
G-NAG3-712

6. AUTHOR(S)

Donald P. Henry, Jr.

7. PERFORMING ORGANIZATION NAME(S) AND ADDRESS(ES)

State University of New York at Buffalo
Department of Civil Engineering
Buffalo, New York 14214

8. PERFORMING ORGANIZATION REPORT NUMBER

None

9. SPONSORING/MONITORING AGENCY NAMES(S) AND ADDRESS(ES)

National Aeronautics and Space Administration
Lewis Research Center
Cleveland, Ohio 44135-3191

10. SPONSORING/MONITORING AGENCY REPORT NUMBER

NASA CR-189079

11. SUPPLEMENTARY NOTES

Project Manager, C.C. Chamis, Structures Division, NASA Lewis Research Center, (216) 433-3252. Report was submitted as a dissertation in partial fulfillment of the requirements for the degree Doctor of Philosophy to the State University of New York at Buffalo, Buffalo, New York in 1987.

12a. DISTRIBUTION/AVAILABILITY STATEMENT

Unclassified - Unlimited
Subject Category 39

12b. DISTRIBUTION CODE

13. ABSTRACT (*Maximum 200 words*)

The focus of this dissertation is on advanced development of the boundary element method for elastic and inelastic thermal stress analysis. New formulations for the treatment of body forces and nonlinear effects are derived. These formulations, which are based on particular integral theory, eliminate the need for volume integrals or extra surface integrals to account for these effects. The formulations are presented for axisymmetric, two- and three-dimensional analysis. Also in this dissertation, two-dimensional and axisymmetric formulations for elastic and inelastic, inhomogeneous stress analysis are introduced. The derivations account for inhomogeneities due to spatially dependent material parameters, and thermally induced inhomogeneities. The nonlinear formulations of the present work are based on an incremental initial stress approach. Two inelastic solutions algorithms are implemented: an iterative; and a variable stiffness type approach. The Von Mises yield criterion with variable hardening and the associated flow rule are adopted in these algorithms. All formulations are implemented in a general purpose, multi-region computer code with the capability of local definition of boundary conditions. Quadratic, isoparametric shape functions are used to model the geometry and field variables of the boundary (and domain) of the problem. The multi-region implementation permits a body to be modeled in substructured parts; thus dramatically reducing the cost of the analysis. Furthermore, it allows a body consisting of regions of different (homogeneous) material to be studied. To test the program, results obtained for simple test cases are checked against their analytical solutions. Thereafter, a range of problems of practical interest are analyzed. In addition to displacement and traction loads, problems with body forces due to self-weight, centrifugal, and thermal loads are considered.

14. SUBJECT TERMS

Body forces; Particular integrals; Two-dimensional; Three-dimensional; Inhomogenous; Initial stress; Incremental; Multi-region; Isoparametric; Shape functions; Sample cases; Computer code

15. NUMBER OF PAGES
262

16. PRICE CODE
A12

17. SECURITY CLASSIFICATION OF REPORT	18. SECURITY CLASSIFICATION OF THIS PAGE	19. SECURITY CLASSIFICATION OF ABSTRACT	20. LIMITATION OF ABSTRACT
Unclassified	Unclassified	Unclassified	

National Aeronautics and
Space Administration

Lewis Research Center
Cleveland, Ohio 44135

Official Business
Penalty for Private Use $300

FOURTH CLASS MAIL

ADDRESS CORRECTION REQUESTED

U.S.MAIL

Postage and Fees Paid
National Aeronautics and
Space Administration
NASA 451

J. Starness
NASA-Langley Research C.
Library - MS 185
Hampton, VA 23665

NASA